GEOLOGICA ULTRAIECTINA

Mededelingen van de
Faculteit Aardwetenschappen
Universiteit Utrecht

No. 188

Benthic foraminiferal response to Late Quaternary variations in surface water productivity and oxygenation in the northern Arabian Sea.

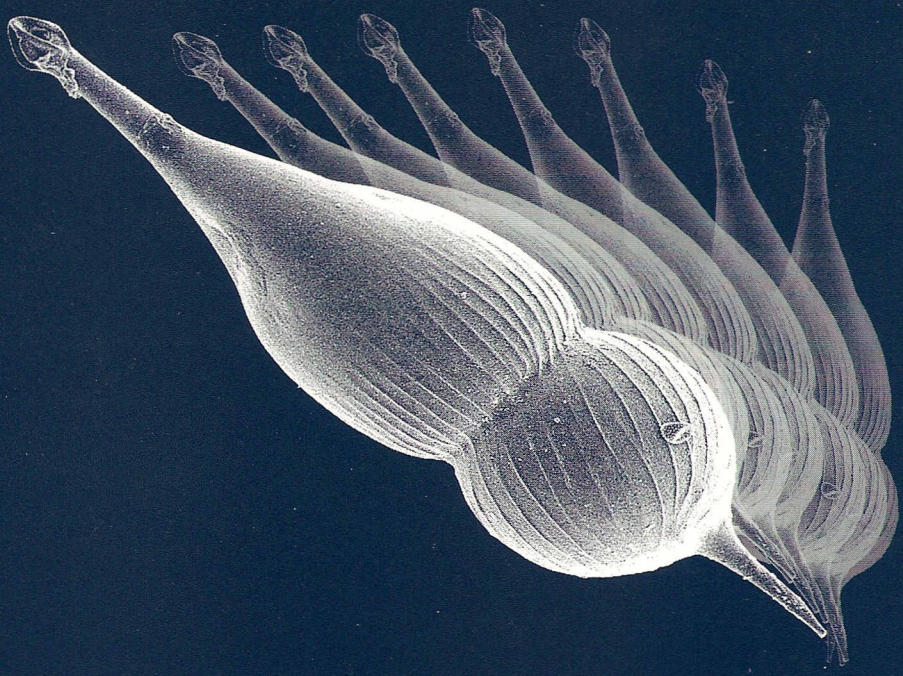

Maryke den Dulk

GEOLOGICA ULTRAIECTINA

Mededelingen van de
Faculteit Aardwetenschappen
Universiteit Utrecht

No. 188

Benthic foraminiferal response to Late Quaternary variations in surface water productivity and oxygenation in the northern Arabian Sea.

Maryke den Dulk

ISBN :90-5744-046-6

Benthic foraminiferal response to Late Quaternary variations in surface water productivity and oxygenation in the northern Arabian Sea.

De response van benthonische foraminiferen op veranderingen in biologische productie en zuurstof in de noord Arabische Zee tijdens het Laat Kwartair.

(Met een samenvatting in het Nederlands)

Proefschrift

ter verkrijging van de graad van doctor
aan de Universiteit Utrecht
op gezag van de Rector Magnificus Prof. Dr. H.O. Voorma
ingevolge het besluit van het College voor Promoties
in het openbaar te verdedigen
op maandag 20 maart 2000 des middags om 14.30 uur

door

Maryke den Dulk
geboren op 11 december 1967, te Cardón

Promotores:

Prof. Dr. J.E. Meulenkamp	Faculty of Earth Sciences Utrecht University
Prof. Dr. G.J. van der Zwaan	Faculty of Earth Sciences Utrecht University Faculty of Biology Nijmegen University

Co-promotores:

Dr. W.J. Zachariasse	Faculty of Earth Sciences Utrecht University
Dr. G.J. Reichart	Faculty of Earth Sciences Utrecht University

Members of the Dissertation committee:

Prof. Dr. P. van Cappellen	Faculty of Earth Sciences Utrecht University
Dr. A.J. Gooday	Southampton Oceanographic Centre Southampton, UK
Prof. Dr J.W. de Leeuw	Netherlands Institute for Sea Research Texel
Dr. A. Mackensen	Alfred Wegener Institute for Polar and Marine Research Bremen, Germany
Prof. Dr. H. Visscher	Faculty of Biology Utrecht University

The research described in this thesis was carried out at the Institute of Paleoenvironments and Paleoclimate Utrecht (IPPU), Faculty of Earth Sciences, Utrecht University, Budapestlaan 4, P.O.Box 80021, 3508 TA Utrecht, The Netherlands. Financial support was provided by the Netherlands Organisation for Scientific Research (NWO, project 750.29.402)

Contents

Chapter 1
Introduction and summary

Doha (Qatar), my residence between 1975-1980:
More than once we were forced to head back to the capital city Doha. We were taken by surprise by suddenly rising sandstorms due to the Shamal winds, in a season which otherwise would be ideal for a trip to the countryside. Thus, heavily disappointed for missing out on a weekend's camping trip to one of Qatar's splendid desolate sandy beaches and shallow lagoons.

Later, during my PhD-studies I learned that on the Arabian peninsula these Shamal winds mark the onset of the Asian summer monsoon.

Continents in the tropical region experience a semi-annual reversal in wind direction called the monsoon. The Asian monsoon system brings seasonal rains in the larger part of the Asian region, influencing agriculture, economics, and the entire ecosystem. People on the Asian continent seriously depend upon the monsoon climate and its predictability. Over 60% of the earth's population lives in this region, which directly states the scale of importance of this phenomenon and the number of people who potentially benefit from studying the mechanisms controlling this climatic system.

The direction and strenght of the Asian monsoon winds is dictated by the atmospheric pressure gradient established between the Asian continent and the subtropical Indian Ocean. The position of the Inter Tropical Convergence Zone in this region and the associated tropical low pressure cell, annually shifts between approximately the tropic of Cancer and 10°S following the cycle of maximum solar heating. The Arabian Sea, located in the north-western part of the Indian Ocean, is enclosed by north-east Africa, the Arabian Peninsula, and India. During summer, heating of the Tibetan Plateau north of India enhances the atmospheric pressure gradient, thus helping to create a powerful monsoon. Moist air attracted from the Indian Ocean moves north over the Arabian Sea in strong southwesterly winds and is forced to rise over the southern slopes of the Himalayas, producing heavy rains over northern India. During winter, the pressure gradient is reversed. Low solar insolation and an increased albedo due to the seasonal snow cover, cause high atmospheric pressures over Central Asia. The resulting cold northeasterly winds are associated with a dry season in India.

Due to the monsoon the Arabian Sea is one of earth's biologically most

productive bodies of water. Prevailing southwestern winds during summer cause upwelling of nutrient-rich subsurface waters. This eutrophic water spurs rapid and widespread growth of marine algae and subsequent marine zooplankton production. Export of organic matter to deeper water and to the sea floor is proportionally high. The breakdown of this exported organic matter, in turn, causes high oxygen consumption within the water column. Combined with moderate rates of mid water ventilation this results in an intense Oxygen Minimum Zone (OMZ) between 150-1200 m water depth. In places where the OMZ intersects the sea floor the low oxygen levels have strong impact on benthic biological and geochemical processes.

Because environmental conditions are extreme, particularly in terms of productivity and oxygenation, the Arabian Sea provides a unique environment to study flux rates at which organic matter is exported from the epipelagic food web, fuelling benthic life below. The extreme OMZ conditions enable us to clearly define the role oxygen plays in the benthic biological system, and on diagenetic processes influencing storage of organic matter and of other components in the fossil record. The resulting knowledge in turn may be put to use in paleoenvironmental studies. Many of these topics, including paleoenvironmental and -climatic variability in the Arabian Sea, are presently addressed in studies conducted by various scientific groups and international research programs.

Paleoenvironmental reconstructions and benthic foraminifera

Biological, chemical and sedimentological parameters reflecting the variability of the environment (so-called proxies) are the main tools to unravel past paleoenvironmental conditions. Among the important biological tools are benthic foraminifera, one celled organisms of which a large number of taxa build a calcite test. Their widespread occurrence, numerical abundance, and high fossilisation potential rank them among the most powerful biological tools to reconstruct paleoenvironments.

At this stage benthic foraminifera are considered particularly useful in reconstructing past changes in surface water productivity and bottom water oxygenation. Studies of dead and living benthic foraminifera, and laboratory studies have led to the notion that oxygen and organic flux are predominant in structuring benthic foraminiferal associations. At the same time a large number of benthic foraminiferal taxa are known to withstand low oxygen- and even anoxic conditions for a longer period of time at a point where most

other meiofaunal and macrofaunal elements are no longer able to cope with the deteriorating conditions. This renders benthic foraminifera as eminently suitable to reconstruct an environment as extreme as the Arabian Sea.

This thesis discusses benthic foraminifera in Late Quaternary records from within and below the northern Arabian Sea OMZ and their interpretation in terms of past changes in surface water productivity and mid-water oxygenation (Chapters 2-5). Because the present contention is that multiproxy studies lead to better assessment of the paleoenvironment, this research has been conducted in a multidisciplinary way. In particular, various geochemical tracers are employed (Chapters 2-4, 6), but a comparison is also made with a number of lithogenic proxies (Chapter 3). The overall picture shows that large variations occurred in the intensity of the OMZ during the last 225 kyr, and that the base of the OMZ occasionally extended well below its present-day position. Variability took place on orbital and sub-orbital time scales and is presumably controlled by 1) changes in summer monsoon wind strength, which controls summer surface water productivity via coastal and open ocean upwelling and thus subsurface oxygen consumption, and 2) deep convective mixing during periods of cold and intensified winter monsoons. The close correlation of sub-orbital monsoon-driven OMZ variability in the Arabian Sea with rapid climatic fluctuations at high northern latitudes suggests a close coupling between high and low latitude climates (Chapter 3).

The development of environmental proxies and continuous scrutiny of their accuracy and reliability is an important part of paleoenvironmental reconstructions. This is evidently due to the complexity of environmental processes, but also because continuous development and employment of new analytical techniques facilitates more detailed analyses and leads to new questions. For example, in studies on living benthic foraminifera microelectrode-technology enables more detailed analyses of microhabitat (in-sediment) distributions in relation to pore-water oxygen gradients. This may raise additional questions, for instance, pertaining to the underlying ecological principles of microhabitat distributions. Most proxies employed have disadvantages in some way, primarily as a result of degradation and/or diagenetic processes, and benthic foraminifera make no exception. Elaborating on our present knowledge of benthic foraminiferal ecology and considering potential pitfalls, Chapter 4 deals with the question how accurately can benthic foraminifers be used as recorders of oxygenation and productivity in paleoenvironmental studies.

Most proxies are not calibrated, and thus provide information on past environmental conditions in relative terms. Yet the need to accurately

reconstruct environmental conditions seems greater than ever, certainly in view of the possible consequences of rapid man-induced environmental changes. As a result continuous efforts are made to quantify observed empirical relationships between proxies and environmental parameters (so-called transfer functions). Chapter 6 explores the perspective of a benthic foraminiferal oxygen transfer function in reconstructing the oxygen history of the Arabian Sea OMZ. It is concluded that the oxygen transfer function produces a potentially reliable quantitative oxygen reconstruction of the oxygen content of bottom waters.

Chapter 2
OMZ intensity, productivity and oxygenation

Benthic foraminiferal response to variations in surface water productivity and oxygenation in the northern Arabian Sea.

Abstract

A 120 kyr benthic foraminiferal record obtained from the base of the Oxygen Minimum Zone (OMZ) at a site in the northern Arabian Sea was studied. Quantitative benthic foraminiferal data were compared with paleoproductivity indices (C_{org} and *Globigerina bulloides*) and indices for bottom water oxygen concentration (Pteropod Preservation Index, Mo/Al, V/Al and Mn/Al). The benthic foraminiferal record revealed two distinct assemblages that show variations in the precession frequency band. A high diversity, high equitability assemblage proliferates in isotopic stages 1, 4 and 5, and has been interpreted to reflect relatively oxygenated bottom water conditions. This assemblage shows a strong covariance with minima in summer monsoon productivity. A low diversity, low equitability fauna, typically with a few species showing high dominances, is considered to reflect low bottom water oxygen conditions related to eutrophic surface water conditions. Dominating species in this assemblage are bolivinids, buliminids and globobuliminids. This assemblage dominates during precession-driven maxima in summer surface water productivity, and also during isotopic stages 2 and 3. We suggest that an intensified and colder glacial winter (NE) monsoon led to increased winter production, which superimposed on the precession driven changes in surface water productivity, resulted in overall poorly oxygenated bottom water during glacial stages 2 and 3. A promising proxy for tracing winter productivity in the northern Arabian Sea is the planktonic foraminifer *Globigerina falconensis*. The benthic foraminiferal species *Rotaliatinopsis semiinvoluta* in particular, is prolific under glacial conditions.

Den Dulk, M., Reichart, G.J., Memon, G.A., Roelofs, E.M.P, Zachariasse, W.J., Van der Zwaan, G.J., Marine Micropaleontology 35 (1998), 43-66.

1. Introduction

The atmospheric circulation in the Arabian Sea region is characterized by an annually reversing wind system, which invokes seasonal changes in hydrography and lithogenic- and biogenic particle fluxes. During the summer monsoon, the combined influence of wind-driven coastal upwelling and open ocean Ekman pumping allows deeper, nutrient-rich waters to rise up in the northwestern Arabian Sea, driving productivity to values that are among the highest known for the open ocean (Wyrtki, 1971; 1973; Swallow, 1984). Winter production on the other hand is generally low except in the northern Arabian Sea, where convective overturn resulting from surface water cooling stimulates surface water productivity (Wyrtki, 1973; Banse, 1984; 1987; Madhupratap et al., 1996).

The combination of high surface water productivity and moderate rates of thermocline ventilation (You and Tomczac, 1993) leads to an intense Oxygen Minimum Zone (OMZ) between 150 and 1200 meters (Wyrtki, 1971; 1973; Deuser et al., 1978; Olson et al., 1993), with oxygen levels below 2 μM (Van Bennekom and Hiehle, 1994). Regions where the OMZ impinges on the slope or submarine highs are characterized by low oxygen conditions at the bottom. Such conditions are known to sustain benthic foraminiferal assemblages characterized by low diversities and high dominances with generally 2 or 3 species constituting up to 80% of the total assemblage (Lutze and Coulbourn, 1984; Perez-Cruz and Machain-Castillo, 1990; Hermelin and Shimmield, 1990; Sen Gupta and Machain-Castillo, 1993; Gooday, 1994; Wells et al., 1994).

Little is known about the distribution of living benthic foraminifers in the Arabian Sea. The only study on living (Rose Bengal stained) benthic foraminifers in the Arabian Sea, is that of Jannink et al. (1998). They show that *Bolivina dilatata* and *Bulimina exilis* are abundantly present within the core of the OMZ, at 500 m. Near the lower boundary of the OMZ, at waterdepths of 1000-1250 m, assemblages are dominated by the species *Uvigerina peregrina*, *B. exilis* and *Rotaliatinopsis semiinvoluta*, whereas *Bulimina aculeata* and *Epistominella exigua* are the most prolific species below the OMZ at depths of 1500-2000 m. A few other studies focused on dead and fossil benthic foraminifers in the Arabian Sea. Zobel (1973) identified a sequence of biofacies types in samples from several depths transects on the Pakistan and Indian Margin. On the Pakistan Margin between 0-350 m she distinguished 5 different biofacies types. A sixth biofacies type characterized by *Bulimina aculeata* occurs below the OMZ. Hermelin and Shimmield (1990) found that benthic foraminiferal faunas in surface sediment samples of the

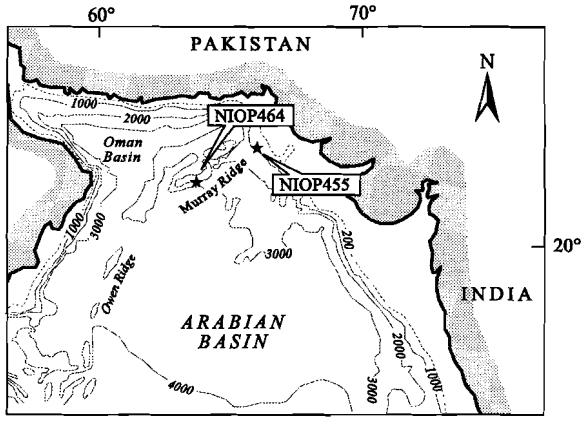

Figure 1. Location of piston core NIOP455 (23.33° N, 65,57° E, waterdepth 1002 m) and NIOP464 (22,15° N, 63,35° E, waterdepth 1470 m).

Arabian Sea are strongly related to the organic carbon content and texture of the sediment. The response of benthic foraminifers to changes in upwelling intensity over the last 10 million years in the northwestern Arabian Sea was studied by Hermelin (1991, 1992). In his 1992 paper he suggests a deepening of the lower boundary of the OMZ between 6.5 and 3.0 Ma. In a more recent paper Hermelin and Shimmield (1995) discuss a late Pleistocene-Holocene benthic foraminiferal record from the Indus Fan region, and suggest that some species show variability in the precession frequency band, perhaps as a response to summer monsoon-driven variations in upwelling and associated food supply. Other species seem to co-vary with the 100 kyr ice volume cycle, possibly due to changes in intermediate and deep water chemistry and the input of nutrients.

In this paper we discuss a 120 kyr record of benthic foraminifers from a sediment core (NIOP455) located on the Pakistan Margin. The interpretation of the benthic foraminiferal census data is compared with that inferred from various geochemical and planktonic foraminiferal data obtained from the same samples. This study is part of a comprehensive study on the dynamics of the OMZ in the northern Arabian Sea for which the material was collected in 1992 during the Netherlands Indian Ocean Programme. Studies are at various stages of completion. In this paper we refer to three studies. One deals with the distribution of living (stained) benthic foraminifers in two transects across the Pakistan Margin (Jannink et al., 1998). Some of the results are mentioned above. A second study (Reichart et al., 1997) discusses the variability in surface

water productivity and the intensity of the OMZ, as inferred from selected geochemical and planktonic foraminiferal data from core NIOP464 recovered from the Murray Ridge. A third paper deals with the possible effect of bottom water oxygen levels on the preservation of organic matter, based on boxcores from within and below the OMZ (Van der Weijden et al., 1999).

2. Material and methods

Piston core NIOP455 was recovered from the base of the present-day OMZ (1002 m) on the Pakistan Margin (Fig. 1) and measures 14.56 m. The sediment essentially consists of alternating greyish-olive to dark olive hemipelagic mud (Fig. 2). Visual observation and X-ray radiographs show several (faintly) laminated intervals. Two thin turbiditic layers occur at the base of the core. No further evidence for mass transport was found. Samples were taken every ~12 cm for geochemical, planktonic foraminiferal and pteropod analyses, and every ~36 cm for benthic foraminiferal counts. The resolution of the benthic foraminiferal record is, therefore, 3 times lower than that of the other proxy records.

The $\delta^{18}O$ record of NIOP455 (Fig. 2) is based on the planktonic foraminiferal species *Neogloboquadrina dutertrei* or *Globigerinoides sacculifer* where *N. dutertrei* was rare. About 100 hand-picked specimens per sample were treated according to standard procedures (see Reichart et al., 1997) and measured on a VG SIRA 24 mass spectrometer. Replicate analyses show a standard deviation of 0.1‰. Isotopic stage boundaries and events in the SPECMAP $\delta^{18}O$ chronology (Imbrie et al., 1984; Martinson et al., 1987) are easily recognized and provide a set of 6 age calibration points, indicating that the $\delta^{18}O$ record of NIOP455 covers isotopic stage 1 to 5, with 5.4 being the oldest event. AMS^{14}C dating on a sample of planktonic foraminifers from 3.88 m below the core top provided an additional calibration point with a ^{14}C-age of 22,940 yr BP, which we converted to 26.1 calendar years (Bard, 1990). Ages of samples were obtained through linear interpolation between these calibration points. Mass accumulation rates (MAR) were calculated using the weight loss upon freeze drying of fixed volume samples and the linear sedimentation rates (LSR).

After freeze drying, part of the samples were thoroughly ground in an agate mortar and dissolved in an $HClO_4$-HNO_3-HF acid mixture. The dried residue was dissolved in 1 M HCl for analysis of Al, Mn, Mo, and V with an ICP-AES (Perkin Elmer OPTIMA 3000). Analytical precision and accuracy

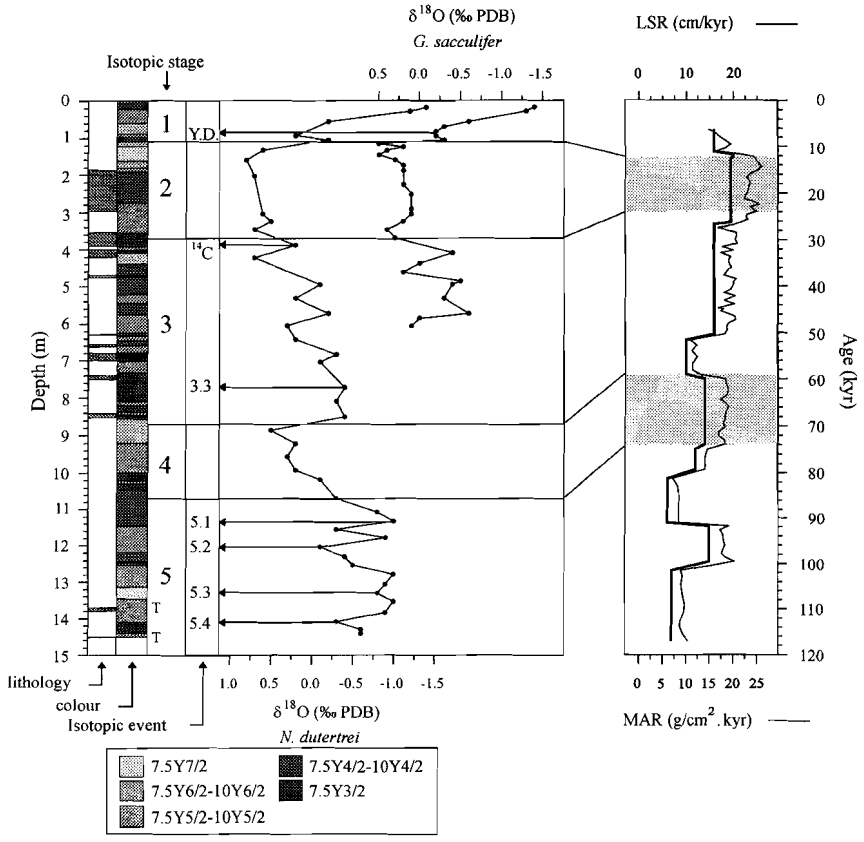

Figure 2 Lithology of NIOP455 (white = homogeneous hemipelagic mud; grey = laminated hemipelagic mud). Sediment colors are given in various grey tones. T = turbidites. The $\delta^{18}O$ of *N. dutertrei* and *G. sacculifer* (relative to the PDB standard) is plotted versus depth and time. Linear sedimentation rate (LSR, cm/kyr) and mass accumulation rate (MAR, $g.cm^{-2}.kyr^{-1}$) are given in the right hand column.

were determined by replicate analyses of samples and by comparison with an international and in-house standard (for more details see Reichart et al., 1997). Relative precision and accuracy were both found to be better than 3%. Elements are normalized to Al to correct for the variable input of terrestrial sediments.

For the analyses of organic carbon (C_{org}) and the isotopic composition of C_{org} ($\delta^{13}C_{org}$), 1 g. of dry sediment was weighted in a centrifuge tube. Carbonate was dissolved in 1 M HCl under mechanical shaking during 12 hours, after which the samples were rinsed in demineralized water in order to remove $CaCl_2$ and subsequently dried. The C_{org} content was determined

volumetrically following dry oxidation with CuO at 900°C in a closed circulation system at $0.2x10^5$ Pa oxygen. The released CO_2 gas was cryogenically separated from the other gasses. The $\delta^{13}C_{org}$ was measured with a VG SIRA 24 mass spectrometer with a precision better than 0.1%. Another aliquot of dry sediment was used to determine C_{org} and N_{tot}, using a Carlo Erba NA1500- CNS analyzer with a relative precision of better than 10‰ for N_{tot} and better than 3‰ for C_{org}. A good agreement was found between the C_{org} contents using this method and the volumetric method.

Quantitative benthic and planktic foraminiferal analyses were performed on the 150-595 μm size fraction of, respectively 44 and 119 samples. Preservation of benthic foraminifers is excellent and preservation of planktic foraminifers is generally good with few fragments. The samples were split into aliquots containing about 250 specimens (using an Otto microsplitter). All foraminifers were mounted, identified and counted. For the benthic foraminiferal census data, forty-four species that show abundances higher than 5% and/or carry relevant ecological information, were subjected to a Principal Component Analysis (PCA). Pteropod abundance is defined by the number of protoconchs per fixed wet sediment volume.

3. The benthic foraminiferal record

3.1 General faunal characteristics and discrimination of assemblage 1 and 2

The frequency distribution of important taxa is illustrated in figures 3 and 4. Quantitatively important taxa are *Bulimina exilis, Rotaliatinopsis semiinvoluta, Bolivina alata,* and *Fursenkoina bradyi.* These species show abundances of >25%. The first two factors of the PCA account for 22% and 9.8%, respectively of the total benthic foraminiferal variation. We limit our discussion to factor one, because this factor discriminates between two ecologically meaningful groups of species, whereas the 2nd PCA-axis cannot be interpreted in simple terms. High positive loadings (>0.6) on the first factor are shown by *Bulimina striata, Gavelinopsis lobatulus, Chilostomella oolina, Monothalameous* spp., *Sphaeroidina bulloides, Cibicides ungerianus, Hyalinea balthica*, and *Hoeglundina elegans* (Table 1). Other contributors (loading >0.5) are *Bulimina alazanensis, Melonis barleeanum, Quinqueloculina* spp, *Cassidulina subglobosa*, and *Cassidulina carinata*. The percentages of all these species are plotted in Figure 3. Elements showing high negative loadings (<-0.36) are *B. exilis, R. semiinvoluta, B. alata, Bolivina pygmaea, Globobulimina* spp., and

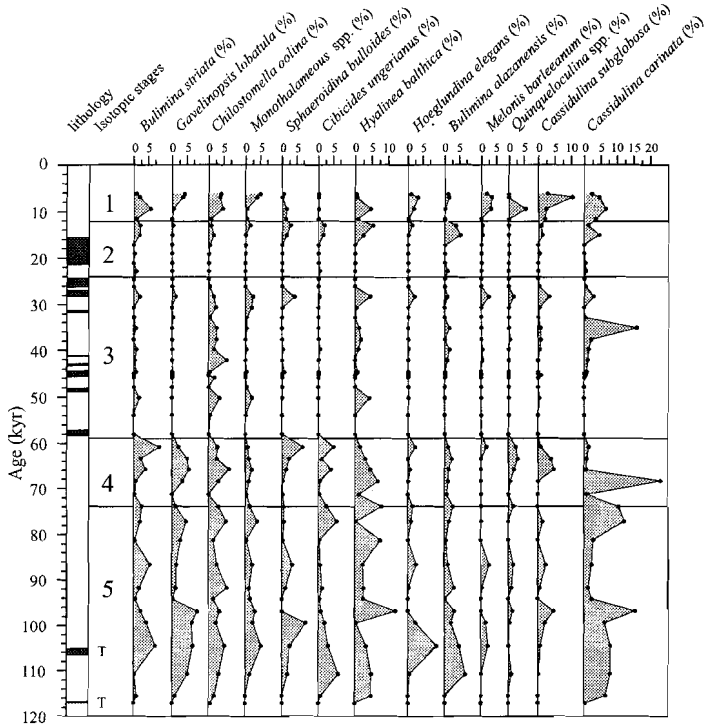

Figure 3 Percentages of species loading positively on benthic Factor 1 plotted versus age.

Bulimina sp.1 (Table 1). The percentages of these species are plotted in figure 4. *F. bradyi* (loading = -0.24) is also plotted in figure 4, because it is quantitatively important.

The general faunal characteristics expressed by the Shannon diversity, equitability, and dominance (= relative abundance of the one most frequent species) show predictable patterns: a high (low) diversity corresponds with high (low) equitability and low (high) dominances (Fig. 5). Dominances range from 8% to about 50%, with highest dominances occurring in the laminated intervals. Dominances in the intervals with high benthic diversity are less than ~20% and on average 10-15%. Figure 5 shows that the Factor 1 scores clearly correlate with the general faunal characteristics. The species loadings on the first PCA axis and the general faunal characteristics, therefore, allow a subdivision of the fauna in two different assemblages. One assemblage, assemblage 1, is diverse and consists of species showing high positive loadings on Factor 1, whereas the other, assemblage 2, is a low diversity assemblage, made up of species showing high negative loadings.

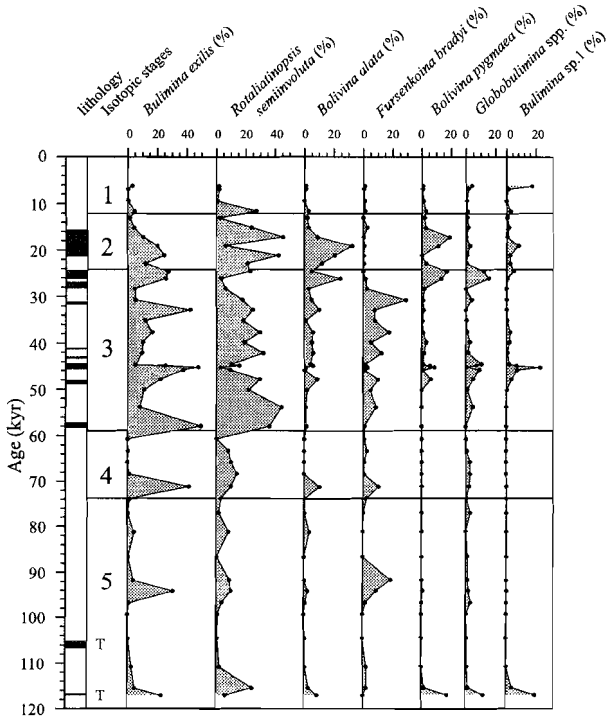

Figure 4 Percentages of species loading negatively on benthic Factor 1 and *Fursenkoina bradyi* plotted versus age.

3.2 Interpreting assemblages 1 and 2

The low diversity and low equitability in assemblage 2 are indicative of faunas thriving under severe dysoxia (Lutze and Coulbourn, 1984; Hermelin and Shimmield, 1990; Denne and Sen Gupta, 1991; Sen Gupta and Machain-Castillo, 1993; Jannink et al.; 1998). In NIOP455, lowest diversity and equitability values are associated with laminated intervals. Intervening homogeneous intervals clearly show evidence of bioturbation by meio- and macrofauna (burrows up to ~1 cm across), whereas there is no evidence of bioturbation in the laminated intervals. These laminated intervals, therefore, represent periods during which the meio- and macrofauna was largely absent, probably due to severe oxygen depletion at the bottom. Assemblage 2 consists of bolivinids, buliminids and globobuliminids, all taxa with infaunal morphological characteristics, such as spherical or elongate test shapes

Table 1.
Factor loadings on factor 1 and 2 for the 44 species employed in the Principal Component Analysis and maximum and average percentages of these species.

Species	Factor 1	Factor 2	Average %	Max (%)
Bulimina striata	0.79	0.42	1.5	8.7
Gavelinopsis lobatulus	0.75	-0.20	1.5	8.5
Chilostomella oolina	0.71	-0.17	2.2	6.9
Monothalameous spp.	0.68	-0.09	1.1	5.4
Sphaeroidina bulloides	0.63	0.47	1.0	8.1
Cibicides ungerianus	0.63	0.01	1.0	6.8
Hyalinea balthica	0.61	-0.48	2.2	12.3
Hoeglundina elegans	0.61	0.32	0.7	9.8
Bulimina alazanensis	0.60	-0.13	1.2	7.1
Melonis barleeanum	0.60	0.54	0.5	3.6
Quinqueloqulina spp.	0.58	0.33	0.5	5.7
Cassidulina subglobosa	0.54	0.08	1.1	10.4
Cassidulina carinata	0.51	-0.40	3.5	23.2
Nummuloculina irregularis	0.48	0.41	0.7	5.8
Fursenkoina sp.1	0.47	-0.06	0.7	7.5
Uvigerina proboscidea	0.44	0.23	1.0	11.1
Pullenia bulloides	0.44	-0.53	2.5	15.1
Uvigerina semiornata	0.42	0.44	0.6	6.3
Triloculina spp.	0.40	0.26	0.3	5.4
Ammonia spp.	0.40	0.52	0.4	6.6
Gyroidina sp.1	0.37	-0.68	0.7	5.1
Bulimina aculeata aculeata	0.35	-0.26	1.6	15.2
Oridorsalis umbonatus	0.34	-0.59	0.7	8.2
Bulimina aculeata marginata	0.30	-0.34	3.9	24.0
Rosalina spp.	0.23	0.41	0.2	6.0
Uvigerina peregrina	0.16	-0.20	2.9	16.3
Cassidulina inflata	0.08	-0.58	1.2	8.5
Osangularia sp.1	-0.17	0.06	1.0	15.0
Ehrenbergina pacifica	-0.17	-0.03	0.3	5.5
Uvigerina porrecta	-0.18	0.07	0.3	7.6
Globobulimina affinis	-0.18	-0.12	0.6	9.6
Bolivina dilatata	-0.19	0.05	0.8	14.6
Globobulimina sp.1	-0.19	0.16	0.6	7.2
Fursenkoina bradyi	-0.24	-0.24	4.1	29.3
Gyroidina polia	-0.26	-0.03	1.6	6.4
Cassidulina bradyi	-0.27	0.19	0.6	12.3
Bolivina seminuda	-0.29	0.15	0.3	8.8
Pullenia quinqueloba	-0.36	-0.03	0.7	6.0
Bulimina sp.1	-0.37	0.15	2.6	23.2
Globobulimina spp.	-0.46	0.13	2.9	15.6
Bolivina pygmaea	-0.54	0.28	2.8	18.9
Bolivina alata	-0.60	0.18	4.7	32.5
Rotaliatinopsis semiinvoluta	-0.60	-0.16	14.4	45.5
Bulimina exilis	-0.74	0.07	12.8	49.5

(Corliss, 1985; Corliss and Chen, 1988). Assemblage 1 on the other hand, contains a substantial number of species with plano-convex or biconvex tests, typical of epifaunal species (Corliss, 1985; Corliss and Chen, 1988). The higher surface area/volume shapes and greater pore density of the infaunal species dominating assemblage 2 is seen as an adaptation to low-oxygen conditions (Corliss, 1985; Bernhard, 1986; Gooday, 1986; Corliss and Emerson, 1990; Corliss, 1991; Bernard, 1992).

C. ungerianus an element of assemblage 1 (Fig. 3), is an important element of a benthic foraminiferal assemblage just below the OMZ in the Arabian Sea (Hermelin and Shimmield, 1990). Apparently this species is intolerant to oxygen depletion. In a study of Mediterranean sapropels, Mullineaux and Lohmann (1981) found *Quinqueloculina* spp. to be the least tolerant taxon to low oxygen bottom water conditions. Furthermore, Barmawidjaja et al. (1992) observed *Quinqueloculina* spp. in the Adriatic Sea only in fair amounts during periods in which the oxygen content of the bottom water was high. In the western Gulf of Mexico *S. bulloides* and *Bulimina mexicana* (= *B. striata*) are part of an assemblage that is abundant in the lower part of the oxygen minimum water with oxygen concentrations between 2.5 and 2.9 ml/l (Denne and Sen Gupta, 1991). In the basins of the middle and outer Californian borderland, *H. elegans* is characteristic of modern slope assemblages with low rates of sedimentation and relatively low oxygen concentrations (0.3-1.1 ml/l) (Douglas, 1981 in: Hermelin and Shimmield, 1990). In the Arabian Sea *H. elegans* is most prolific just below the OMZ, but remains present, though with significantly lower percentages, in the basal part of the OMZ (Hermelin and Shimmield, 1990). *H. elegans* is likely to be sensitive

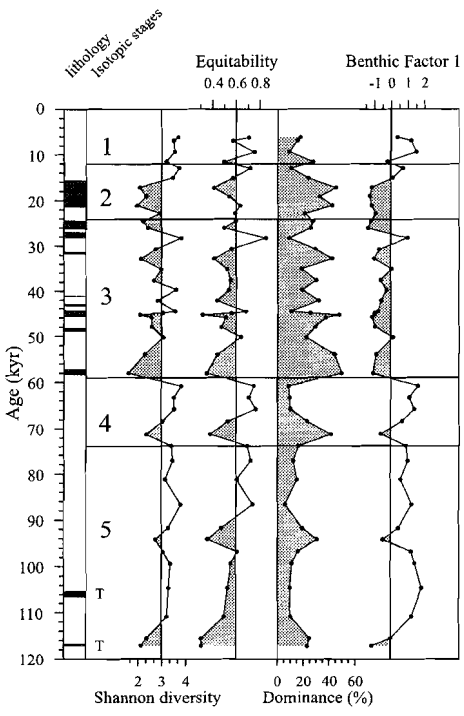

Figure 5 Shannon diversity, equiability, dominance and scores for benthic Factor 1 plotted versus age.

to dissolution because of its aragonitic shell, and in areas with low oxygen concentrations its shell may easily dissolve due to lowered alkalinity. Therefore, directly or indirectly, through dissolution, *H. elegans* becomes less frequent under lower oxygen conditions. In accordance with these observations, Kaiho (1994) classified *B. striata*, *S. bulloides*, and *H. elegans* as suboxic indicators, whereas he considered *Cibicides* spp. and *Quinqueloculina* spp. to be indicative of well-oxygenated bottom-waters. We find all these species to be part of assemblage 1. *C. oolina* is one of the species showing highest positive loadings on Factor 1 (Table 1, Fig. 3). This species, however, is generally associated with low oxygen levels (Kaiho, 1994 and references therein). Given that *C. oolina* has been reported to have a deep infaunal habitat (Corliss, 1985; Corliss and Emerson, 1990; Miao and Thunell, 1993; Alve and Bernhard, 1995), this species could have occupied levels close to the oxic/anoxic front deep in the sediment under oxic bottom water conditions. Species of assemblage 1, therefore reflect a complex sequence of epi- to infaunal species, suggestive of a deep redox front under relatively well-ventilated conditions.

The dominance of assemblage 2 in the laminated intervals indicates that the species of this assemblage are tolerant to low oxygen concentrations of the bottom water. However, this does not imply that oxygen is the prime ecological control on these species. The low oxygen levels presumably have originated from a high flux of organic matter. Tolerance to oxygen depletion then provides a competitive edge enabling these species to utilize the trophic resources associated with the high organic load. Hermelin and Shimmield (1990) found *B. pygmaea* and *Bulimina* sp.1 to be dominant in the benthic assemblage from the Arabian Sea OMZ, between 200-600 m, where organic carbon accumulation is most prolific. Denne and Sen Gupta (1991) found *B. alata* to be a significant contributor to a deltaic assemblage in the present-day discharge area of the Mississippi, which is a zone of high surface water productivity. *B. exilis* is one of the species with a strongly negative loading on Factor 1 (-0.74) and which shows very high dominances (~50%, Table 1, Fig. 4). According to Jonkers (1984) *B. exilis* can be regarded as 'an eutrophic species flourishing under low oxygen and high food conditions'. Caralp (1984) proposed that *B. exilis* flourishes under conditions of rapidly accumulating organic matter of high nutritive quality. Later, Caralp (1989) linked *B. exilis* to little altered, labile organic matter. A study on living, stained benthic foraminifers from the Pakistan Margin (Jannink et al., 1998) supports these suggestions; high numbers of *B. exilis* are found in the fine fraction (63-150 μm) of samples from the OMZ at the end of the summer. The small size of

these specimens is characteristic of large standing stocks in areas of high production, and may result from rapid reproduction under "optimum conditions" characterized by abundant food (Phleger and Soutar, 1973). The literature thus suggests that *B. exilis* flourishes under high, pulse-like fluxes of organic matter, thereby tolerating low oxygen conditions. *R. semiinvoluta*, an endemic species from the Indian Ocean (Loeblich & Tappan, 1988), also has a strongly negative loading on Factor 1 (-0.60, Table 1, Fig. 4), but little is known about its habitat preferences. The study on living (stained) benthic foraminifera revealed high numbers of *R. semiinvoluta* in the fine fraction (63-150 μm) at the end of the summer monsoon, at 1000 and 1250 m water depth (Jannink et al, 1998). These high numbers near the base of the OMZ suggest preferences for enhanced food supply under modest low-oxygen bottom water conditions.

All evidence together suggests that the dominance of infaunal species in assemblage 2 reflects low bottom water oxygen conditions and a high flux of organic matter. The more complex composition of assemblage 1 indicates more oxygenated conditions.

3.2 Downcore variability in assemblages 1 and 2

Figure 5 shows that assemblage 1 (positive factor scores) dominates in isotopic stages 1, 4 and 5, which suggests that relatively well oxygenated bottom water conditions prevailed during these periods. The generally positive scores in isotopic stages 4 and 5, are interrupted by three short intervals with negative scores at around 116, 93 and 71 ka, which is roughly every 23 kyr. These intervals represent periods of decreased oxygen content in the bottom water. The 23 kyr variability in the score plot (Fig. 6) may indicate that the benthic foraminiferal fauna responded to precession driven (23 kyr) changes in surface water productivity and organic carbon fluxes. Factor 1 scores in isotopic stages 2 and 3 are almost all negative. This causes a strong glacial-interglacial contrast, which probably explains the 100 kyr signal in the spectrum of the Factor 1 score plot (Fig. 6). The overall negative scores in stages 2 and 3 suggest that, superimposed on the precession driven variability, low bottom water oxygen conditions prevailed during this period due to either an additional flux of organic matter, decreased mid-water ventilation, or a combination of both.

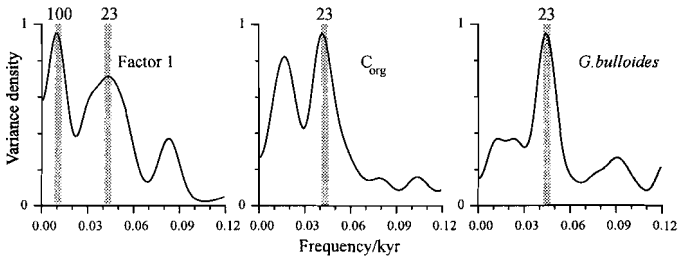

Figure 6 Spectra of the benthic Factor 1 score plot and the record of organic carbon and *G. bulloides*. Spectral estimates are based on a Parzen smoothing window with 100 lags and an interpolated time interval of 1 kyr, resulting in a bandwidth of 0.0185. Spectral densities are normalized and plotted on a linear scale.

4. Geochemical and planktonic foraminiferal proxies for paleo-productivity and OMZ intensity

4.1 Proxies for paleoproductivity

A potential proxy for past changes in surface water productivity is the organic carbon concentration in the sediment (Müller and Suess, 1979). The organic carbon (C_{org}) record of NIOP455 shows relatively high percentages around 115, 95 and 73 ka and overall higher values in isotopic stages 2 and 3 (Fig. 7a). A major C_{org} peak (~6%) is recorded around 45 ka.

Admixing of terrigenous organic matter and changes in organic carbon preservation resulting from fluctuations in sedimentation rates and bottom water oxygen content, however, may interfere with the surface water productivity related component of the organic carbon record. To assess the contribution of land-derived organic matter, we measured $\delta^{13}C_{org}$ and the C-N ratio of C_{org}. Figure 7b shows that C_{org} values are positively correlated with $\delta^{13}C_{org}$ values. Taking a $\delta^{13}C_{org}$ value of -26‰ for land-derived and of -20‰ for marine organic matter (Fontugne and Duplessy, 1986; Jasper and Gagosian, 1990), we can calculate that 80% of the organic matter has a marine origin, which increases to almost 100% in samples with maximum C_{org} values. This implies that a higher C_{org} content is associated with more marine produced organic matter and not with increased land-derived organic matter. C-N ratios vary between 10 and 18 (Fig. 7c), which is within the typical range for marine organic matter (Jasper and Gagosian, 1990; Calvert et al., 1995). If admixing of

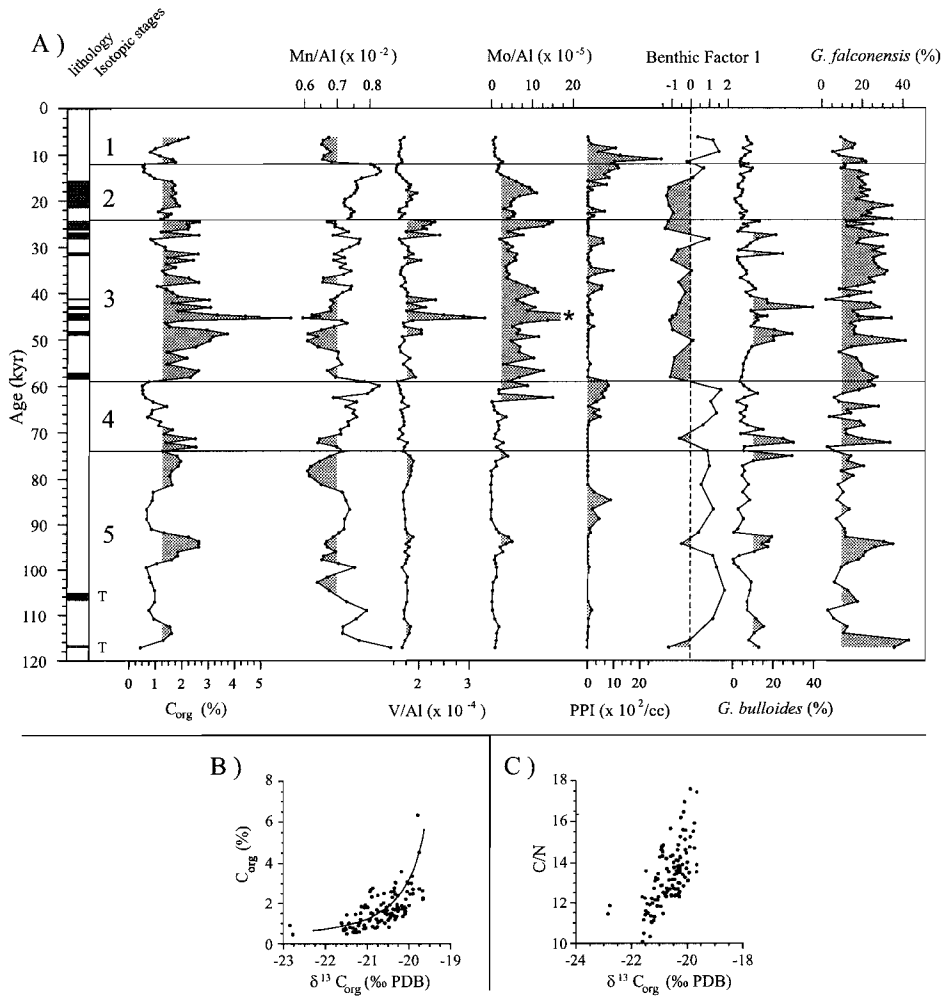

Figure 7 A) C_{org}, Mn/Al, V/Al, Mo/Al, pteropod index (PPI), scores for benthic Factor 1 and percentages of *G. bulloides* and *G. falconensis* plotted versus age. Cut-off value of ~70x10^{-5} in the Mo/Al curve is indicated. B) Relationship between $\delta^{13}C_{org}$ and C_{org} content. Curve indicates general trend, with increasing organic carbon content the $\delta^{13}C_{org}$ approaches marine values of ± -20‰ PDB. C) Relationship between C/N and $\delta^{13}C_{org}$. Apparent correlation between C/N and $\delta^{13}C_{org}$ is caused by decreasing relative importance of inorganic nitrogen on the C-N ratio with increasing organic matter content.

terrigenous organic matter played a significant role in shaping the C_{org} curves, C/N-ratios should increase towards terrestrial values (generally >30; Tyson, 1995), with increasing C_{org} contents. Figure 7c shows that high C-N ratios

correlate with less negative $\delta^{13}C_{org}$, which again indicates the absence of a significant contribution of land-derived organic matter in NIOP455 (Müller et al., 1994). Müller and Suess (1979) argued that sedimentation rates should increase 10 fold to cause a 2 fold increase in C_{org} values. This is significantly more than the 2.5 fold changes in the sedimentation rate of NIOP455 (Fig. 2). Fluctuations in sedimentation rates can, thus, be disregarded as a major factor in shaping the C_{org} record. All evidence together indicates that changes in the primarily marine produced organic matter are caused by changes in organic matter preservation linked to OMZ intensity and/or variations in surface water productivity. The effect of low bottom water oxygen levels on the preservation of organic matter is a heavily debated subject (e.g. Calvert and Pedersen, 1992; Pedersen et al., 1992; Dean et al., 1994). In a recent paper of Van der Weijden et al. (1999), it is shown that organic matter is enriched at places where the OMZ impinges the submarine topography. This enrichment is attributed to enhanced preservation of C_{org} under anoxic bottom water conditions. Downcore variations in $C_{org,}$ thus, include a preservational effect.

The planktonic foraminifer *Globigerina bulloides* is a eutrophic species proliferating in the productive upwelling area off Oman, and has been used as a foraminiferal proxy for summer productivity in the Arabian Sea (Prell et al, 1980; Prell, 1984; Cullen and Prell, 1984; Prell, 1993). In NIOP455, *G. bulloides* varies between 1 and 40 %, with high abundances occurring around 113, 93 ka and between 68-76, 42-52, and 24-32 ka (Fig. 7a). These peak abundances correlate with C_{org} maxima, which indicates that, although variations in $C_{org,}$ include a preservational effect, the C_{org} record of NIOP455 is primarily shaped by changes in surface water productivity.

Frequency analysis shows that the proxy records for surface water productivity (i.e. percentages C_{org} and *G. bulloides*) vary strongly in the 23 kyr frequency band (Fig. 6). This together with the observation that fluctuations in the C_{org} content and *G. bulloides* of NIOP455 are in phase with those recorded at the Murray Ridge (Reichart et al., 1997) and the Oman Margin (Murray and Prell, 1991; Clemens et al., 1991; Anderson and Prell, 1993) indicates that the surface water productivity changes recorded at site NIOP455 reflect precession driven changes in summer monsoon upwelling.

4.2 Proxies for OMZ intensity

Variations in past bottom water oxygen levels are recorded by the Pteropod Preservation Index (PPI) and redox sensitive elements such as Mo, V

and Mn. Past variations in OMZ intensity can be reconstructed by using a combination of these proxies.

Variations in the PPI (Fig. 7a) reflect changes in aragonite preservation, since pteropod shells are made up of aragonite. The present-day Aragonite Compensation Depth (ACD) in the northern Arabian Sea lies within the OMZ at about 500 m (Berger, 1977). This shallow position is caused by oxidation of organic matter in the watercolumn, which reduces the (solution) pH and carbonate saturation values due to CO_2 addition and the oxidation of ammonia to nitrate (Canfield and Raiswell, 1991). Hence, enhanced pteropod preservation probably reflects a substantial weakening of the OMZ, whereas the absence of pteropods is probably indicative of an intense OMZ. Pteropod preservation spikes in NIOP455 indicate that the ACD deepened from the present-day depth of 500 m to at least 1000 m during the deposition of these intervals. Major PPI peaks are present around 85 ka and at the end of isotopic stage 4 and 2 (58-66 ka and 8-14 ka, Fig. 7a). Several minor peaks are observed in isotopic stage 3.

Dysoxic conditions reduce Mn (IV) to its soluble Mn (II) state, resulting in depleted values of Mn/Al in the sediment. Surface sediments deposited within the present-day OMZ are depleted in Mn (Van der Weijden et al., 1999), because low oxygen conditions prevent the recycling of Mn oxides. Only when the surface sediments are oxygenated, can porewater Mn concentrations get sufficiently high to form Mn carbonate phases (Calvert et al., 1996). Because Mn carbonate is preserved during burial to anoxic conditions, Mn can be used as a paleoredox proxy. Low values of Mn/Al are recorded around 10, 25, between 36 and 58, and around 75, and 94 ka. Highest values are observed at the end of isotopic stages 2 and 4 (Fig. 7a).

Mo and V are transported to the sediments as reduced species and released from the sediments by oxidation. The accumulation of these metals is, therefore, favored by dysoxic bottom waters at the time of deposition (Ripley et al., 1990; Shaw et al., 1990; Breit and Wanty, 1991). During burial the sediment remains anoxic so the primary Mo and V redox signal remains preserved. Hence, Mo and V can be used as reliable proxies for the intensity of the OMZ. High Mo/Al values correlate with high V/Al values and characterize isotopic stages 2 and 3 (Fig. 7a). Minor V/Al and Mo/Al peaks are observed around 76, 95, and 114 ka.

Figure 7a shows that low Mn/Al values generally correspond with (moderately) high Mo/Al and V/Al values and vica versa. Highest Mo/Al and V/Al values are recorded in the laminated sediments of isotopic stages 2 and 3, which is in agreement with their deposition under low oxygen levels as

inferred from the absence of bioturbation. Pteropod preservation spikes correlate well with high Mn/Al values. Pteropods are absent in the laminated sediments. Combining the results of these proxies, thus, indicate that bottom water oxygen levels were periodically severely depressed at the site of NIOP455.

5. Comparison of benthic foraminiferal score plot with the proxy records for paleoproductivity and OMZ intensity

5.1 Variability on a precessional timescale

On a precessional time scale, high productivity conditions (indicated by high C_{org} content and high abundances of *G. bulloides*) correlate with low Mn/Al values, high Mo/Al and V/Al values, and zero PPI values. High PPI, and high Mn/Al values, on the other hand, are associated with a low C_{org} content and low abundances of *G. bulloides* (Fig. 7). This close correspondence between proxy data for paleoproductivity and OMZ intensity point to low (high) bottom water oxygen levels and a shallow (deep) ACD at times of high (low) productivity conditions. This relationship, furthermore, suggests that variations in OMZ intensity on a precessional time scale result from variations in mid-water oxygen consumption rates. Figure 7 also shows that high productivity conditions and low bottom water oxygen levels at site NIOP455 are associated with assemblage 2, whereas assemblage 1 dominates under low productivity conditions and high bottom water oxygen levels, which is in agreement with the (micro)habitat requirements of assemblage 1 and 2 as concluded earlier in this paper from a perusal of the benthic foraminiferal literature.

5.2 The dominance of assemblage 2 in glacial stages 2 and 3.

In the previous section we have shown that the benthic foraminiferal record varies on a precession time scale. This precession-scale variability is clear in the regular alternation of assemblages 1 and 2 during isotopic stages 4 and 5, but it is less evident in isotopic stages 2 and 3. The sustained flourishing of assemblage 2 in stages 2 and 3, together with overall high C_{org} and Mo/Al values (Fig. 7a), suggest that this period is marked by persistent eutrophic conditions with severe bottom water oxygen depletion. The exclusive

presence of laminated sediments in stages 2 and 3 is another argument for (periodically) severe bottom water depletion during this period.

However, *G. bulloides* is only intermittently present at high abundances in stages 2 and 3 (Fig. 7a). Hence, the sustained higher surface water productivity during these stages cannot be attributed to summer monsoon productivity alone. Moreover, surface water productivity linked to the summer monsoon has been shown to vary primarily on the precession band of orbital forcing (see also Reichart et al.,1997). We, therefore, suggest that a significant part of the phytoplankton productivity during stages 2 and 3 took place during the winter.

Today winter productivity is relatively high in the northern Arabian Sea due to the erosion of the summer nutricline by convective mixing to about 100 m (Banse, 1984; Bauer et al., 1991; Madhupratap et al., 1996). It is conceivable that deeper winter mixing, due to a colder winter monsoon during stages 2 and 3, stimulated winter production in the northern Arabian Sea, thereby contributing to an overall higher annual production during this period. Supportive evidence for a colder winter monsoon comes from Emeis et al. (1994), who concluded from a SST record off Oman that the winter (NE) monsoon was more effective in cooling the Arabian Sea at glacial times.

Increased winter production during glacial stages 2 and 3 may also be inferred from the overall high percentages of the planktonic foraminiferal species *Globigerina falconensis* during this period (Fig. 7a). Cullen and Prell (1984) and Brock et al. (1992) observed maximum abundances of this species in surface sediment samples from the northern Arabian Sea, which they correlated with a greater seasonality in this region, although, without explaining the cause of this relationship. We suggest that the correlation of *G. falconensis* to seasonality is related to winter productivity resulting from convective mixing, which today is most effective in the nothernmost Arabian Sea (Madhupratap et al., 1996). If the flourishing of *G. falconensis* in the northern sector of the Arabian Sea is, indeed, related to winter productivity, then the record of this species in NIOP455 would suggest increased winter production during stages 2 and 3. Within this context it is significant, that in one of the very few tow and trap studies in which *G. falconensis* is distinguished from *G. bulloides*, the former species is listed as a winter species (tow data from the cool subtropical North Atlantic - Be et al., 1971). Hermelin and Shimmield (1995) explained the glacial-interglacial variability in a deep marine benthic foraminiferal record from the western Arabian Sea by changes in intermediate and deep water chemistry and nutrient input to the ocean. Increased glacial wind strength could have enriched the surface water

with wind borne nutrients resulting in increased surface water productivity. In view of the results of NIOP455, increased winter (NE) monsoon productivity may provide an alternative explanation for the observed glacial-interglacial variability in the deep marine benthic foraminiferal record, discussed by Hermelin and Shimmield (1995).

The specific conditions associated with stages 2 and 3 are reflected in the benthic foraminifers by the dominance of assemblage 2 and at the species level by the overall high percentages of *R. semiinvoluta* (Fig. 4). Living *R. semiinvoluta* shows highest abundances near the base of the OMZ (Jannink et al., 1998). One explanation for this is that this species is adapted to rapid changes in bottom water oxygen content, which may occur at the base of the OMZ on a seasonal or interannual basis, or even on a longer time scale. The rapid variations in C_{org}, Mo, V, pteropod preservation and *G. falconensis* in stages 2 and 3 (Fig. 7a), suggest rapid fluctuations in winter surface water productivity and associated bottom water oxygen content, which may have favoured *R. semiinvoluta* during this period. If *R. semiinvoluta* is particularly favoured by increased variability in bottom water oxygen content during glacial stages 2 and 3, then longer time series in the Arabian Sea may show increased abundances of this species in older glacial stages as well.

6. Conclusions

The benthic foraminiferal record in the northern Arabian Sea core NIOP455 contains two distinctly different assemblages. Assemblage 2 consists of *B. exilis, R. semiinvoluta, B. alata, B. pygmaea, Globobulimina* spp., and *Bulimina* sp.1, species which are known from other studies to flourish under high C_{org} flux and low bottom water oxygen conditions. Assemblage 1, characterised by *B. striata, G. lobatula, C. oolina, Monothalameous* spp., *S. bulloides, C. ungerianus, H. balthica*, and *H. elegans*, is intolerant to bottom water oxygen depletion and dominates during periods of low C_{org} flux.

The 120 kyr benthic foraminiferal- and paleoproductivity records are strongly shaped by changes in summer monsoon productivity, with summer monsoon productivity maxima being associated with maxima in OMZ intensity and a dominance of assemblage 2, whereas summer productivity minima correspond with a weak OMZ and a dominance of assemblage 1. The sustained flourishing of assemblage 2 during isotopic stages 2 and 3 is suggested to be the result of an overall higher winter surface water

productivity during this period, which is superimposed on precession driven changes in summer surface water productivity.

Acknowledgements.

This research was carried out in a joint Dutch-Pakistan marine geosciences program, as part of the Netherlands Indian Ocean Program 1992-1993. We thank the director and our colleagues A.R. Tabrez and A.A. Khan of the National Institute of Oceanography, Karachi, for their co-operation. Chief scientist of the cruise was W.J.M. van der Linden. We thank the crew and technicians of the R.V. Tyro for their professional help in collecting the material. Thanks are also due to L.J. Lourens and H.J. Visser for analytical support, and G. Nobbe, A. van Dijk, H. de Waard, G.J. van het Veld, and G. Ittman for laboratory support. The reviews by J.O.R Hermelin and an anonymous referee are highly appreciated. This research was funded by the Netherlands Organization for Scientific Research (NWO). This is publication 980302 of the Netherlands School of Sedimentary Geology (NSG).

Chapter 3
Sub-orbital OMZ variations

Multiple monsoon-controlled breakdown of oxygen-minimum conditions during the past 30,000 years documented in laminated sediments off Pakistan.

Abstract

Late Holocene laminated sediments from a core transect centred in the oxygen minimum zone (OMZ) impinging at the continental slope off Pakistan indicate stable oxygen minimum conditions for the past 7000 calendar years. High SW-monsoon-controlled biological productivity and enhanced organic matter preservation during this period is reflected in high contents of total organic carbon (TOC) and redox-sensitive elements (Ni, V), as well as by a low-diversity, high-abundance benthic foraminiferal *Buliminacea*-association and high abundance of the planktic species *Globigerina bulloides* indicative of upwelling conditions. Surface water productivity was strongest during SW monsoon maxima. Stable OMZ conditions (reflected by laminated sediments) were found also during warm interstadial events (Preboreal, Bølling/Allerød , and Dansgaard-Oeschger events), as well as during the peak glacial times (17-22.5 ka, all ages in calendar years). Sediment mass accumulation rates were at a maximum during the Preboreal and Younger Dryas periods due to strong riverine input and mobilization of fine-grained sediment coinciding with rapid deglacial sea-level rise, whereas eolian input generally decreased from glacial to interglacial times. In contrast, the occurrence of bioturbated intervals from 7-10.5 ka (early Holocene), in the Younger Dryas (11.7-13 ka), from 15-17 ka (Heinrich event 1), and from 22.5-25 ka (Heinrich event 2) suggest completely different conditions of oxygen-rich bottom waters, extremely low mass and organic carbon accumulation rates, a high-diversity benthic fauna, all indicating lowered surface-water productivity. During these intervals the OMZ was very poorly developed or absent and a sharp fall of the aragonite compensation depth favoured the preservation of pteropods. The abundance of lithogenic proxies suggests aridity and wind transport by northwesterly or northeasterly winds during these periods coinciding with the North Atlantic Heinrich events and dust peaks in

Von Rad, U., Schulz, H., Riech, V., Den Dulk, M., Berner, U., Sirocko, F., Paleogeograpghy, Paleoclimatology, Paleoecology 152 (1999) 129-161.

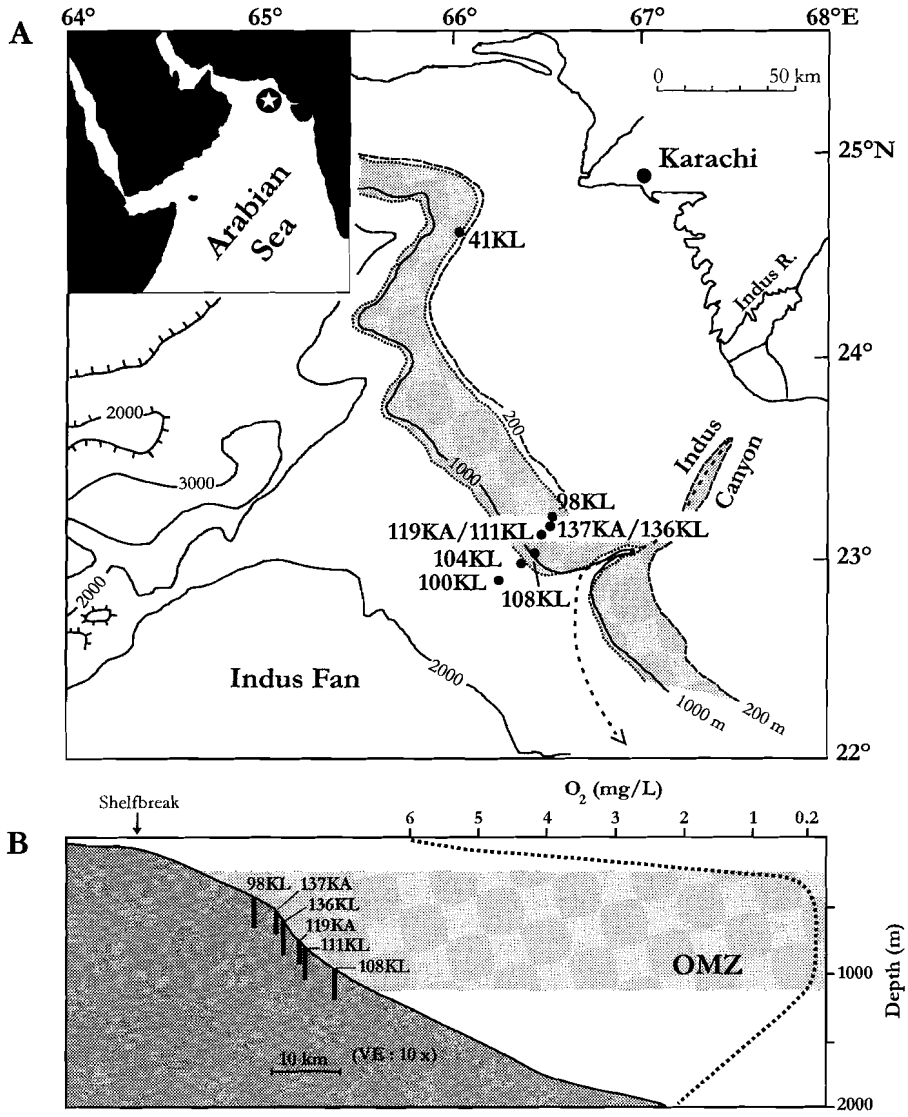

Figure 1 A. Area of investigation off Pakistan with location of cores off the Indus delta discussed in this paper. Inset shows Arabian Sea and SO90-survey area Stippled area indicates oxygen-minimum zone (OMZ) impinging on the continental slope. B. Profile across the Indus slope with location of OMZ cores (see Fig. 2) and oxygen content within the water column.

the Tibetan Loess records. The correlation of the monsoon-driven OMZ variability in the Arabian Sea with the rapid climatic fluctuations in the high northern latitudes suggests a close coupling between the climates of the high and low latitudes at a global scale.

1. Introduction

High eolian and fluvial input from the surrounding continents, as well as monsoon-induced upwelling of nutrient-rich sub-surface waters make the Arabian Sea one of the most productive oceanic areas in the world. Satellite data of the chlorophyll (pigment) distribution in the surface waters (Banse, 1987) and time series of particle fluxes from sediment traps suggest that surface water productivity is strongest in the north-western Arabian Sea linked with the conspicuous coastal and open ocean upwelling cells off Oman (among others, Prell et al., 1990). Sea surface cooling leads to convection processes and injection of nutrients into the subsurface waters; this leads to high biological productivity in the waters of the North-eastern Arabian Sea that continues after the upwelling season off Oman into the winter monsoon (Madhupratap et al., 1996).

Today, an expanded, persistent oxygen minimum zone (OMZ) can be observed in the entire northern Arabian Sea at intermediate water depths. In the north-eastern Arabian Sea (Fig. 1A) a marked OMZ impinges on the continental slope between 250 and 1000 m water depth (Fig. 1B; Wyrtki, 1973;) resulting in the preservation of mm-scale laminated (varved) sediments (Von Stackelberg, 1972; Schulz et al., 1996; Von Rad et al., in press). A high-salinity tongue (derived from the Persian Gulf Outflow Water) at 200-350 m water depth forms the top of the OMZ and contributes to the stratification of the OMZ waters by preventing the vertical mixing of surface water with the oxygen-poor (<1ml/L) Indian Ocean Central Water (Schulz et al., 1996; Reichart et al., 1998). Although low-oxygen conditions in the Arabian Basin at intermediate depths are also influenced by the lateral advection of oxygen-depleted waters from the south-east and from the Persian Gulf Water (Olson et al., 1993), there is general agreement that the intensity of the OMZ conditions in the Arabian Sea is mainly controlled by surface water productivity and hence influenced by monsoonal climate variations, responding to the intensity of northern hemisphere summer insolation (Altabet et al., 1995; Reichart et al., 1997).

The OMZ off the Indus delta (Fig. 1B) is characterised by extremely low

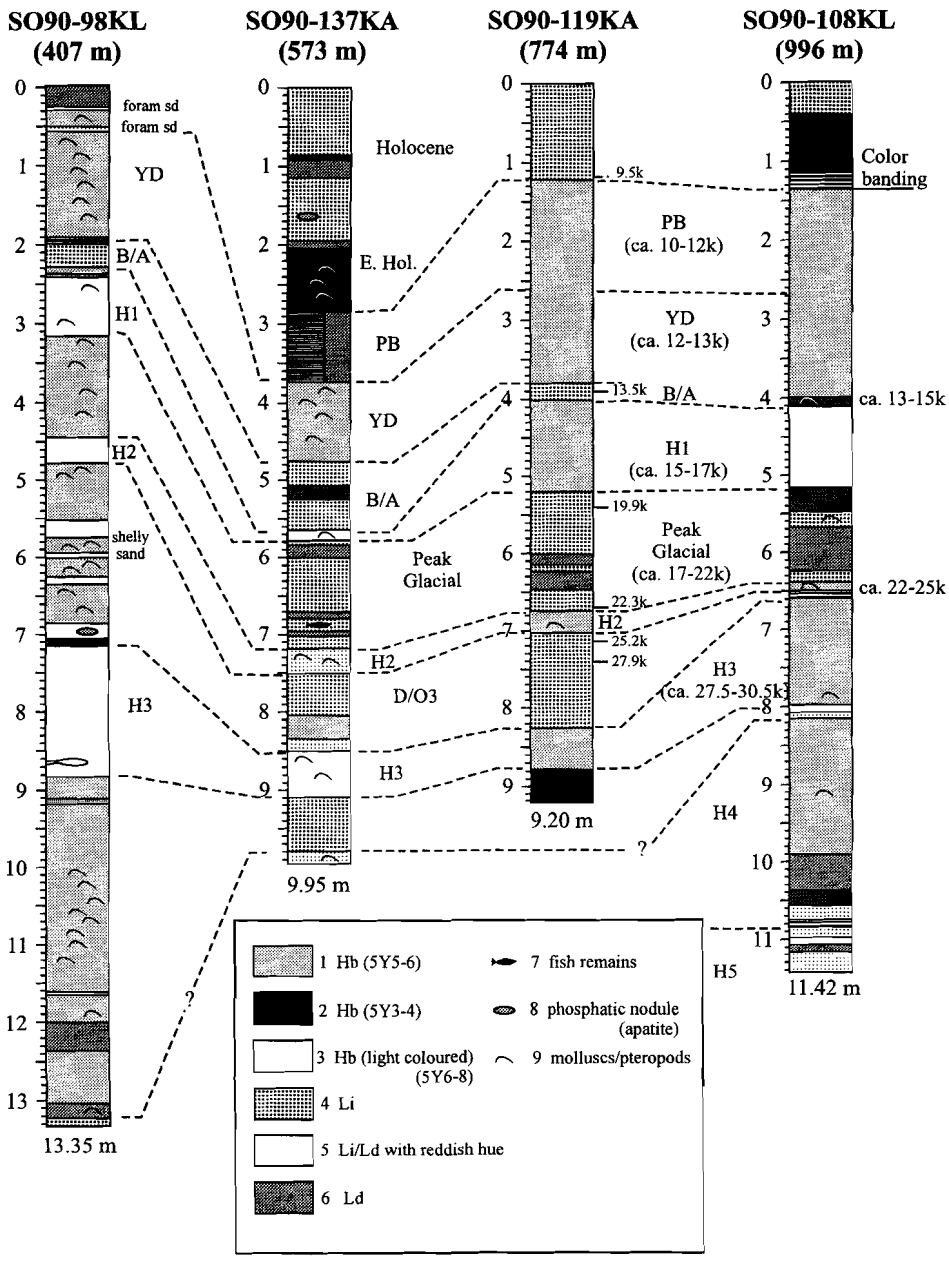
SO90-98KL
(407 m)
SO90-137KA
(573 m)
SO90-119KA
(774 m)
SO90-108KL
(996 m)
foram sd
foram sd
YD
B/A
H1
H2
shelly
sand
H3
13.35 m
Holocene
E. Hol.
PB
YD
B/A
Peak
Glacial
H2
D/O3
H3
9.95 m
9.5k
PB
(ca. 10-12k)
YD
(ca. 12-13k)
13.5k
B/A
H1
(ca. 15-17k)
19.9k
Peak
Glacial
(ca. 17-22k)
22.3k
H2
25.2k
27.9k
H3
(ca. 27.5-30.5k)
H4
9.20 m
?
Color
banding
ca. 13-15k
ca. 22-25k
H5
11.42 m
1 Hb (5Y5-6)
2 Hb (5Y3-4)
3 Hb (light coloured)
(5Y6-8)
4 Li
5 Li/Ld with reddish hue
6 Ld
7 fish remains
8 phosphatic nodule
(apatite)
9 molluscs/pteropods

Figure 2 Lithofacies, chronostratigraphy and correlation of four selected cores from the OMZ off the Indus delta (400-996 m water depth; see also Fig. 1B). Legend of lithofacies: *Li,Ld* = indistinctly, distinctly laminated; *Hb* = homogeneous bioturbated. Stratigraphy: *YD* = Younger Dryas; *B/A* = Bølling-Allerød; *D/O* = Dansgaard-Oeschger event; *H1...4* = Heinrich events; *PB* = Preboreal. Chronostratigraphy from ^{14}C dates, oxygen isotope stratigraphy and colour stratigraphy. Note that the Heinrich 1 (H1) event (duration about 1.5 ka) is represented in core 119KA by 100 cm, and in 108KL by 120 cm, whereas in 137KA it is condensed to 20 cm. Cores 119KA and the sister core 111KL are ^{14}C dated. Some ^{14}C dates from 111KL (spliced into 119KA) are shown (for all dates see Fig. 3).

oxygen contents in the bottom water. The surface sediments from box cores at the same station are devoid of bioturbation features and benthic macrofauna, although benthic foraminifera are present. Piston and kasten (10m-long, 30x30 cm-diameter box) cores show that during the late Holocene only laminated sediments were deposited along the continental slopes of Pakistan and western India indicating stable oxygen minimum conditions at the sea floor for the past 7000 years as observed today (Von Rad et al., 1995, Schulz et al., 1996, Von Rad et al, in press).

In contrast, the pre-Holocene sediments are characterised by frequent alternations of dark olive-grey, organic-rich, laminated intervals and light-coloured, carbonate-rich, bioturbated (homogeneous) sections (Von Rad et al., 1995). This alternating facies pattern can be correlated over a wide range of water depths (Fig. 2) and suggests strong fluctuations of the OMZ and monsoonal productivity during the last glacial/interglacial cycle.

The intensity of the Indian monsoon system varied strongly on a precessional (23 ka) variability (Clemens et al., 1991; Reichart et al., 1997). Recently, Schubert et al. (1998), using the record of core SO90-94KL (about 100 km seaward of core 137 KA), demonstrated precessional productivity cycles based on dinosterol, alkenone and total chlorin concentration maxima coinciding with TOC maxima. Higher-resolution paleoclimatic records have emphasised the general instability of Late Pleistocene climate in timescales of a few millenia, centuries or even decades, e.g. the warm interstadials or Dansgaard-Oeschger events [1] (Johnsen et al., 1992; Dansgaard et al., 1993) and cool stadials or Heinrich events (Broecker et al., 1992; Grousset et al., 1993; Bond et al., 1993). Sirocko et al. (1996) and Schulz et al (1998) presented

[1] Although Dansgaard-Oeschger events and Heinrich Layers (or events) were originally defined only for the Greenland ice cores and North Atlantic Ocean sediments, we discovered in the Arabian Sea the exact time equivalents of these events (without inferring the same origin). In this paper we use these terms chronostratigraphically in the broader sense without adding "time equivalents of..." in each case.

evidence for a relationship between low-latitude monsoonal climatic variability and the rapid temperature fluctuations seen in the Greenland ice record (GISP-2; Dansgaard et al., 1993). Sediment cores from intermediate water depths off Pakistan (e.g., cores 111KL, 136 KL; Figs. 1; 3) reveal a distinct pattern of laminated, organic carbon-rich intervals reflecting strong monsoonal productivity and OMZ intensity that can be correlated to the mild interstadial climatic events in the North Atlantic region. These dark-coloured, indistinctly to distinctly laminated intervals appear as equivalents to the Greenland Dansgaard-Oeschger interstadials.

In contrast, periods of lowered south-west monsoonal intensity, indicated by bioturbated, organic carbon-poor intervals, are associated with periods of high-latitude atmospheric cooling and the injection of meltwater into the surface waters of the North Atlantic, resulting in low productivity and carbonate dissolution. The light-coloured, bioturbated intervals of the Arabian Sea cores correspond to periods of extremely light $\delta^{18}O$ ratios in the GISP2 ice core indicating cool air temperatures over Greenland and the northern North Atlantic. This applies particularly for the massive intervals of bioturbated, $CaCO_3$- and pteropod-rich sediments which can be correlated to the Younger Dryas cool period at 13-11.7 ka B.P. and to the Heinrich Events H1 to H3 in the northern North Atlantic. In order to study the origin of the laminated and bioturbated slope sediments and the history of the OMZ during the past 30,000 years in detail, we selected a high-sedimentation rate 10 m-Kasten core SO90-137KA (23°07.3′N, 66° 29.8′E, 573 m water depth) from the centre of the OMZ (Fig. 1B), located about 140 km north-west of the Indus delta and 30 km north-west of the conspicuous Indus Submarine Canyon. Core 137KA is situated at the "upper slope scarp", a distinct increase in slope gradient between 500 and 800m, where *Parasound* records show a hemipelagic drape by postglacial, well-layered slope deposits (Von Rad and Tahir, 1997).

2. Methods

Sediment samples are generally spaced at 10-cm intervals representing an average time resolution of about 300 years. After freeze-drying, we investigated bulk samples for $CaCO_3$-content, total organic carbon (TOC), X-ray fluorescence (XRF) and X-ray diffraction analysis (XRD; aragonite, quartz), as well as for studies on the coarse fraction (> 63 μm). $CaCO_3$ was determined from the CaO values of the XRF, and from the difference of total

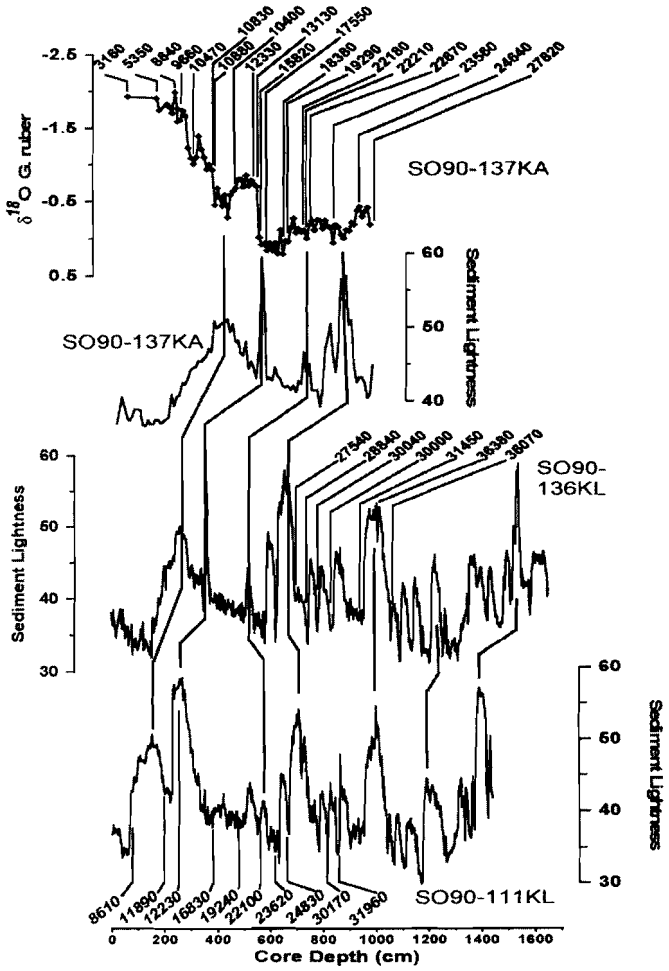

Figure 3 Correlation of OMZ core SO90-137KA with core SO90-136KL (same position, 568 m w.d.) and nearby core SO90-111KL (775 m w.d.), based on oxygen isotopes or sediment lightness (*MINOLTA*) records (low values indicate laminated, dark-coloured, TOC-rich, suboxic facies, values >50 indicate light-coloured, bioturbated intervals with carbonate-rich, oxidised sediments). Numbers depict uncorrected AMS and conventional radiocarbon ages for comparison.

carbon minus TOC, measured by the LECO carbon combustion method using a LECO CS 344 instrument. The inorganic geochemical composition of the sediments was analysed by standard XRF- methods. All bulk XRF values are re-calculated on a carbonate-free basis or standardised to Al to eliminate

varying dilution effects by the biogenic fraction, or correct for the contribution of the terrigenous fraction, respectively.

Quartz, aragonite, and dolomite contents were quantified using a program combining XRD and XRF data (Meyer and Klosa, 1997). From the coarse silt fraction (20-63 μm) we determined semi-quantitatively quartz, feldspar and chlorite by measuring peak heights or integral intensities.

Silt and clay fractions (< 63μm) were determined after H_2O_2 and acetic acid treatment. Subsamples of the carbonate-free lithogenic fraction were wet-sieved to obtain the <20 μm fraction for XRD analyses, then separated by pipette analysis into three size fractions <2 μm, 2-6.3 μm and 6.3-20 μm.

The <2 μm and <20 μm fractions were analysed by XRD. Aragonite and quartz contents were studied on the <20 μm fraction in 52 samples, grain size of lithogenic material <63 μm in 45 samples.

Coarse fraction analyses of the lithogenic and biogenic contents were generally made on subfractions of the sand fraction obtained by careful washing using a 63 μm -screen. Quantitative analyses of benthic and planktic foraminifera were performed on the 150-595 μm fraction of 30 samples. The concentration of pteropod debris was counted from the 250-315 μm fraction. These samples were split by an Otto microsplitter into aliquots containing about 250 specimens. Benthic foraminifera were mounted into a Chapman-slide and subsequently identified. The census data have been subjected to a principal component analysis (PCA), selecting species that show abundance higher than 5% carrying statistically meaningful information.

Sediment colour was quantified using a hand-held *MINOLTA* chromameter CR-2002 with an opening of about 1 cm. Generally, low sediment lightness values correspond to dark, organic-rich and frequently indistinctly to distinctly laminated intervals. High sediment lightness reflects light-coloured and frequently bioturbated intervals that contain much less organic carbon (% of dry weight) and much more $CaCO_3$. Curvilinear regression techniques show that there is a close correlation (correlation coefficients >0.9) between sediment lightness and the percentage of TOC.

In a semi-quantitative way the degree of bioturbation between the end members "distinctly laminated" and completely homogenised (bioturbated) intervals can be estimated from our X-radiographs (Fig. 4), as described for the Santa Barbara Basin sediments (Behl and Kennett, 1996). We used the following "bioturbation scale" (see Fig. 6): (1) distinctly laminated sediments (Ld) with continuous, <1 μm thick laminations, suggesting an "anaerobic" environment (< ca. 0.2 ml O_2/L; all values from Savdra et al., 1984; Wetzel, 1991); (2) indistinctly laminated intervals (Li) with discontinuous, diffuse or

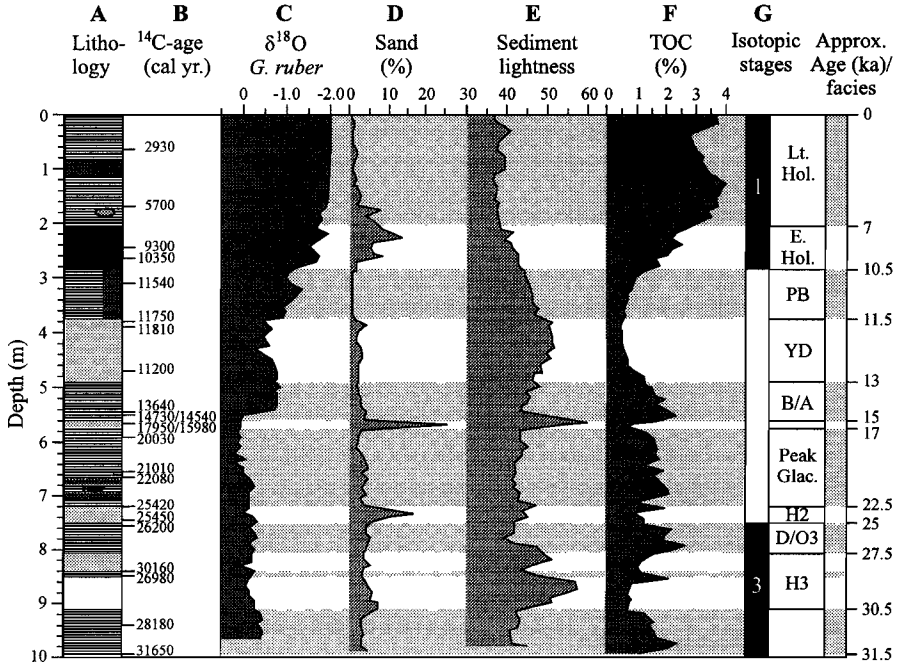

Figure 4 A: Lithofacies profile of core 137KA showing stratigraphy (abbreviations in Fig. 2). Note frequent alternations of laminated (dashed pattern) and bioturbated sediment intervals. B: ^{14}C dates converted into calendar years (for age model see Table 1). C: δ^{18}O G ruber. D: sand content (% >63 μm). E: sediment lightness (Minolta chromameter; low values = dark sediment). F: TOC . G: oxygen isotope stages and approximate age (ka) (partly after Bølling/Allerød Von Rad et al., 1995).

irregular laminations suggesting an anaerobic to dysaerobic environment (ca. 0.2-0.5 ml O_2/L); (3) alternating bands of faint, diffuse lamination surrounded by homogenised sediments, indicating a "dysaerobic environment" (ca. 0.5-2 ml O_2/L); and (4) completely homogenised, bioturbated sediments (Hb) without any primary fabrics preserved ("aerobic environment" > ca. 2ml O_2/L).

We obtained a high-resolution planktonic foraminiferal δ^{18}O record of *Globigerinoides ruber (white)* for cores 137KA based on 10 cm sampling intervals. For oxygen isotope-stratigraphy, 20-25 specimens of the near-surface dwelling planktic foraminiferal species *Globigerinoides ruber (white)* were picked from the 315-500 μm -fraction. The preparation of the foraminiferal calcite was performed at Kiel University with the Carbo-Kiel automated preparation system, linked to a Finnegan MAT 251 mass spectrometer that

allows subsequent measurements of stable carbon and oxygen isotopes. Bulk organic matter was prepared at BGR for carbon isotope measurements using the methods described in Schoell (1984) and subsequent analyses using a Finnegan MAT 251 mass spectrometer at BGR, Hannover. Isotope ratios of oxygen and carbon are reported in δ-notation relative to the international Pee Dee Belemnite (PDB) standard. In the uppermost section only a few samples could be extracted for isotope stratigraphy due to dissolution effects on the foraminiferal fauna. Since the core was sampled immediately on board, artificial dissolution can be excluded. However, based on porewater profiles and XRF data, core 137KA shows now significant differences to the other cores, where planktonic foraminifera are frequent and exceptionally well preserved through their entire core length (e.g., the 8 m-long Holocene $\delta^{18}O$ profile of core 43KL, Schulz et al., 1996).

Dry bulk sediment densities were determined using large sample volumes (ca. 30 cm^3). Mass accumulation rates of organic carbon (MAR C_{org}) bulk sediment and of individual sediment components were calculated from the equation of Bordovsky (1965) and after Thiede et al. (1982).

23 samples were selected for radiocarbon dating. Ten conventional ^{14}C-ages on the coarse fraction (> 63 μm) were obtained using 15 cm^3 miniature counters of the radiocarbon laboratory of the Geowissenschaftliche Gemeinschaftsaufgaben (GGA), Hannover. Thirteen AMS-^{14}C ages on monospecific planktic foraminiferal calcite were provided by the Leibniz-Labor für Altersbestimmung und Isotopenforschung, Universität Kiel (Table 1). Conventional radiocarbon ages (T1/2=5568 years) were corrected for a local ocean reservoir effect of -640 years (Schulz et al., 1998) and then converted to a calendar timescale following Stuiver and Braziunas (1993) and Bard et al. (1997). These ages were compared with 17 radiocarbon age data from nearby cores 136 KL and 111 KL and with the stratigraphic evidence from the $\delta^{18}O$ record (Fig. 3). Between the age points sediment ages were interpolated assuming constant sedimentation rates. All calculations and age assignments are based on a calendar timescale and are expressed as calendar years before present (cal. yr BP).

Table 1
C-14 age data of Core SO90-137KA with corrections (see text).

Lab. Nr.	Depth (cm)	Facies	Species	^{14}C-age (yr BP)	1σ (yr)	1σ (yr)	Cal. age (yr BP)
Hv19651	60-67	lam	C.F.	3,160	+160	-160	2,930
KIA128	173-177	lam	G.s.	5,350	+50	-50	5,700
KIA129	243-247	biot	G.r.	8,660	+60	-60	9,300
Hv9652:	260-267	biot	C.F.	9,660	+255	-255	10,350
KIA2481	310-320	lam	G.s.	10,470	+50	-50	11,540
KIA130	383-387	biot	G.r.	10,830	+110	-110	11,750
Hv19653	385-395	biot	C.F.	10,880	+250	-250	11,810
Hv19654	465-472	biot	C.F.	10,400	+230	-230	11,200
Hv19525	540-547	lam	G.F	12,330	+290	-290	13,640
KIA131	550-555	lam	G.r.	13,200	+150	-150	14,730
KIA132	550-555	lam	C.s	13,050	+90	-80	14,540
KIA133	563-567	biot	G.r.	15,820	+110	-110	17,950
KIA134	563-567	biot	Pt.	14,210	+160	-150	15,980
KIA135	585 590	lam	G.r.	17,550	+230	-230	20,030
Hv19655	650-657	lam	C.F.	18,380	+540	-540	21,010
KIA136	663-667	lam	G.r.	19,290	+290	-280	22,080
KIA137	723-727	biot	G.r.	22,180	+430	-410	25,420
Hv19656	740-747	biot	C.F.	22,210	+540	-540	25,450
KIA2958	753-757	biot/lam	G.s.	22,870	+220	-210	26,200
KIA138	843-847	lam	G.r.	26,440	+700	-650	30,160
Hv 19526	845-850	lam	C.F.	23,560	+1460	-1230	26,980
Hv19657	945 952	lam	C.F.	24,640	+1060	-890	28,180
Hv 19868	990-995	biot	C.F.	27,820	+640	-640	31,650

Calibrated (calendar) ages calculated with a reservoir age of 640 years, corrected after Bard et al. (1987) and Stuiver and Braziunas (1993). Hv numbers refer to conventional ^{14}C dates based on coarse fractions (C.F.) (biogenic debris); all other dates are AMS^{14}C dates based on *Globigerina sacculifer* (G.s.), *Gobigerina ruber* (G.r.), or pteropods (Pt.).

3. Stratigraphy

Based on $\delta^{18}O$ stratigraphy, radiocarbon chronology and on the correlations outlined in Figures 2 and 3, we suggest that core SO90-137KA represents a complete sediment record spanning the past 30,000 - 32,000 years and extending to Marine Isotope Stage 3 (Figs. 3,4). Only the uppermost laminated section of the last 500-1000 years may be disturbed or even partly missing due to the coring process and handling of the 10-m long kasten corer on deck (we used box core 112KG from the same locality for the near-surface sediments). Our age model for core 137KA includes 15 stratigraphic age points

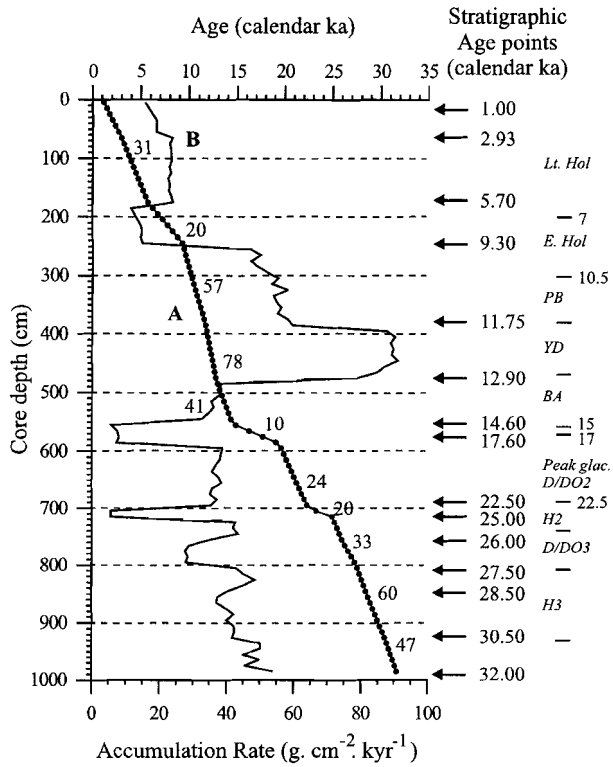

Figure 5 Core depth versus age (in calendar years) relationship of core 137KA (A) and (B) mass accumulation rate (bulk sediment . $cm^{-2}.kyr^{-1}$) plotted versus age (calendar ka). Linear sedimentation rates (cm/ka) are attached to curve A.

for the last 32,000 years including an assumed age of 1000 years for the core top (Table 1, Figs. 2, 5). In Figure 3 we correlate the lithostratigraphy and radiocarbon age data of core SO90-137KA with those of core SO90-136KL (from the same position) and nearby core SO90-111KL (also from the OMZ). Confirmed by these radiocarbon data, the upper section of core 137KA between 0 and 570 cm bsf (below sea floor) represents the Holocene, Younger Dryas and Bølling/Allerød chronozones (Figs. 2,3,4). The interval of Termination I of this high-sedimentation rate core shows significant high-frequency variability similar to the series of monsoonal events previously shown in deep-sea core SO42-74KL from the south-western Arabian Sea (Sirocko et al., 1993). After the Younger Dryas Period we note abrupt deglacial jumps, generally with decreasing shifts towards lighter values between 395 cm and 335 cm bsf with a small intermittent minimum centred at

365 cm, from 305 cm to 275 cm, and from 255 to 245 cm bsf (Fig. 4C). Prior to this succession of late deglacial events we note a broad maximum in $\delta^{18}O$ between 395 and 455 cm bsf giving clear evidence for the Younger Dryas climatic period in the northern Indian Ocean. This interval is preceded by a 90 cm thick interval of distinctly to indistinctly laminated sediment with again slightly lighter ratios representing the Bølling/Allerød climatic interval in the Arabian Sea between 14,600 and about 12,900 cal yr BP. Termination IA is represented in core 137KA with less fine structure coinciding with a narrow severely bioturbated interval which is lithologically in sharp contact with the under- and overlying laminated strata.

We observe dark-coloured, indistinctly to distinctly laminated sediments (documenting a strong OMZ) during five intervals: (1) the late Holocene (the last 7,000 years), (2) the Preboreal period (11.7-10.5 ka) (3) between the abrupt deglacial warming events of Termination 1A (midpoint age: 16.5 ka) and 1B (ca. 11.7 ka BP), suggesting the presence of an equivalent Bølling/Allerød climatic interval (13-15 ka) in the Arabian Sea (Figs. 3, 4), (4) during the peak glacial period (17 - 22.5 ka) and (5) from 25 to 27.5 ka BP. In contrast, light-coloured, bioturbated intervals occur in the early Holocene from 7-10.5 ka, during the Younger Dryas (11.7 to 13 ka; Fig. 4), at the equivalent of Heinrich event H1 from 15 to 17 ka (Fig. 7B), from 22.5 to 25 ka (H2) and from 27.5 to 30.5 ka, at the base of the isotopic stage 2/3 boundary. In core 137KA sedimentation rates of the laminated intervals range between 31 cm/kyr (Late Holocene) and 57 cm/kyr (Preboreal; Fig. 5). For the bioturbated intervals sedimentation rates range from 10 cm/kyr (H1) to 78 cm/kyr (Younger Dryas; Fig. 5). Total mass accumulation rates show maxima during the Younger Dryas (90 $g.cm^{-2}.kyr^{-1}$) and minimum values (5-7 $g.\ cm^{-2}.kyr^{-1}$) during the H1 and H2 events (Fig. 5). However, along the continental margin the thickness of the individual bioturbated intervals (e.g., the light-coloured, bioturbated interval of the H1 interval) is highly variable: this interval is only 12 cm in core 137KA, whereas in nearby core 119KA, the same unit is about 120 cm thick (Fig. 2). We suggest that the bioturbated sediments may be winnowed by strong bottom currents during periods of a weakened OMZ. Hence accumulation rates of bulk sediment and individual components are highly variable from core to core for the bioturbated intervals. However, our correlations and stratigraphic data from more than 30 cores along the Pakistani continental margin (including the cores presented in Figs 2 and 3) revealed a spatially and temporally consistent facies pattern of alternations between bioturbated and laminated intervals (Schulz et al., unpublished data). Facies and paleoclimatic evolution during seven time slices from the record of

core 137KA covering the past 30,000 yr (partly after Sirocko et al., 1993; 1996; see also Fig. 13). The suggested ages of the major lithostratigraphic units (Fig. 2; Table 3) are based on our stratigraphic model, derived from isotope stratigraphies of many SO90 cores from the Indus slope and the slope west of Karachi , correlated with core SO42-74KL (Sirocko et al., 1993).

4. Lithofacies and Biofacies

The light-coloured, bioturbated intervals of core 137KA (Fig. 4) commonly coincide with coarser-grained pteropod layers and contain less TOC and more biogenic sand and terrigenous silt (Figs. 4, 7). The main sediment components are biogenic carbonate and clay- to fine silt-sized terrigenous detritus. Skeletal opal is extremely rare in our sediments, although diatoms and radiolarians are present (especially in the near-surface sediments), and dinoflagellates are abundant in plankton tows from the surface waters (unpublished data by H. Oberhänsli). Hence most biogenic opal is being dissolved while settling through the water column or on the seafloor.

In general, the change from laminated to bioturbated facies, i.e. from anoxic to oxic bottom water conditions, is rather abrupt (A. Wetzel, personal communication, 1997; see also "bioturbation index" in Fig. 6A). During the oxic intervals the content of bottom water oxygen, documented by *Phycosiphon, Planolites* and other large "bio-deformational structures" (with indistinct outlines and features which destroy pre-existing structures), must have been rather high. It is noteworthy that the laminated intervals between 4.8 and 7.1 m bsf contain large individual burrows (2-6 mm diameter), probably from deep-burrowing crustaceans. The laminated intervals below 7.5 m bsf contain many individual, large "bio-deformational structures". Individual *Thalassinoides*-type large burrows extend down from the bioturbated intervals ("piping down" structures) into the laminated facies for up to 45 cm, whereas normally the penetration depth of burrows (mainly dependant on oxygenation and benthic food availability) down into the laminated facies is only about 3-5 cm (A. Wetzel, 1991 and personal communication, 1997).

Compared with the varved sequences of the sediments from the Karachi slope (Von Rad et al., in press), the individual laminae in core 137KA are very thin and indistinct (bioturbation index 2-3). This is due to a comparatively lower sedimentation rate (generally 20-50 cm/kyr; Fig. 5) than at the Karachi slope (>60 cm/kyr) leading to very fine-scale micro-bioturbation and to

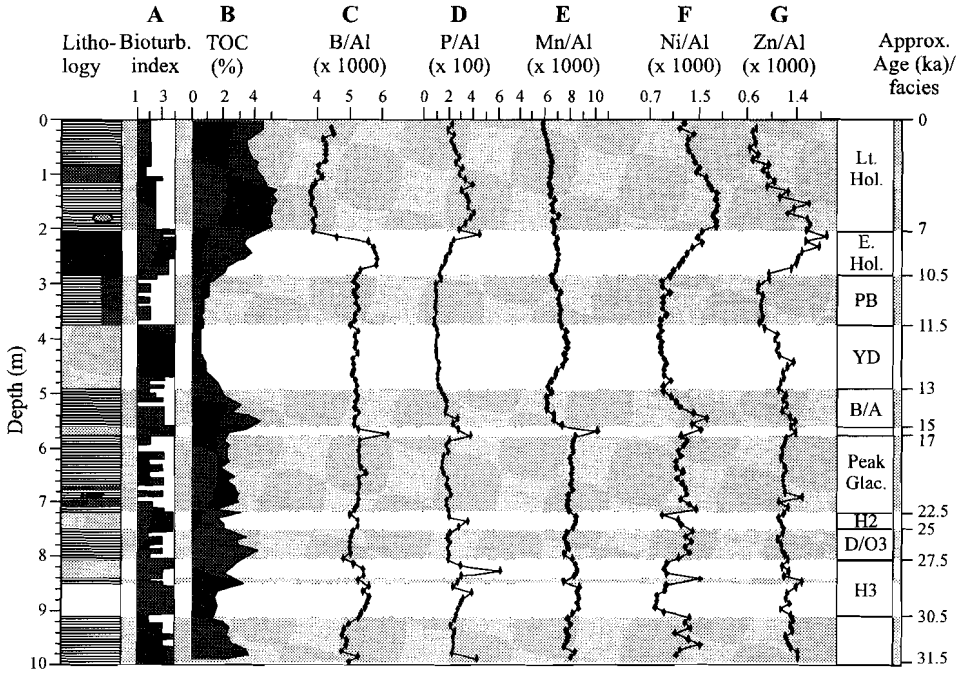

Figure 6 Lithofacies profile of core 137KA with proxies indicating productivity and/or bottom water oxygen conditions (laminated intervals are shaded). A: bioturbation index (Ld = distinctly laminated/"anaerobic environment"; Li indistinctly laminated/anaerobic - dysaerobic environment; Li/Hb slightly bioturbated with faint diffuse laminations/dysaerobic environment; Hb= homogenised-bioturbated/aerobic environment; see chapter 3). B: TOC (calculated carbonate free); C: Ba/Al x 1000; D: P/Al x 100; E: Mn/Al x 1000; F: Ni/Al x 1000; G: Zn/Al x 1000 . Note the strong minima in the TOC, P/Al, Ni/Al ratios during the T1B (H1) and YD intervals, whereas Ba/Al is negatively correlated to TOC and Ni/Al and hence not a productivity, but a terrigenous proxy off Pakistan.

lower accumulation rate of fluvial silty clay.

Macrofaunal benthic remains (echinoids, brittle stars, crustaceans, gastropods, and pelecypods) and pteropods are clearly enriched in the homogeneous, bioturbated oxic facies (Fig. 8B). Fish remains occur in both facies, but whole fish, including the soft parts, are preserved only in the laminated sediments, e.g. at 6.85 m bsf (Fig. 4).

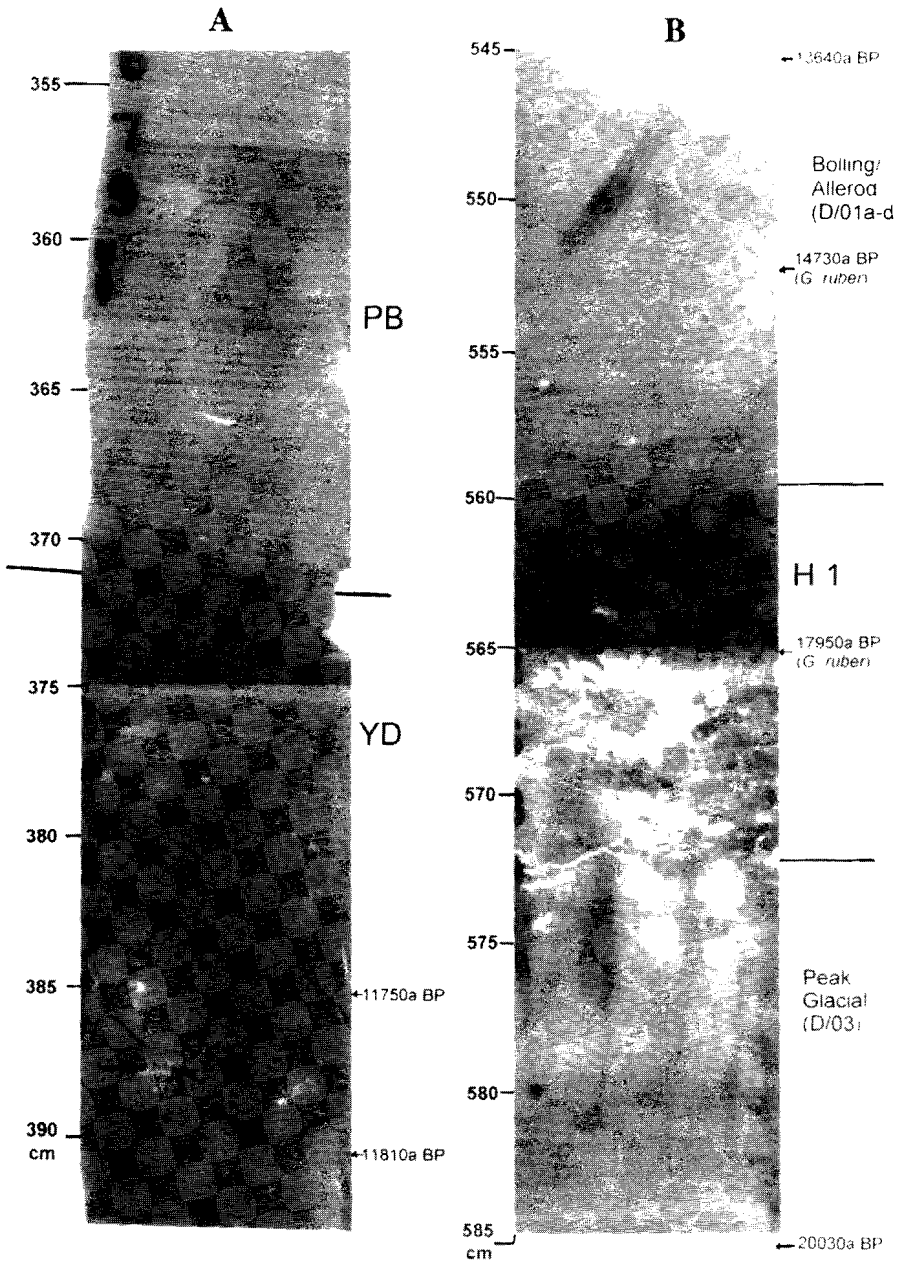
A
355
360
365
370
375
380
385
390
cm
PB
YD
11750a BP
11810a BP
B
545
550
555
560
565
570
575
580
585
cm
13640a BP
Bolling/
Allerod
(D/01a-d)
14730a BP
(G. ruber)
H 1
17950a BP
(G. ruber)
Peak
Glacial
(D/03)
20030a BP

5. Carbonate production, preservation, dilution and dissolution

More than 99% of the sand fraction of the bioturbated sediments consists of biogenic material, mainly planktonic and benthonic foraminifera, pteropods, diverse macrobenthos, fish remains, and copepods. The contents of the biogenic sand (Fig. 4D) show a general downcore-coarsening trend and several maxima generally coinciding with the bioturbated sections. Upcore, the average sand content (background values below the marked maxima) decreases continuously. All laminated intervals contain < 5% biogenic sand, compared to up to 27% sand content in the bioturbated sections. Within the uppermost 1.5 m of core 137KA (6 ka - Present), the sand content is < 3%.

Very small proportions of the total carbonate content are of lithogenic (reworked) origin . The detection of Tertiary and Cretaceous nannofossils (P. Cepek, personal communication, 1995), proves the presence of reworked (probably wind-blown) detrital carbonates. According to XRD data dolomite contents are < 3%. In smear slides we observed traces of dolomite rhombs (20-40 μm).

The bulk $CaCO_3$ content decreases from the top of isotope stage 3 (Fig. 8) to the Holocene. Except for the bioturbated interval of the Younger Dryas, all bioturbated intervals coincide with carbonate maxima. The main carbonate peaks are in the early Holocene, at the Termination 1A (H1), and in the sediment interval corresponding to Heinrich event 3. The general upcore decrease of the mean $CaCO_3$ content is strongly influenced by a continuous upcore increase in fluvial input. A strong supply of detritus from the Indus (see below) can be assumed for the last 3,000 years, around the Younger Dryas, and the Preboreal (Fig. 10). Carbonate minima were determined in the Preboreal and in the near-surface sediments. In general, the $CaCO_3$ curve (Fig. 8A) shows clear maxima in the peaks glacial (LGM) and stadials (Heinrich events). In the near-surface part of the core (0-0.5 m) and between 3 and 3.6 m bsf (Preboreal) most of the carbonate in the laminated sediments consists of nonbiogenic matter. These are minima in the curves for bulk $CaCO_3$ and the coarse-grained biogenic debris and detrital silicates.

Since TOC does not correlate with the degree of dissolution of

Figure 7 X-radiograph photos of core 137KA showing characteristic sediment texture and structures. A: Rapid change from dark-coloured, fine-grained , laminated sediment (Preboreal) to bioturbated, pteropod-rich, coarse-grained, light-coloured sediments (Younger Dryas; H1). B: Laminated Bølling/Allerød and Peak Glacial interrupted by thin bioturbated Heinrich 1 layer.

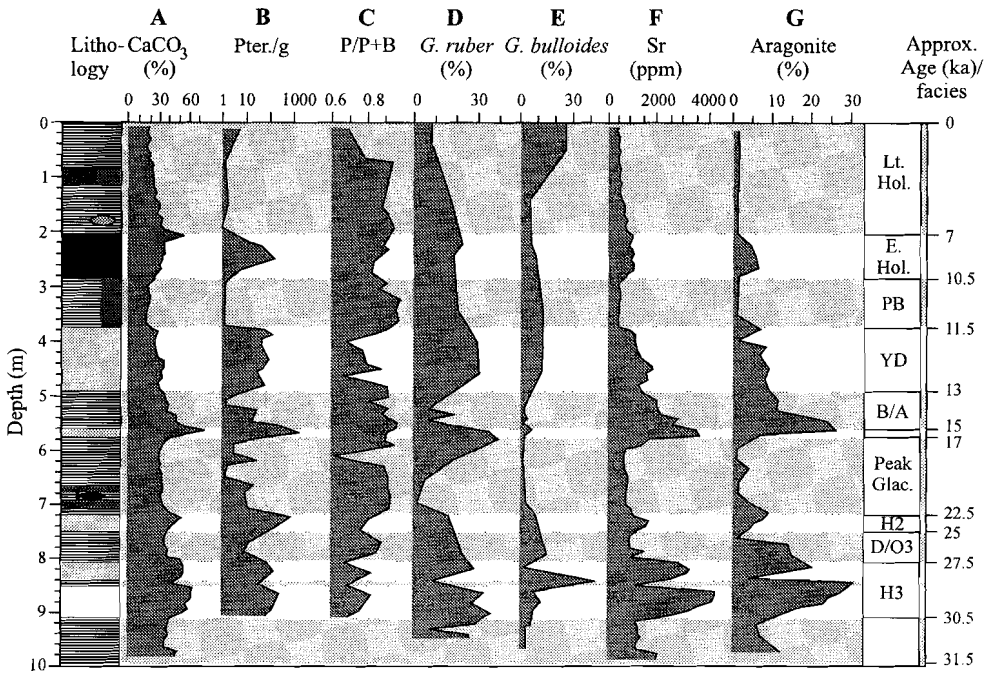

Figure 8 Lithofacies profile of core 137KA showing biogenic proxies (laminated intervals are shaded) A: % $CaCO_3$; B: pteropods (gram per sample from coarse fraction analysis; C: plankton/benthos ratio (only from foraminifera); D: *G.ruber* (% of total planktic foraminiferal fraction); E: *G. bulloides* (% as *G.ruber*); F: Sr (ppm); G: aragonite (from XRF and XRD analysis). For explanation of abbreviations see Fig. 2.

foraminifers, we think that - apart from the top several meters - the $CaCO_3$ contents in core 137KA (Fig. 8A) generally reflect variations in surface water productivity and terrigenous dilution, and only to a minor degree variations in dissolution. Although the water depth at site 137KA is relatively shallow, supralysoclinal dissolution can influence foraminiferal calcite and thus contribute to modifying the shape of the bulk $CaCO_3$ curve. Low bulk $CaCO_3$ and aragonite contents and high degree of fragmentation of the foraminifers suggest that the preservation of carbonate decreases rapidly upcore within the top several meters of the core that contain the highest TOC contents. The foraminifers in the laminated sediments, however, are generally better preserved than in the bioturbated beds. The more intense fragmentation in the bioturbated sections is probably caused by the burrowing and feeding activities of the megabenthos and not by dissolution.

The aragonite content of the bulk sediments ranges from 3 to 27% (Fig.

8G). This curve correlates with that for pteropod abundance (Fig. 8B), Sr (Fig. 8F) and bulk $CaCO_3$ contents (Fig. 8A). Aragonite maxima of > 20% coincide also with the bulk $CaCO_3$ maxima at 5.55-5.65 m bsf (H1) and at about 8-9 m bsf (H3). The absolute pteropod maxima (Fig. 8B) are at 3.85 m bsf (Younger Dryas), 7.25 m bsf (LGM), and especially at 5.65 m bsf (H1). In the top 5 meters of the core aragonite contents are < 10% with only a few juvenile specimens being present in the Holocene sediments. The most recent occurrence of pteropods is at 2.25 m bsf in the early Holocene. The absence of pteropods in the Holocene correlates with the disappearance of arenaceous foraminifers and macrobenthos. The most recent carbonate maximum is caused by an elevated proportion of planktonic foraminifers and coincides with the lowest aragonite contents. Towards the top of core 137KA we note an extreme decrease of $CaCO_3$, by terrigenous (fluvial) dilution and/or increase foraminiferal dissolution during the latest Holocene. Dilution by fluviatile detritus also results in low contents of aragonite and foraminiferal sand and in a poorly developed $CaCO_3$ maximum of the Younger Dryas horizon. The strong Sr and $CaCO_3$ maxima are caused by pteropod spikes in the Heinrich layers H1-3.

Aragonite preservation maxima show a positive correlation with phases of good aeration of the intermediate water, i.e., the (planktonic) pteropods occur together with a highly diversified micro- and macrobenthos. Aragonite maxima correlate better with the bioturbated intervals than with the TOC minima (Von Rad et al., 1995; Reichart et al., 1998). The laminated sediments near the Preboreal do not contain aragonite although TOC is low. This indicates a rise of the ACD caused by climate changes (see Melkert et al., 1992). According to Zobel (1973) there is no direct relationship between the abundance of pteropods in plankton hauls and that in the underlying surface sediments. The pteropod maximum in continental slope sediments is at 50-150 m water depth, which explains the rare occurrence of pteropods in the topmost sediments of core 137KA (570 m water depth). Judging from the pteropod contents in our surface sediments, today's aragonite compensation depth is at approximately at 500 ± 200 m (in the centre of the present OMZ). Periodically, especially during less productive periods (Early Holocene, Younger Dryas, and H1-H3 events), the ACD off the Indus delta was substantially lowered, down to at least 1000 m water depth, since core 108KL (Fig. 2) still contains pteropod layers. Pteropod preservation peaks coincide with stadials (Heinrich events) and glacials around 29 ka, 27-26 ka (H3), 25-22.5 ka (H2), 17-15 ka (H1), 13-11.8 ka (Younger Dryas), and at about 9.3 -7 ka

(early Holocene), but also with the Bølling/Allerød interstadial (15-13 ka; Fig. 8B,G).

Table 1

Factor loadings of benthic foraminiferal species

	Factor 1		Factor 2
Variance	25.3		13.8
Miliolids	0.91	*Osangularia culter*	0.80
Lagenids	0.87	*Pullenia quinqueloba*	0.75
Lenticulina spp.	0.82	*Bolivina dilatata*	0.67
Sphaeroidina bulloides	0.82	*Hanzawaia boueana*	0.64
Bulimina marginata	0.80	*Trifarina angulosa*	0.52
Textularia spp.	0.77	*Gyroidina orbicularis*	0.50
Hyalinea baltica	0.73	*Spiroplectammina* spp.	0.45
Shallow water species	0.66	*Uvigerina peregrina*	0.28
Bulimina striata	0.60	Shallow water species	0.26
Chilostomella oolina	0.58	*Globobulimina* spp.	0.24
Trifarina angulosa	0.55	*Bulimina marginata*	0.21
Cibicides pseudoungerianus	0.53	*Chilostomella oolina*	0.13
Agglutinated species	0.48	*Ehrenbergina pacifica*	0.13
Bolivinita quadrilatera	0.44	*Hyalinea baltica*	0.11
Gyroidina orbicularis	0.42	*Bolivinita quadrilatera*	0.11
Hanzawaia boueana	0.25	*Tritaxia tricarinata*	0.10
Cassidulina subglobosa	0.24	*Lagenids*	0.07
Spiroplectammina spp.	0.14	*Cassidulina carinata*	0.06
Cassidulina carinata	0.13	*Bolivina seminuda*	0.04
Tritaxia tricarinata	0.11	*Sphaeroidina bulloides*	0.00
Ehrenbergina pacifica	0.09	*Miliolids*	-0.15
Osangularia culter	-0.06	*Cassidulina subglobosa*	-0.16
Bolivina pygmaea	-0.15	*Bulimina* sp.1	-0.22
Pullenia quinqueloba	-0.16	*Bulimina exilis*	-0.25
Bolivina dilatata	-0.18	*Globobulimina affinis*	-0.27
Uvigerina peregrina	-0.23	*Lenticulina* spp.	-0.29
Globobulimina affinis	-0.24	*Cassidulina bradyi*	-0.30
Bolivina seminuda	-0.28	*Bolivina pygmaea*	-0.31
Bolivina alata	-0.28	*Textularia* spp.	-0.38
Cassidulina bradyi	-0.31	*Bulimina striata*	-0.38
Bulimina sp.1	-0.40	*Cibicides pseudoungerianus*	-0.45
Globobulimina spp.	-0.51	*Bolivina alata*	-0.48
Bulimina exilis	-0.58	Agglutinated species	-0.49

6. Benthic and Planktonic Foraminifera

As discussed before, the diversity of the benthic fauna, the $CaCO_3$, pteropod and biogenic sand contents are higher in the bioturbated than in the laminated sediment. The benthos in the lower Holocene section is dwarfed. During the Younger Dryas and the H1 event benthic activity was very strong, indicated by luxuriant macrobenthos and large benthic foraminifera including *Cibicides*, arenaceous foraminifera and crustaceans. In general, the plankton/benthos ratio decreases downcore (Fig. 8C). The largest macrobenthos (including echinids) is present in H3, suggesting well ventilated bottom water conditions very suitable for benthic life.

Results of the quantitative benthic foraminiferal analyses are shown in Figure 9. This figure shows simple diversity and the abundance of a number of important benthic foraminiferal taxa, together with PCA (principal component analysis) Factor 1 and PCA Factor 2. Factor 1 and Factor 2 account for 25.3% and 13.8%, respectively of the benthic foraminiferal variation. Table 2 lists the taxa incorporated in the PCA and shows their loadings on the first two factors.

The benthic foraminiferal results suggest that the OMZ varied substantially in intensity during the late Pleistocene-Holocene. Changes in intensity, however, do not appear to be dominantly driven by Glacial-Interglacial cycles, since lithological changes, associated with fluctuations in bottom-water oxygen concentrations, occur at higher frequency (cf. Schulz et al., 1998; Reichart et al.,1997, 1998).

The score plot of Factor 1 (Fig. 9M) displays a clear relation to lithology:

(1) low or negative scores, correspond to laminated intervals, where the benthic fauna shows lowest diversity and highest relative abundance (25-75%); factor 1 is negatively loaded by *Bulimina exilis, Globobulimina* spp., *Bulimina* sp.1, *Bolivina seminuda, Uvigerina peregrina, Cassidulina bradyi, Bolivina alata, Bolivina dilatata.* These species are generally associated with low bottom-water oxygen concentrations and/or high TOC flux.

(2) Species contributing to the positive scores on Factor 1 (Fig. 9M) are characteristic of homogeneous intervals; they represent a relatively diverse and equitable association with low dominance; the main components are Miliolids, Lagenids s.l., *Lenticulina* spp., *Sphaeroidina bulloides, Bulimina marginata, Textularia* spp., and *Bulimina striata.* The high-diversity fauna indicates higher bottom-water oxygen concentration and/or lower TOC-flux, compared to the conditions that prevailed during the deposition of the laminated sediments.

Benthic Factor 1 illustrates that distinct changes in the benthic

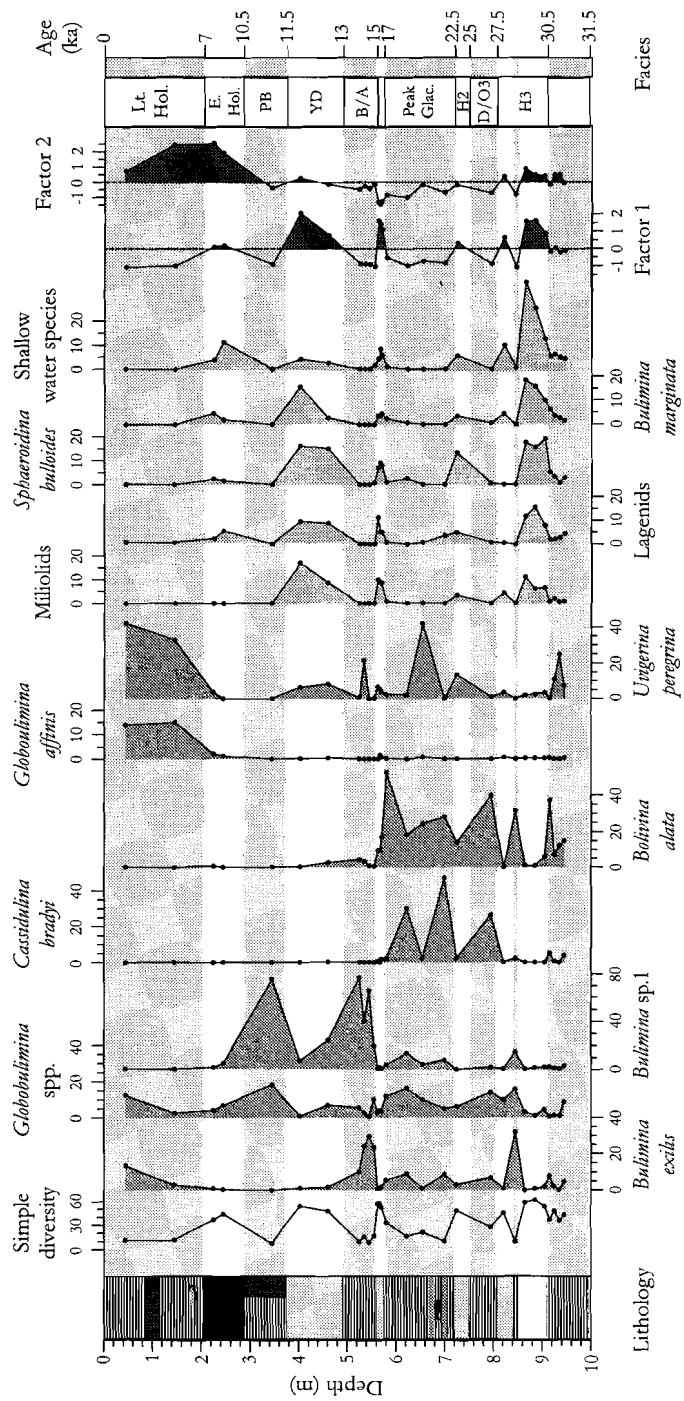
Depth (m)
Lithology
Simple diversity
Globobulimina spp.
Bulimina exilis
Bulimina sp.1
Cassidulina bradyi
Bolivina alata
Globobulimina affinis
Uvigerina peregrina
Miliolids
Lagenids
Sphaeroidina bulloides
Bulimina marginata
Shallow water species
Factor 2
Factor 1
Age (ka)
Facies
Lt. Hol.
E. Hol.
PB
YD
B/A
Peak Glac.
H2
D/O3
H3

foraminiferal fauna covary with the major changes in lithology; i.e. laminated sediments contain a typical low-diversity assemblage dominated by *Buliminids, Uvigerinids, Bolivinids, Cassidulinids* and *Globobuliminids*, and a high-diversity fauna characterises the sand-rich bioturbated beds. A suite of shallow-water species, as *Cibicides lobatulus* and a group constituted by *Rosalinids, Discorbidae, Ammonia* sp, *Nonion scaphum* (Murray, 1991), is also relatively abundant in the homogeneous intervals (Fig. 9).

A low-diversity, dwarfed benthic foraminiferal fauna, as found in the laminated intervals, is indicative of faunas thriving under severe dysoxia (Zobel, 1973; Lutze and Coulbourn, 1984; Hermelin and Shimmield, 1990; Denne and Sen Gupta, 1991; Sen Gupta and Machain-Castillo, 1993; Jannink et.al., 1998). Furthermore, dominance of taxa characterising the laminated sections (i.e., *Buliminids, Uvigerinids, Bolivinids, Cassidulinids* and *Globobuliminids*), is generally associated with low bottom-water oxygen concentrations and/or high TOC flux (Lutze and Coulbourn, 1984; Hermelin and Shimmield, 1990; Perez-Cruz and Machain-Castillo,1990; Sen Gupta and Machain-Castillo, 1993; Gooday, 1994; Wells et al., 1994). In contrast, a number of taxa observed in the homogeneous sections (e.g. Miliolids, Lagenids, *S. bulloides, B. striata*), have been associated with oxic benthic environments (Hermelin and Shimmield, 1990; Denne and Sen Gupta, 1991; Barmawidjaja et al., 1992; Kaiho, 1994). The benthic signal in the laminated sediments of SO90-137KA suggests low bottom water oxygen conditions and high TOC flux, which is in good agreement with the preservation of laminae, absence of macrofaunal remains, and enhanced concentrations of organic carbon.

The high-diversity fauna in the bioturbated intervals suggests higher bottom-water oxygen concentrations compared to the conditions prevailing during the deposition of the laminated sediments. The benthic foraminiferal fauna in these bioturbated sections contains about 15% shallow-water forms which might have been reworked from the shelf/uppermost slope, although the good preservation (no signs of corrosion) and the lack of sorting argue against downslope transport by currents. It seems therefore more likely that

Figure 9 Benthic factor loadings (Factor 1 and 2), simple diversity and percentages of species loading most negatively and most positively on benthic Factor 1 (see Table 2). Laminated intervals are dashed. Benthic foraminifera representative for anoxic/suboxic conditions are *Bulimina exilis, Globobulimina* ssp., *Bulimina* sp.1, *Cassidulina bradyi* (only pre-Younger Dryas), *Bolivina alata* (only pre-Younger Dryas) and *Uvigerina peregrina*. The miliolids, lagenids, *Sphaeroidina bulloides* and *Bulimina marginata* are characteristic of normal (oxic) bottom water oxygen conditions.

during periods of improved oxygen conditions at the sea floor, species from shallower sites (especially the lower part of the photic zone, since most are not exclusively epiphytic) migrate downslope and invade the formerly stressed environment.

The score plot of Factor 2 (Fig. 9N) shows negative to low positive values from 9.9-3.4 m bsf (Pleistocene sediments). Species contributing to negative scores are agglutinated species, *Bolivina alata, Cibicides pseudoungerianus, Bulimina striata, Textularia* spp., *Bolivina pygmaea. and Cassidulina bradyi.* Significantly positive scores are shown from 3.4 m bsf to the core top (Holocene sediments). This shift from negative to significantly positive scores is caused by the increase in abundance of *Osangularia culter, Pullenia quinqueloba, Bolivina dilatata, Hanzawaia boueana, Trifarina angulosa* and *Gyroidina orbicularis.*

The pattern of Factor 2 shows a change in the benthic foraminiferal composition from Pleistocene to Holocene sediments. In conjunction with this transition large-sized (>595 μm) benthic foraminifers, which are common in the Pleistocene bioturbated beds disappear in the early Holocene. Agglutinated foraminifera are completely lacking in the lower Holocene bioturbated beds.

Apparently, the pattern of factor 2 (Fig. 9N) is associated with the change from glacial to interglacial conditions. The Holocene assemblage corresponds to the highest TOC values recorded in core SO90-137KA. Apparently, many of the large Pleistocene species, characteristic of the Pleistocene bioturbated intervals, disappeared 12 ka ago and do not occur in the Recent surface samples, not even in well-oxygenated environments (A. Thies, oral comm., 1997). This indicates that a new faunal balance, possibly related to a change in quantity and/or quality of organic flux, is established in the Holocene.

From the planktonic foraminifera *G. bulloides* (Fig. 8E), indicating enhanced surface water productivity (due to upwelling or lateral advection of nutrient-rich waters), is more abundant in laminated intervals (e.g., Late Holocene, Dansgaard/Oeschger events) than in bioturbated section, where *G. ruber* is more common (Fig. 8D). *Globoratalia truncatulinoides* (not shown) which indicates intensified winter mixing (Reichart et al., 1998) does not occur in surface sediments, but only sporadically, e.g. in the laminated sediments of the Bølling/Allerød (5.65 m bsf).

Maxima of the planktonic/benthonic foraminifera ratio (Fig. 8C) are characteristic of high-productivity periods (Late Holocene and interstadial or Dansgaard/Oeschger events) which are characterised by high mass accumulation rates of organic carbon (Fig. 11).

7. Geochemical variability of sediments: results and discussion

7.1 Terrigenous (non-carbonate) proxies: fluvial input and wind-borne dust

The non-carbonate silt and clay fractions represent the terrigenous fraction, mainly transported by rivers. The profile of core 137KA shows a downcore decrease of the terrigenous clay (Fig. 8A) and an increase of the silt fraction (Fig. 10B) from the Holocene to the last Glacial. There is a considerable range of the grain size parameters, e.g. from 22 to 57% in the <2 µm carbonate-free fraction (Fig. 10A). Beginning at 5.45 m bsf (H1) we note conspicuous upcore-fining. Surprisingly, the glacial biogenic sand maxima (Fig.4) coincide with maxima of the terrigenous 20-63 µm fraction (Fig. 10B) and the bioturbated intervals of the core with optimal benthic life conditions contain more biogenic and terrigenous coarse fraction material. Generally, the coarse silt contents range from 0.7 to 41% in the carbonate-free fraction. Three absolute minima can be observed: (1) near the surface, (2) at 3.30-3.60 m bsf (Preboreal), and (3) at about 5 m bsf (Bølling/Allerød). In general, the quartz contents (calculated on a carbonate-free basis; Fig. 10C) increase downcore from 14% to a maximum of 32% . The reddish stain of the sediments of the Preboreal (Fig. 3) indicates clay-sized material transported by the Indus River from the north. The quartz maxima are in the bioturbated intervals and coincide with the coarse silt maxima (Fig. 10B). However, the bulk quartz contents do not decrease as strongly upcore as terrigenous coarse silt, since the increasing proportion of clay (Fig. 10A) in the younger sediments adds also to quartz. The high coarse silt/quartz ratio in the Pleistocene sediments is apparently due to the small proportion of quartz-bearing fine fractions.

In general, the SiO_2 contents (carbonate-free fraction) decrease upcore (Fig. 10D). This trend correlates with the upcore decrease in silt content (Fig. 10B) and the upcore increase in clay content (Fig. 10A). This general trend is interrupted by abrupt changes in SiO_2 and Al_2O_3 contents at 2.1 and 5.6 m bsf and a broad maximum for Al_2O_3 between 2.5 and 5.3 m bsf. The Al_2O_3 contents (carbonate-free) increase upcore from 10-3 m bsf, and again from 2 m bsf to the top (Fig. 10E). The broad TiO_2 maximum between 1 and 2 m bsf does not correlate with any coarse silt maximum. Apparently, TiO_2 is contained in both the fine and coarse terrigenous fractions.

The carbonate-free K_2O and TiO_2 values (Fig. 10G,H), as well as the Rb/Al values (Fig. 10F), are negatively correlated with coarse silt content (bioturbated sequences). Additionally, the K_2O values form a broad maximum

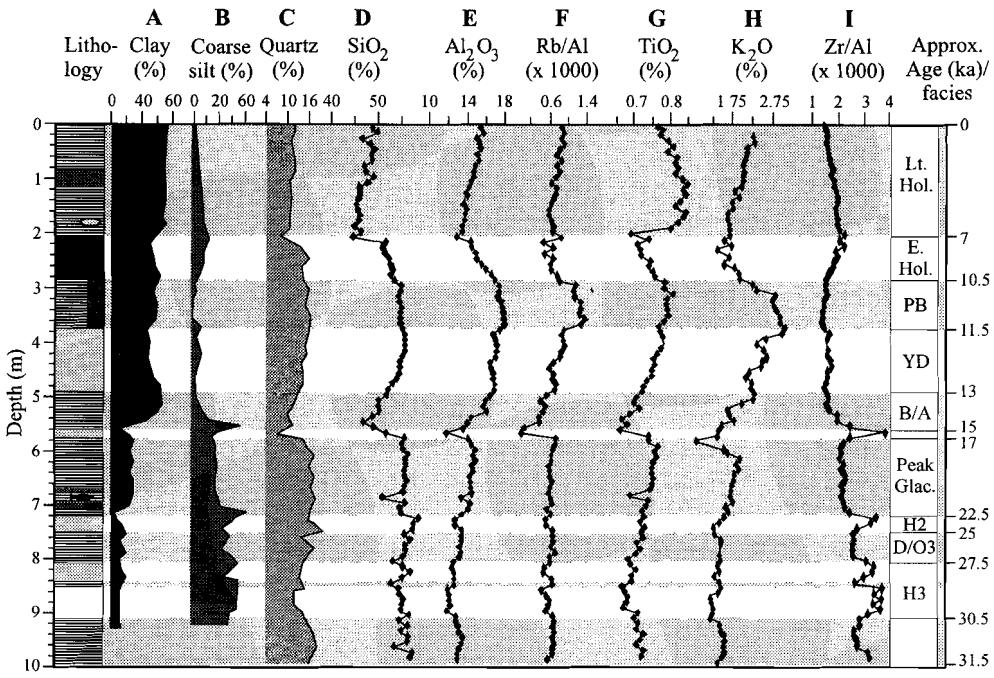

Figure 10 Lithofacies profile of core 137KA (laminated intervals are dashed) showing lithogenic (terrigenous) proxies (all geochemical percentages calculated carbonate-free). A: lithogenic clay (< 2 μm); B: coarse silt (20-63 μm) fraction; C: quartz; D: SiO_2; E: Al_2O_3; F: Rb/Al x 1000, G: TiO_2; H: K_2O; I: Zr/Al x 1000. Legend: see Fig. 8.

between 2.9 and 4.4 m bsf (Preboreal, partly Younger Dryas) and significant minima at 5.65 m bsf (H1) and 2.1 m bsf correlating with $CaCO_3$ maxima in the bulk sediment, whereas the wide K_2O and Rb/Al maxima correlate with minima for $CaCO_3$ (Fig. 8A), TOC, TiO_2, P/Al, and Ni/Al (Fig. 6). The scatter plot of K_2O versus clay, a proxy for fluvial deposition (<2 μm fraction; Fig. 12A), shows moderately good correlation of the two parameters: the Heinrich layers H1-4 have the lowest K_2O and clay percentages and the Preboreal sediments maxima in both properties.

The general upcore increase of fluvial material is reflected by enhanced clay, K/Al, Al_2O_3, Fe_2O_3 , and Rb/Al contents (Figs. 10, 12). After a short-term decrease in supply of river-transported matter from 7 and 6 ka, the fluvial input increased again around 6 ka in the mid-Holocene. The increase in the clay fraction, particularly during the last 15 ka, was probably caused by an enhanced river input (Fig. 10A). K_2O and Rb are probably derived from illite and micas (biotite, muscovite) transported by the Indus River (Satyaranyana

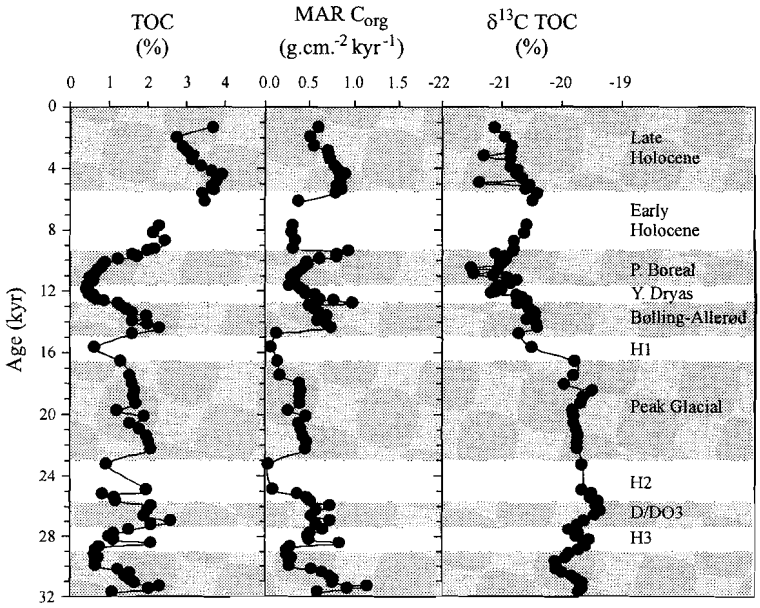

Figure 11 Time series (chronology) of various properties of core 137KA versus age (laminated intervals are shaded). A: TOC; B: mass accumulation rate of TOC (g .cm^{-2}.ka^{-1}); C: δ^{13}C of bulk organic carbon.

and Ramana, 1994). This is also shown by the abundance of "mica-rich mud" deposited on the middle shelf off the Indus River (Von Stackelberg, 1972).

The clay minima at 7 ka and 15 ka correlate with minima in the Al_2O_3 curve (Fig. 10). The (carbonate-free) TiO_2 content (Fig. 11F), is considerably higher above 2.3 m (7 ka). This might indicate an increased amount of matter supplied laterally from the Narmada and Tapti Rivers, which transport Ti-bearing minerals from the Deccan trap basalts (Douglass, 1996). The K_2O content (Fig. 10G) correlates with the clay content, because K is mainly contained in clay minerals (particularly muscovite-illite), although a small proportion is derived from silt-sized K-feldspar. A broad maximum for K_2O (Fig. 10H) and for (carbonate-free) Al_2O_3 (Fig. 10E) occurs between 3 and 5 m bsf in core 137KA (Terminations 1A and B) at the end of the Pleistocene. The nonbiogenic coarse silt contents (Fig. 10B) decrease considerably in this part of the core. The low (carbonate-free) TOC content between 3 and 5 m bsf (Fig. 6) also indicates the strong dilution by fine-grained, river-transported material. We explain this by elevated precipitation in the watershed causing the increased supply of fluvial matter. Such a distinct monsoon event at about 11.5 k calendar years BP is documented in many cores from the Arabian Sea

(Sirocko et al., 1996). It proves that the SW monsoon was very intense during the transition to the Preboreal (Fig. 12; Table 3).

The Mg/Al (not shown), Zr/Al and Ti/Al ratios (only TiO_2 shown), normally used as wind strength indicators in pelagic areas of the Arabian Sea (Shimmield and Mowbray, 1991; Sirocko et al., 1996; Sirocko, 1996; Reichart et al., 1997), and pointing to an elevated eolian input after the last glacial period, cannot be used as wind proxies in the river-dominated area of the Indus slope. Zr is an important lithogenic component originating from very resistent heavy minerals (zircon, ilmenite), reworked from the continents by rivers and concentrated on the shelf as heavy mineral placers. Maxima of coarse silt content, quartz and Zr/Al , Mg/Al (not shown) at Termination 1A (H1), H2 and H3 (Fig. 10B,C,I), are conspicuous, but they might have been caused either by eolian input or by reworking from the emerged shelf areas during sea level lowstands.

In general, the downcore plot of clay and coarse silt contents (Fig. 10A,B) shows the long-term trend of greater accumulation of coarse silt during the Pleistocene. This trend is interrupted by periodic maxima within the bioturbated core intervals, which might have been caused by enhanced input of coarse silts (during periods of strong winds and continental aridity) or a reduced input of fine-grained fluvial sediment (Prins and Weltje, 1999) during the stadials of the Heinrich events H1-3.

The Ba/Al ratio can be a proxy for (1) productivity in upwelling areas (biogenic Ba), or (2) for terrestrial Ba (reworked barite); (3) the Ba/Al ratio can be also influenced by secondary (diagenetic) mobilization due to changes in redox conditions within the sediments, where sulfate reduction takes place. In core 137KA the Ba/Al ratio (Fig. 6C) is rather constant and low (if compared with pelagic cores), with a small maximum in the bioturbated section of the lower Holocene and a minimum in the top 2 m (upper Holocene). Opposite to the findings of Shimmield and Mowbray (1991) and Sirocko et al. (1996) from the upwelling area off Oman and Reichart et al. (1997) from the Murray Ridge, the Ba contents in core 137KA show no positive correlation with P, TOC and Ni, suggesting that the amount of biogenic Ba is probably very low

Figure 12 Correlation diagrams (scatter plots) of various element or oxide concentrations from core 137KA. A: K_2O (calculated carbonate free; proxy for Indus River mica) versus clay < 2 μm; B: Zr (ppm) versus TiO_2 ; C: Ba (ppm) versus Al_2O_3; D: Sr (ppm) versus CaO (%); E: TOC (%) versus Ni (ppm); F: TOC (%) versus P_2O_5 (%). ACD = aragonite compensation depth. Legend: see Fig. 8 trends

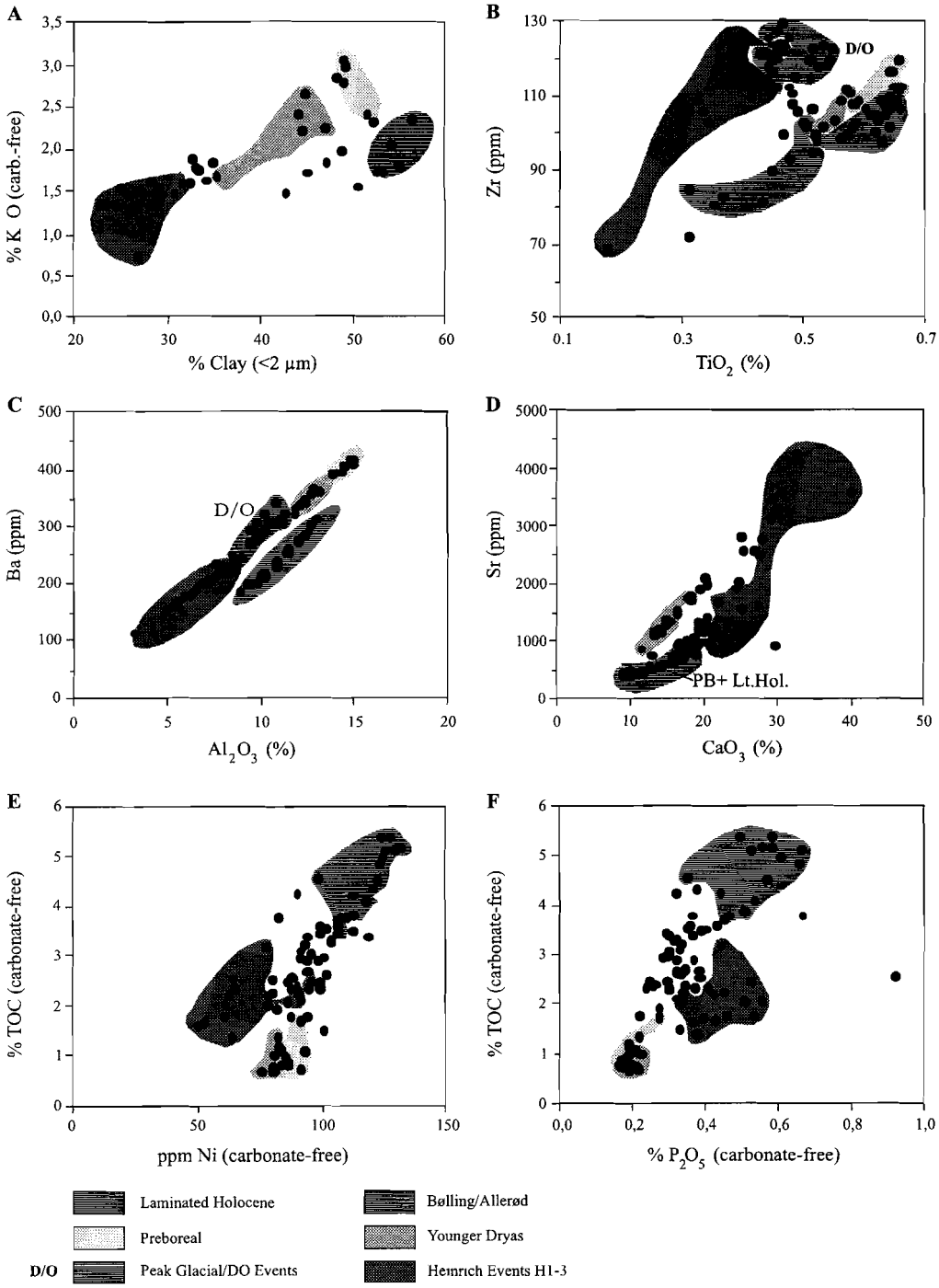
A
% K O (carb.-free)
% Clay (<2 μm)
B
Zr (ppm)
TiO_2 (%)
D/O
C
Ba (ppm)
Al_2O_3 (%)
D/O
D
Sr (ppm)
CaO_3 (%)
PB+ Lt.Hol.
E
% TOC (carbonate-free)
ppm Ni (carbonate-free)
F
% TOC (carbonate-free)
% P_2O_5 (carbonate-free)
Laminated Holocene
Preboreal
D/O
Peak Glacial/DO Events
Bølling/Allerød
Younger Dryas
Heinrich Events H1-3

(actually a scatter plot shows even a negative correlation of Ba with TOC). Apparently, the Ba signal is obscured, since Ba becomes mobilised in suboxic sediments due to sulfate reduction in organic matter-rich sediments and diffuses upwards, until sulfate concentrations are high enough for $BaSO_4$ to be precipitated (Dymond et al., 1992; Von Breymann et al., 1992). Although increasing reduction of sulfate with depth was determined in core 137KA by Dietrich and Marchig (1996), this geochemical trend does not affect the Ba/Al curve (Fig. 6C). However, a scatter plot between Ba and Al_2O_3 , the latter a typical terrigenous proxy (Fig. 12C), shows the excellent positive correlation of both properties in two separate subparallel, very distinct trends. Hence Ba is probably mainly of detrital origin (lack of correlation with productivity indicators such as TOC or P) and cannot be used as a paleo-productivity proxy in the highly productive nearshore sediments off Pakistan. The Ba/Al ratio might also be influenced by diagenetic mobilization at a redox boundary, since there is a strong decrease of Ba/Al at the Early/Late Holocene boundary (at 2.1 m bsf; Fig. 6C).

7.2 Productivity and redox sensitive proxies

TOC, V/Al, Ni/Al, Zn/Al, and P/Al are important indicators of paleo-productivity and -reduced conditions (Fig. 6).

In the pre-Younger Dryas Pleistocene section, TOC (Figs. 6B, 11) shows a conspicuous variability, which correlates with the alternations of bioturbated and laminated intervals (Von Rad et al., 1995). Figure 11A shows the TOC accumulation plotted against age with strong maxima in the Late Holocene (around 5 ka), during the Bølling/Allerød, the Peak Glacial and the Dansgaard/Oeschger Event 3. Strong minima occur during the Younger Dryas and the early part of the Preboreal, and during the Heinrich events H1-H3.

Total organic carbon (Fig. 11A) shows maxima in the Late Holocene (around 5 ka), during the Bølling/Allerød, the Peak Glacial and the Dansgaard/Oeschger Event 3. From 4 to 1.4 m bsf there is a continuous upcore increase in the TOC values from 0.5 to 3.8%. The absolute maximum of organic carbon is found in the upper Holocene sediments (Fig. 4F). TOC maxima are often associated with fish debris (especially in the late Holocene and peak glacial).

Due to dilution the TOC profile is generally negatively correlated with $CaCO_3$ (Fig. 8A) and terrigenous material. Hence the TOC contents of the

bioturbated sediments are lower than those of the laminated intervals (Figs. 4F, 6B). TOC minima occur during the Younger Dryas and the early part of T1B (Preboreal), and during the Heinrich events H1-H3. The conspicuous TOC minimum in the Preboreal and the Younger Dryas (Fig. 4F, 11A) correlates with maxima of various detrital (fluvial) constituents (Fig. 10). The bioturbated interval between 2.1 and 2.8 m bsf lacks the expected TOC minimum, i.e., the lower Holocene sediments are anomalous.

Carbon isotope ratios of bulk organic carbon vary between -19.5 and -21.6‰ suggesting a predominantly marine origin (Fig. 11C). This is supported by microscopic (organic petrographic) analyses which indicate that more than 90% of the organic matter are amorphous and of marine (phytoplankton) origin (Lückge et al., 1997). We observe an increase of ^{12}C from peak glacial times with fairly stable $\delta^{13}C$ values of about -19.7‰ to values between -20 and -21.5‰ during the Late Holocene (Fig. 11C). As the terrestrial fraction of the organic carbon remains nearly constant, this isotope shift can be explained by an increasing amount of dissolved carbon dioxide in the surface waters (Popp et al., 1989; Rau et al., 1989).

Maxima in sedimentary organic carbon are mainly driven by increased surface water paleoproductivity caused by strong SW monsoon conditions and coastal upwelling off Oman. In the upper part of the profile, the changes in organic carbon content occur less frequently and the concentrations are higher than in the pre-Younger Dryas sediments. Moreover the correlation between TOC (carbonate-free; Fig. 6B) and (carbonate-free) clay (Fig. 10A) is not close, indicating that adsorption of organic matter on clay minerals is not the main control of sedimentary organic carbon. The increase in TOC coinciding with the Al_2O_3 minimum between 1 and 2 m (middle Holocene) (Fig. 10E) also indicates elevated productivity. In the pre-Younger Dryas sediments, an enhanced fluvial input appears to coincide with increased productivity and/or better preservation of organic matter (see also Calvert et al., 1995).

Of the geochemical species entering the sediment via biogenic material, phosphate is an important constituent of fish remains. Since sea floor photographs revealed dead fish on the sea floor in the central OMZ off Karachi, the marked enrichment of fish remains in the laminated sediments might be caused by lack of oxygen in the bottom water. It might also be caused by higher surface water productivity (G.J. Reichart, personal communication, 1998). The mean phosphate content in the carbonate-free fraction (0.17%) corresponds to that of pelagic clay (0.15%). The phosphate minimum (0.1%) between 3 and 5 m bsf results from strong dilution with

Table 3

Facies and paleoclimatic evolution during seven time slices from the record of core 137KA covering the past 30,000 yr (partly after Sirocko et al.,1993; 1996; see also Fig. 13).

Time slices	Approx. age	Structure	Colour (lightness value)	Texture	Accum. Rate ($g.cm^{-2}.yr^{-1}$)	TOC, redox-sens. elements	Productivity (carbonate prod.-proxies)
Late Holocene	0-7	laminated	(dark) olive-grey, grey (>40)	very fine grained (<μm)	moderate (10-20)	TOC-rich (>3%) high Ni/Al, V/Al, Cr, Zn contents	mod. high P/Al contents (23% carbonate)
Early to Mid-Holocene	7-10.5	bioturbated (deeper sites are laminated see Fig. 2)	light grey (40-45)	lower clay and higher sand contents than late Holocene	low (ca. 10)	lower TOC (<2%) Ni/Al, and higher Mn/Al contents than late Holocene content	mod. high (>20% carbonate)
Preboreal	10.5-11.7	laminated (other sites are bioturbated ; Fig. 2)	(reddish-) grey (Indus R.) (>45)	clay max. (coarse silt and sand contents)	high (50-60)	TOC reduced by fluvial dilution low Ni/Al, V/Al high Mn/Al content	low P_2O_5 content; 17% carbonate
Younger Dryas	11.7-13	bioturbated	light grey (45-50)	moderate clay, coarse silt and sand contents	very high up to 90	low TOC, Ni high Mn/Al contents	low product., high 37% carbonate
Bølling-Allørod equivalent	13-15	laminated	grey > 50	low sand concentration	moderate up to 40	high P_2O_5, V, Ni contents high (-2% TOC)	low product., high (37%) carbonate
Late Glacial pteropod spikes (Heinrich event quivalents	H1: 15-17 H2: 22.5-25 H3: 27.5-30.5	bioturbated	light grey/ white (50-60)	coarse-grained (high terrig. and biogenic sand content	very low (<7)	oxic conditions (<1% TOC)	very low (macro-benthos and planktonic forams)
Peak glacial, and older D/O events	17-22.5, and >25	laminated	olive-grey >40	less clay, mod. Sand and coarse silt content	moderate (30-50)	TOC, Ni/Al, Cr/Al, V/Al, etc., high, espec. at 18 ka (LGM)	P/Al high, slightly more biogenic sand

Second column shows suggested ages of major lithostratigraphic units that are based on our stratigraphic model, derived from isotope stratigraphies of many SO90 cores from the Indus slope and west of Karachi , correlated with core SO42-74KL (Schulz et al., 1996; and unpublished data).

Table 3 (continued)

Arag. comp. depth (pterop.)	Fluvial input (K_2O, Al_2O_3 clay)	Wind input (coarse silt, Zr/Al, qtz, etc.)	SW monsoon strength	NE monsoon strength	Sea level (reworking)	Comments (bottom-water oxygen levels, productivity terrigenous input)
shallow ACD (low arag./pteropod contents)	strong input by Indus River (high clay, K_2O, Al_2O_3 contents)	none; minima of coarse silt, qtz, SiO_2, Zr/Al	strong	very low	high (minimal reworking)	Stable, intensified OMZ and productivity maximum, but Indus River input strong. TOC mainly of marine (phytoplankton) origin 7–4 ka humid interval, after 4 ka increasingly arid.
mod. strong (K_2O, Al_2O_3,Rb/Al) strong riverine input at 8 ka	none (no Northwester lies reaching site)	v. strong (7–10 ka)	low			OMZ less strong at site than during late Holocene. Elevated productivity, reduced deep mixing, high oxygen consumption. Indus River input very strong at 8 ka (early Holocene humid period).
shallow ACD, low arag./Sr contents (fluvial dilution)	very strong, maxima of clay, K_2O, TiO_2,SiO_2	none (sea level high)	at 11.5 ka major intensification	low	major SL rise around 11.3 ka (T1B)	Low productivity and strong fluvial dilution (mica-rich clay material from Indus River), but bottom-water oxygenation is low at this site).
deep ACD, high aragonite, pteropod Sr content	mod. high (but low K_2O)	mod. strong (coarse silt, qtz, Zr/Al, TiO_2)	weak	strong (fluvial dilution)	YD-lowstand (but rising) SL after YD reduced winnowing	Fully oxic conditions with well developed benthic life. Biogenic sand and bulk carbonate decreasing upcore due to fluvial dilution.
shallow ACD, low aragonite/ pteropod contents	fluvial input, increasing upcore	moderate (decreasing upcore)	mod. strong (decreasing upcore)		major SL rise at 16–15 ka (T1A)	Moderately high productivity and well developed OMZ; low river discharge.
deep ACD, very strong pteropod maxima	very low (?)	strong (max. dust flux off Arabia >)	weak (low product., no upw. off Oman)	moderate (winter mixing)	off Indus delta strong reworking (Zr max.)	Fully oxic conditions, strong reworking, strong dust input at low productivity levels.
shallow ACD, low aragonite/ pteropod contents	very low (?)	very strong, at peak glacial, high Zr/Al content	moderate, decreasing upcore	strong at 18 ka (peak glacial)		Peak glacial: poorly oxygenated bottom waters (stable OMZ) and comparatively high productivity. Hyperarid condition in hinterland at LGM?

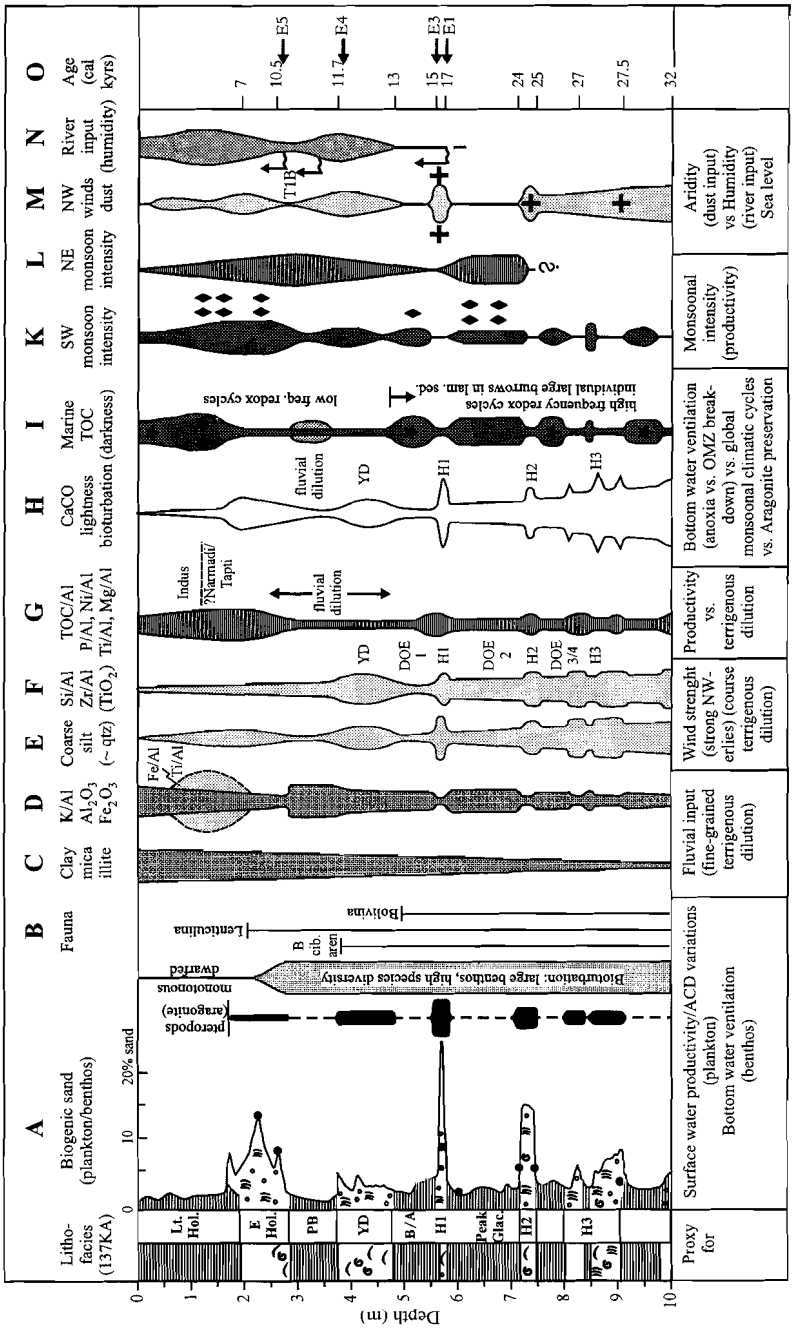
A
B
C
D
E
F
G
H
I
K
L
M
N
O
Litho-facies (137KA)
Biogenic sand (plankton/benthos)
Fauna
Clay mica illite
K/Al Al2O3 Fe2O3
Coarse silt (~ qtz)
Si/Al Zr/Al (TiO2)
TOC/Al P/Al, Ni/Al Ti/Al, Mg/Al
CaCO lightness bioturbation
Marine TOC (darkness)
SW monsoon intensity
NE monsoon intensity
NW winds dust
River input (humidity)
Age (cal kyrs)
Depth (m)
20% sand
pteropods (aragonite)
monotonous
dwarfed
Bolivina
Lenticulina
B cib. aren
Bioturbation: large benthos, high species diversity
Lt. Hol.
E Hol.
PB
YD
B/A
H1
Peak Glac
H2
H3
Fe/Al
Ti/Al
Indus
?Narmada/ Tapti
fluvial dilution
YD
DOE 1
H1
DOE 2
H2
DOE 3/4
H3
fluvial dilution
YD
H1
H2
H3
low freq. redox cycles
high frequency redox cycles
individual large burrows in lam. sed.
T1B
E5
E4
E3
E1
7
10.5
11.7
13
15
17
24
25
27
27.5
32
Proxy for
Surface water productivity/ACD variations (plankton)
Bottom water ventilation (benthos)
Fluvial input (fine-grained terrigenous dilution)
Wind strenght (strong NW-erlies) (course terrigenous dilution)
Productivity vs. terrigenous dilution
Bottom water ventilation (anoxia vs. OMZ break-down) vs. global monsoonal climatic cycles vs. Aragonite preservation
Monsoonal intensity (productivity)
Aridity (dust input) vs Humidity (river input) Sea level

fluvial material. There is also a detrital component for this element and some of the P maxima are in the bioturbated sediments, correlating with Zr maxima. This suggests enrichment by winnowing. The general increase in P/Al content (Fig. 6D) at the beginning of the Holocene and the decrease in the late Holocene correlates with the curves for TOC, Ni/Al, and Zn/Al (Fig. 5B,F,G). Therefore, we note an elevated productivity during the Holocene (with a peak around 5 ka BP; Fig. 11C) for the Pakistan margin similar as determined for the north-western part of the Arabian Sea (Sirocko, 1995).

The broad TOC minimum in the Preboreal and Younger Dryas (Fig. 6B) correlates with P/Al, Ni/Al, and Zn/Al minima (Fig. 6D,F,G), whereas maxima of these elements correlate with TOC maxima and are hence indicative of strong OMZ conditions. The P/Al ratio (carbonate-free; Fig. 6D) correlates positively with the Ni/Al ratio (Fig. 6F), especially from 0 to 5 m bsf. P/Al and TOC correlate less well, especially at high P and TOC contents, because some of the Pleistocene P peaks are in the bioturbated intervals below the TOC-rich sections. The TOC and P/Al curves show both similarities and differences: both curves have an extended minimum between 3 and 5 m bsf and generally higher values from 2-0 m bsf (upper Holocene). However, the P/Al peaks of the Pleistocene sequence are close to the upper boundary of the bioturbated intervals, somewhat deeper than the TOC peaks.

Of the trace elements of biogenic origin Ni (and to a lesser degree also Zn) have a depth profile that is very similar to that of TOC with maxima in the

Figure 13 Summary of general trends and downcore variability of various proxies in litho-, bio- and chemical facies of core 137KA. Paleoclimate (monsoonal intensity), humidity/fluvial input, aridity/wind dust input by Northwesterlies) and paleoenvironmental (bottom water ventilation) interpretation is also added (for more explanation see Table 3). Abbreviations: Lithofacies and stratigraphy: see Fig. 4; column B: P/B = plankton/benthos ratio, b = dwarfed benthos (Bulimina, Buliminella, Uvigerina), B = macro-benthos, B = large macro-benthos; Cib = Cibicides, aren = arenaceous foraminifera, crust = crustaceans, ech = echinids, foraminiferal symbol = many planktonic foraminifera, crossed foraminiferal symbol = highly fragmented planktonic foraminifera, cop = copepods, fish symbol = fish remains (large symbol: many fish remains). Column C: note upward fining. Column E: "coarse silt" refers to lithogenic 20-63 µm fraction. Column H: "sediment lightness" correlates with bioturbation index (see Fig. 5A), H1-H3 = Heinrich events, D/O 1-5 = Dansgaard/Oeschger events (see Schulz et al., 1998), * = suboxic conditions, ** suboxic/anoxic conditions. Column K: paleomonsoon intensity, diamond = weak upwelling, double diamond = strong upwelling. Column M: + = arid, ++ maximum dust input from Arabia, Iran and Persian Gulf, vertical arrow = major sea level rise. Column O: E1-E5 = climatic events after Sirocko et al. (1993, 1996).

laminated and minima in the bioturbated sequences (Fig. 6F,G). The Ni/Al values form a broad maximum in the Holocene (3000–6000 years), but in the Preboreal to the Bølling/Allerød there is a broad minimum. Scatter plots of TOC versus Ni (Fig. 12E) show a positive correlation, with the Late Holocene laminated sediments having the highest TOC and Ni (or P_2O_5) percentages (see chapter 7.5). The Ni/Al ratio in core 137KA (Fig. 6F) is related to the nutrient cycle and reflects, the accumulation of organic matter, i.e. productivity. Also Zn/Al (Fig. 6G) shows a distinct maximum in the Holocene sediments (apparently also a productivity signal), although Zn/Al, unlike Ni, does not correlate with the laminated Pleistocene sequences.

The Mn/Al curve (Fig. 6E) resembles- in mirror image- that for Al_2O_3 (Fig. 10E), more than that for Ba/Al (Fig. 6C) and has roughly the opposite trend as the TOC curve (Fig. 6B). The rapid change in composition clearly marks the transition from H1 to the Bølling/Allerød interstadial, followed by a wide maximum in the uppermost Pleistocene (Younger Dryas and Preboreal). The low Mn contents (about 0.05-0.07% in the carbonate-free fraction) are mainly due to the reducing conditions at the surface of the suboxic sediments and within the sediment. This prevents precipitation of Mn oxides from the seawater and results in the re-dissolution of those oxides precipitated in oxygenated bottom water. Additionally, high sedimentation rates lessen accumulation of authigenic precipitates.

8. Conclusions and comparison with other monsoon records

8.1 Variations of the monsoonal climate during the past 30,000 years

The long-term trends of the paleoenvironmental and paleoclimatic evolution during the past 30,000 years are summarised in seven time slices in Table 3 and shown in Figure 13. The multiple millenial-scale changes from laminated to bioturbated sediments suggest significant changes in bottom water ventilation, surface water productivity and continental aridity in sub-Milankovich cycles (Sirocko et al., 1993; Sirocko, 1996).

The present interval of a stable and expanded OMZ conditions in the Intermediate Indian Ocean water masses between 200 and 1200 m water depth (Fig. 1B) has been one of the longest and, with respect to the preservation of organic matter, one of the most intense during the last 30 ka. Temporal changes of the bottom water oxygen content occurred less frequently than during the less stable climate of the Late Pleistocene (marine isotopic stage 2).

The change from the Pleistocene high-frequency cycles to the lower-frequency cycles begins in the Younger Dryas period, as clearly documented in the TOC profile (Fig. 4F). During the Pleistocene the oxic-anoxic cycles have a higher frequency than during the Holocene.

8.2 Suborbital variability of OMZ conditions and surface water productivity

We interpret the multiple intercalation between laminated and bioturbated intervals in our cores as temporal changes in the oxygenation of bottom waters.

The cyclicity of laminated/bioturbated intervals and the variability of monsoonal circulation, continental aridity, and bottom water ventilation is forced by suborbital (sub-Milankovich) variability in bottom-water oxygen concentration, paleoclimate, and (monsoonal) circulation system. For the record of the past 30 ka, we found comparable laminated/bioturbated intervals in core 137KA, as other authors in other subtropical/tropical environments: high-resolution studies on the history of monsoon circulation, productivity and the variability of OMZ conditions from the north-western Arabian Sea (Sirocko et al., 1996), the north-eastern Arabian Sea (Reichart, et al., 1997; 1998; Schulz et al., 1998), as well as from the Santa Barbara Basin (Behl and Kennett, 1996) and the Cariaco Basin (Peterson et al., 1991; Hughen et al., 1996) indicate global mechanisms for these short-term climatic oscillations. From the Santa Barbara Basin, Behl and Kennett (1996) described 19 laminated intervals attributed to interstadials (Dansgaard-Oeschger events) and correlated with the GISP2 ice core record. In the South China Sea sediments two regimes of monsoonal circulation are recorded; the glacial to interglacial, millenial-scale changes in the East Asian monsoon climate which can also be correlated to Heinrich and Dansgaard/Oeschger events of the Pakistan Margin and of the high latitudes (e.g., the Greenland ice record) led to major changes in seasonal wind intensity, as well as highly variable dust and moisture fluxes (Wang et al. in press).

Apparently, the paleoclimate/paleo-circulation in the Northern Arabian Sea fluctuated between two extremes: (A) oxygen-deficient bottom water (OMZ) and (B) fully oxygenated bottom water conditions (breakdown of OMZ).

8.3 Suboxic conditions (strong OMZ)

The influence of a stable and expanded OMZ during the past is reflected in the dark, TOC-rich and distinctly to indistinctly laminated sediments, deposited during the Late Holocene, the Preboreal , the Bølling/Allerød, the peak glacial (ca. 17-22.5 k cal yr) and Dansgaard/Oeschger event equivalents 3 and 4. In the northern Arabian Sea these interglacial/interstadial periods and the peak glacial are characterised by relatively cool (ca. 20-23°C) sea surface temperatures, high surface water productivity, deepening of the mixed layers, and injection of nutrients into the photic zone during a strong summer monsoon (Reichart et al., 1998). Also the lack of any macrobenthos, the low-diversity, high-abundance benthic foraminiferal fauna (dwarfed *Buliminacea* facies) in the laminated sediments indicates suboxic conditions and an intensified, expanded OMZ which was apparently stable for several ka. An abrupt climate and ventilation change at the beginning of the Bølling/Allerød interstadial is characterised by an increase in fluvial proxies, minimum of dust proxies, and increased accumulation rates of organic matter. This appears to be a global phenomenon, since it was also found in the African Rift Valley, the Red Sea and other areas of the Northern hemisphere (Broecker et al., 1998).

Carbon isotope and organic petrographic analyses indicate that >90% of the TOC is of marine (phytoplankton) origin, and hence a fairly reliable proxy for enhanced productivity. However, also the preservation of organic matter is enhanced in the OMZ due to reduced or missing bioturbation and absence of labile Mn (Van der Weijden et al., 1999). Surface water productivity (documented by maxima of *Globigerina bulloides*, abundant fish remains, high contents of TOC and redox-sensitive elements or productivity indicators, such as V, Ni, Zn, P) was strongest during periods with SW monsoon maxima , e.g. the late Holocene and interstadials. Planktonic $\delta^{18}O$ data and abundance of *G. bulloides* in the laminated surface sediments do not indicate upwelling conditions (*sensu stricto*), but enhanced productivity due to lateral advection of nutrient-rich waters from the upwellingcentre off Oman, mainly during the SW monsoon (Schulz et al., 1998; Reichart et al., 1997).

The concentration of terrigenous proxies, such as clay content, K/Al and TiO_2 in the middle Holocene and of reddish stain in the Preboreal is explained by enhanced SW monsoon winds causing more precipitation and increased input of illite, mica, and Ti- and Fe-rich minerals by the Indus, Narmadi and Tapti Rivers.

8.4 Fully oxygenated conditions (breakdown of OMZ conditions)

Oxygenated bottom water conditions during the Early Holocene, the Younger Dryas, and the Heinrich events are characterised by light-coloured, bioturbated sediments rich in carbonate, aragonite (pteropods) and Mn, as well as by low TOC accumulation rates and minima of redox-sensitive elements. This indicates lowered surface-water productivity and fully oxygenated bottom water conditions supporting a "normal" high-diversity benthic fauna (including a high-diversity macrofauna of crustaceans, echinoids, *Dentalium* sp.; Fig. 13). The decrease in *G. bulloides* and increase of *G ruber* in the bioturbated sediments (especially in the Younger Dryas and during Heinrich 1-3 events) suggests that productivity was low. A strong lowering of the ACD favoured the preservation of the aragonitic pteropods which are negatively correlated with the intensity of the OMZ. Hence the carbonate maxima are partly due to a lowered ACD and not caused by enhanced productivity or reduced terrigenous dilution.

Periods of strong offshore winds caused extensive convective turnover in the water column (linked to occurrence of *G. truncatulinoides*) during the winter (intensified NE monsoon), whereas the decreased intensity of the SW monsoon reduced the surface water productivity (Reichart et al., 1998).

The benthic foraminiferal associations are exceptionally well preserved in the bioturbated intervals and are distinctively different from typical shelf faunas, having no modern analogues in recent core-top samples. We interpret these specific faunal associations to reflect distinct periods of better oxygenation and changing carbon fluxes at OMZ depths.

The abundance of lithogenic proxies (e.g., coarse silt, quartz, and Zi/Al) suggests aridity and wind transport during the stadials (Heinrich events), although reworking from the emerged wide shelf areas cannot be excluded.

8.5 Influence of deglacial sea level rise

Times of increased fluvial sediment supply to the Indus slope with high accumulation rates coincide with humid phases (intensified monsoon) during the early Holocene and times of rapid rises of the global sea level (Figs. 5,13). At the end of the Younger Dryas (Termination 1B and Preboreal), sea level rose rapidly to 40 m below the present day level and large parts of the shelf became flooded. Whereas the sediment supply to the deep-sea fans was reduced (Weber et al., 1997), enhanced fluvial supply by the Indus River was

noted on the continental slope during the transgression (mobilization and downslope reworking of fined-grained material). During sea level lowstands (such as the Younger Dryas) a mixing process could also have been promoted by the termination of input of highly saline waters from the Persian Gulf and Red Sea into the northern Arabian Sea eliminating the stable stratification of the oxygen-poor Intermediate Indian Ocean Water.

8.6 Teleconnections with Dansgaard-Oeschger and Heinrich Events

We assume that during cool periods over the northern hemisphere bioturbated intervals in the north-eastern Arabian Sea formed at times of weakened SW monsoons under warm, saline surface waters and slightly lowered productivity. This resulted in the breakdown of the OMZ conditions that are typical of strong SW monsoon conditions and high productivity periods, as experienced today.

The sedimentary record of core 137KA and of nearby cores (e.g., 111KL, 136KL; Fig. 3) suggests that monsoonal climatic and OMZ variability during the past 110 ka can be correlated with the Dansgaard-Oeschger and Heinrich events of the Greenland ice cores; the striking similarity between the air temperature above the Greenland ice sheet and the marine record in the north-eastern Arabian Sea point to a teleconnection and global forcing mechanisms acting extremely rapidly (Schulz et al., 1998). Atmospheric circulation (water vapour) changes may have triggered the monsoonal circulation and hence forced the intensification of the OMZ off Pakistan. We do not yet know the ultimate cause for these teleconnections between high and low latitudes. On the one hand, Porter and Zhisheng (1995) have reported distinct peaks in the size distributions of aerosol particles found in the Chinese loess plateau correlated to the Heinrich events H1 to H6 and explained to reflect stronger east Asian winter monsoonal winds in the West Pacific; they postulated an inter-hemispheric connection between Greenland and central Asia by stronger westerlies blowing towards the loess plateau during cool periods, cooling the Asian plateaux, reducing the interhemispheric pressure gradients and, hence, the intensity of the SW-monsoon. On the other hand, it is also possible that climate changes in the tropical monsoonal system (forced by winds reacting to pressure gradients between the south Asian high plateaux and the ocean) triggered millenial-scale climate changes within the higher latitudes.

Acknowledgements

We are very grateful to our colleagues who have co-operated with us on our PAKOMIN cores, especially to Steven Calvert (Vancouver), Gregory Cowie (Edinburgh), Peter Dietrich (Freiberg), Andreas Lückge (BGR), Vesna Marchig (BGR),), Sonja Schulte and Jürgen Rullkötter (Oldenburg), Andrea Thies (Kiel), Hedi Oberhänsli (Potsdam), Andreas Suthhof and Tim Jennerjahn (Hamburg). We also thank Mebus Gey (Geologische Gemeinschaftsaufgaben, Hannover) and Pieter Grootes (Kiel) for conventional/AMS-^{14}C datations and Hans Erlenkeuser (Kiel) for oxygen isotope measurements. Andreas Wetzel (Basel) helped with information on bioturbation structures. Andreas Wetzel (Basel), Jan-Willem Zachariasse (Utrecht), and especially Gert-Jan Reichart (Utrecht) kindly read the manuscript and gave many helpful comments. We are very grateful for constructive criticism by the reviewers Fred Jansen, Patricia Wells, and especially for the very thorough review by Ralph Schneider. Thanks are due to the German Federal Ministry of Education, Research and Technology (BMBF) for funding cruise SO90 (Project No. 03 G 0090A).

Chapter 4
Benthic foraminiferal proxies

Benthic foraminifera as proxies of organic matter flux and bottom water oxygenation? A case history from the northern Arabian Sea

Abstract

Benthic foraminifera have been quantified in two sediment cores from a topographic high (Murray Ridge) in the northern Arabian Sea. One core is from a station within the present-day Oxygen Minimum Zone (OMZ), the other from a station below the OMZ. Changes in the intensity of the OMZ, linked to monsoonal climate variability, had a strong impact on benthic foraminiferal composition and accumulation rates. At the shallower OMZ station (920 m) an intensification of the OMZ resulted in lower diversities and high dominances of low oxygen tolerant species. The deeper station (1470 m) was far less affected, though at least once during the last 225,000 years the benthic faunal composition and accumulation rates show evidence for a deepening of the base of the OMZ to a level close to or even below 1470 m. We suggest that percentages of miliolids can be used for rapid reconstruction of periods of increased ventilation in the northern Arabian Sea and are a promising proxy for tracing changes in bottom and pore water oxygenation in general. OMZ conditions are characterised by high abundances of deep infaunal species and increased burial efficiency of organic matter. The proportion of deep infaunal species appears to be a measure for the anoxic burial efficiency of organic matter and not a direct measure for the arriving flux at the seabed. Results, furthermore, show that benthic foraminiferal accumulation rates cannot be used as a proxy for surface water productivity under the prevalence of severe dysoxia.

Den Dulk, M., Reichart, G.J., Van Heijst, S., Zachariasse, W.J, Van der Zwaan, G.J., Palaeogeography, Palaeoclimatology, Palaeoecology, in press.

1. Introduction

Benthic foraminifera have long been recognized for their potential in marine paleo-environmental studies. Over the past two decades, this has become particularly evident for their use in reconstructing changes in paleoproductivity and bottom water oxygenation. Studies of dead and living benthic foraminifera have shown that benthic foraminiferal distribution patterns are closely related to the organic carbon flux and the organic carbon content of the sediment (e.g. Mackensen et al., 1985; Altenbach and Sarnthein, 1989, Caralp, 1984, 1989; Jorissen et al., 1992; Gooday, 1993;Van der Zwaan et al., 1990; Schmiedl et al., 1997; Fariduddin and Loubere, 1997; De Stigter et al., 1998; Altenbach et al., 1999). Other studies have demonstrated the sensitivity of the assemblage composition to changes in oxygen levels of the bottom water and within the sediment (e.g. Lutze and Coulborn, 1984; Corliss, 1985; Perez-Cruz and Machain-Castillo, 1990; Hermelin and Shimmield, 1990; Corliss and Emerson, 1990; Bernhard and Reimers, 1991; Moodley and Hess, 1992; Bernhard, 1992, 1993; Sen Gupta and Machain-Castillo, 1993; Gooday, 1994; Wells et al., 1994; Loubere, 1996; Jannink et al., 1998). As a result, the general contention is that oxygen and food supply are the main factors controlling the spatial and in-sediment distribution of benthic foraminifera (e.g. Jorissen et al., 1995). Although much progress has been made in benthic foraminiferal ecology, the relevant question still seems to be how accurately can benthic foraminifers be used as reliable recorders of oxygen and productivity in paleo-environmental studies? To address this question we studied the benthic foraminiferal records from the last 225 kyr of two sediment cores from the northern Arabian Sea. Present-day surface water conditions at these two stations are comparable but bottom water conditions are quite different.

2. Study area

In the present-day northern Arabian Sea, the combination of high surface water productivity and moderate rates of thermocline ventilation (You and Tomczak, 1993) leads to an intense Oxygen Minimum Zone (OMZ) between 150 and 1200 meters (Wyrtki, 1971; 1973; Deuser et al., 1978; Olson et al., 1993) with oxygen levels below 0.05 ml/l (Van Bennekom and Hiehle, 1994). Surface water productivity shows a large semi-annual variability, and is highest during summer, when strong southwest monsoonal winds induce coastal and open ocean upwelling off Oman (Wyrtki, 1971; 1973; Smith and Bottero,

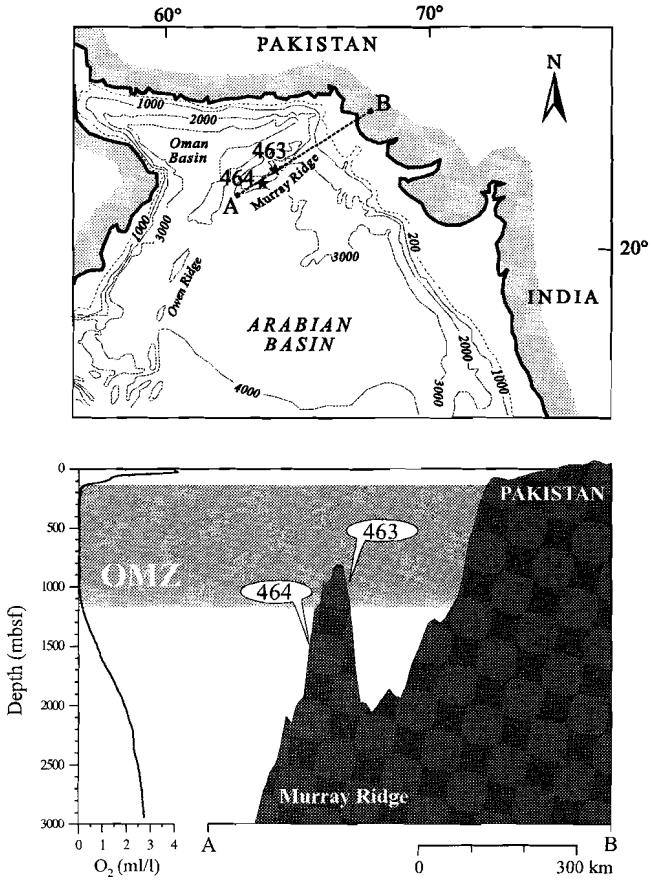

Figure 1a) Location of NIOP463 (22° 32'.9 N, 064° 02'.8 E, water depth 920 m) and NIOP464 (22° 15'.4 N, 063° 35'.1 E, water depth 1470 m). 1b) Oxygen profile is from CTD station NIOP458 (22° 00'.3 N, 63° 50'.4 E) and profile of seafloor topography is along dashed line in Fig. 1a. Grey shading depicts the OMZ

1977; Swallow, 1984; Brock et al., 1992). This allows deeper nutrient-rich waters to rise, resulting in productivity values that are among the highest known for the open ocean. In winter relatively weak, dry and cold northeastern winds are prevailing. Production is generally low except in the region off Pakistan, where convective overturn due to surface water cooling stimulates productivity (Wyrtki, 1973; Banse, 1987; Bauer et al., 1991; Madhupratap et al., 1996). Annual productivity rates are between 200 and 400 $gC.m^{-2}.yr^{-1}$ (Kabanova, 1968; Qasim, 1982; Codispoti, 1991).

Temporal variations in OMZ intensity occur at orbital and sub-orbital

time scales (Altabet et al, 1995; Reichart et al., 1997, 1998; Den Dulk et al., 1998; Schulz et al, 1998; Von Rad et al, 1999). These changes are presumably linked to 1) changes in summer monsoon wind strength, which via coastal and oceanic upwelling controls summer surface water productivity and subsurface oxygen consumption (Altabet et al, 1995; Reichart et al., 1997; Schulz et al, 1998), 2) deep convective mixing during periods of cold and intensified winter monsoon (Reichart et al., 1998), and 3) changes in production of intermediate and deep water masses (Olson et al., 1993; Zahn and Pedersen, 1991; Rohling and Zachariasse, 1996). In a previous study on an OMZ sediment core from the Pakistan Margin (NIOP455) we showed that benthic foraminifers proved to be well suited for tracing past changes in surface water productivity and OMZ intensity in the northern Arabian Sea (Den Dulk et al., 1998). The present study extends the former by comparing changes in benthic foraminiferal composition and benthic foraminiferal accumulation rates in two cores from sites of Murray Ridge with contrasting bottom water oxygen conditions. Core NIOP463 is located in the dysoxic lower part of the OMZ ($[O_2] < 0.05$ ml/l), whereas the other core, NIOP464, is located ~65 km to the west and below the OMZ ($[O_2] \sim 0.9$ ml/l). The implicit assumption in our study is that the time-averaged conditions at our core sites are very similar as far as surface water processes are concerned. With this basic assumption we consider modern or fossil local differences as subordinate to the large-scale and long-term environmental overprint.

3. Material and methods

Cores NIOP463 and -464 were collected in 1992 during the Netherlands Indian Ocean Program. Both core stations are located on the Murray Ridge at 920 m (base OMZ) and 1470 m (below OMZ) water depth, respectively (Fig. 1). The sediments essentially consist of homogenous, dark-greenish to light greenish/gray hemipelagic mud. Visual observation and X-ray radiographs show several distinctly to faintly laminated intervals in NIOP463. Samples were taken for benthic foraminiferal counts, organic carbon, elemental and oxygen isotope analyses. Sample resolution for benthic foraminferal analyses is ~17 cm (=~2400 yrs) for NIOP463 and ~13 cm (=~2000 yrs) for NIOP464. For geochemical analyses sample resolution is about half that distance.

The $\delta^{18}O$ record of NIOP463 and -464 (Fig. 3, 4) is based on measuring about 100 hand-picked specimens of the planktonic foraminiferal species

Neogloboquadrina dutertrei per sample on a mass spectrometer (VG SIRA 24). Samples were treated according to standard procedures with international and in-house standards (NBS-14, -18). Replicate analyses show a standard deviation of 0.1‰ for $\delta^{18}O$.

For the analyses of organic carbon (C_{org}), about 1 g of dry sediment was weighed in a centrifuge tube. Carbonate was dissolved in 1 M HCl under mechanical shaking for 12 hours, after which the samples were rinsed with demineralized water in order to remove $CaCl_2$ and subsequently dried. The C_{org} content was determined using a CNS-analyser (Fisons NA 1500). An aliquot of the samples was thoroughly ground in an agate mortar after freeze drying and before dissolution of 250 mg in 5 ml of a 6.5: 2.5: 1 mixture of $HClO_4$(60%)-HNO_3(65%) and H_2O and 5 ml HF(40%) at 90 °C. The dried residue was dissolved in 1 M HCl for analysis of Al, Mn, and V with an ICP-AES (Perkin Elmer OPTIMA 3000). Analytical precision and accuracy were determined by replicate analyses of samples and by comparison with international (SO-1, SO-3) and in-house standards. Both were found to be better than 3%. To distinguish changes that are not caused by dilution with $CaCO_3$ or a variable input of terrestrial sediments, elements are normalized to Al.

For the benthic foraminiferal analyses, we processed 88 samples from NIOP463 and 108 samples from NIOP464. The sediment was freeze dried, dry weighed, washed, and wet sieved. The residues of the 150-595 μm fraction were split into aliquots containing at least 200 and generally about 250 specimens (using an Otto microsplitter). Although many small species do not occur in this larger size fraction, it is generally accepted that the 150-595 μm fraction accurately reflects environmental change. All specimens were picked, mounted on slides, identified and counted. The general faunal characteristics are expressed as Shannon diversity, equitability and dominance (= percentage of most frequent species), and are based on all species identified prior to (generic) grouping for the statistical analyses. Taxa and species groups that display abundances higher than 5% were selected for statistical analyses in SPSS (constitutes at least 70% of benthic foraminiferal assemblage). The frequency data were subjected to a principal component analysis, cluster analysis and spectral analysis (see for instance Reichart et al. (1998) for discussion of spectral analysis method employed). The matrix of similarity coefficients between species and Shannon diversity and dominance, respectively, was used for ordination of the species against Shannon diversity and dominance. Benthic Foraminiferal Accumulation Rates (BFAR's) were calculated by multiplying numbers per volume and linear sedimentation rates.

Table 1
AMS ^{14}C ages for two levels in core NIOP463

Sample	Depth (cm)	^{14}C ages (yr BP)	$^{14}C_{cor.}$ ages (yr BP)	$^{14}C_{cal.}$ ages (yr BP)
GrA-352	10.5	12,010±90	11,610	13,750
GrA-350	84.5	16,700±100	16,300	20,000

Pteropod preservation is defined by an index which ranges from 0 to 3 (0 = no pteropods, 1 = few small fragments, 2 = many medium sized fragments, 3 = abundant medium sized fragments). The planktonic foraminifer *Globorotalia truncatulinoides* is occasionally present in low quantities (≤ 3% in quantitative planktonic foraminiferal counts). Therefore, *G. truncatulinoides* is quantified by counting numbers in 27 (of 45) fields in a rectangular picking tray to a maximum of 30 specimens.

The chronology of both cores is based on linear interpolation between $\delta^{18}O$ events, of which the age was obtained by calibrating these events to an orbital-tuned $\delta^{18}O$ record (details, in Reichart et al., 1998). Two additional calibration points were provided by AMS^{14}C datings in NIOP463 (Table 1). The ^{14}C ages were calibrated to the U/Th timescale (Bard et al., 1990) and corrected for a reservoir age of 400 year (Bard, 1988). Table 2 lists SPECMAP $\delta^{18}O$ events (Imbrie et al., 1984) and their ages (Martinson et al., 1987), which were identified in the $\delta^{18}O$ record of core NIOP464 (Reichart et al., 1997), plus their converted ages using the orbital-tuned time scale of Reichart et al. (1998). Each core contains two full glacial cycles. The base of NIOP463 and NIOP464 have extrapolated ages of ~205 ka and ~225 ka, respectively. Linear sedimentation rates vary between 3.4 and 17.6 cm/kyr in NIOP463 and between 3.5 and 13.5 cm/kyr in NIOP464.

4. Results

4.1 Mn, V, and organic carbon records

Variations of the redox sensitive elements manganese (Mn) and vanadium (V) (Fig. 2) record past changes in oxygen levels of the bottom water and can be used to reconstruct variations in OMZ intensity. Mn (IV) is reduced to its soluble Mn (II) state under dysoxic conditions, which might result in the loss of Mn from the sediment. Surface sediments deposited within the present-day OMZ are depleted in Mn (Van der Weijden et al., 1999), because low oxygen

Table 2.
Table 2 lists SPECMAP $\delta^{18}O$ events (Imbrie et al., 1984) and their ages (Martinson et al., 1987), which were identified in the $\delta^{18}O$ record of core NIOP464 (Reichart et al., 1997), plus their converted ages using the orbital-tuned time scale of Reichart et al. (1998).

SPECMAP-event (Imbrie et al., 1984)	Event age (Martinson et al., 1987)	Age in orbital-tuned time scale (Reichart et al., 1998)
2	12.05	14.50
3	24.11	23.41
3.3	50.21	56.25
3.31	55.45	61.44
4	58.96	64.30
5	73.91	76.95
5.1	79.25	81.50
5.3	99.38	102.50
5.5	123.82	128.15
6	129.84	131.70
6.3	142.28	144.26
6.41	161.34	161.71
6.42	165.35	165.42
6.5	175.05	176.65
6.6	183.30	183.00
7	189.61	190.16
7.1	193.07	193.00
7.2	200.57	204.92
7.3	215.54	219.48

conditions prevent the recycling of Mn-oxides. Only when surface sediments are oxygenated can porewater Mn-concentrations get sufficiently high to form Mn-carbonate phases (Calvert et al., 1996). Because Mn-carbonate is preserved during burial under anoxic conditions, Mn can be used as a paleoredox proxy. Vanadium is transported to the sediments as a reduced species that is released from the sediments by oxidation. Therefore the accumulation of V is favoured by dysoxic bottom waters at the time of deposition (Ripley et al., 1990; Shaw et al., 1990; Breit and Wanty, 1991). The primary redox signal remains preserved during subsequent burial under anoxic conditions. Mn/Al values vary between 60-90x10^{-4} and V/Al values between 15-30x10^{-4} in NIOP463. Low Mn/Al values in NIOP463 are recorded around 192, 170, 148, between

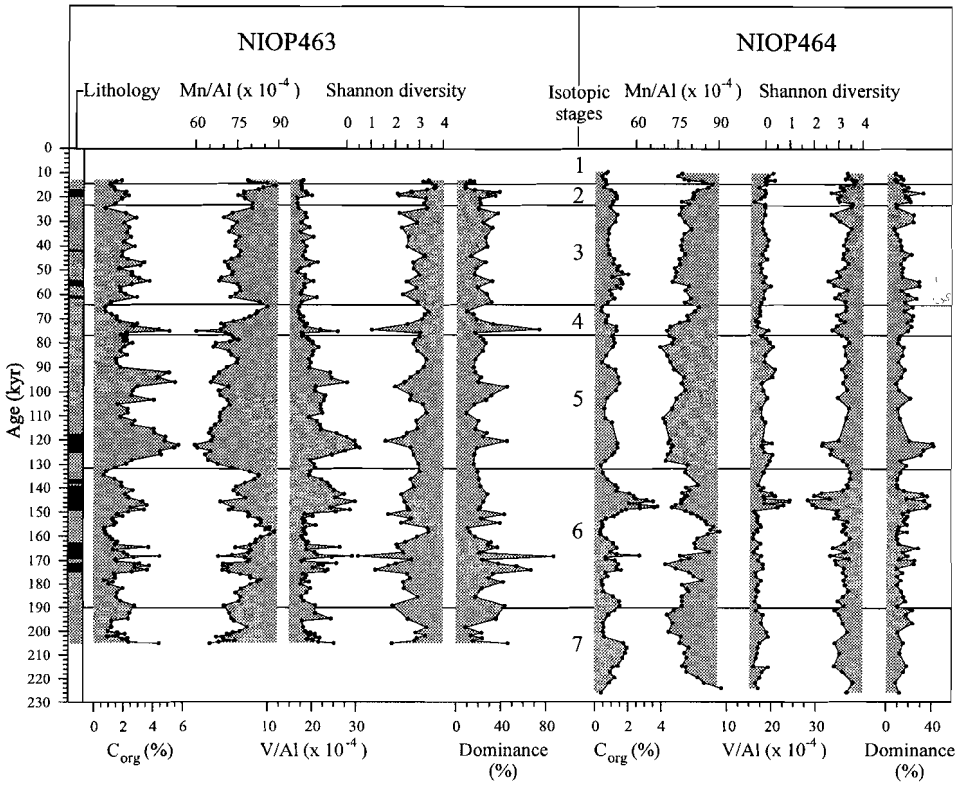

Figure 2 Organic carbon (%), V/Al-, Mn/Al-, Shannon diversity and dominance for NIOP463 and -464 plotted versus age. Laminated intervals in NIOP463 are shown in the first column.

130 and 70, and between 60 and 25 ka and generally correlate with high V/Al values (Fig. 2). Variability in Mn/Al is less in NIOP464; i.e. lowest values are around $70x10^{-4}$. Only one peak (around 148 ka) of about $25x10^{-4}$ is observed in the V/Al record of NIOP464. High Mn/Al values in NIOP464 are time-equivalent with the high values in NIOP463. Also the peak values ~148 ka in the V/Al record of NIOP464 correlates with elevated values in NIOP463.

Figure 2 also presents variations in the organic carbon content and the occurrence of laminated intervals. Organic carbon values vary between ~0.5% and ~6% in NIOP463. Maximum values are generally lower (≤ 3%) in NIOP464, but correlate with high C_{org} values in NIOP463. Laminated intervals occur in NIOP463 only and are associated with relatively high C_{org} values, low Mn-Al, and high V-Al ratios.

4.2 Benthic foraminiferal patterns

The benthic foraminiferal records of NIOP463 and -464 show distinct changes in overall composition. Dominances range from 7.5% to 87% in NIOP463 and from 7.5% to 39% in NIOP464. Intervals with high benthic diversity contain about 40-50 different taxa with dominances being on average between 10-15%. In low-diversity intervals, the number of taxa decreases to less than 20 or to around 10 in the most extreme cases. The distributions of quantitatively important taxa are illustrated in Figures 3 and 4. In NIOP463 these taxa are *Bolivina alata*, *Bolivina dilatata*, *Bulimina exilis*, *Cassidulina carinata*, *Ehrenbergina pacifica*, *Globobulimina affinis*, *Osangularia* spp, *Rotaliatinopsis semiinvoluta*, *Uvigerina* spp. and *Uvigerina proboscidea* (Fig. 3). In NIOP464 *Bulimina aculeata*, *B. exilis*, *C. carinata*, *Cassidulina subglobosa*, *Chilostomella oolina*, *E. pacifica*, *Fursenkoina bradyi*, *R. semiinvoluta*, *Uvigerina* spp, *U. proboscidea* are the most common taxa (Fig. 4). They all display peak abundances of more than 20%.

Cluster analysis shows that taxa with similar distribution patterns are grouped by hierarchical clustering into five clusters (Fig. 5). The close correlation of *C. oolina* and *F. bradyi* in cluster I is primarily based on their co-occurrence in NIOP464; *C. oolina* shows low percentages (< 3%) in NIOP463. A number of elements of cluster III, e.g. *Ceratobulimina pacifica*, *Hanzawaia boueana*, *Karreriella bradyi*, *Astrononion* spp., are characteristic of, or primarily occur in, NIOP464. Miliolids, grouped in cluster III, are very diverse. The assemblage is dominated by species belonging to *Quinqueloculina*, *Pyrgo*, *Nummuloculina*, *Triloculina*, and *Sigmoilopsis*. Most of the species that are quantitatively important in one, or both, core(s) are joined in clusters IV and V.

Table 3 lists the correlation coefficients between Shannon diversity and

Table 3.
Correlation coefficients of Shannon diversity with dominance and equitability, respectively, in NIOP463 and -464.

	Shannon diversity	
	NIOP463	NIOP464
Dominance	- 0.92	-0.87
Equitability	0.87	0.71

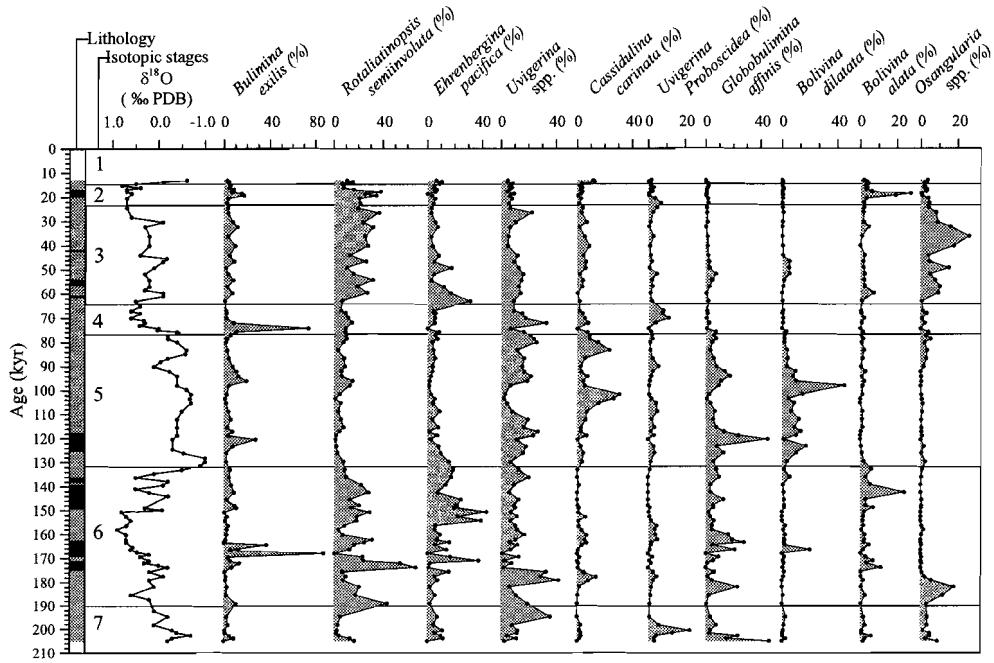

Figure 3 Percentages of quantitatively important species in NIOP463 plotted versus age. Laminated intervals are shown in the first column

equitability and dominance, respectively in NIOP463 and -464. They are highly correlated in both cores and show predictable patterns; i.e. a high (low) Shannon diversity corresponds with high (low) equitability and low (high) dominances. Down core variations in Shannon diversity and dominance are shown in Figure 2. Generally, diversities are highest in NIOP464, whereas dominances are highest in NIOP463. In NIOP463 some marked intervals with low benthic diversity are observed; these are only partly reflected in NIOP464.

The relationship between the general faunal characteristics and the benthic frequency data in NIOP463 and -464 is illustrated in Figure 6. Benthic foraminiferal species are ordinated along the faunal dominance and diversity gradients, using similarity coefficients. In the scatter-plots of the similarity coefficients the benthic foraminifera are separated along a gradient from species typically occurring under high diversity/low dominance to low diversity/high dominance. It can be seen that the hierarchical cluster analysis successfully differentiated the species that are separated along this gradient (Fig. 5). In both records *R. semiinvoluta* and *B. exilis* (elements of cluster V)

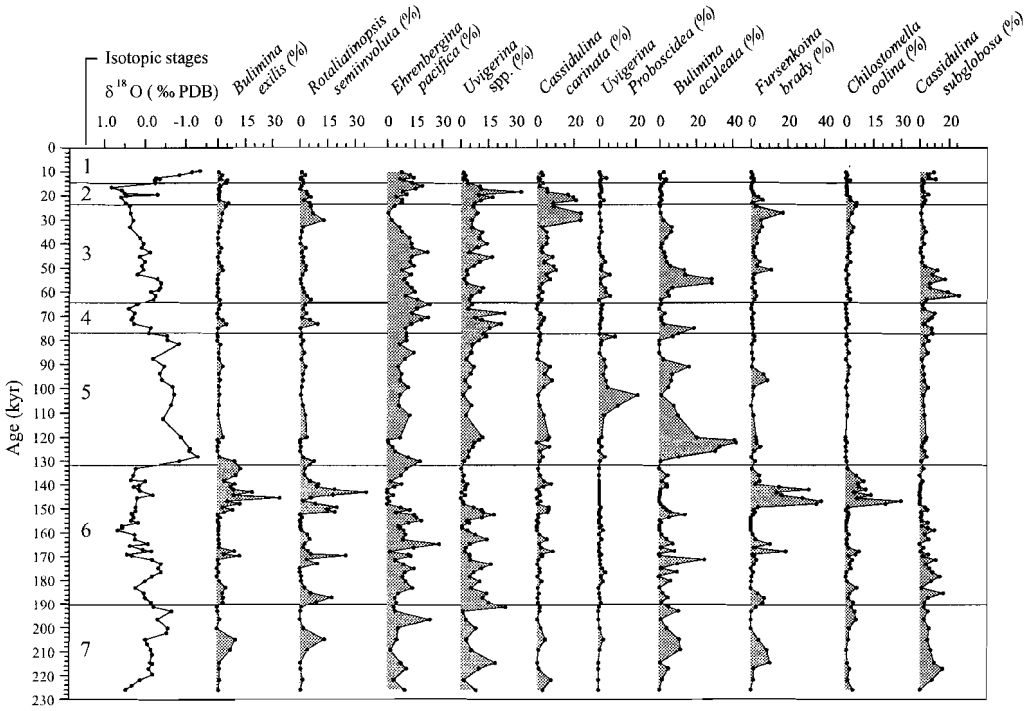

Figure 4 Percentages of quantitatively important species in NIOP464 plotted versus age.

plot relatively high on the dominance axis and low on the diversity axis. This pattern is the same, although somewhat less clearly so, for other members of cluster V and some of cluster IV (*Uvigerina* spp.). Species of cluster III (e.g. miliolids, *S. bulloides* and *Cibicides bradyi*) plot at the other extreme of the diversity and dominance axes. Still quite negatively related to dominance and positively related to diversity are several species of cluster II. Thus individual taxa in both cores roughly order the same with respect to the general faunal characteristics.

The average faunal composition in NIOP463 and -464 is illustrated in pie diagrams (Fig. 6). The diagrams reveal a substantial difference between the two cores. Whereas elements of clusters IV and V make up the majority of the fauna in NIOP463, elements of cluster II and III are more important in NIOP464. These results show that the benthic foraminiferal associations from the core presently located in the OMZ (NIOP463), are distinctly different from the core below the OMZ (NIOP464), which is also suggested by the lower diversities and higher dominances prevailing in the OMZ core.

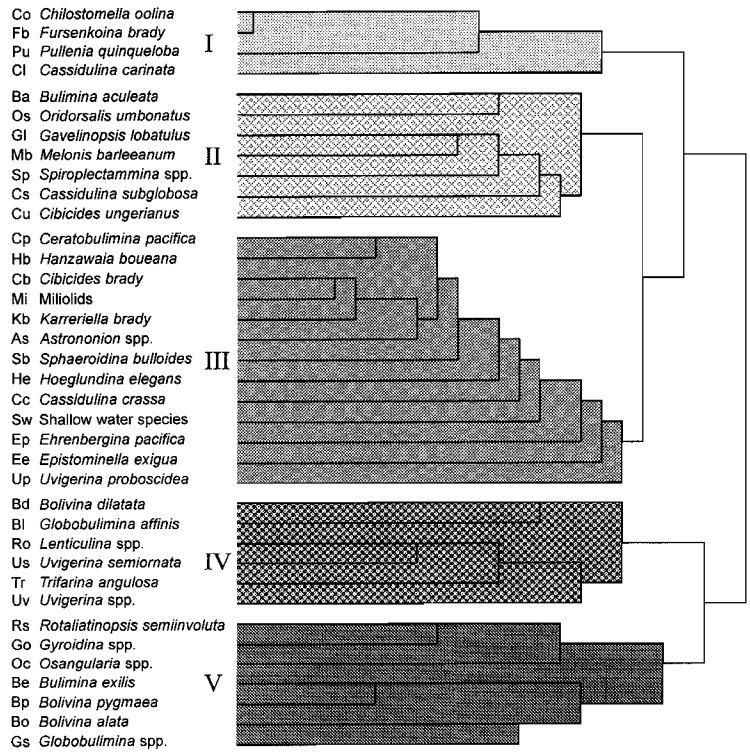

Figure 5 Cluster diagram of 37 benthic foraminiferal species in NIOP463 and -464. Individual clusters are given roman numbers I-V.

5. Discussion

5.1 The productivity and oxygen regime of the cores

Downcore variations in organic carbon can be correlated throughout the northern Arabian Sea and across a wide depth range (within and below the OMZ), and covary with changes in other proxy records for surface water productivity (e.g. Ba/Al, *Globigerina bulloides*: Clemens et al., 1991; Murray and Prell, 1992; Shimmield, 1992; Anderson and Prell, 1993; Ten Kate et al., 1994; Reichart et al.,1997, 1998; Den Dulk et al., 1998, Des Combes, 1999; Von Rad et al, 1999). The C_{org} records in the northern Arabian Sea, therefore, are primarily shaped by changes in surface water productivity, and show a strong variability in the precession band of orbital forcing, with maxima being associated with maxima in summer monsoon intensity related to northern

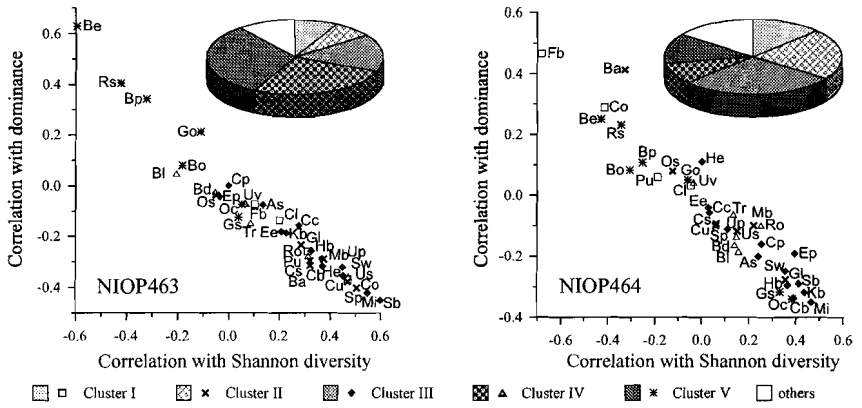

Figure 6 Scatter diagrams show the benthic foraminiferal species (codes listed in Figure 5) ordinated along dominance and diversity gradients using similarity coefficients. Pie diagrams illustrate the relative contribution of the clusters from the cluster diagram (Fig. 5) to the overall fauna composition in NIOP463 and -464. 'Others' contain low-frequency and unidentified species.

hemisphere summer insolation (Reichart et al., 1997, 1998). Altabet (1995), Reichart et al. (1997, 1998), Den Dulk et al. (1998), and Von Rad et al. (1999) have shown by using a variety of proxies that periods of high surface water productivity are associated with an intense OMZ and vice versa. A similar relationship is suggested by the concurrent maxima in C_{org} and V/Al, and minima in Mn/Al in NIOP463 and -464 (Fig. 2).

In view of the fact that the stations of NIOP463 and -464 are located in an open ocean setting only ~65 km apart, we assume that export productivity rates are similar at both stations. The difference in water depth (550 m), however, results in less organic matter arriving at the sediment-water interface of the deeper station NIOP464, due to the ongoing decay of organic matter with depth. Incorporating primary productivity and water depth in the equation from e.g. Betzer et al. (1984) or Berger and Wefer (1990), it can be calculated that the difference in settling flux between the two stations should amount to about 25-30% in an oxic water column. For example, with an initial primary production of 200 $gC.m^{-2}.yr^{-1}$, the C_{org} fluxes arriving at the stations are 9.8 $gC.m^{-2}.yr^{-1}$ at NIOP463 and 7.3 $gC.m^{-2}.yr^{-1}$ at NIOP464. Yet, considerable larger inter-core differences in C_{org} are observed: in intervals with high organic carbon content, C_{org} concentrations are generally 50-70% higher in NIOP463 (Fig. 2). Even if one corrects for the lower flux arriving at the deeper station NIOP464, differences are high, which was the reason for Reichart (1997) to conclude that there is a large difference in organic matter

burial efficiency between stations NIOP463 and NIOP464. The reason for this is that NIOP463 experienced more severe periods of dysoxic bottom water conditions than NIOP464. Reichart (1997) calculated that during periods of an intense OMZ the burial efficiency of organic matter at station NIOP463 was 2.5 times higher that at station NIOP464. Besides the Mn/Al and V/Al records, the different bottom water oxygen history at both stations is also nicely reflected in the presence of laminated intervals in NIOP463 and their absence in NIOP464 (Fig. 2).

5.2 Benthic foraminiferal response to changes in bottom water oxygenation

Differences in the bottom water oxygen history between the two stations are reflected in the benthic foraminiferal record. As pointed out before, species belonging to cluster IV and V are more frequent in NIOP463, whereas those belonging to cluster III proliferate in NIOP464 (Fig. 6). The majority of the species of cluster IV and V are known as markers of oxygen deficient waters (Phleger and Soutar, 1973; Miller and Lohmann, 1982; Lutze and Coulbourn, 1984; Hermelin and Shimmield, 1990; Miao and Thunell, 1993; Sen Gupta and Machain-Castillo, 1993; Jannink et al., 1998). The overall less aerated conditions at station NIOP463 are also reflected in the generally lower diversities and higher dominances (Fig. 2). Whereas low diversity intervals are not so pronounced in NIOP464, percentages of species belonging to cluster III clearly show similar patterns in both cores (Fig. 7). Species belonging to Cluster III are thriving in diverse associations with relatively low dominances. This indicates that they are characteristic for non-stressed conditions. Moreover, a number of these species (e.g. miliolids, *C. ungerianus*, *C. bradyi*, *S. bulloides*) are known to be intolerant to oxygen stress (Mullineaux and Lohmann, 1981; Denne and Sen Gupta, 1991; Barmawidjaja et al.,1992; Kaiho,1994). High joint frequencies of cluster III species are, therefore, indicative of a well-oxygenated benthic environment. As the redox-proxy records, their co-varying patterns suggest that changes in bottom and pore water oxygenation affected both stations. Spectra, furthermore, show that Cluster III species vary strongly in the 23 kyr frequency band (Fig. 8). This confirms a close correspondence with precession induced changes in surface water productivity and OMZ intensity.

Miliolids are rare or absent in oxygen deficient environments (Mullineaux and Lohmann, 1981; Nolet and Corliss, 1990; Moodley et al., 1998b; Jannink et. al., 1998; Jorissen, 1999) and can thus be regarded as sensitive oxygen markers. In NIOP463 their occurrence is, indeed, sporadic. If present, they

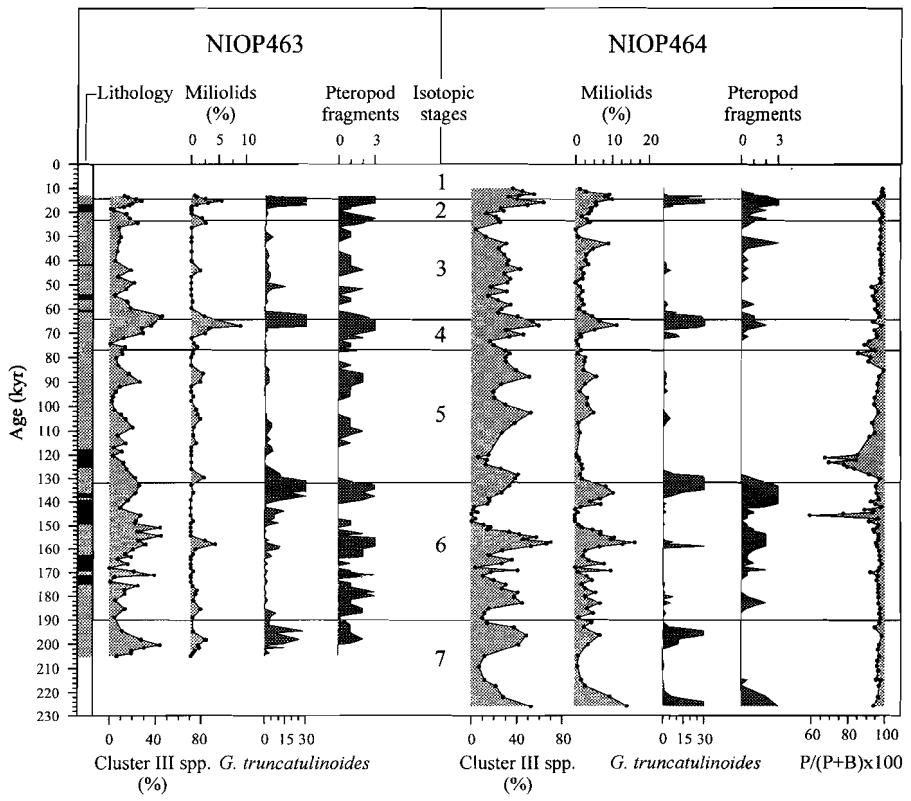

Figure 7 Records of Cluster III species (%), miliolids (%), occurrences of *G. truncatulinoides*, and pteropod preservation of NIOP463 and -464, and planktic to benthic foraminiferal ratio's (=P/P+B) of NIOP464 plotted versus age. Laminated intervals in NIOP463 are shown in the first column.

suggest a better ventilation of the OMZ. The far more persistent occurrence of miliolids in NIOP464, suggests an overall better oxygenation of the benthic environment. Similar to the cluster III species, percentages of miliolids show time equivalent maxima in both cores, which should mark periods during which the OMZ was at least substantially weakened. Most of these periods of better oxygenation in both cores are characterised by occurrences of the planktonic foraminifer *Globorotalia truncatulinoides* (Fig. 7). Reichart et al. (1998) interpreted the occasional presence of *G. truncatulinoides* as indicative of intensified winter mixing, resulting in the breakdown of the OMZ. A breakdown of the OMZ during periods corresponding with intervals of *G. truncatulinoides* is in agreement with our benthic record, which, furthermore,

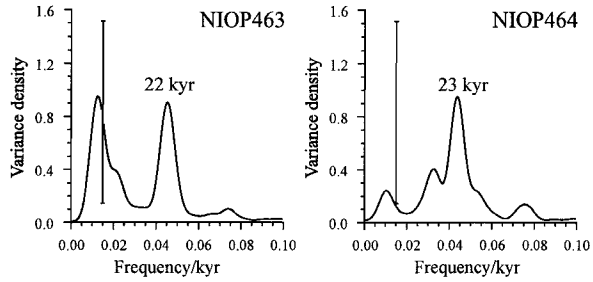

Figure 8 Spectra of Cluster III species in NIOP463 and -464. Spectral estimates are based on a Parzen smoothing window with 190 lags and an interpolated time interval of 1 kyr, resulting in a bandwidth of 0.0097. Spectral densities are normalized and plotted on a linear scale. Vertical bar indicates 95 % confidence limit.

suggests that counting miliolids is a rapid tool for reconstructing past changes in bottom and pore water oxygenation.

A potential caveat in the use of miliolids is their solution prone test (Corliss and Honjo, 1981; Machain-Castillo et al., 1998), which might lead to reconstructed bottom water oxygenation levels which are too low. Although the present-day lysocline in the Arabian Sea lies well below the OMZ at ~3000 m water depth, calcite dissolution can occur at shallower depths. This so-called supralysoclinal dissolution occurs at or close to the sediment water interface due to the release of CO_2 during oxic decomposition of organic matter (Morse and Mackenzie, 1990). Furthermore, within the OMZ oxidation of ammonia to nitrate and the addition of CO_2 as a consequence of oxygen consumption, lowers the solution pH and carbonate saturation (Canfield and Raiswell, 1991). Dissolution only takes place at or close to the sediment water interface because the increase in alkalinity brought about by sulfate reduction deeper in the organic rich sediments enhances carbonate preservation. Figure 7 shows that in NIOP463 absence of miliolids covaries with intervals devoid of pteropods. These minima in the pteropod preservation index, furthermore, correspond with maxima in C_{org} (%) (Fig. 2).

Since pteropod shells are made up of aragonite and are more susceptible to dissolution than the calcitic miliolid group, this suggests that only at times of enhanced sea surface productivity and an intense OMZ, miliolids might have been affected by supralysoclinal dissolution. Although supralysoclinal dissolution may occur during oxic decomposition of organic matter, particularly intense supralysoclinal dissolution has been related to dysoxic (OMZ) conditions (Berelson et al., 1996). This implies that the absence of miliolids in NIOP463 at times of enhanced sea surface productivity could be (partly) due to selective dissolution. Furthermore, that differences in

supralysoclinal dissolution may explain the differences between percentages of miliolids in NIOP463 and -464 in these intervals.

Similar differences between percentages of miliolids in NIOP463 and -464, however, also occur in intervals with pteropods preserved in both cores (Fig. 7). These cannot be attributed to supralysoclinal dissolution, thus are more likely caused by changes in bottom and pore water oxygenation. Although we cannot exclude that the absence of miliolids in NIOP463 is (partly) due to selective dissolution, fluctuations in miliolids in NIOP464 do not seem to be strongly influenced by supralysoclinal dissolution. The ratio of planktic/benthic foraminifers in NIOP464 shows only 2 intervals (around 120 ka and 145 ka) where P/B ratio's are significantly reduced (Fig. 7). This could indicate a significant loss of $CaCO_3$ through dissolution because planktonic foraminifers are more prone to dissolution than benthic foraminifers (Douglas and Woodruff, 1981). Reichart et al (1997) already concluded that the low carbonate values around 120 ka and 145 ka in NIOP464, are likely to be the result of decreased pelagic carbonate production and/or increased supralysoclinal dissolution during a period of high surface water productivity. In summary, we conclude then that dissolution may have contributed to the shaping of the miliolid pattern, but we hold the opinion that their fluctuations are predominantly driven by variations in bottom and pore water oxygenation.

5.3 Microhabitats, bottom water oxygenation and organic matter

Benthic foraminifera are considered particularly useful for estimating paleoflux since they are more resistant to diagenetic changes caused by dissolution or oxidation than for example planktonic foraminifera or accumulation of organic carbon (Corliss and Chen, 1988). These authors suggested a close relation between the percentage of infauna and organic flux. Recently, Jorissen et al. (1995) summarized most ideas on foraminiferal microhabitat distribution in a simple but attractive model in which the infaunal distribution was thought to be limited by oxygen in eutrophic environments, and by food in oligotrophic ones. However, Jannink et al. (1998) have shown the existence of a flourishing benthic foraminiferal community in the severely dysoxic bottom waters of the northern Arabian Sea OMZ, indicating that oxygen itself is no limiting factor. Moodley et al. (1998) showed that the formation of H_2S in combination with anoxic conditions is possibly the actual limiting factor in benthic foraminiferal survival. H_2S is produced during sulfate reduction as organic matter is oxidised

Table 4.

Epifauna	
Cibicides ungerianus	2, 7, 12, (13, SI)
Epistominella exigua	1, 7, 10, 11, 12
Gavelinopsis lobatulus	(3, E/SI), 10, (13*, SI)
Hanzawaia boueana	1*
Oridorsalis umbonatus.	1, (3, T), 7, 10, (13, E/SI)
Shallow water species	10*
Shallow infauna	
Astrononion spp.	(1*, I), (13*, II)
Cassidulina crassa	11
Cassidulina carinata	10
Ceratobulimina pacifica	
Cibicides bradyi	(2*, II), (3, T), (7, I)
Ehrenbergina pacifica	
Gyroidina spp.	(1, E), (7, E), 10
Hoeglundina elegans	(2, E), (3, E/SI), 6, 10, (13, E/SI)
Karreriella bradyi	13
Miliolids	(1, E), (2, E), (3, E), 6, (7, E), 10, 13
Osangularia spp.	
Pullenia quinqueloba	(2*, II), (7, SI/II), 13
Lenticulina spp.	(1, E), 2, (3, E/SI)
Sphaeroidina bulloides	13
Spiroplectammina spp.	
Trifarina angulosa	(1, I), 2, 3, 7, 11
Uvigerina spp.	(1, I), 2, 3, 6, 7, 9, 10, 13
Uvigerina semiornata	2*, 11*, 13*
Intermediate infauna	
Bulimina aculeata	(2, SI), (9, SI), 12
Cassidulina subglobosa	(1*, I), (7*, E)
Melonis barleeanum	2, (6, DI), 7, 10, 11, 13
Rotaliatinopsis semiinvoluta	12
Uvigerina proboscidea	(3, SI)
Deep infauna	
Bolivina alata	
Bolivina dilatata	4, 10, 11, 12
Bolivina pygmaea	
Globobulimina affinis	2, 5, 6, 8, 9
Bulimina exilis	6, 10
Chilostomella oolina	2, 3, 5, 6, 7, 10, 13
Fursenkoina bradyi	2, 7, 8*
Globobulimina spp.	3, 7, 10, 11, 13

when other, thermodynamically more favourable, oxidants are exhausted. The results of Jannink et al. (1998), thus, implies that sulfate reduction is absent in surface sediments from the present-day northern Arabian Sea OMZ. This supports the conclusion reached by Van der Weijden et al. (1999).

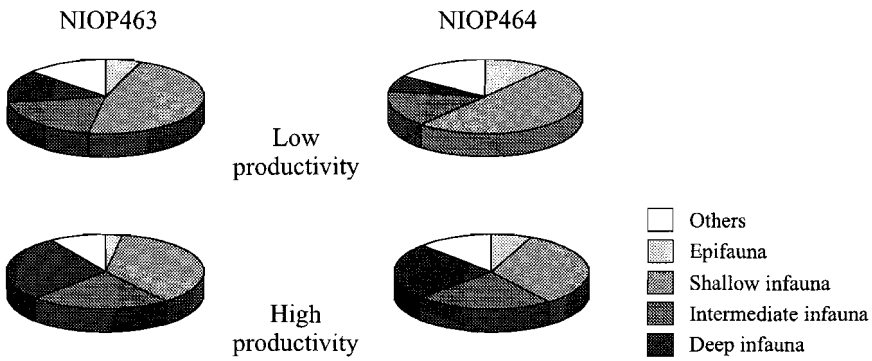

Figure 9 Pie diagrams illustrate the proportion of each microhabitat group in the average faunal composition under low and high productivity conditions in NIOP463 and -464. Samples were arbitrarily grouped using lower (higher) than 1.5% C_{org} indicating low (high) productivity conditions in NIOP463, and using lower (higher) than 1.2% C_{org} indicating low (high) productivity conditions in NIOP464. 'Others' contain low frequency and unidentified species.

In Table 4 we summarise the faunal distribution in NIOP463 and -464 in terms of preferred position of species in the sediment column. Although species microhabitat distribution is very dynamic, certain species are frequently reported as epifaunal, shallow- , intermediate- or deep infaunal (Corliss, 1985, 1991; Corliss and Chen, 1988; Corliss and Emerson, 1990;

Table 4 Arbitrary subdivision of benthic foraminifera into microhabitat categories based on the following references: 1) Corliss and Chen (1988); 2) Corliss (1991); 3) Rathburn and Corliss (1991); 4) Barmawidjaja (1992); 5) Bernhard (1992); 6) Buzas et al. (1993); 7) Gooday (1994); 8) Kitazato (1994); 9) McCorkle et al. (1997); 10) Guichard (1997); 11) De Stigter et al. (1998); 12) Jannink et al. (1998); 13) Jorissen et al. (1998). In a number of cases no references were found or taxa were classified differently (or data suggest taxa should be classified differently). In the latter case the references are between brackets, and added are abbreviations reflecting the categories the taxa were assigned to by these authors: E = Epifauna, SI = Shallow infauna, II = Intermediate Infauna, DI = Deep Infauna, I = Infauna, and T = transitional II/DI. * indicates references classifying comparable species, or species differently named. We, furthermore, included results from Jannink et al., (1998), because this paper discusses living (Rose Bengal Stained) benthic foraminifera from the northern Arabian Sea. However, subdividing the foraminifera into microhabitat categories is somewhat difficult in this case. In the northern Arabian Sea high productivity /low oxygen setting the overall in-sediment penetration depth is shallow and does not reflect an extended microhabitat partitioning (Jannink et al.,1998).

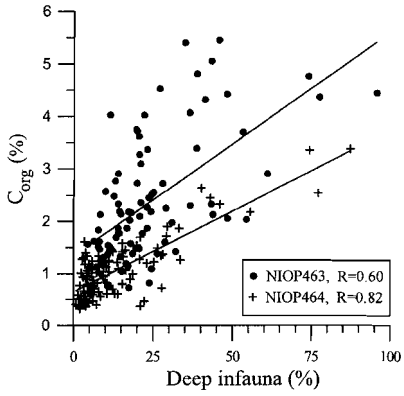

Figure 10 Scatter-plot of deep infaunal species (%) versus C_{org} (%).

Rathburn and Corliss, 1994; Barmawidjaja et al., 1992; Bernhard, 1992; Buzas et al., 1993; Gooday, 1994; Kitazato, 1994; McCorkle et al., 1997; Guichard, 1997; De Stigter et al., 1998; Jannink et al., 1998; Jorissen et al., 1998; Jorissen and Wittling, 1999). The prefixes deep and shallow are used in a relative sense, since with the upward migration of the sulfide producing front, deep infaunal species could be forced to live close to the sediment-water interface. Figure 9 shows the properties of each of the four categories in both cores under low and high productivity conditions. The figure demonstrates that deep infaunal species are most abundant under high productivity conditions, and vice versa. This implies that a positive correlation should exist between C_{org} (%) and percentages of deep infaunal species, which is indeed seen in the plot of C_{org} values and joint frequencies of deep infaunal species (Fig. 10). Since the higher C_{org} concentrations in NIOP463 are presumably explained by a higher anoxic burial efficiency, Figure 10 also suggests that the proportion of deep infaunal species is a measure for the storage of organic matter and not directly for the arriving flux at the seabed. Highest epifaunal and shallow infaunal frequencies occur under low productivity conditions (Fig. 9). Species of Cluster III are all classified shallow infaunal or epifaunal. We concluded earlier that this group is sensitive to oxygen variations and for this reason it is unsuited for reconstructing past changes in organic flux and export productivity.

5.4 Benthic Foraminiferal Accumulation Rates and oxygen

Benthic foraminiferal accumulation rates (BFAR's) are often used as a proxy for surface water productivity since benthic foraminiferal densities correlate with the C_{org} content in the sediment (Herguera and Berger, 1991). However, this relationship between BFAR and C_{org} content is based on samples from oxic environments, and might break down in less oxygenated environments because benthic numbers are thought to be very sensitive to

bottom water oxygen concentrations (Verhallen, 1991; Van der Zwaan and Jorissen, 1991; Moodley et al. 1997). The general idea is that with decreasing bottom water oxygen levels the total meiofaunal benthic biomass first increases due to decreased predation by, and competition with the declining macrofauna (Verhallen, 1991). At a certain critical oxygen content meiofaunal standing stocks start to rapidly diminish (Josefson and Widbom, 1988) and eventually only the microbial communities remain, although recent experiments have shown that many benthic foraminiferal species are very resistant to prolonged anoxia (Josefson and Widbom, 1988; Bernhard, 1993; Alve and Bernhard, 1995; Bernhard and Alve, 1996; Moodley et al., 1998a,b).

To evaluate the potential use of BFAR for paleoproductivity reconstructions under various stages of dysoxia we compared BFAR's in the studied cores. Sedimentation rate is critically for calculating BFAR's. Inaccuracies in sedimentation rates are inevitable because calculated average sedimentation rates between calibration points may actually be variable, resulting in BFAR's which are too low or too high. We assume, however, that major inter-core differences cannot be attributed to large differences in sedimentation rates, because both cores are tuned similarly using the precession cycle. This allows for maximal inter-core differences of about 5 kyr per individual cycle, which could result in maximum inaccuracies in average sedimentation rates per precession cycle of 5/23 of the sedimentation rate. Changes in BFAR's are several times higher than what can be explained by tuning inaccuracies. To further discuss BFAR results we used the equation:

$$J(z) = 31 + 1.06\ BFAR \qquad \text{Eq.1 (Herguera and Berger, 1991)}$$

to calculate J(z) values for both cores. J(z) is flux arriving at depth z. We recalculated primary production ([PP] = $gC.m^{-2}.yr^{-1}$) values to compare BFAR's from different depth's, using J(z) in the following way:

$$J(z) = ((2\sqrt{PP})*PP)/Z + ((5/\sqrt{PP})*PP)/\sqrt{Z} \qquad \text{Eq.2 (Berger and Wefer, 1990)}$$

Calculated PP values vary between 44 $gC.m^{-2}.yr^{-1}$ and 1623 $gC.m^{-2}.yr^{-1}$ for NIOP463 and between 78 $gC.m^{-2}.yr^{-1}$ and 1868 $gC.m^{-2}.yr^{-1}$ for NIOP464 (Fig. 11). The majority of the PP-values in both cores varies between 300 $gC.m^{-2}.yr^{-1}$ and 700 $gC.m^{-2}.yr^{-1}$. Lowest calculated PP-values are in the range of modern open ocean low productivity settings (Berger et al., 1989), and might be realistic for periods of low surface water productivity. Peak values are about 6 times higher than present annual primary productivity rates in the northern Arabian Sea (= 200-400 $gC.m^{-2}.yr^{-1}$; Kabanova, 1968; Qasim, 1982; Codispoti,

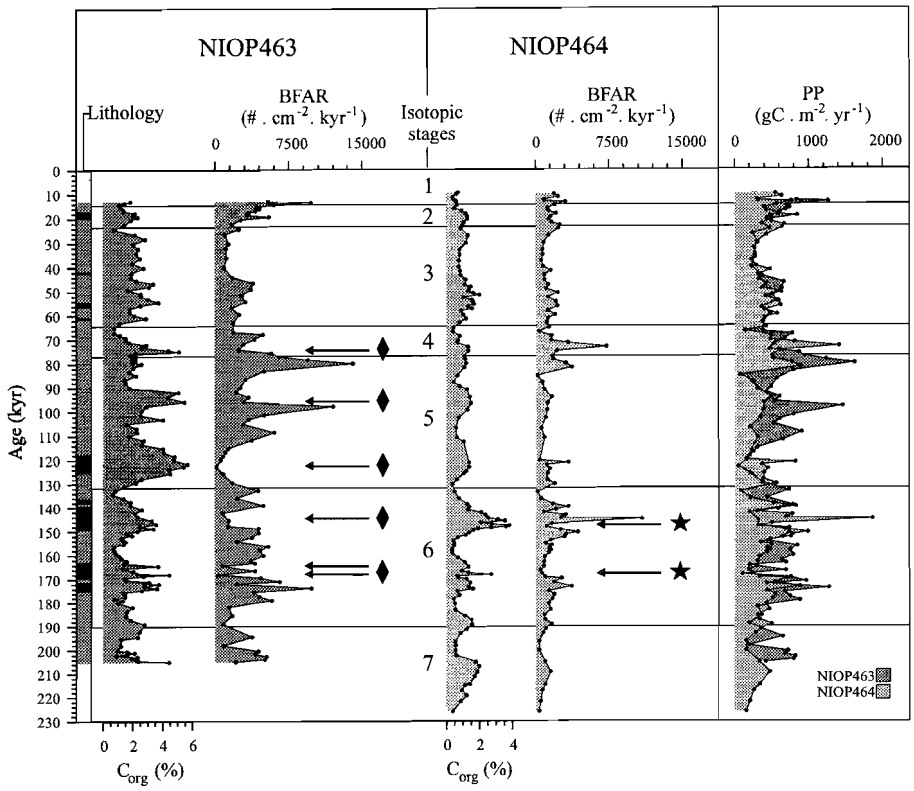

Figure 11 C_{org}, BFAR, and reconstructed primary productivity (PP) values for NIOP463 and -464 plotted versus age. Diamonds and stars indicate the strongly decimated faunas under high productivity conditions in NIOP463 and -464, respectively. Laminated intervals in NIOP463 are shown in the first column.

1991). Because these annual PP-rates of 200-400 $gC.m^{-2}.yr^{-1}$ are common for modern high productivity upwellings areas (Berger et al., 1989), the calculated peak values are considered unrealistic. Even the upper limit of the majority of the calculated PP-values is still about 2 times the annual primary productivity rate in the northern Arabian Sea. All this seems to indicate that the equations using BFAR's for flux and primary productivity estimates do not apply to suboxic/dysoxic environments. BFAR values correspond with those by De Stigter (1996) and of Naidu and Malmgren (1995), both from high productivity or stressed environments. Therefore, our high calculated BFAR's support the idea that under reduced oxygen levels the meio- and microfauna density increases, probably due to a decreased predation and competition by

the macrofauna. This in turn results in PP-values that are too high for samples from sediments deposited under suboxic/dysoxic bottom water conditions.

Figure 11 shows that the calculated PP patterns of NIOP463 and -464 do not co-vary for the larger part of the record. PP values are generally higher in NIOP463 than in NIOP464. In several short intervals (around 73, 97, 124, 165, and 168 ka, indicated by diamonds) the pattern is reversed. These intervals are characterised by high C_{org} values. Most intervals where PP values are higher in NIOP463 than in NIOP464, are characterised by relatively low C_{org} values. All this indicates that at times of high surface water productivity and an intense OMZ, BFAR's increased at the deeper station NIOP464 and decreased at the OMZ station NIOP463. The most likely explanation for this is that the benthic foraminiferal community, as observed in the 150-595 μm fraction, is strongly decimated at station NIOP463 during these periods due to severe oxygen stress. BFAR's in NIOP463, thus, seem significantly influenced by changes in bottom water oxygenation. The overall positive correlation between BFAR and C_{org} in NIOP464, suggests that BFAR's are essentially a reflection of the organic flux at this station. Figure 11, however, shows 2 intervals at ~147 ka and ~167 ka (indicated by stars) where maximum C_{org} values are accompanied by low BFAR's, suggesting that during these two periods bottom water oxygen levels were also severely depressed at station NIOP464. This, in turn, indicates that at ~147 ka and ~167 ka the OMZ should have expanded considerably to a depth of at least 1470 m. Furthermore, calculated BFAR's (and PP values) at ~73 ka and ~145 ka in the BFAR-curve of NIOP464 seem exceptionally high (Fig. 11). In both cases these peak values correlate with low BFAR's in NIOP463. The most likely explanation for this is that they reflect periods of (moderate) oxygen stress at site 464, as a result of which predation/competition pressure by the macrofaunal community decreased and the benthic foraminiferal fauna densities increased. Although BFAR's occasionally reach very low values, no barren intervals were observed. This corroborates studies which showed that benthic foraminifera can survive prolonged periods of anoxia (Alve and Bernhard, 1995; Moodley et al., 1997, 1998a).

5.5 Accumulation rates of the various microhabitat categories

In Figure 12 we have reconstructed changes in average accumulation rates of the various microhabitat categories listed in Table 4 under high and low productivity and bottom water oxygen conditions. In both cores the epifaunal

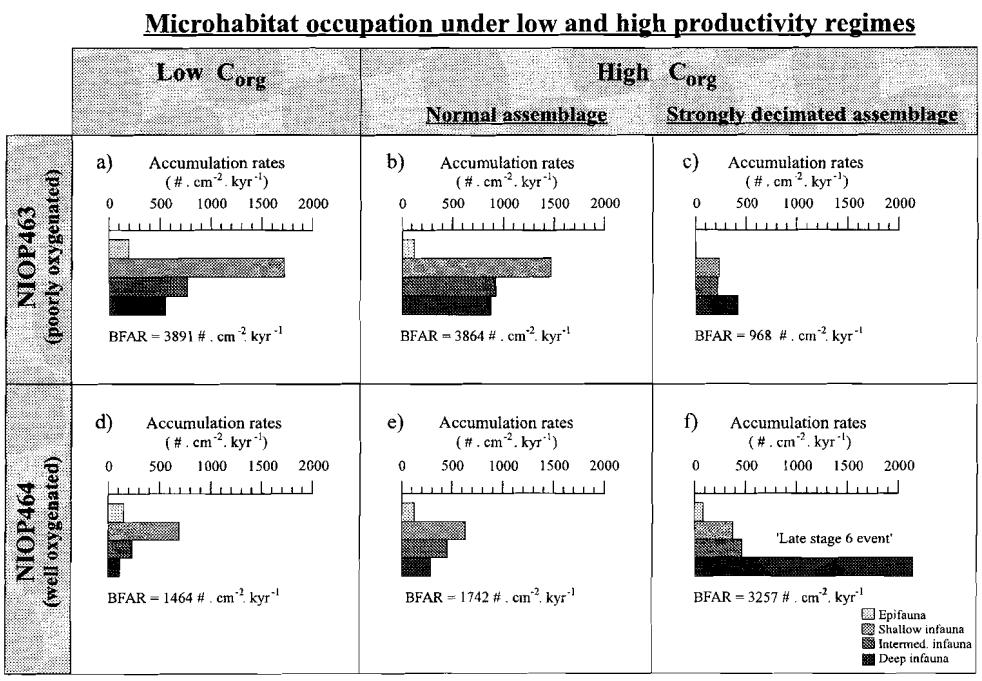

Figure 12 a-f) Average accumulation rates (AR) of the microhabitat groups under low (a, d) and high productivity conditions (b, c, e, f) in NIOP463 and -464. Samples were arbitrarily grouped using lower (higher) than 1.5% C_{org} indicating low (high) productivity conditions in NIOP463, and using lower (higher) than 1.2% C_{org} indicating low (high) productivity conditions in NIOP464. We, furthermore, subdivided the "high productivity" sample groups into two groups: one with normal BFAR's and one where BFAR's indicate a strongly decimated benthic foraminiferal fauna (Fig. 12c and 12f). Figures 12c and 12f show the effect of severe oxygen stress on the distribution of the microhabitat groups. Below the histograms average BFAR and Primary Productivity (PP) values are given. PP values are calculated using the average BFAR values (see text Ch. 5.4).

group is most frequent under conditions of presumably, relatively low surface water productivity (Fig. 12a, -d). In these cases a relatively steep increase in abundances from deep to shallow infauna is observed. One would expect that with increasing ventilation of the OMZ the fauna is able to penetrate deeper into the sediment (Jannink et al., 1998). Therefore, in the on-average much better ventilated core NIOP464, one may expect fullest in-sediment occupation.

Figure 12b shows that the pattern of microhabitat occupation changed under high productivity conditions at the OMZ station NIOP463. The

infaunal pattern is less steep, which is primarily due to an increase in the deep infaunal group. We presume that especially the deep infaunal species are able to profit of the increased food availability induced by the higher organic carbon burial efficiency under depleted bottom water oxygen conditions. It is likely that during these conditions the total in-sediment penetration is low and the redox front resides rather close to the sediment-water interface. This is confirmed by field data of Jannink et al. (1998). Furthermore, the decrease in oxygen content of the bottom water is directly reflected in a reduction of the epifaunal group (Fig. 12b). Although initially deep infaunal species tolerate the oxygen deficiency, the overall decrease in BFAR's (Fig 12c) indicates that severe dysoxia eventually seriously affects all infaunal groups. This results in a gradual decrease in abundances from deep infauna to epifauna, or a 'reversed' in-sediment occupation pattern.

Figure 12f shows the average accumulation rates for the four microhabitat groups at station NIOP464 between 140 and 150 ka. This interval stands out for the high C_{org} and V/Al values (Fig. 2) and large amplitude changes in BFAR (Fig. 11). The average abundance distribution of the four groups is comparable to that shown in Figure 12c, except for the extremely high average abundances of the deep infaunal group. High amplitude changes in BFAR between 140 and 150 ka suggest that environmental conditions for the deep infaunal group changed rapidly from near lethal to near optimum. These rapidly changing environmental conditions were most likely caused by severely depressed bottom water oxygen conditions. This conclusion would corroborate with that of Reichart (1997) for the high C_{org} values between 140 and 150 ka in NIOP464. The conclusion he reached was that this interval experienced enhanced C_{org} preservation due to low bottom water oxygen conditions, resulting from an expanded OMZ in late oxygen isotope stage 6. Although the OMZ had significantly expanded during at least one and possibly three periods in the last 225 kyr, neither cores contain barren intervals. Therefore, it is unlikely that the redox level at which sulfate is reduced resided at the sediment water interface for a considerable period of time, although Bernhard (1993) showed that some taxa survived relatively low sulfide concentrations. Yet, residence of the sulfide producing front in the water column, thus under completely anaerobic conditions, would have resulted in toxic conditions followed by barrenness (Moodley et al., 1998b).

6 Conclusions

Comparison of two northern Arabian Sea benthic foraminiferal records, from within and below the present-day OMZ, reveal differences in benthic foraminiferal composition and accumulation rates associated with changes in the intensity of the OMZ. During periods with an intense OMZ a low-diversity fauna, with high dominances of low-oxygen tolerant species, proliferates in the OMZ core. Equivalent time periods in the record from below the OMZ show generally higher diversities. This difference is explained by a difference in oxygenation of the bottom water between the two sites, which implies that during periods characterised by a pronounced OMZ the base of the OMZ was positioned between 920 m and 1470 m.

At least once and possibly three times in the past 225,000 yrs the OMZ expanded to a level close to or below 1470 m. Evidence for this deepening of the base of the OMZ is provided by high percentages of low-oxygen tolerant, deep infaunal species. Increased burial efficiency of organic matter due to severe oxygen depletion is most likely responsible for the good correlation between high C_{org} concentrations and the proportion of deep infaunal species.

During periods with a less intense OMZ benthic foraminiferal faunas in both cores are characterised by a high diversity, low dominances, and maximum percentages of miliolids. We suggest that percentages of miliolids can be used for rapid reconstruction of periods of increased ventilation in the northern Arabian Sea and are a promising proxy for tracing changes in bottom and pore water oxygenation in general.

High amplitude changes in BFAR between 140-150 ka in the core from below the OMZ suggest that environmental conditions changed rapidly from near optimum to near lethal. Low BFAR's in the OMZ core, associated with periods of a pronounced OMZ, can be explained by a strongly decimated benthic foraminiferal community. Both indicate that severe dysoxia directly affects the reliability of BFAR's in the 150-595 μm fraction for the reconstruction of paleoproductivity.

Acknowledgements

This research was carried out as part of the Netherlands Indian Ocean Program 1992-1993. Material was collected during the D-cruises of the program. Chief scientists of the D-cruises were W.J.M. van der Linden and C.H. van der Weijden. The director and our colleagues A.A. Khan, G.M.

Memon, and A.R. Tabrez of the National Institute of Oceanography, Karachi, are thanked for their co-operation. The collection of the material would not have been possible without the professional help of crew and technicians of the R.V. Tyro. Thanks are due to L.J. Lourens, H.J. Visser, G. Nobbe, A. van Dijk, H. de Waard, G.J. van het Veld, and G. Ittman for analytical and laboratory support. We also thank A. Almogi-Labin and an anonymous reviewer for their usefull remarks. This research is supported by the Netherlands Geosciences Foundation, with financial aid from the Netherlands Organization for Scientific Research (NWO).

Chapter 5
An overview

Variations in thickness and intensity of the northern Arabian Sea Oxygen Minimum Zone over the past 225 kyr: benthic foraminiferal evidence.

Abstract

Benthic foraminifera have been quantified in four piston cores from the northern Arabian Sea. One core was recovered from the centre of the Arabian Sea Oxygen Minimum Zone (OMZ) (SO90-137KA), two from the base of the OMZ (NIOP455 and -463), and one from below the OMZ (NIOP464). In this paper a comparison is made between the variations in benthic foraminiferal fauna in these cores. Changes in the intensity of the OMZ, linked to monsoonal climate variability, strongly influenced the benthic foraminiferal fauna. During periods with an intense OMZ a low-diversity fauna, with high dominances of low-oxygen tolerant, deep infaunal species, proliferates in all OMZ cores. Equivalent time periods in the core from below the OMZ show generally higher diversities. Periods with no, or only a very weak OMZ are marked by a high diversity assemblage, maximum percentages of miliolids, high PB-ratio's, no supralysoclinal dissolution, good preservation of pteropods and the occurrence of the deep-dwelling planktonic foraminifers *Globorotalia truncatulinoides* and/or *Globorotalia crassaformis*. These changes are primarily linked to the precession cycle, with a well-developed OMZ during times of maximum summer and minimum winter monsoon intensity. The OMZ is virtually absent during times characterised by minimum summer and maximum winter monsoon. This is presumably caused by lower sea surface productivity combined with local ventilation of the intermediate waters through convective mixing during winter. Glacial-interglacial variability in the OMZ cores, shown by dominances of deep infaunal species and *Rotaliatinopsis semiinvoluta*, presumably reflects increased winter productivity during glacials. Elevated percentages of deep infaunal species and of *R. semiinvoluta* in the core from below the OMZ, probably mark periods with an extended OMZ. At least during one of these periods there is a dominance of deep infaunal species in this core, which suggest that the OMZ expanded to a depth of at least 1470 m. The expansion of the OMZ at glacial times might be related to reduced inflow of modified NADW and RSW.

* *In close collaboration with*
G.J. Reichart, W.J. Zachariasse, and G.J. Van der Zwaan,

1. Introduction

The northern Arabian Sea Oxygen Minimum Zone (OMZ) is a mid-water layer with extremely low oxygen values (<2 μM; Van Bennekom and Hiehle, 1994), which has a strong impact on biological, geochemical and sedimentological processes in places where the OMZ intersects the sea floor (Hermelin and Shimmield, 1990; Jannink et al, 1998; Van der Weijden et al., 1999). Evidence provided by a variety of proxies indicates that large changes occurred in the intensity of the OMZ over the past 225 kyr, and that this variability took place on orbital and sub-orbital time scales (Altabet et al, 1995; Reichart et al., 1998, Von Rad et al, 1999; Den Dulk et al, 1998, submitted). Variability is presumably controlled by 1) changes in summer monsoon wind strength, which via coastal and open ocean upwelling controls summer surface water productivity and subsurface oxygen consumption (Altabet et al, 1995; Den Dulk et al, 1998; Von Rad et al., 1999), and 2) deep convective mixing during periods of cold and intensified winter monsoons (Reichart et al., 1998). To what extent past variability in intermediate and deep water circulation influenced the intensity of the OMZ is unclear.

In three previous papers it was shown that benthic foraminifera are useful for reconstruction of past variations in surface water productivity and OMZ intensity in the northern Arabian Sea (Von Rad et al, 1999; Den Dulk et al, 1998, in press). It was also shown that the OMZ occasionally expanded well below it's present-day depth (Den Dulk et al, in press). All these conclusions were based on a comparison between benthic foraminiferal and geochemical data in four sediment cores from within and below the northern Arabian Sea OMZ. In this paper we will review temporal variations in benthic foraminiferal composition and density in these cores in order to present a comprehensive picture of the long-term history of the OMZ. We particularly address the questions on which time scales and by which processes the OMZ periodically expanded.

2 Study area

Thermocline water in the Arabian Sea originates from the inflow of about 6 Sv. Indian Central Water (ICW, Swallow, 1984) and ~0.7 Sv. Persian Gulf Water (PGW) and Red Sea Water (RSW, Wyrtki, 1971; Olsen et al., 1993). The inflow at intermediate depths of dominantly oxygen poor ICW ($[O_2] \approx 1$ $mL.L^{-1}$; Olsen et al, 1993) in combination with high organic particle fluxes and associated high rates of sub-surface oxygen consumption leads to an intense Oxygen Minimum Zone between 150 and 1200 meters (Wyrtki, 1971; 1973;

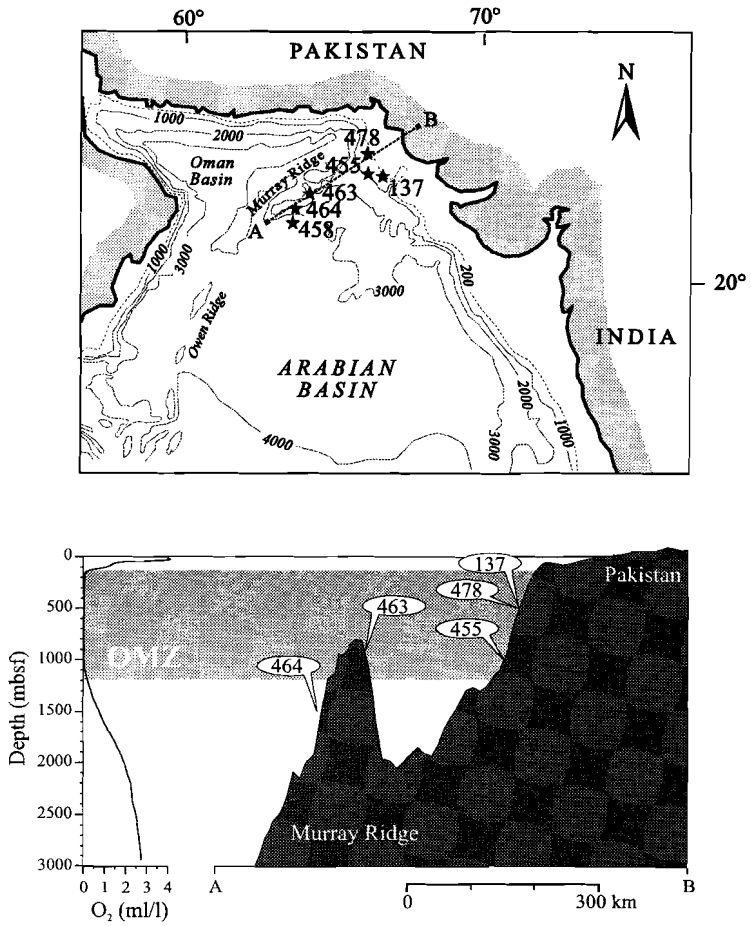

Figure 1 Location of cores NIOP455, -463, -464, -478 and SO90-137KA. Below is shown the oxygen profile from CTD station NIOP458 (22°00 N, 63°50 E) and the position of the cores along the depth transect, indicated by the dashed line (A-B) on the location map. Shading depicts the OMZ.

Deuser et al., 1978; Olson et al., 1993).

Surface water productivity in the Arabian Sea shows large semi-annual variability due to a reversal in monsoonal wind direction. In summer strong, warm and humid southwestern winds cause coastal- and open ocean upwelling off Oman, resulting in surface water productivity values that are among the highest known for the open ocean (Wyrtki, 1973; Smith and Bottero, 1977; Swallow, 1984; Brock et al., 1992). During winter, cold and dry northeastern winds cause surface waters to cool, setting the stage for convective mixing which stimulates sea surface productivity offshore Pakistan (Wyrtki, 1973;

Banse, 1984; 1987; Bauer et al., 1991; Madhupratap et al., 1996). Annual productivity rates in the Arabian Sea are between 200 and 400 $gC.m^{-2}.yr^{-1}$ (Kabanova, 1968; Qasim, 1982; Codispoti, 1991).

Table 1
Core locations and water depth of studied cores.

Station	latitude (N)	longitude (E)	depth (m)
NIOP455	23°33'.2	065°57'.2	1002
NIOP463	22°32'.9	064°02'.8	920
NIOP464	22°15'.4	063°35'.1	1470
NIOP478	24°12'.7	065°39'.7	565
SO90-137KA	23°07'.3	066°29'.8	573

3 Material and methods

Piston cores NIOP455, -463, -464 and -478 from the northern Arabian Sea were collected during the 1992 cruise of the Netherlands Indian Ocean Program. Cores NIOP455, -463, and -478 were recovered from depths within the OMZ (NIOP478 from the centre and NIOP455 and -463 from the base), whereas NIOP464 comes from below the OMZ (Fig. 1, Table 1). SO90-137KA is a high-sedimentation rate, 10 m Kasten core (30x30 cm diameter box), collected during the SONNE Cruise 90 (Von Rad et al., 1995) from the centre of the OMZ at the Karachi Margin (Fig. 1, Table 1). Cored sediments essentially consist of homogeneous, dark-greenish to light greenish/grey hemipelagic mud. Visual observation and X-ray radiographs show several distinctly to faintly laminated intervals in NIOP455 and -463. SO90-137KA shows an alternation of homogenous and laminated sediments over its full length (Von Rad et al., 1999). Sample resolution for benthic foraminiferal analyses is ~36 cm (=~2900 yrs) for NIOP455, ~17cm (=~2400 yrs) for NIOP463, ~13 cm (=~2000 yrs) for NIOP464. For planktic foraminiferal- and geochemical analyses sample resolution is about a third that distance in NIOP455, and about half that distance in NIOP463, and NIOP464. In NIOP478 sample resolution for benthic and planktic foraminiferal counts and geochemical analyses is ~10 cm (=~527 yrs). In SO90-137KA sample resolution for benthic foraminiferal analyses is ~35 cm (=~1050 yrs) and for geochemical analyses sample resolution is about a third that distance.

Oxygen isotope records have been published elsewhere (NIOP-cores: Reichart et al., 1998; Den Dulk et al, 1998, in press; SONNE-core: Von Rad et al., 1999). The chronology in the NIOP-cores is based on linear interpolation

Table 2
AMS ^{14}C datings and conversion to calendar ages, and linear sedimentation rates (LSR) in NIOP455, -463, 464, and SO90-137KA.

Station	Sample	Depth (cm)	^{14}C ages (yr BP)	$^{14}C_{cor.}$ Ages (yr BP)	$^{14}C_{cal.}$ Ages (yr BP)	LSR (cm/kyr)	LSR stages 2 and 3 (cm/kyr)
NIOP455		388		22,940	26,100	3.4-17.6	5-7.7
NIOP463	GrA-352	10.5	12,010±90	11,610	13,750	3.4-17.6	10.6-24.4
	GrA-350	84.5	16,700±100	16,300	20,000		
NIOP464						3.5-13.5	
NIOP478		264			15,200	6.5-33.2	
		1028.5			24,000		
		1110			33,000		
SO90-	Hv19651	60-67	3160±160		2930	18.8-212.5	
137KA	KIA128	173-177	5350±50		5700		
	KIA129	243-247	8660±60		9300		
	KIA130	383-387	10830±110		11,750		

between $\delta^{18}O$ events, of which the age was obtained by calibrating these events to an orbitally-tuned $\delta^{18}O$ record (details in Reichart et al., 1998). Additional calibration points were provided by AMS^{14}C datings (Table 2). Based on the ages of several distinct C_{org} maxima, which can be correlated throughout the northern Arabian Sea (Fig. 2), there was a need to slightly change the age model of SO90-137KA (Von Rad et al., 1999). Sedimentation rates based on linear interpolation are given in Table 2.

Benthic foraminiferal counts were performed on 45 samples of NIOP455, 88 samples of NIOP463, 108 samples of NIOP464, and 29 samples of SO90-137KA. Planktic foraminiferal counts were performed on 119 samples of NIOP455, 147 samples of NIOP463, 117 samples of NIOP464, and 142 of NIOP478. The sediment was freeze dried, dry weighed, washed, and subsequently sieved. The residues of the 150-595 μm fraction were split into aliquots containing about 250 specimens using an Otto microsplitter. Specimens were picked, identified, mounted in slides, and counted. The benthic foraminiferal census data were subjected to a Principal Component Analysis (SPSS). The PCA was executed on the total data set for species and species groups that show abundances higher than 5%. The general faunal characteristics are expressed as Shannon diversity, equitability and dominance (= percentage of most frequent species) and based on the amount of species identified prior to (generic) grouping for the statistical analysis. Benthic Foraminiferal Accumulation Rates (BFAR's) were calculated by multiplying total benthic numbers per fixed volume and linear sedimentation rates. In part of the samples of NIOP455 and -463, and all samples of NIOP478, total

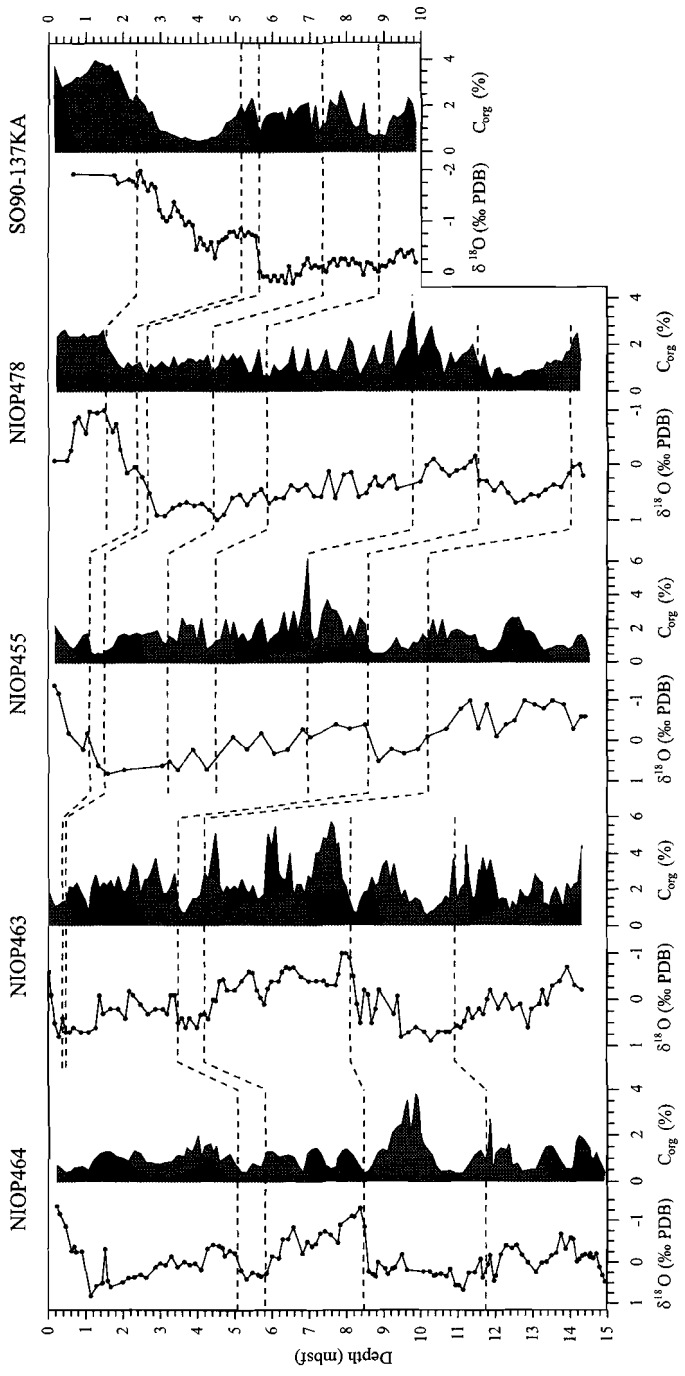
SO90-137KA
NIOP478
NIOP455
NIOP463
NIOP464
Depth (mbsf)
δ18O (‰ PDB)
Corg (%)

benthic foraminiferal numbers were obtained through counting benthic foraminifers that are associated with the planktic foraminiferal counts.

For NIOP455, -463, -464 and -478 organic carbon was measured on a CNS analyser (Fisons NA 1500) after removal of carbonate. The carbonate was extracted by mechanical shaking with 6M HCl for 12 hours, after which the samples were rinsed with demineralised water in order to remove $CaCl_2$, and dried. The analytical precision and accuracy were determined by replicate analyses of samples and by comparison with an international (BCR-71) and in-house standard (F-TURB and MM-91). The relative standard deviations, analytical precision and accuracy were better than 3%. The organic carbon content in SO90-137KA (Von Rad et al., 1999) was measured using an element analyser (LECO CS 344)

4 Benthic foraminiferal composition and -accumulation rates

Changes in the overall composition of the benthic foraminiferal fauna in NIOP455, -463, -464 and SO90-137KA are very well reflected by the general faunal characteristics. In all four cores they show predictable patterns with a low Shannon diversity generally corresponding with low equitability and high dominances (Table 3). Quantitatively important taxa (> 30% in at least 1 of the studied cores) are *Bolivina alata*, *Bolivina dilatata*, *Bolivina pygmaea*, *Bulimina aculeata*, *Globobulimina affinis*, *Bulimina exilis*, *Bulimina* sp.1, *Cassidulina bradyi*, *Cassidulina carinata*, *Ehrenbergina pacifica*, *Fursenkoina bradyi*, *Rotaliatinopsis semiinvoluta*, and *Uvigerina* spp.. Dominance ranges are 7.5-87% in NIOP463, 8.5-77% in SO90-137KA, 9-50% in NIOP455, and 7.5-39% in NIOP464. High-diversity intervals contain about 40-50 different taxa with dominances being on average between 10-15%. In low-

Table. 3
Correlation coefficients between Shannon diversity and simple diversity, dominance, equitability and Factor 1 scores, respectively.

	Shannon diversity			
	NIOP464	NIOP463	NIOP455	SO90-137KA
Simple diversity	0.88	0.93	0.94	0.97
Dominance	-0.87	-0.92	-0.92	-0.89
Equitability	0.71	0.87	0.72	0.58
Factor 1	0.57	0.77	0.87	0.89

Figure 2 $\delta^{18}O$ (in ‰ PDB) and organic carbon records of NIOP455, -463, -464, -478 and SO90-137KA. Profiles can be correlated in great detail as indicated by the dashed lines.

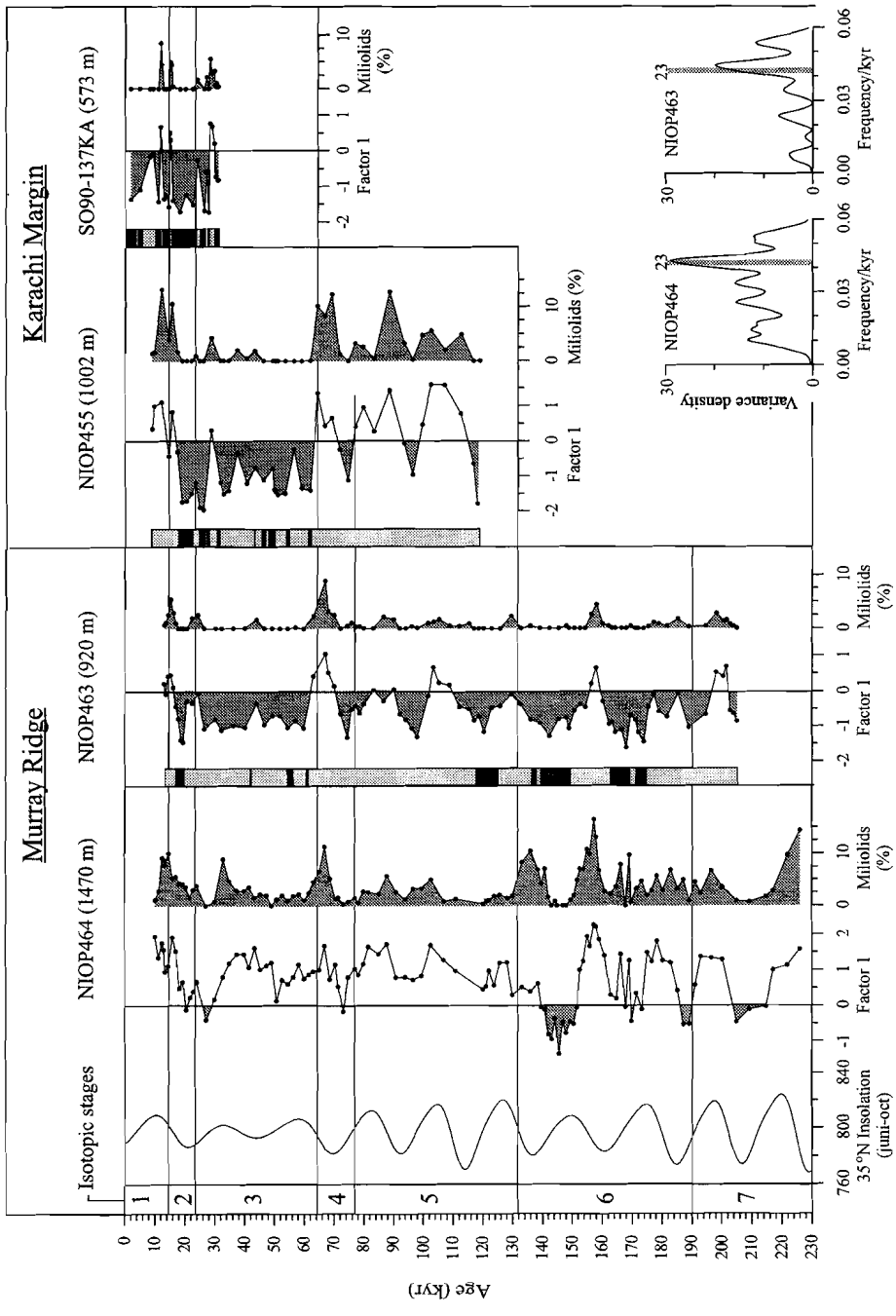
Murray Ridge
Karachi Margin
Isotopic stages
NIOP464 (1470 m)
NIOP463 (920 m)
NIOP455 (1002 m)
SO90-137KA (573 m)
Factor 1
Miliolids (%)
Variance density
Frequency/kyr
35°N Insolation (juni-oct)
Age (kyr)

Figure 3 Factor 1 scores and percentages of miliolids in NIOP464, -463, -455 and SO90-137KA plotted versus age. Laminated intervals in NIOP463, -455 and SO90-137KA are indicated in black. Spectra of Factor 1 scores in NIOP463 and -464 are based on a Welch-1 filter with a 6 dB bandwith of 7.29×10^{-3} in NIOP464 and 8.19×10^{-3} in NIOP463. Variance densities are plotted on a linear scale.

diversity intervals the number of taxa decreases to less than 20, and to around 10 in the most extreme cases.

We performed a standardised PCA on all census data to compare the fauna composition at the species level between the cores. The first axis of PCA accounts for 14.9% of the total benthic foraminiferal variation which is significant for a standardised multivariate analysis. Higher order axis account for less than 8% of the total variation each, and do not show any meaningful trend. The taxa incorporated in the PCA and their loadings on the first axis are listed in Table 4. High positive loadings (> 0.5) on Factor 1 are shown by *Astrononion* spp., *Cibicides bradyi*, *Gavelinopsis lobatulus*, *Hoeglundina elegans*, *Karreriella bradyi*, lagenids, *Melonis barleeanum*, miliolids., *Sphaeroidina bulloides*, and *Spiroplectammina* spp.. Species displaying high negative loadings (< -0.20) are *B. alata*, *B. pygmaea*, *B. exilis*, *Bulimina* sp.1, *C. bradyi*, *Globobulimina* spp., *G. affinis*, and *R. semiinvoluta*.

Data in Table 3 indicate that Factor 1 is positively correlated with

Table 4.
Species loadings on Factor 1 resulting from principal component analysis of the census data of NIOP455, -463, 464, and SO90-137KA.

Species	Factor 1
Cibicides brady	0.66
Miliolids	0.65
Gavelinopsis lobatulus	0.65
Melonis barleeanum	0.63
Karreriella brady	0.59
Spiroplectammina spp.	0.57
Lagenids	0.57
Astrononion spp.	0.55
Hoeglundina elegans	0.53
Sphaeroidina bulloides	0.52
Oridorsalis umbonatus	0.47
Cassidulina subglobosa	0.43
Cibicides ungerianis	0.37
Pullenia bulloides	0.35
Ehrenbergina pacifica	0.32
Bulimina striata	0.29
Hanzawaia boueana	0.28
Shallow water species	0.25
Bulimina aculeata	0.25
Cibicides pseudoungerianis	0.23
Uvigerina proboscidea	0.22
Cassidulina carinata	0.10
Lenticulina spp.	0.09
Chilostomella oolina	0.06
Hyalinea balthica	0.04
Pullenia quinqueloba	0.03
Uvigerina semiornata	-0.04
Gyroidina spp.	-0.05
Osangularia spp.	-0.05
Uvigerina spp.	-0.08
Tritaxia tricarinata	-0.13
Fursenkoina brady	-0.16
Bolivina seminuda	-0.19
Bolivina dilatata	-0.19
Cassidulina brady	-0.23
Globobulimina affinis	-0.25
Bulimina sp.1	-0.26
Bolivina pygmaea	-0.39
Globobulima spp.	-0.46
Bolvina alata	-0.47
Rotaliatinopsis semiinvoluta	-0.55
Bulimina exilis	-0.58

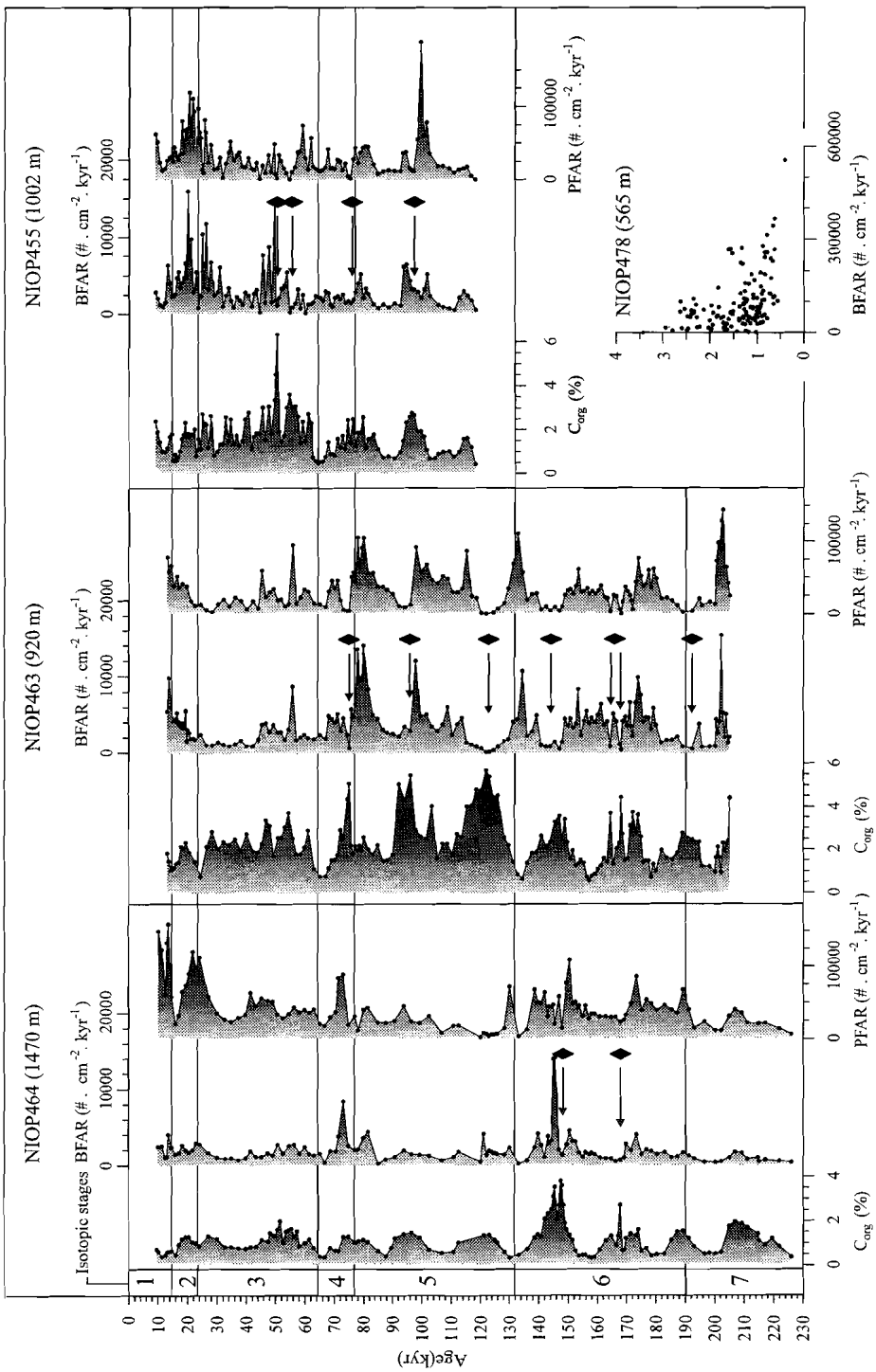
NIOP464 (1470 m)
NIOP463 (920 m)
NIOP455 (1002 m)
NIOP478 (565 m)
Isotopic stages
BFAR (#. cm-2. kyr-1)
PFAR (#. cm-2. kyr-1)
Corg (%)
Age(kyr)

Shannon diversity and equitability, and consequently negatively correlated with high dominances in the cores from the northern Arabian Sea (NIOP455, -463, and SO90-137KA). Factor 1 is weakly correlated with these faunal characteristics in the core from below the OMZ (NIOP464). The good correlation between Factor 1 and general faunal characteristics indicates that Factor 1 discriminates between two distinctly different assemblages; 1) a high-diversity assemblage, of which the species are positively loaded on Factor 1 and, 2) a low-diversity assemblage, made up of species with negative loadings.

Figure 3 shows down- and inter-core variations and spectra of Factor 1. Furthermore, laminated intervals are indicated. Laminated intervals are always associated with negative Factor 1 scores. Distinct correlatable changes in Factor 1 scores occur in the OMZ cores (NIOP455, -463 and SO90-137KA). Equally large changes occur in the core taken from below the OMZ (NIOP464), but in contrast to the OMZ cores scores are overall positive. Nevertheless both patterns show strong covariance. Spectral analyses show a strong 23 kyr frequency in the score plots of NIOP464 and -463 (Fig. 3). Comparison with the precession-dominated 35° N insolation curve (averaged over june to october) indicates that minimum in the score plots correlate with maxima in the insolation curve, although with a considerable time lag (Fig. 3). Variability on a glacial-interglacial time scale is particular clear in the score plot of NIOP455, with overall negative values in stages 4, 3, 2 and overall positive values in stage 5. Variability on a sub-orbital time scale is reflected in short term fluctuations of laminated and bioturbated sediments. This particularly holds true for stage 4, 3, and 2. If resolution permits (e.g. SO90-137KA) then these short term alternations are accompanied by similar short term fluctuations in the benthic foraminifera. Figure 3 further shows systematic differences between NIOP455 and -463 in spite of the fact that both cores are from similar depths from within the OMZ. Overall the amplitude of the changes in the scores of NIOP455 are larger than in the time equivalent part of NIOP463. In addition the scores in stages 2, 3, 4 are more negative in NIOP455, whereas the scores corresponding with the insolation minima of stage 5 are more positive.

Figure 4 shows Benthic and Planktonic Foraminiferal Accumulation Rates (BFAR's and PFAR's) for NIOP455, -463, -464. BFAR's for NIOP478 are added in a scatterplot with organic carbon (%). BFAR's vary between 50 #.cm^{-2}.kyr^{-1} and 55600 #.cm^{-2}.kyr^{-1}. Maxima in BFAR's are lowest for the core from

Figure 4 C_{org} (%), Benthic Foraminiferal Accumulation Rates (BFAR's), and Planktonic Foraminiferal Accumulation Rates (PFAR's) in NIOP464, -463, -455 plotted versus age and scatterplot of C_{org} (%) versus BFAR's in NIOP478. Diamonds indicate intervals with high organic carbon values and low PFAR's and BFAR's.

below the present-day OMZ (NIOP464) and highest for the core from the centre of the OMZ (NIOP478). BFAR patterns show little similarity. Comparison with the organic carbon record shows that in NIOP464 high BFAR's generally correlate with high C_{org} values (Fig. 4). In NIOP463 and -455 a partly reverse pattern is observed; high BFAR's correlate with low C_{org} values. The scatterplot of BFAR's and C_{org} of NIOP478 shows that high BFAR's correlate consistently with low C_{org} values. PFAR's vary between 50 $\#.cm^{-2}.kyr^{-1}$ to 190000 $\#.cm^{-2}.kyr^{-1}$. PFAR patterns show strong similarity with BFAR's in NIOP455, -463, and 464.

5 Discussion

5.1 Temporal variations in benthic foraminifera

Factor 1 is basically independent of the geographic location of the cores. Scores show correlatable changes between the Murray Ridge and Karachi Margin, but also between cores from within and below the OMZ (Fig. 3). This implies that the Factor 1 score plot reflects the benthic foraminiferal response to environmental changes that affected the entire northern part of the Arabian basin.

Factor 1 discriminates between two ecologically contrasting benthic foraminiferal assemblages. The low-diversity assemblage is indicative of low oxygen conditions and/or eutrophic surface water conditions (e.g. Lutze and Coulborn, 1984; Perez-Cruz and Machain-Castillo, 1990; Hermelin and Shimmield, 1990; Sen Gupta and Machain-Castillo, 1993; Gooday, 1994; Wells et al., 1994; Jannink et al. 1998). Species dominating this assemblage have been classified as deep infaunal because have been repeatedly recorded living at considerable depth in the sediment under well-ventilated conditions (Corliss, 1985, 1991; Corliss and Chen, 1988; Corliss and Emerson, 1990; Rathburn and Corliss, 1994; Barmawidjaja et al., 1992; Bernhard, 1992; Buzas et al., 1993). This is often where reducing conditions occur pointing to absence of free oxygen, which indicates that these deep living taxa must be highly tolerant to low oxygen conditions. When under low bottom water oxygen conditions redox-levels shallow, this group of deep infaunal species is thought to move up to the sediment-water interface and to gradually replace the less low oxygen tolerant epifauna and shallow infaunal species (Van der Zwaan et al, 1999). They eventually will dominate the living, dead and fossil assemblages. The high-diversity assemblage, on the other hand, consists of a large variety of epifaunal to shallow infaunal species and low frequencies of deep infaunal species. This points to a full in-sediment occupation with a deep position of the redox front. The high-diversity assemblage, therefore, suggests relatively

well-ventilated conditions.

Fluctuations in Factor 1 scores, thus, reflect alternating periods of high (low) surface water productivity and an intense (weak) OMZ (see also, Den Dulk et al., 1998, in press, Von Rad et al, 1999). Similar contrasting surface and bottom water conditions are inferred from geochemical and planktonic foraminiferal proxy records and from the presence/absence of laminated sediments (Reichart et al., 1997, 1998, Den Dulk et al., 1998, in press, Schulz et al. 1996, Von Rad et al, 1999). High/low productivity conditions are on a precessional time scale presumably related to changes in summer monsoon wind strength, which via coastal and open ocean upwelling controls summer surface productivity (Clemens et al., 1991; Murray and Prell, 1992; Shimmield, 1992; Anderson and Prell, 1993; Ten Kate et al., 1994; Reichart et al.1997, 1998; Den Dulk et al., 1998). The intensity of the OMZ, in turn, is strongly related to variations in surface water productivity via subsurface oxygen consumption (Altabet et al, 1995; Reichart et al., 1997, 1998; Den Dulk et al., 1998). Variability in summer productivity, however is not the only factor that determines OMZ intensity. There is evidence that periods with a weak summer monsoon were characterised by cold and intensified winter monsoonal winds, and that these conditions caused periodically deep convective mixing resulting in a breakdown of the OMZ (Reichart et al., 1998).

5.2 Area-dependent variations: Murray Ridge versus Karachi Margin

Cores NIOP455 and -463 are from about the same water depth, but different geographic locations (Karachi Margin and Murray Ridge, respectively). They were recovered near the base of the OMZ slightly above the steep oxycline, which implies that in the present-day situation both sites are characterised by severely depleted bottom water oxygen conditions (Van Bennekom and Hiehle, 1994; Van der Weijden et al., 1999). The score plot of both cores nicely shows the precession driven changes in OMZ intensity (Fig. 3). The score plots, however, also show significant differences between NIOP455 and -463. Scores in stages 2 and 3 are on the average distinctly more negative in NIOP455 than in NIOP463. Conversely, scores for stage 5 are more positive in NIOP455 compared to NIOP463. The more negative factor 1 scores during stages 2 and 3 in NIOP455 compared to NIOP463 seem to be largely determined by the much higher percentages of the deep infaunal species in NIOP455. Conversely the more positive Factor 1 scores during stages 5 and stage 1 is to a large extent reducible to the much higher percentages of miliolids in NIOP455.

The higher percentages of the deep infaunal species in stages 2 and 3 of

NIOP455 (Fig. 5), suggest that during stages 2 and 3 redox boundaries resided closer to the sediment-water interface at the Karachi Margin compared to the Murray Ridge. This can either be caused by regional differences in productivity or a difference in bottom water oxygenation. Den Dulk et al (1998) previously suggested (based on the elevated percentages of the planktonic foraminiferal species *Globigerina falconensis*) that an intensified and colder glacial winter (NE) monsoon could have increased winter production during glacial stages 2 and 3, which would explain the sustained flourishing of deep infaunal species during these stages. Since NIOP455 lies to the northeast of NIOP463 one might suggest that strengthening of the northeast monsoon during glacial productivity maxima caused a disproportionate increase of winter productivity. The possibility of elevated winter productivity at site NIOP455 during stages 2 and 3 can be tested by calculating the average primary productivity (PP) for this period at both sites. Average C_{org} values for stages 2 and 3 in NIOP455 and -463 are comparable (Fig. 4), but the average sedimentation rate during this time span is 2 to 3-fold higher in NIOP455 compared to NIOP463 (Table 2). In stages 2 and 3 C_{org} accumulation rates at site NIOP455, therefore, should have been 2 to 3 times higher than at site NIOP463. In part these higher C_{org} accumulation rates can be explained by better preservation caused by these higher sedimentation rates (Müller and Suess, 1979). It is therefore important to reconstruct the original flux that arrived at the sediment water interface during stages 2 and 3 at both sites. Since both cores are from about the same water depth, the organic matter flux that arrived at the seafloor depends primarily on primary productivity. Using the equations of Sarnthein et al. (1988) or Berger et al. (1989), it can be calculated that primary productivity at the Karachi Margin (NIOP455) was ~195 $g.m^{-2}.yr^{-1}$ for stages 2 and 3, which is about 30 $g.m^{-2}.yr^{-1}$ higher compared to the Murray Ridge area. The higher abundances of deep infaunal species during stages 2 and 3 at site NIOP455 most likely resulted from an excess supply of food and a more shallow position of the redox boundaries due to an increase in winter productivity at the Karachi Margin. Supportive evidence for this more stable (year-round) bottom water oxygen depletion during stages 2 and 3 at the Karachi Margin comes from the more frequently occurring laminated sediments in NIOP455 (Fig. 3).

The much higher percentages of miliolids at the Karachi Margin during stage 5 is problematic. From the literature (Mullineaux and Lohmann, 1981; Nolet and Corliss, 1990; Moodley et al., 1998b; Jannink et. al., 1998; Jorissen, 1999) and from in-house studies (Jannink pers. comm.;Van der Zwaan et al., submitted) it is concluded that miliolids are intolerant of reduced oxygen levels. Abundance fluctuation in miliolids from NIOP464 and -463, therefore has been earlier interpreted in terms of varying bottom and pore water oxygen conditions (Den Dulk et al., in press). The difference in stage 5 miliolid

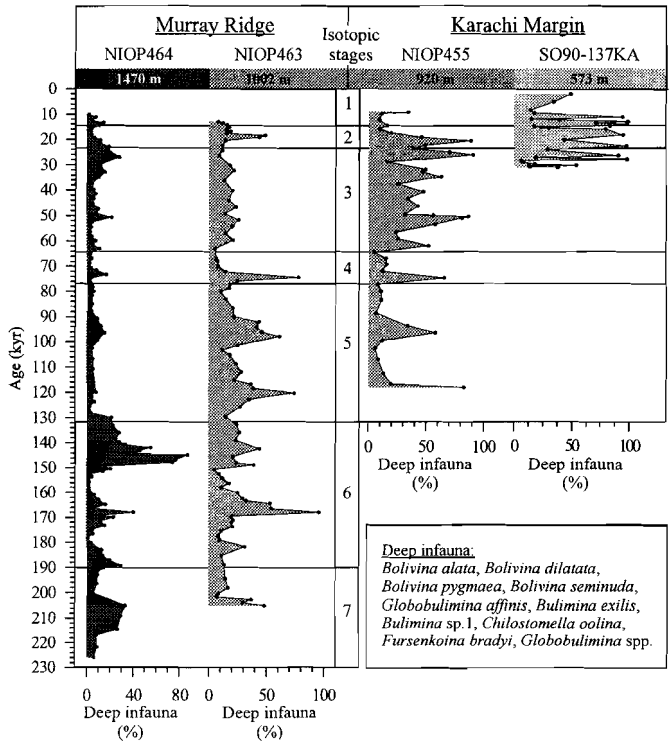

Figure 5 Percentages of deep infaunal species in NIOP464, -463, -455, and SO90-137KA plotted versus age. Text explains what species are included in the deep infaunal group.

abundances between NIOP455 and -463 thus suggests that the Karachi Margin was on the average better oxygenated than at the Murray Ridge during stage 5. The cause of this difference in oxygenation however remains puzzling. One can speculate that this difference reflects the gradient in summer productivity since the advected nutrient load reaching NIOP455 during summer is less than at the more "upstream" location site NIOP463.

5.3 Depth-dependent variations: Within versus below the OMZ

The overall benthic foraminiferal composition clearly differs between cores from within and below the OMZ. Factor 1 scores (Fig. 3) indicate that the benthic foraminiferal record from below the OMZ (NIOP464) is characterised by higher benthic foraminiferal diversities and lower

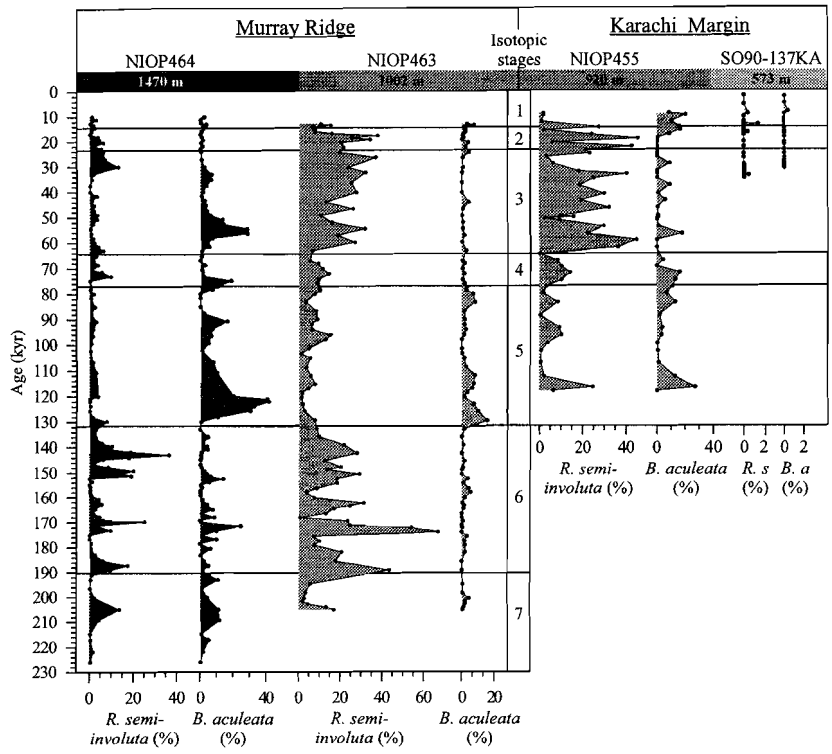

Figure 6 Percentage of *R. semiinvoluta* and *B. aculeata* in NIOP464, -463, -455, and SO90-137KA plotted versus age.

dominances of taxa tolerant to low oxygen conditions, even during periods of high surface water productivity and an intensified OMZ (Den Dulk et al, in press). This is, furthermore, illustrated by the down-core pattern of deep infaunal species (Fig. 5), which indicates that overall bottom and pore water oxygen concentrations were highest at the site from below the OMZ (NIOP464). There are, however, several glacial high productivity intervals in NIOP464, in which deep infaunal species significantly increase (20-35 %). The maximum of 88% around 145 ka is suggestive of a substantial decrease in bottom and pore water oxygenation. In NIOP455 and -463, deep infaunal taxa reach percentages of 40-90% during most periods characterised by an intense OMZ. All laminated intervals in SO90-137KA, show deep infaunal abundances of about 90%. This clearly illustrates that maximum deep infaunal abundances are associated with the most intense oxygen depleted bottom waters. This, in turn, supports the idea that the deep infaunal maximum (88%) in NIOP464 at around 145 ka reflects a deepening of the base of the OMZ to

at least 1470 m. In a previous paper it was shown that such a deepening agrees well with observed changes in the redox-sensitive elements Mn and V (Den Dulk et al, in press)

Additional information on the occasional deepening of the OMZ comes from the distribution of *R. semiinvoluta*, a species endemic to the Indian Ocean (Loeblich and Tappan, 1988). Living *R. semiinvoluta* shows highest abundances near the base of the OMZ (~800 - ~1300m) in surface sediments of the Karachi- and Makran Margin, (Jannink et al., 1998; A. Thiess and W. Kuhnt, pers. comm. 1999). Also the dead association from the Karachi Margin show a maximum of 10-30% at the base of the OMZ (NIOP-unpublished data). Off Somalia *R. semiinvoluta* reaches maximum relative abundances of ~6% in the combined living and dead assemblage at 789m in the basal part of the OMZ (E.M. Ivanova, pers. comm. 1999). The OMZ off Somalia is seasonally ventilated at depths near 400 m, resulting in somewhat different oxygen profiles compared to the Pakistan Margin with oxygen levels of 0.35-0.5 ml/l in the basal part of the OMZ (Van Bennekom et al., 1995). Combined with the data from the Pakistan margin, this implies that *R. semiinvoluta* proliferates within a narrowly defined oxygen range of about 0.01-0.5 ml/l, corresponding with the lower part of the OMZ and slightly deeper.

Down-core distributions (Fig. 6) show that in agreement with the present-day distribution, *R. semiinvoluta* is very rare (< 2%) in SO90-137KA, which is presently located in the centre of the OMZ. In NIOP455, and -463 this species shows overall higher abundances during glacial intervals (30-60%). Generally low abundances, however with several distinct maxima associated with glacial C_{org} maxima are observed in NIOP464 from below the OMZ. Highest percentages in NIOP464 occur immediately before and after the peak of deep infaunal species around 145 ka (Fig. 5). This pattern suggests a severe deepening and subsequent shallowing of the base of the OMZ with *R. semiinvoluta* being replaced by deep infaunal species under the most severe oxygen depletion. In NIOP464, there are several other peaks (around 30, 170, 187 and 206 ka) in the combined percentages of deep infaunal species and *R. semiinvoluta* that are associated with glacial C_{org} maxima (Fig. 6). Also these periods probably mark periods with an expanded OMZ, although not as dramatic as the deepening recorded at 145 ka.

A number of species are characteristic of the living and dead fauna from below the OMZ, such as *M. barleeanum, O. umbonatus,* and *B. aculeata* (Zobel, 1973; Hermelin and Shimmield, 1990; Jannink et al., 1998). These species are also more common in NIOP464 from below the OMZ (Fig. 6). In particular, *B. aculeata* shows maximum percentages (20-40%) around 54, 75, 92, and 122 ka, intervals which corresponds with C_{org} maxima. Jannink et al. (1998) have shown that *B. aculeata*, is one of the most prominent species in the living

fauna between 1500 and 2000 m. They concluded that *B. aculeata* must be an opportunistic bathymetrically deeper dwelling species, not particularly dependent on high amounts of fresh and unaltered organic matter, but certainly thriving under a high flux. Since several C_{org} maxima in NIOP464 are characterised by high percentages of *B. aculeata* (Fig. 4 and 6) the lower boundary of the OMZ during these periods most likely resided close to its present-day position.

5.4 The influence of bottom water oxygenation on benthic and planktic foraminiferal accumulation rates

Under normal, oxygenated conditions planktic and benthic foraminifera respond proportionally to changes in sea surface productivity. This results in planktic/benthic (PB-) ratios which basically depend on water depth (Van der Zwaan et al., 1990; De Stigter et al., 1998). PB-ratios, however, can also reflect changes in bottom water oxygenation. Bottom water oxygen controls PB-ratio's directly through influencing benthic foraminiferal densities (Verhallen, 1991; Van der Zwaan and Jorissen, 1991; Moodley et al. 1997; Den Dulk et al, in press), and may indirectly affect PB-ratio's through preferential supralysoclinal dissolution of planktic foraminifers. PB-ratios in NIOP464 show two distinct minima, one around 120 ka and the other around 145 ka (Fig. 7). NIOP463 and -455 show a higher number of co-varying minima.

Although the present-day lysocline in the Arabian Sea lies well below the OMZ (~3000m) water depth, calcite dissolution can occur at shallower depths. This so-called supralysoclinal dissolution occurs at or close to the sediment water interface due to the release of CO_2 during oxic decomposition of organic matter (Morse and Mackenzie, 1990). Furthermore, within the OMZ oxidation of ammonia to nitrate and the addition of CO_2 as a consequence of oxygen consumption, lowers the solution pH and carbonate saturation (Canfield and Raiswell, 1991). Dissolution only takes place at or close to the sediment water interface because the increase in alkalinity brought about by sulphate reduction deeper in the organic rich sediments enhances carbonate preservation.

Since calcite is less soluble than aragonite, we can safely assume that sediments containing aragonite are unaffected by supralysoclinal dissolution. Pteropods are common pelagic organisms constructing aragonitic tests. Therefore, pteropod preservation can be used to reconstruct changes in aragonite preservation. The present-day Aragonite Compensation Depth (ACD) lies within the OMZ at about 500 m (Berger, 1977). Since NIOP455, -463 and -464 are from stations well below the present-day ACD, enhanced pteropod preservation in these cores point to a substantial deepening of the

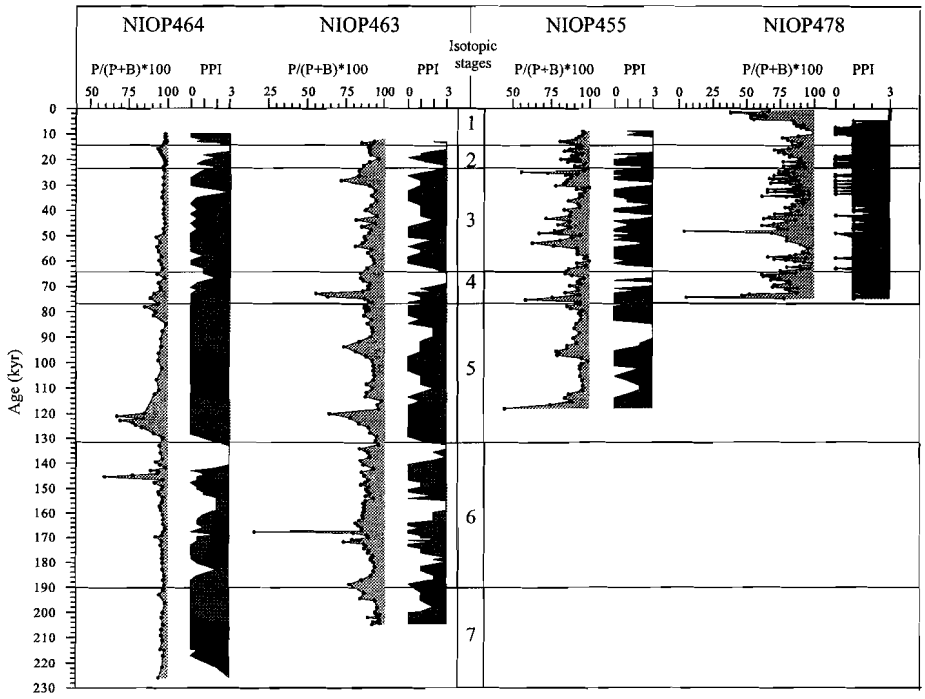

Figure 7 Planktic/benthic (P/P+B) ratio's and Pteropod Preservation Index (PPI) in NIOP455, 463, 455, and 478.

ACD (Fig. 7). Periods with a deep ACD correspond to minima in summer monsoon productivity and OMZ intensity (Reichart et al., 1997, 1998; Den Dulk et al., 1998). This implies that only at times of enhanced sea surface productivity and an intense OMZ, PB-ratio's might have been seriously affected by supralysoclinal dissolution.

Figure 7 shows that PB minima correlate with intervals devoid of pteropods. These minima, therefore, might be attributed to preferential supralysoclinal dissolution of planktic foraminifera. Figure 4 shows that a number of the C_{org} maxima in NIOP455 and -463 are associated with PFAR- and PB minima (diamonds, Fig. 4). This, indeed, suggests that supralysoclinal dissolution periodically played a substantial role (Fig. 4). PFAR minima also correlate with minima in BFAR (Fig. 4). It seems difficult to asses the effect of supralysoclinal dissolution on the benthic foraminifera. However, benthic foraminifera show few fragmented specimens, indicating that supralysoclinal dissolution of benthic foraminifera is probably negligible. Therefore, the minima in BFAR are more likely related to a strong reduction in the benthic

foraminiferal fauna caused by severe oxygen depletion during periods of high summer monsoon productivity (see also Den Dulk et al., in press). Severe but more persistent oxygen most likely explains the negative correlation between BFAR and C_{org} in NIOP478 (Fig. 4). In several intervals in NIOP463 highest BFAR-values are observed immediately before and/or after BFAR minima (e.g. ~78 ka, and ~98 ka, Fig. 4). This pattern most likely reflects enhanced benthic foraminiferal production due to reduced predation under reduced oxygen conditions before and after maximum oxygen stress. The BFAR- and PFAR record in the cores from the present-day OMZ, thus, indicates that minima in PB-ratios either result from preferential dissolution of planktic foraminifera or from enhanced benthic foraminiferal production.

The two distinct PB minima of NIOP464 are correlative with PFAR minima, suggesting that these are influenced by supralysoclinal dissolution. Minima in PFAR, however, do not necessarily point to dysoxic bottom waters, because supralysoclinal dissolution may also occur due to oxic decomposition of organic matter below the OMZ. The PB minimum around 145 ka further, correlates with a minimum in BFAR. This combination provides good evidence for decreased bottom water oxygenation and deepening of the base of the OMZ to 1470 m, in agreement with elevated percentages of *R. semiinvoluta* and high percentages of deep infaunal species. The PB minimum around 120 ka, on the other hand, correlates with relatively high BFAR's. This suggests that although supralysoclinal dissolution may have affected the PB-ratio at this level, bottom water conditions remained relatively ventilated. Also the peak in *B. aculeata* and associated low abundances of deep infaunal species, suggests that the PB minimum at 120 ka is not associated with a deepening of the OMZ. Figure 4 shows a second BFAR minimum around 164 ka in NIOP464, which does not correspond with a PB minimum. This minimum is coincident with elevated percentages of *R. semiinvoluta* and deep infaunal species and, therefore, may also indicate a deepening of the base of the OMZ close to or even below 1470 m.

6. A comprehensive picture of the long-term history of the OMZ

Orbital changes in the intensity and thickness of the OMZ over the past 225 kyr are summarised in the schematic reconstruction of Figure 8. The most obvious variability in OMZ intensity is on a precession time scale. Periods with no, or only a very weak OMZ are marked by a high diversity assemblage, maximum percentages of miliolids, high PB-ratio's, no supralysoclinal dissolution and good preservation of pteropods. These periods are also characterised by intensified winter convection because of the presence of the deep dwelling planktonic foraminifers *G. truncatulinoides* and/or *G.*

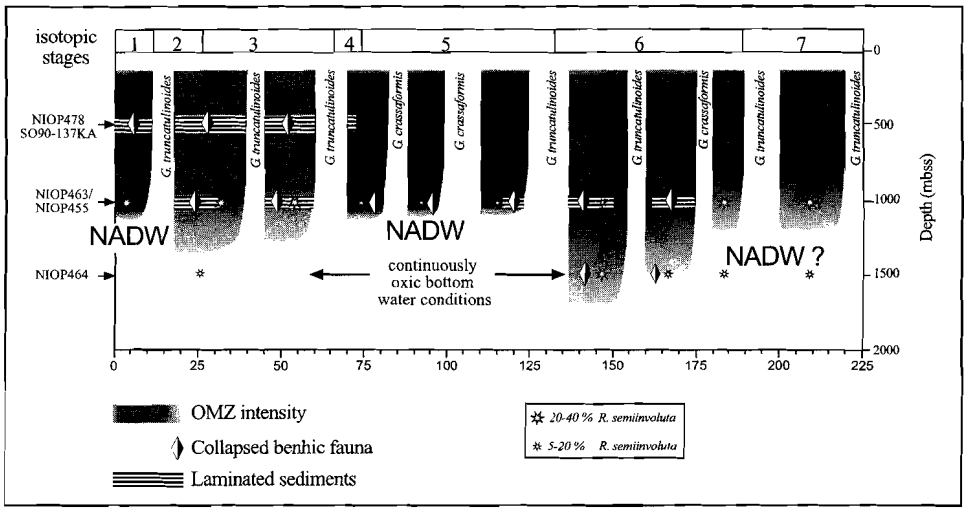

Figure 8 Schematic reconstruction of OMZ intensity and thickness over the past 225,000 yrs. Horizontal axis represents time; vertical axis represents water depth (m). Periods of a well-developed OMZ are shaded with darkest shading for the most intense OMZ. Occurrences of the planktonic foraminifers *G. truncatulinoides* and *G. crassaformis* depict ventilated intervals. Diamonds, asterix and stripes, indicate minima in BFAR, frequencies of *R. semiinvoluta*, and laminated intervals, respectively. Changes in OMZ intensity are primarily linked to precession driven changes in summer monsoon productivity. An expanded and possibly weaker OMZ occurred during glacial productivity maxima

crassaformis (Reichart et al., 1998). Deep winter mixing during these periods apparently introduced sufficient oxygen at intermediate depths to sustain a highly diverse benthic fauna. The intervals in between these evidently well-ventilated periods are characterised by a low-diversity fauna with high dominances of deep infaunal species and no or few miliolids. These intervals mark periods with a well-developed OMZ and maximum summer monsoon productivity. The sediments are occasionally laminated, although according to the benthic foraminiferal fauna this not necessarily indicates lowest oxygen levels.

Apart from changes on a precession time scale, OMZ intensity also shows a glacial-interglacial periodicity (Fig. 8). During glacial precession-driven

productivity maxima the lower depth limit of the OMZ seems slightly depressed compared to interglacials. This is based on elevated percentages of *R. semiinvoluta* and deep infaunal species in NIOP464. Moreover, in stage 6 the benthic foraminiferal fauna was strongly decimated twice at site NIOP464 (Fig. 4), which in combination with high abundances of deep infaunal species suggests that the OMZ expanded to a depth of at least 1470 meter. During the interglacial precession-driven productivity maxima of stage 5 the lower depth limit of the OMZ remained at its present-day position. Evidence for this comes from high relative abundances of the deeper dwelling species *B. aculeata* during these intervals in NIOP464, indicating that bottom water oxygen conditions at this deeper site were comparable to today (Fig. 6). BFAR minima together with high dominances of deep infaunal species in NIOP455 and -463 indicate an intense OMZ for these sites during these intervals. Schenau et al. (1999), however, concluded that the lower depth limit of the OMZ experienced maximum expansion during the precession-driven productivity maxima of stage 5. Their modelled variation in thickness of the OMZ is based on the redistribution of Mn, assuming a 100% Mn relocation efficiency from sediments deposited within the OMZ to the deeper part of the basin. In view of the benthic foraminiferal results, Mn relocation efficiency might be related to differences in OMZ intensity, rather than to changes in OMZ thickness. This would imply that high productivity conditions during interglacial stage 5 are accompanied by a very intense, but not expanded OMZ. Since the OMZ expanded to a depth of at least 1470 meter during the later part of glacial stage 6, and taking into account the minimal Mn redistribution at that time (Schenau et al., 1999), we may conclude that during this period the OMZ was less intense.

7. The role of deep and intermediate water circulation on OMZ thickness and intensity

Thermocline water in the northern Arabian Sea is primarily replenished by Indian Central Water (ICW, Tomczak and Godfrey, 1994). ICW is formed in the subtropical convergence of the southern hemisphere and enters the northern Indian Ocean in the western boundary current. Because the transfer of ICW between the hemispheres is restricted to the southwest monsoon season the net transfer rate is small (Tomczak and Godfrey, 1994). This results in sluggish circulation of ICW in the northern Indian Ocean; the ICW rapidly ages with increasing distance to its source region. ICW, therefore, supplies little oxygen to the thermocline water in the Arabian Sea. Antarctic Intermediate Water (AIW) which constitutes thermocline water in the southern Indian Ocean, does not contribute to ICW. A strong hydrological

front at 10° S blocks the progression of AIW into the northern Indian Ocean (Wyrtki, 1973; Boyle, 1994; Tomczak and Godfrey, 1994). The northern Arabian Sea is filled by Indian Deep Water (IDW) from 3800 m up to the base of the OMZ. The deepest parts of the Arabian basin contain Antarctic Bottom Water (AABW). The properties of IDW in the high salinity core near 40°E south of the equator, match the properties of North Atlantic Deep Water (NADW) in the Atlantic sector of the Southern Ocean (Tomczak and Godfrey, 1994). Therefore, IDW is considered to be of northern Atlantic origin carried into the Indian Ocean via diversions from the Upper Circum Polar current and directly via South Africa (Wyrtki, 1973; Tomczak and Godfrey, 1994). IDW is modified along the way into the Arabian basin by mixing with thermocline water above, upwelling of AABW from below and injection of Red Sea Water (RSW) and Persian Gulf Water (PGW) at intermediate depth (Tomczak and Godfrey, 1994). Outflow of PGW and RSW occurs at about 300 m and 800 m waterdepth, respectively.

Present-day hydrography suggests that the inflow of IDW and the northward flow of ICW must somehow control the lower depth limit of the OMZ. Periods in which we have evidence for an expanded OMZ correspond with glacial productivity maxima. It is generally believed that during comparable periods large changes in global deep water circulation occurred, and that glacial NADW formation was reduced (Boyle, 1988; Duplessy, 1988; Oppo and Leman 1993; Oppo et al., 1995). This suggests that IDW, or modified NADW, was significantly reduced and/or had other sources. Changes in the relative inflow of both water masses, therefore, could have been responsible for the inferred variability in thickness of the OMZ. Apart from IDW and ICW changes in RSW may also have influenced the lower depth limit of the OMZ. Presently the inflow of RSW in the northern Arabian Sea invokes a steepening in the density gradient at depths close to the base of the OMZ (Wyrtki, 1973). However, a lowering of global sea level during glacials would have seriously curtailed the outflow of RSW into the Arabian Sea (Rohling and Zachariasse, 1996). This might have resulted in a reduced density gradient at glacial times favouring an expanded OMZ during episodes of increased productivity. Expansion of the OMZ during 2 periods in stage 6 are, therefore, probably related to glacial-interglacial changes in IDW and RSW inflow.

8 Conclusions

We reconstructed intensity and thickness of the Arabian Sea OMZ for the last 225,000 yrs using benthic foraminifers. Changes are primarily linked to

the precession cycle, with a well-developed OMZ during times of maximum summer and minimum winter monsoon intensity. The OMZ is virtually absent during times characterised by minimum summer and maximum winter monsoon. This is presumably caused by lower sea surface productivity combined with local ventilation of the intermediate waters through convective mixing during winter. The OMZ was most intense during interglacials, but reaches maximum thickness during glacials. The expansion of the OMZ at glacial times might be related to reduced inflow of modified NADW and RSW. The occasionally very intense OMZ during interglacials must be due to a high sub-surface oxygen consumption associated with high summer surface productivity, while deeper water experienced sufficient inflow of modified NADW and RSW, so that the base of the OMZ was close to its present-day position.

Acknowledgements

The director and our colleagues at the National Institute of Oceanography in Karachi, Pakistan are thanked for their good cooperation in the Netherlands Indian Ocean Program. We also thank our German colleages, particularly Ulrich von Rad, Hartmut Schulz, and Andrea Thiess. The NIOP-cores used in this study would not have been recovered without the skilled technicians of the NIOZ, Texel. Willem van der Linden and Cees van der Weijden were chief scientists during the Utrecht NIOP cruises. Analytical support came from G. Nobbe, M.A. van Alphen, H. de Waard, G.J. Ittman, G. van het Veld, and A van Dijk. This research was funded by the Netherlands Organisation of Scientific Research (NWO).

Chapter 6
An oxygen transfer function

Oxygenation history of the Arabian Sea Oxygen Minimum Zone over the past 225 Ka: Application of a benthic foraminiferal transfer function.

Abstract

In this paper we explore the possibilities and limitations of a benthic foraminiferal transfer function in reconstructing the oxygenation history in a complex environment as the Arabian Sea Oxygen Minimum Zone (OMZ). Using data of living (Rose Bengal stained) foraminifera we show that foraminiferal reaction on the OMZ is sharp. The observed relationship between oxygen and the benthic foraminiferal distribution in the various microhabitats, possibly relates to the succession of redox fronts. Foraminifera respond sharply at the Mn reduction front, followed deeper in the sediment by a change at the Fe reduction front. In the Arabian Sea sediments the Mn and NO_3 reduction fronts are too closely spaced to conclude to differential foraminiferal response. One group of foraminifera seems to be restricted to the oxic microhabitat. This group of foraminifera is used in the context of an oxygen transfer function, which we subsequently applied to the benthic foraminiferal census data from two northern Arabian Sea cores covering the past 225 kyr. The results of the transfer function are furthermore checked using the down core patterns of the redox elements Mn and V, and discussed in view of living benthic foraminiferal patterns. It is concluded that the transfer function produces potentially reliable quantitative (μMol/l) oxygen reconstructions.

* *In close collaboration with*
G.J. Van der Zwaan, N.T. Jannink, and W.J. Zachariasse.

1. Introduction

Over the past decades intensive research has led to a better appraisal of benthic foraminiferal ecology. Instead of regarding these unicellular organisms as trustworthy tools for salinity or temperature, we now consider them rather reliable tracers of oxygen and organic flux (Gooday 1994; Van der Zwaan et al., 1999). Although much has been clarified, there still remain a considerable amount of issues which need further study. For instance, although we know that many benthic foraminifera withstand periods of dysoxia (e.g. Alve and Bernhard, 1995; Moodley et al., 1998), we lack any knowledge how they precisely cope with these adverse conditions. Bernhard (1996) summarised a number of possible metabolic pathways. From this review it is clear that the foraminiferal strategy versus oxygenation is probably highly diversified.

At this stage the potential of benthic foraminifera to estimate past variations in oxygenation is rather vague. Often qualitative terms as "well ventilated" or "dysoxic" are employed (e.g. Den Dulk et al., in press), although Kaiho (1994, 1999) attempted to quantify the relation between benthic foraminifera and oxygenation. The main problem in this respect is the fact that much data collection takes place under poorly constrained conditions. In the first place, many observations pertain to the distribution of dead assemblages, for instance versus oxygen conditions as measured at one moment in time. It should be realised that the dead assemblage is a time-averaged reflection of considerable seasonal variation. Also the oxygen measurements are often not representative since variation in oxygenation over the year can be substantial. Moreover, the measurements are often carried out somewhere in the water column, instead of close to the sediment-water-interface, i.e. the actual living space of foraminifera. If living assemblages are studied, a further problem is that they are displaying variations which is not always synchronous with environmental change. For instance, deterioration of water column properties can be coped with over a rather long time by adult individuals, and as such not readily reflected in the assemblage. In the meantime reproduction might be seriously affected resulting in assemblage response lagging the environmental change.

The only way to overcome these problems is an analysis of living assemblages over an extended period of time, following the population dynamics and the environmental changes over a longer time series. Further detailed observations of processes at the sediment-water interface are essential. Such series are becoming available now, and these will lead to better insights in the foraminiferal response to oxygenation.

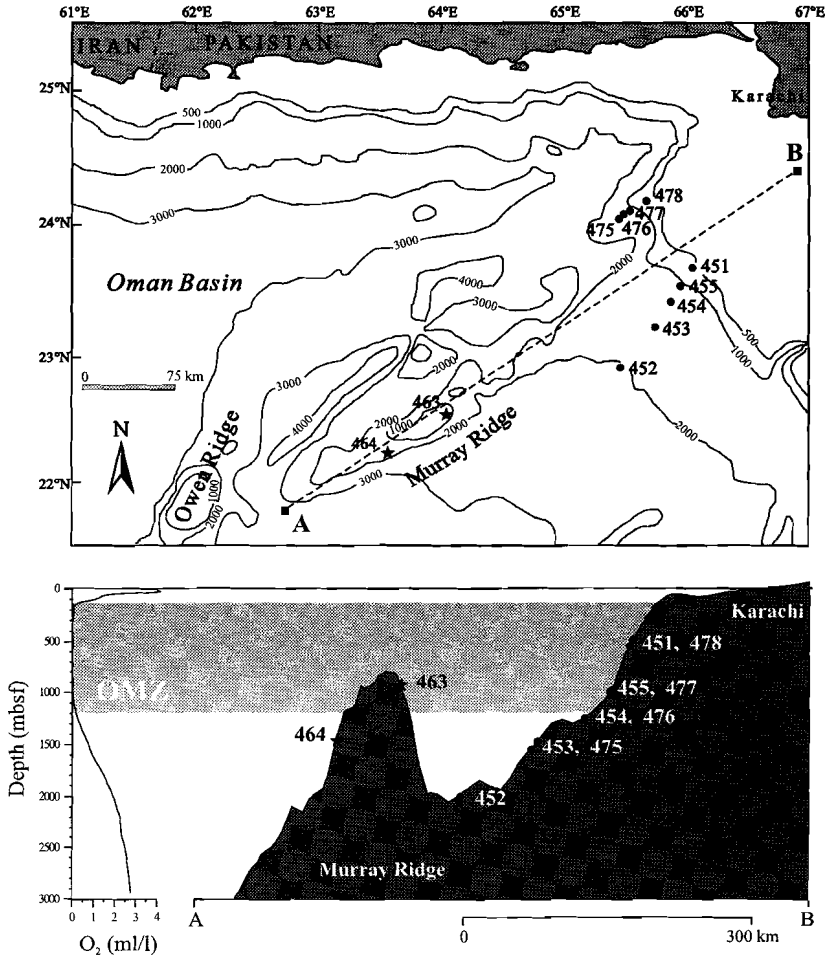

Figure 1 a) Location map of sites NIOP451-455 (Transect I), NIOP475-478 (Transect II), NIOP463 and NIOP464. 1b) Oxygen profile is from CTD station NIOP458 (22° 00'.3 N, 63° 50'.4 E) and the profile of seafloor topography is along the dashed line in Fig.1a. Grey shading depicts the OMZ.

In previous papers (Den Dulk et al., 1998, and in press) we used benthic foraminifera in a multi-proxy approach to reconstruct the history of the Arabian Sea Oxygen Minimum Zone (OMZ). This pronounced oceanic zone varies in intensity and thickness over time, depending on the amount of surface water productivity and the depth of winter mixing (Reichart et al., 1998). Up to this point however, we were not able to quantify past oxygen

conditions over time. In this paper we aim at reconstructing the oxygenation history over the past 225 kyr, employing benthic foraminiferal census data from two cores taken at 920 m and 1470 m depth, i.e. at the lower boundary and below the present day OMZ. We will use a recently developed transfer function based on distributional patterns of living benthic foraminifers (Van der Zwaan et al., submitted). As such, this study is meant as a validation of this transfer function, and to explore its potential pitfalls. To further elucidate foraminiferal patterns under anoxic conditions we include census data from nine boxcores taken from depths within and below the Arabian Sea OMZ. Using these data, the distribution of living benthic foraminifera in the northern Arabian Sea and the occurrence of in-sediment redox fronts can be compared.

2. Material and methods

Living (Rose Bengal stained) benthic foraminifera were collected from nine box cores of two parallel down-slope transects covering depths from 500 to 2000m (Fig. 1). Processing of the samples and resulting faunal patterns were discussed in detail by Jannink et al. (1998). Samples in the 63-150 μm size fraction were studied only from the uppermost sediment layer, but benthic foraminiferal patterns in the 150-595 μm were quantified for every half cm slice down to 2 cm and every 1 cm slice further down to 10 cm. The patterns as obtained by Jannink et al. (1998) will be compared with data on the in-sediment distribution of redox elements. Analyses on the occurrence of Mn, Fe and NO_3 were carried out by the shipboard party, Mn and Fe on bulk sediment, and NO_3 on pore waters. For details the reader is referred to Van der Linden et al. (1994). Faunal data and distribution of redox elements were analysed and compared using conventional statistical techniques (cluster analysis) and RDA analysis (Ter Braak et al., 1998), respectively.

Piston cores NIOP463 and -464 were collected in 1992 during the Netherlands Indian Ocean Program. Both core stations are located on the Murray Ridge at 920 m (base OMZ) and 1470 m (below OMZ) water depth, respectively (Fig. 1, Table 1). The sediments essentially consist of homogenous, dark-greenish to light greenish/gray hemipelagic mud. Visual observation and X-ray radiographs show several distinctly to faintly laminated intervals in NIOP463. Samples were taken for benthic foraminiferal counts, elemental and oxygen isotope analyses. Sample resolution for benthic foraminiferal analyses is ~17 cm (= ~2400 yrs) for NIOP463 and ~13 cm (=

Table 1
List of NIOP-box and piston cores, their location and waterdepth.

NIOP cores		Latitude (N)	Longitude (E)	Depth (m)
Box	451	23°41',4	066°02',9	495
	455	23°33',3	065°57',2	998
	454	23°26',9	065°51',2	1254
	453	23°14',0	065°44',0	1555
	452	22°56',4	065°39',7	2001
	478	24°12',7	065°30',9	556
	477	24°07',6	065°28',9	1000
	476	24°06',1	065°28',9	1226
	475	24°11',9	065°26',8	1472
Piston	463	22°32',9	065°02',8	920
	464	22°15',4	065°35',1	1470

~2000 yrs) for NIOP464. For geochemical analyses sample resolution is about half that distance. The chronology of NIOP463 and -464 is based on linear interpolation between $\delta^{18}O$ events, of which the age was obtained by calibrating these events to an orbitally-tuned $\delta^{18}O$ record (Reichart et al., 1998; Den Dulk et al., in press).

For the analyses of organic carbon (C_{org}), about 1g of dry sediment was weighed in a centrifuge tube. Carbonate was dissolved in 1 M HCl under mechanical shaking for 12 hours, after which the samples were rinsed with demineralized water in order to remove $CaCl_2$ and subsequently dried. The C_{org} content was determined using a CNS-analyser (Fisons NA 1500). An aliquot of the samples was thoroughly ground in an agate mortar after freeze drying and before dissolution of 250 mg in 5 ml of a 6.5: 2.5: 1 mixture of $HClO_4$(60%)-HNO_3(65%) and H_2O and 5 ml HF(40%) at 90 °C. The dried residue was dissolved in 1 M HCl for analysis of Al, Mn, and V with an ICP-AES (Perkin Elmer OPTIMA 3000). Analytical precision and accuracy were determined by replicate analyses of samples and by comparison with international (SO-1, SO-3) and in-house standards. Both were found to be better than 3%. To distinguish changes that are not caused by dilution with $CaCO_3$ or a variable input of terrestrial sediments, elements are normalised to Al.

For the benthic foraminiferal analyses, we processed 88 samples from NIOP463 and 108 samples from NIOP464. The sediment was freeze dried, dry weighed, washed, and wet sieved. The residues of the 150-595 μm fraction were split into aliquots containing at least 200 and generally about 250

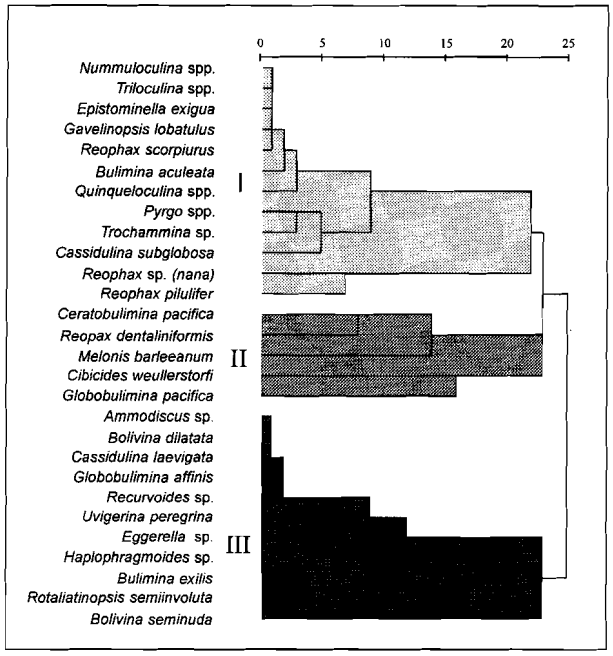

Figure 2 Cluster diagram of 23 dominant benthic foraminiferal species in the living (Rose Bengal stained) assemblages of northern Arabian Sea transect I. Individual clusters are given roman numbers I-III.

specimens (using an Otto microsplitter). Although many small species do not occur in this larger size fraction, it is generally accepted that the 150-595 μm fraction accurately reflects environmental change. All specimens were picked, mounted on slides, identified and counted. The general faunal characteristics and faunal patterns were discussed in detail by Den Dulk et al. (in press).

3. Results

Living foraminiferal patterns were described in detail by Jannink et al. (1998). The quantitative data show that many foraminiferal taxa are living below the uppermost cm, although in this surface layer standing stocks of all species are highest. Living foraminifera are present in substantial numbers even in the centre of the OMZ, suggesting that these taxa are able to survive anaerobic conditions over longer periods of time. The cluster diagram shows that a number of assemblages can be distinguished (Fig. 2), which is basically

the result of the species distribution along the oxygen stress gradient. The most stress tolerant assemblage (= group III) consisting of *Bolivina seminuda*, *Ammodiscus* and *Cassidulina laevigata* is most frequent in the centre of the OMZ. Other species frequent within but reaching highest percentages just below the OMZ are *Globobulimina pacifica*, *Eggerella*, *Rotaliatinopsis semiinvoluta*, *Uvigerina peregrina*, *Recurvoides* and *Globobulimina affinis*. The most diverse assemblage (= group I) is dominated by *Reophax* taxa, *Epistominella exigua* and miliolids. This one is most abundant at the deepest stations below the OMZ, where oxygen concentrations are much higher (Fig. 1).

Using the census data of Jannink et al. (1998), we plotted the abundances of the three groups as derived from the cluster analysis against depth in the sediment column, and water depth (Fig. 3). Within the OMZ, faunal penetration is not very deep compared with that below the OMZ. However, even in the anoxic deepest parts of the sediment column within the OMZ fauna remains present and the most stress-tolerant assemblage is occurring even rather abundantly.

In Fig. 3 we compared the faunal abundance patterns with the distribution of the redox elements Mn, NO_3 and Fe. These elements indicate various stages in the oxidation-reduction process. It can be seen that the elements follow each other with increasing depth in the sediment. There is a similarity in the successive distribution of these redox elements and the distribution of the various benthic groups. This similarity suggests that these patterns are possibly causally related. This idea is further strengthened if we consider the results of RDA analysis (Fig. 4). It can be seen that the taxa as *Cibicides wuellerstorfi*, *Reophax* species and miliolids are arranged around the Mn-axis. One species is distributed along the Fe-axis (*Globobulimina pacifica*) indicating the most intense redox state. Other species are distributed between both redox fronts, some taxa close to Mn (*Quinqueloculina*) and others closer to the Fe-front (as *Bolivina dilatata* and *U. peregrina*).

The distribution of the bathymetrically deepest occurring faunal group is unambiguous. The taxa belonging to this group occur only in waters below the OMZ which are relatively well-aerated. Even then these taxa do not penetrate deep into the sediment (Fig. 3) where they would encounter decreasing oxygen levels. This suggests that they are dependent on the presence of free oxygen. This idea has been further checked using data from the Arabian Sea and Atlantic Ocean (Guichard, 1997). In Fig. 5 we plotted Average Living Depths (ALD's) of all species occurring in the Arabian Sea

Transect I Indian Ocean:

Comparison between some redox elements and foraminiferal groups

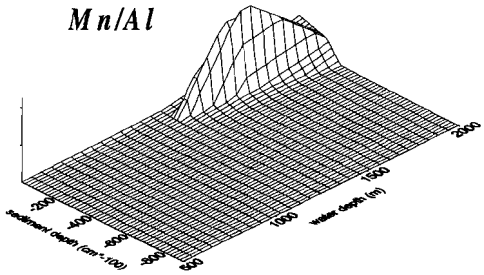

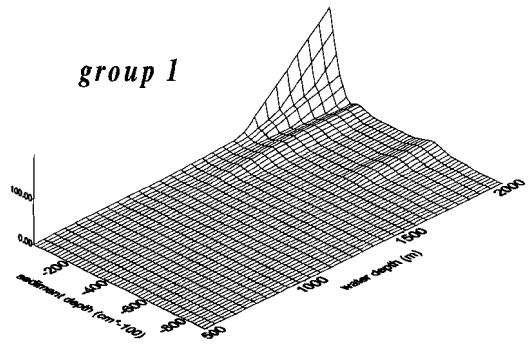

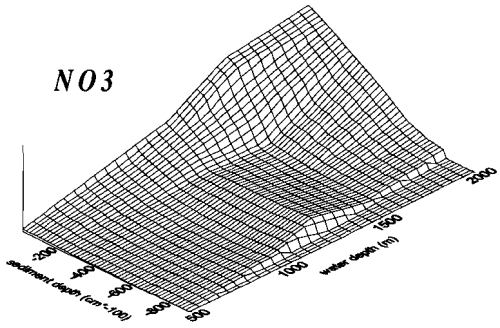

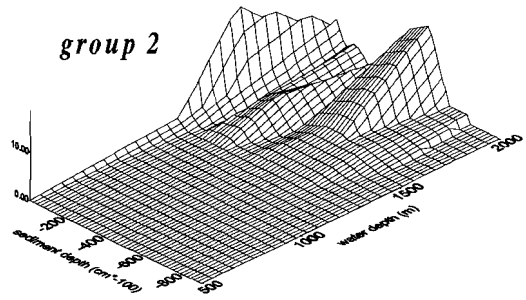

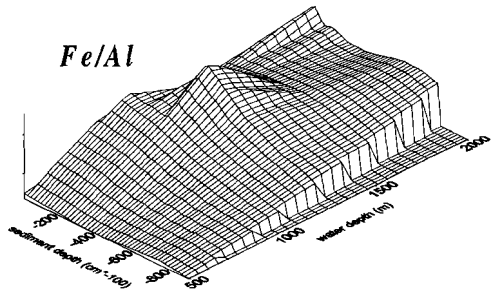

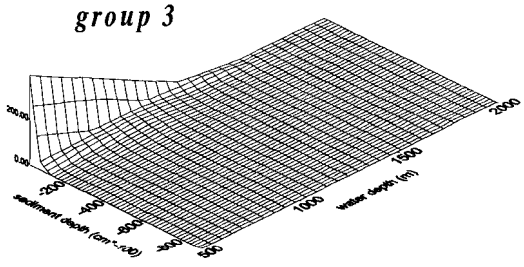

(Jannink et al., 1998), and compared these with ALD's of taxa in the Atlantic Ocean off NW Africa (Guichard, 1997). The latter data are used here since the Atlantic environments off NW Africa are similar to the Arabian Sea; both are high productivity upwelling areas. The benthic foraminiferal ALD's of all stations indicate that the species are closely packed and that together they inhabit the total environmental range from the sediment-water interface down to 10 cm in the sediment. This suggests that benthic foraminiferal niche dimensions overlap considerably and are not well separated.

The suggestion that some taxa live predominantly in the aerated parts of the sediment column, was recently further substantiated by Van der Zwaan et al. (submitted). They show that a group of species ("oxyphilic") is living always in the topmost cm layers or, in case of the presence of an OMZ, in sediments below well-ventilated waters. It appeared to be possible to regress the relative abundance of these taxa (expressed as percentage of the total calcareous assemblage) against oxygen. The oxygen values used in the regression analysis were measured with probes and reflect the contents at the sediment-water interface. The percentage of oxyphilic taxa was calculated as proportion of the total sum of calcareous species, to avoid possible negative effects of bad preservation of fragile agglutinated taxa (Van der Zwaan et al., submitted). The resulting regression can be represented using the formula:

$$[\text{Oxygen concentration } \mu\text{Mol/l}] = 7.9602 + 5.95^{*}\{\%\text{ oxyphilic taxa}\}.$$

We applied this transfer function to reconstruct the oxygenation history of two cores located at the base and below the modern OMZ and covering the past 225 kyr. Species employed in the transfer function are *Cibicides wuellerstorfi*, *C. kullenbergi*, *C. ungerianus*, *C. pseudoungerianus*, *Lenticulina* spp., *Rosalina* spp., *Gavelinopsis* spp., *Sphaeroidina bulloides* and miliolids. These taxa were considered to be oxyphilic by Van der Zwaan et al. (submitted) based on the distribution on the Atlantic and Indian Oceans, and in the shallower Adriatic Sea and Levantine Basin.

In Fig. 6 the oxygen history is shown in μM/l. The record shows considerable variation in both cores over the past 225 kyr. The reconstruction suggests that on average core NIOP463 was deposited under rather low

Figure 3 Plots of redox elements (Mn, NO_3 and Fe), and groups as derived from the cluster analysis against depth in the sediment column. Plots are of northern Arabian Sea transect I.

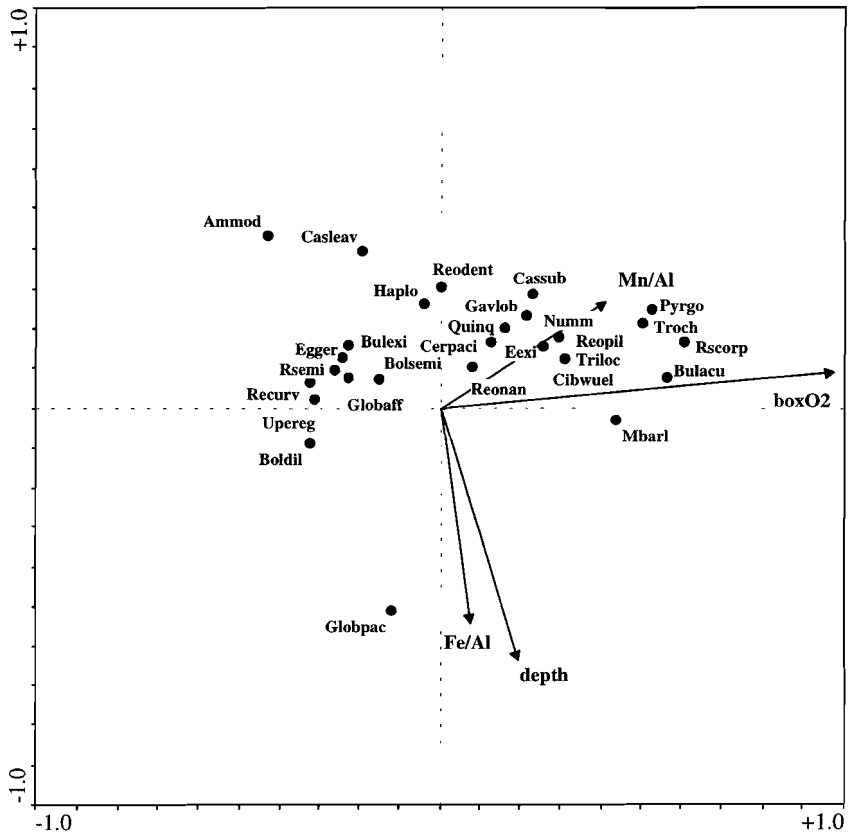

Figure 4 Ordination diagram based on Redundancy Analysis (RDA) of percentages of species in northern Arabian Sea transects I and II.

oxygen contents, the average concentrations being around 40 µMol/l (~0.9 ml/l). The oxygen contents at the sediment-water interface were generally much higher at the site of core NIOP464. The figure further shows that the oxygenation history as quantified by the transfer function, is supported by the pattern of the redox elements. Combinations of high values of Mn/Al and low of V/Al (indicating well aerated waters) and high V/Al values and low Mn/Al values (indicating oxygen deficient waters) co-vary with the oxygenation curve based on the transfer function. Figure 6 also shows the patterns in organic carbon contents for both cores. It is obvious that on the average core NIOP463 is characterised by higher C_{org} contents, resulting in

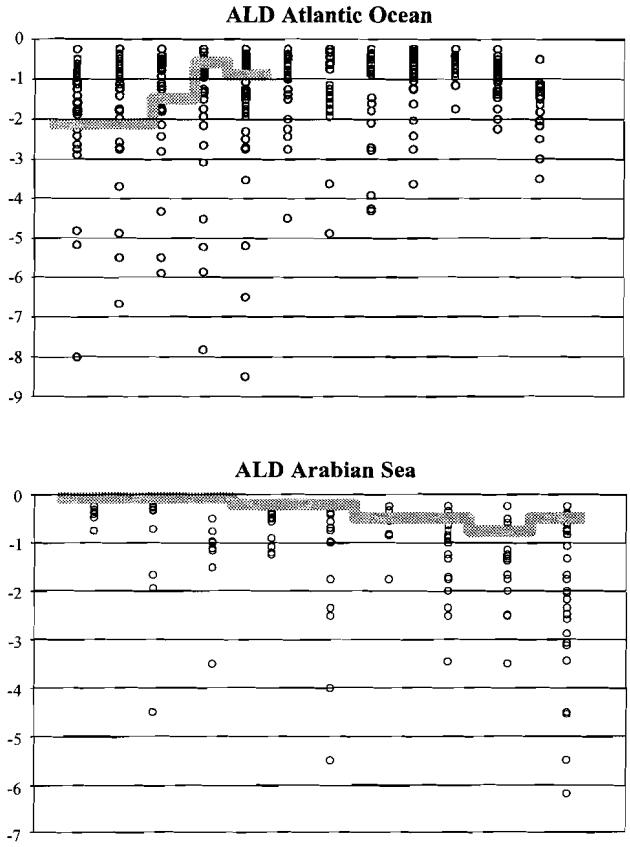

Figure 5 Average living depths (ALD's) of species occurring in the Arabian Sea and the Atlantic Ocean off NW Africa (Guichard, 1997) going from shallow (left) to deeper sites (right). Grey shading indicates zero oxygen level. This level is based on the Manganese reduction front in the Arabian Sea boxcores, and on probe analysis in the boxcores from the Atlantic Ocean.

higher oxygen consumption rates and lower oxygen contents at the sediment water interface. The overall correlation between organic carbon and the oxygen contents in NIOP464 is rather poor, suggesting that accumulation of organic matter is not the only factor controlling bottom water oxygenation. However, high organic carbon maxima in both cores coincide with low reconstructed oxygen values, and vice versa.

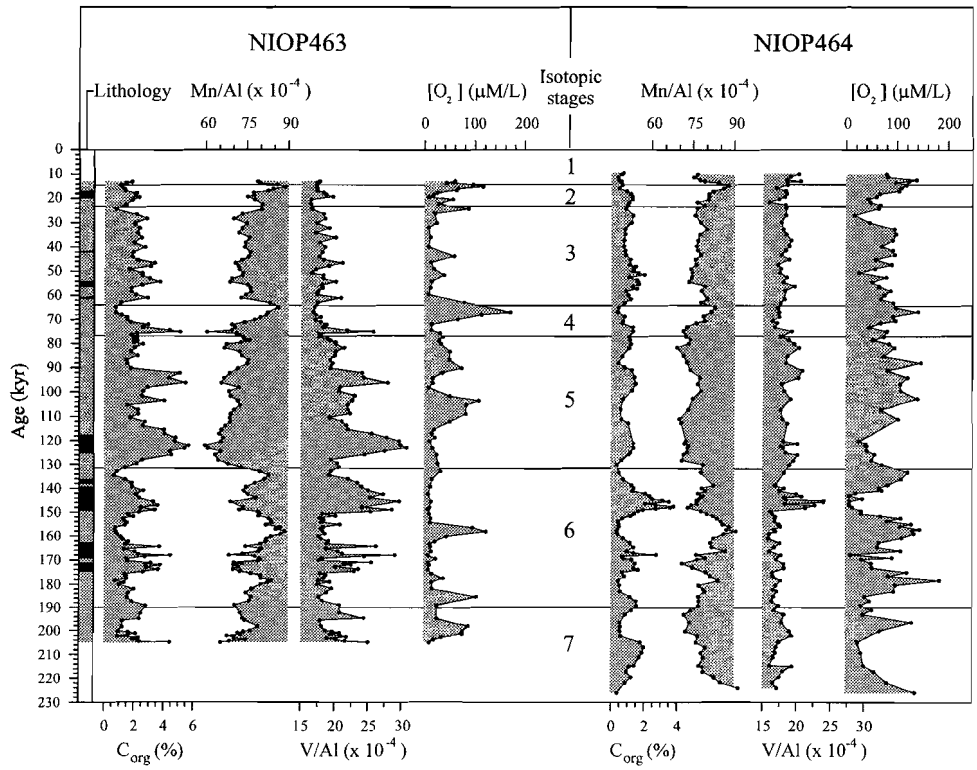

Figure 6 Organic carbon (%), V/Al-, Mn/Al-, and reconstructed oxygen concentrations (µM/L) in piston cores NIOP463 and -464 plotted versus age. Laminated intervals in NIOP463 are shown in the first column.

4. Discussion

Our data set on living foraminifera is too meagre to perform extended statistical analyses. We therefore are not in the position to prove that there is a statistically significant relationship between the various groups of benthic foraminifera and the succession of redox fronts. Jorissen et al. (1998) already pointed out that benthic foraminiferal microhabitat patterns were structured partly by the nitrate-reduction front. Van der Zwaan et al. (1999) formulated theoretical reasons that a relationship between the redox succession and foraminiferal patterns is likely. Our data are indeed suggestive for such a pattern certainly if we view the coherency between the foraminiferal patterns and that of the Mn front. This front is the interface where free oxygen

disappears and the insoluble Mn-oxides are reduced to soluble compounds. Experimental evidence (Alve and Bernhard, 1995; Moodley et al., 1997, 1998a,b) renders it likely that many foraminiferal taxa are able to survive anoxic conditions for some time, although it is not known whether they are able to reproduce under these conditions. Also the similarity of the patterns displayed by the *Bolivina* and *Globobulimina* taxa and the Fe front suggests that foraminiferal distribution is structured by redox fronts. However, coincidence of these patterns does not prove the causality. Although, at first sight a correlation between the transition from oxic to anoxic sediments is likely, it is more difficult to understand why other redox fronts would invoke foraminiferal change. Our first problem in this respect is that we are not aware what metabolic pathways are employed (compare Bernhard, 1996). Secondly, it could be possible that relationships between foraminifera and redox fronts are not straightforward, but coupled to foraging patterns. As Van der Zwaan et al (1999) suggested, it could be possible that facultative anaerobes selectively predate on bacterial suites, which in turn are stratified according to successive redox zones. The stratification of specific bacterial suites according to successive redox zones is certainly true, as has been shown in extensive research summarised by for instance Laanbroek (1990). Although a coupling of benthic foraminiferal groups to certain redox fronts could be true, it is far from clear how this should work. Experimental work is still in progress which will certainly elucidate part of the problem. There is, however, already experimental evidence pertaining to the role of one of the deeper redox fronts. Evidence suggests that this sulphide producing front is limiting: Moodley et al. (1998a) show that the combination of anoxia and sulphide production is lethal to many species, although they certainly survive for some time at lower concentrations (Bernhard, 1993).

Van der Zwaan et al. (submitted) suggests that there is a group of (oxyphilic) taxa which avoids stressed conditions and preferably inhabits only aerated, and thus often the top sediment layer. They considered four different areas (Arabian Sea, Atlantic Ocean, Levantine Basin and Adriatic Sea) and concluded that the abundance patterns of these species reflect variability in the oxygen contents at the sediment water interface. Even accepting this relationship, it remains difficult to understand why the proportion of such taxa would co-vary with oxygen. In many instances oxygen has been regarded as limiting factor, i.e. it decides on the presence-absence of a species and not on its abundance (see Van der Zwaan et al., 1999, for extensive discussion). In the model of Van der Zwaan et al. (submitted) the relationship between the abundance of oxyphilic taxa and increased oxygen can be explained by

assuming that for these taxa the amount of inhabitable space increases with lowering of the redox front. Hence, they have increasing opportunities to proliferate and respond by increased abundances under well-aerated conditions. Also in our data on living foraminifera, we clearly have a group of taxa which avoids lowered oxygen contents at the sediment-water interface or deeper in the sediment column. This group contains taxa which were not mentioned by Van der Zwaan et al. (submitted), such as *Bulimina aculeata*. However, for the purpose of the oxygen reconstruction, we restricted ourselves to species which were found to be oxyphilic also in other regions. In that way we prevent mistakes by using an incidental occurrence which has not been confirmed in other regions and under different conditions.

The reconstructed oxygen record of Fig. 6 represents the variation of the oxygen contents at the sediment-water interface over the past 225 kyr, and suggests that the actual concentrations were frequently very low. Many times oxygen levels at site NIOP463 dropped to values below 0.5 ml/l (or below 25 μMol/l), a value too low for most macrofaunal species (e.g. Tyson and Pearson, 1991). In this respect the reconstructed oxygenation curve is certainly supported by independent faunal evidence: in many parts of the succession we observe signs of meagre macrofaunal presence as for instance evidenced by the preservation of laminated sediments. According to the reconstruction, at site NIOP464 the values were always above this critical limit, and consequently no laminated sediments were found. Apparently, macrofaunal bioturbation remained present throughout the depositional history of this core.

Taken together the records suggest that NIOP463 has been located within the OMZ (see also Den Dulk et al., in press). At this site periods of an intense OMZ clearly alternate with periods characterised by a weakened OMZ, as has already been concluded by Reichart et al. (1997, 1998) and Den Dulk et al. (1998, in press). Over its entire history the deeper core NIOP464 has been substantially better ventilated than NIOP463, which is logical if its present-day position below the OMZ is taken into account. Independent evidence for the reconstructed oxygenation history is provided by the redox elements Mn and V. In an extensive discussion Reichart et al. (1997) and Den Dulk et al. (1998, and in press) point out that with decreasing oxygenation first higher concentrations of Mn and then high concentrations of V occur. Especially if V concentrations are high, bottom water oxygenation is low. The advantage of the reconstructed oxygen record compared with the record of the redox elements becomes immediately evident: oxygen conditions are quantified and make it possible to put constraints on the degree of ventilation of the OMZ during its history. Redox elements only qualitatively indicate oxygenation

history and moreover have the disadvantage that elemental concentrations do not co-vary linearly with oxygenation. With decreasing oxygenation Mn concentrations initially increase, but subsequently decrease.

The variability in reconstructed oxygen curves, suggests that if bioproduction is solely held responsible for the reduced oxygen contents, the variation in organic flux should have been enormous. In view of the overall high average organic fluxes as reconstructed for this system (Den Dulk et al., in press) this seems untenable. Instead, it seems much more realistic to assume that variation in oxygenation was caused by variation in oxygen supply. As pointed out by Reichart et al. (1998) periodic deep convective mixing during periods of a weakened OMZ, seems a far more likely mechanism. The reconstruction indicates that in spite of periodically increased ventilation, maximum reconstructed oxygen concentrations are moderately high (around 150 μMol/l ≈ 4 ml/l) even during the best ventilated periods.

5 Conclusions

We conclude that the distribution of benthic foraminiferal microhabitats is probably associated with redox fronts. However, the reason for this is far from clear. It is evident that some taxa are able to withstand anoxic conditions, which in the Arabian Sea OMZ are of a semi permanent nature. Other taxa seem to be restricted to the well oxygenated microhabitat. These species were employed to reconstruct the oxygenation history of the northern Arabian Sea over the past 225 kyr. The patterns as derived from the oxygen transfer function seem totally acceptable if compared with a detailed pattern of redox elements. Also independent macrofaunal evidence, as expressed in the absence of bioturbation, supports the results obtained from the oxygen transfer function.

Epilogue

Since the initial observation that benthic foraminifera are vertically stratified within the sediment column (Corliss, 1985) a large number of papers addressed this topic. It became clear that a distinction should be made between oligotrophic, generally deep ocean environments, and more eutrophic continental margin regions. Significant differences in composition and in-sediment occupation patterns exist between these settings (Gooday and Rathburn, 1999; Van der Zwaan et al., 1999). Particularly when in eutrophic regions high rates of mid-water oxygen consumption also causes severely depleted bottom water oxygen conditions. In low oxygen environments a low number of species, of which 2 or 3 are dominant, characterise the assemblage. These observations resulted in the conclusion that food and oxygen are the prime ecological factors in structuring benthic foraminifera both horizontally and vertically. Jorissen et al. (1995) summarised most ideas on in-sediment, foraminiferal microhabitat distribution in a conceptual model (the TROX model). Applied to a transect going from eutrophic to oligotrophic environments the model shows that infaunal penetration is shallow at the eutrophic edge. Here, due to the high organic load oxygen consumption is high. Consequently the position of the redox zone is shallow. Therefore, in-sediment distribution under eutrophic conditions is thought to be limited by oxygen. Going to more oligotrophic environments infaunal penetration becomes deep(er) because oxygen consumption is less and redox zones are deeper in the sediment. In oligotrophic environments oxygen consumption is low. The redox zone resides deep in the sediment and does not limit infaunal penetration. In this case, however, it is the lack of food in deeper sediment layers which prevents deep infaunal habitation; infaunal penetration is shallow. However, the way oxygen actually structures benthic foraminifera in eutrophic environments is far from clear. We know that benthic foraminifera are probably highly tolerant to oxygen stress and that a considerable number of species persist below the level of free oxygen (e.g. Jannink et al., 1998; Moodley et al., 1998b). Recent studies suggest that successive redox fronts are involved in foraminiferal distribution. Van der Zwaan et al. (1999) added this feature to the initial TROX-model and included a third element likely to structure microhabitats, viz. competition for food and space (Fig. 1). They attempted through this modification to identify processes which affect both distribution and abundance of benthic foraminifera, instead of describing depth distributions or occurrences as in TROX. TROX-2 schematically shows

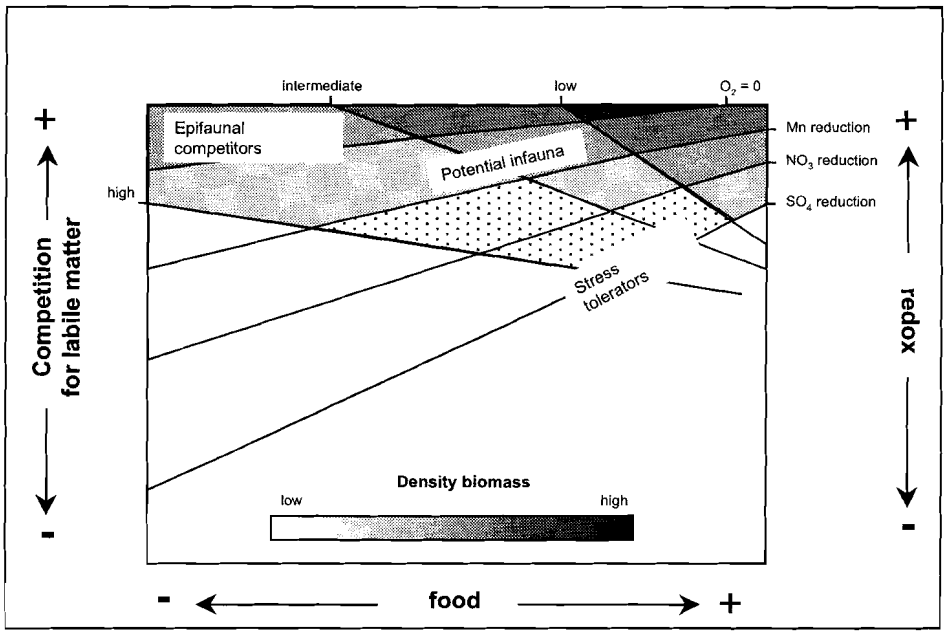

Figure 1 TROX-2 model. Shown is the effect that redox gradients and competition for labile organic matter have on faunal density and distribution of species. Both competition and redox gradients are regulated, in turn, by organic flux (=food) (after Van der Zwaan et al., 1999).

the effect that redox gradients and competition for labile organic matter have on faunal density and the depth distribution of species. In turn both competition and redox gradients are regulated by organic flux (Van der Zwaan et al., 1999).

Oxygen gradients in the benthic environment are not only regulated by the flux arriving at the sea floor, but also by oxygen concentrations in the overlying water column, in turn regulated by oxygen advection. The result of oxygen consumption and advection affects overall composition, density and the depth distribution of benthic foraminiferal species. Characteristic benthic foraminiferal assemblages are found in low oxygen settings, but particularly because microhabitat partitioning appears to be highly complex, the real proxy value of benthic foraminifera in reconstructing oxygenation remains somewhat enigmatic. Moreover, because the flux arriving at the sea floor and oxygen concentrations in the overlying water column are intimately linked to surface water productivity, separating the effect of productivity and

ventilation is considered to be problematic. This is also the case in the Arabian Sea, since high surface water productivity and the intense OMZ results in high organic fluxes and low oxygen conditions in places where the OMZ impinges on the continental slope. Past changes in oxygenation took place on orbital and sub-orbital time scales (Reichart et al., 1998, Von Rad et al, 1999; Den Dulk et al, 1998, and in press). Variability on these time scales is controlled by 1) changes in summer monsoon wind strength, which via coastal and open ocean upwelling controls summer surface water productivity and subsurface oxygen consumption (Altabet et al, 1995; Den Dulk et al, 1998; Reichart et al., 1997, 1998; Von Rad et al., 1999), and 2) deep convective mixing during periods of cold and intensified winter monsoons (Reichart et al., 1998).

Common benthic foraminiferal tools in reconstructing paleoproductivity and bottom water oxygenation are the overall faunal assemblage characteristics, such as dominance, diversity and benthic number (or accumulation rates). The combination of dominance and simple or Shannon diversity generally illustrates the oxygenation history quite nicely in cores collected from depth within the present-day Arabian Sea OMZ. Low (high) diversity and high (low) dominances in these cores reflect alternating periods of an intense and weak OMZ (Chapter 1, 2, 3, and 4).

Dominance and diversity seem less sensitive in recording changes in OMZ intensity at sites below the present-day Arabian Sea OMZ (Chapter 3). This is logical if the position below the OMZ is taken into account. Variability in OMZ intensity, however, is clearly reflected in the group of miliolids both within and below the OMZ (Chapter 3, 4). The latter group shows maximum abundances during periods of a weak OMZ and is rare or absent during periods of an intense OMZ. We therefore concluded that percentages of miliolids can be used for rapid reconstruction of the intensity of the OMZ (Chapter 3). Whether the observed variability in OMZ intensity is forced by surface productivity or by ventilation cannot be decided from the benthic foraminifers. Evidence for changes in the ventilation of the Arabian Sea OMZ is derived from the abundance pattern of some deep-dwelling planktonic foraminiferal species (Reichart et al., 1998). In many instances oxygen has been regarded as limiting factor, i.e. it controls the presence-absence of a species and not its abundance (see Van der Zwaan et al., 1999, for extensive discussion). On the basis of living benthic foraminiferal distribution patterns from the Atlantic, Arabian Sea, and the shallower Adriatic Sea and Levantine Basin, Van der Zwaan et al. (submitted) classified miliolids among a group of epifaunal and shallow infaunal elements which seem to be restricted to the oxic microhabitat. The relative abundance of this 'oxyphilic' group appeared

positively correlated with oxygen contents at the sediment-water interface. This relationship has been quantified resulting in an oxygen transfer function (Van der Zwaan et al., submitted). The observed relationship between oxyphilic taxa and oxygenation can be explained by assuming that for these taxa the amount of inhabitable space increases with a lowering of the redox front. Hence, they have increasing opportunities to proliferate and respond by increased abundances under well-oxygenated conditions. The reconstructed oxygenation history for the cores from below the present-day OMZ using the oxygen transfer function, however, indicates larger variability than that shown by the miliolid record. This is understandable if we assume that below a critical oxygen level miliolids are almost completely absent. Both the transfer function and benthic diversity are based on a larger portion of the assemblage and should therefore record more subtle changes in oxygenation than those recorded by the miliolids and the geochemical proxies Mn/Al and V/Al (Chapter 3, 5). For example, the V-Al ratio documents only one interval in which the OMZ expanded, whereas the benthic foraminifers document three of such intervals.

Although single species occurrences may give insight in the quality of organic matter they are extremely difficult to use as proxies of organic flux (Van der Zwaan et al., 1999). For example, peak occurrences of *Bulimina exilis*, a marker species of high concentrations of fresh or unaltered organic matter (Caralp, 1989), only marks part of all the precession-driven high productivity periods in the OMZ core from the Murray Ridge (Chapter 3). The reason for this is that peak occurrences are not controlled by organic matter flux alone, but also by bottom water oxygenation and inter-specific competition as is summarised in TROX-2. In fact, *B. exilis* belongs to the group of stress tolerators or deep infaunal species (see TROX-2), which live at considerable depth in the sediment under oxygenated conditions at the sediment surface. Because oxygen is no longer acting as a limiting parameter for species occupying this deep infaunal compartment, food should be deciding on their abundance. This implies that their variability in all cases should mark changes in surface water productivity. Unfortunately under normal oxygenated conditions at the sediment surface this microhabitat is sparsely occupied, which will result in a weak reflection in down core percentages, as is observed in the core from below the OMZ. In the Arabian Sea record deep infaunal species only regularly dominate the benthic foraminiferal assemblages in cores collected from the present-day OMZ (Chapter 4). Their strong relation to both OMZ conditions and organic flux is further indicated by the correlation with high organic carbon concentrations

of the sediment (Chapter 4). These high organic carbon concentrations, in turn, have been related to increased burial efficiency under anoxic conditions (Van der Weijden et al., 1998). This implies that deep infaunal species could reflect the storage capacity of organic matter more than the flux arriving at the sea bed (Chapter 4).

The first Factor of multivariate analysis also suggests a relationship with productivity. The factor 1 scores in all Arabian Sea cores correlate nicely with the organic matter content. The latter parameter can be considered as a proxy for productivity, since fluctuations can be correlated in great detail between cores from within and below the OMZ (Reichart et al., 1998). Also in various other studies the first factor correlates with the organic carbon content of the sediment (e.g. Hermelin and Schimmield; Loubere, 1996; Kuhnt et al., 1999), which corroborates the prime ecological role food has in structuring benthic foraminifera. At the same time it should be realised that also oxygenation is incorporated in this axis. However, a combination of benthic foraminiferal proxies may give insight in the role of productivity and oxygenation. For example, in the Arabian Sea core from below the OMZ the combination of high dominances and low diversity values around 120 ka suggest bottom water oxygen depletion (Chapter 3). Positive Factor 1 scores in this same interval, particularly supported by high percentages of the bathymetrically deeper dwelling species *Bulimina aculeata*, on the other hand, point to relatively ventilated bottom water conditions (Chapter 4). The likely conclusion is that productivity was high but the core site was below the OMZ. This, in turn, suggest that the faunal assemblage characteristics are also sensitive to changes in competition for food and space and changes in oxygen gradients as a function of organic flux.

Benthic Foraminiferal Accumulation Rates (BFAR's) for cores from within the OMZ indicate that BFAR's cannot be used as proxy for surface water productivity under anoxic to dysoxic conditions (Chapter 3). This agrees well with the suggestion made by Van der Zwaan et al. (1990) a decade ago. On the basis of a review of relevant literature and an extensive data set these authors concluded that benthic numbers are dependent on pelagic flux, but that this relation might break down in strongly oxygen-deficient areas. TROX-2 illustrates that benthic foraminiferal densities increase with increasing food supply. Benthic foraminiferal densities will be extremely high in low oxygen settings in response to the high food supply and a likely decrease in predation/competition pressure by the macrofaunal community. However, severely oxygen depleted conditions, possibly in combination with changing redox conditions, are limiting resulting in a reduction in benthic

foraminiferal densities. In line with this pattern BFAR's from below the present-day OMZ are generally positively correlated with the organic carbon content of the sediment. In cores from within the OMZ, BFAR's point to a strongly decimated fauna during periods of an intense OMZ. The high BFAR's just before and after a minimum in BFAR, then, are likely explained by a decrease in predation/competition pressure by the macrofaunal community under (moderate) oxygen stress. However, the high BFAR's prevailing in the low productivity and well-oxygenated intervals of the OMZ core from the Murray Ridge (Chapter 3), are not very well understood. This may indicate that for example organic carbon regeneration processes or other diagenetic processes may influence benthic foraminiferal densities as well.

In living assemblages strong seasonal changes are observed, which when tracable in fossil assemblages could contribute significantly to paleoenvironmental reconstructions. In the northern Arabian Sea seasonality is high with substantial fluxes in summer and winter, and low inter-monsoon fluxes, but little is known whether these seasonal differences are reflected (qualitatively and/or quantitatively) in the benthic foraminiferal assemblages. Overall higher percentages of the deep infaunal group during stages 2 and 3 in the core from the Karachi Margin compared to the Murray Ridge core have been attributed to a larger winter flux of organic matter on the Karachi Margin. There are more differences in the benthic foraminiferal fauna between the Karachi and Pakistan Margin cores, but because we lack seasonal data these differences are presently difficult to explain.

In the living assemblages of the northern Arabian Sea *Rotaliatinopsis semiinvoluta*, proliferates within a defined oxygen range of about 0.01- 0.5 ml/l in the lower part of the OMZ and slightly deeper. On basis of this distribution pattern Jannink et al (1998) previously concluded that *R. semiinvoluta* could be a marker species for the lower boundary of the OMZ. Rare occurrences in the core from the centre of the OMZ and common occurrences in cores from the base of the OMZ, indeed, agree with such relation (Chapter 5). High percentages in the core from below the OMZ then are likely explained by a deepening of the base of the OMZ. The use of *R. semiinvoluta* seems evident in roughly reconstructing the position of the lower boundary of the Arabian Sea OMZ, but the causal relation is unclear. Wishner et al. (1998) summarised on basis of a number of papers that in contrast to the oxygen minimum zone per se, the upper and lower boundaries of OMZs appear to be locations of elevated biological and biogeochemical activity. They also showed an increase in subsurface zooplankton biomass across the 0.05-0.1 ml/l oxygen gradient of the lower edge of the Arabian Sea

OMZ. All this seems to indicate, as was previously suggested by Jannink et al (1998), that *R. semiinvoluta* is related to specific food conditions associated with the transitional conditions between those in the OMZ and those in somewhat deeper less eutrophic water. Unfortunately *R. semiinvoluta* is endemic to the Indian ocean, but one may speculate that different species could mark this niche in other oceans.

The extent of supralysoclinal dissolution is of some concern. Particular intense supralysoclinal dissolution has been related to dysoxic (OMZ) conditions (Berelson et al., 1996). In line with this observation Planktonic Foraminiferal Accumulation Rates (PFAR) suggest that supralysoclinal dissolution has, indeed, affected carbonate preservation at times of an intense OMZ in the shallow cores. Since benthic foraminifera are less prone to dissolution than planktonic foraminifera, both groups are not necessarily equally affected. The gloss of benthic foraminifera do show differences between intervals that are presumably affected by dissolution and those that are not, but overall few fragmented specimens were observed. In fact, it appears to be very difficult to estimate the effect of dissolution. As an extreme point of view one may argue that the benthic foraminiferal patterns are shaped entirely by variations in supralysoclinal dissolution. We, however, feel that this is not likely to be the case, because this would imply selective dissolution off all "oxic" species, thereby excluding deep infaunal species of which some have fragile tests. More importantly, down-core patterns can be well explained considering distribution patterns of living (Bengal Rose stained) benthic foraminifera in the Arabian Sea and in other high productivity/low oxygen environments.

A central conclusion of this thesis is that benthic foraminifers are well suited for the reconstruction of late Quaternary variations in thickness and intensity of the northern Arabian Sea Oxygen Minimum Zone (OMZ) (Chapters 2, 3, 4, and 5). Benthic foraminifera have potential in quantifying past changes in oxygenation (Chapter 5). An unresolved question is the effect of seasonality on benthic foraminiferal fauna in the Arabian Sea and the actual potential of benthic foraminifera in reconstructing summer and winter monsoon productivity. We think that future research should focus on this topic, before more effort is put into detailed analysis of benthic foraminifera in the context of proxy application for Arabian Sea paleoenvironmental reconstructions. A study on living-dead turn over rates may also elucidate the effect of supralysoclinal dissolution.

References

Altabet, M.A., Francois, R., Murray, D.W., and Prell, W.L., 1995. Climate-related variations in denitrification in the Arabian Sea from sediment $^{15}N/^{14}N$ ratios. Nature 373, 506-509.

Altenbach, A.V., and Sarnthein, M., 1989. Productivity Record in Benthic Foraminifera. In: W.H. Berger, V.S. Smetacek, G. Wefer. (Eds.), Production of the Ocean: Present and Past. Chichester, England, Wiley-Interscience, pp. 255-269.

Altenbach, A.V., Pflaumann, U., Schiebel, R., Thies, A., Timme, S., and Trauth, M., 1999. Scaling percentages and distributional patterns of benthic foraminifera with flux rates of organic carbon. J. of Foram. Res. 29, 173-185.

Alve, E. and Bernhard, J.M., 1995. Vertical migratory response of benthic foraminifera to controlled oxygen concentrations in an experimental mesocosm. Mar. Ecol. Prog. Ser. 116, 137-151.

Anderson, D.M. and Prell, W.L., 1993. A 300 kyr record of upwelling off Oman during the late Quaternary: Evidence of the Asian southwest monsoon. Paleocanography 8, 193-208.

Banse, K., 1984. Overview of the Hydrography and associated biological phenomena in the Arabian Sea, off Pakistan. In: B.U. Haq and J.D. Milliman, (Eds.), Marine Geology and oceanography of the Arabian Sea and coastal Pakistan. Van Nostrand Reinhold, New York, pp. 271-303.

Banse, K., 1987. Seasonality of phytoplankton chlorophyll in the central and northern Arabian Sea. Deep-Sea Res. 34, 713-723.

Bard, E., 1988. Correction of accelerator mass spectrometry ^{14}C ages measured in planktonic foraminifers: paleoceanographic implications. Paleoceanography 3, 635-645.

Bard, E., Hamelin, B., Fairbanks, R.G. and Zinder, A., 1990. Calibration of the ^{14}C timescale over the past 30,000 years using mass spectrometric U-Th ages from Barbados corals. Nature 345, 405-410.

Bard, E., Rosteck, F., and Sonzogni, C., 1997. Interhemispheric synchrony of the last deglaciation inferred from alkenone palaeothermometry. Nature 385, 707-710.

Barmawidjaja, D.M., Jorissen, F.J., Puskaric, S. and Van der Zwaan G.J., 1992. Microhabitat selection by benthic foraminifera in the northern Adriatic Sea. J. Foram. Res. 22, 297-317.

Bauer, S., Hitchcock, G.L. and Olson, D.B., 1991. Influence of monsoonally-forced Ekman dynamics upon surface layer depth and plankton biomass distribution in the Arabian Sea. Deep-Sea Res. 38, 531-553.

Bé, A.W.H., Vilks, G., and Lott, L., 1971. Winter distribution of planktonic foraminifera between the Grand Banks and the Caribbean. Micropaleontol. 17, 31-42.

Behl, R.J., and Kennett, J.P., 1996. Brief interstadial events in the Santa Barbara Basin, NE Pacific, during the past 60 kyr. Nature 379, 243-246.

Berelson, W.M., McManus, J., Coale, K.H., Johnson, K.S., Kilgore, T., Burdige, D., and Pilskaln, C., 1996. Biogenic matter diagenis on the seafloor: A comparison between two continental margin transects. J. of Mar. Res. 54, 731-762.

Berger, W.H., 1977. Deep-sea carbonate: pteropod distribution and the aragonite compensation depth. Deep-Sea Res. 25, 447-452.

Berger, W.H., and Wefer, G., 1990. Export production: seasonality and intermittency, and paleoceanographic implications. Palaeogeogr., Palaeoclimatol., Palaeoecol. (Global Planet. Change Sect.) 89, 245-254.

Berger, W.H., Smetacek, V.S., and Wefer, G., 1989. Ocean productivity and paleoproductivity- An overview. In: W.H. Berger, V.S. Smetacek, G. Wefer. (Eds.), Production of the Ocean: Present and Past. Chichester, England, Wiley-Interscience, pp. 255-269.

Bernhard, J.M., 1986. Characteristic assemblages and morphologies of benthic foraminifera from anoxic, organic-rich deposits: Jurassic through Holoceen. J. of Foram. Res. 16, 207-215.

Bernhard, J.M., 1992. Benthic foraminiferal distribution and biomass related to pore-water oxygen content: central California continental slope and rise. Deep-Sea Res. 39, 585-605.

Bernhard, J.M., 1993. Experimental and field evidence of Antarctic foraminiferal tolerance to anoxia and hydrogen sulfide. Mar. Micropaleontol. 20, 203-213.

Bernhard, J.M., and Alve, E., 1996. Survival, ATP pool, and ultrastructural characterization of benthic foraminifera from Drammensfjord (Norway): response to anoxia. Mar. Micropaleontol. 28, 5-17.

Bernhard, J.M., and Reimers, C.E., 1991. Benthic foraminiferal population fluctuations related to anoxia: Santa Barbara Basin. Biogeochemistry 15, 127-149.

Betzer, P.R., Showers, W.J., Laws, E.A., Winn., C.D., Di Tullio, G.R., and Kroopnick , P.M., 1984. Primary productivity and particle fluxes on a transect of the equator at 153° W in the Pacific Ocean. Deep Sea Res. 31, 1-11.

Bigg, G.R. and Jiang, D., 1993. Modelling the late Quaternary Indian Ocean circulation. Paleoceanography 8, 23-46.

Bond, G., Broecker, W.S., Johnsen, S., McManus, J., Labeyrie, L.D., Jouzel, J., and Bonani, G., 1993. Correlations between climate records from North Atlantic sediments and Greenland ice. Nature 365, 143-147.

Bordovsky, O.K., 1965. Accumulation of organic matter in bottom sediments. Mar. Geol. 3, 33-82.

Boyle, E.A., 1988. Cadmium: chemical tracer of deep water paleoceanography. Paleoceanography 3, 471-489.

Breit, G.N. and Wanty, R.B., 1991. Vanadium accumulation in carbonaceous rocks: a review of geochemical controls during deposition and diagenesis. Chem. Geol. 91, 83-97.

Brock, J.C., McClain, C.R., Anderson, D.M., Prell, W.L., and Hay, W.W., 1992. Southwest monsoon circulation and environments of recent planktonic foraminifera in the northwestern Arabian Sea. Paleoceanography 7, 799-813.

Broecker, W.S., Bond, G., Klas, M., Clark, E., and McManus, J., 1992. Origin of the northern Atlantic Heinrich events. Climate Dyn. 6, 265-273.

Broecker, W.S., Peteet, D., Hajdas, I., Lin, J., and Clark, E., 1998. Antiphasing between rainfall in Africa's rift valley and North America's Great Basin. Quat. Res. 50, 12-20.

Buzas, M.A., Culver, S.J., and Jorissen, F.J., 1993. A statistical evaluation of the microhabitats of living (stained) infaunal benthic foraminifera. Mar. Micropaleontol. 20, 311-320.

Calvert, S.E., and Pedersen, T.F., 1992. Organic carbon accumulation and preservation in marine sediments: How important is anoxia ? In: J. Whelan and J.F. Farrington, (Eds.), Organic matter. Colombia Univ. Press, New York, pp. 232-263.

Calvert, S.E., Bustin, R.M., and Ingall, E.D., 1996. Influence of water column anoxia and sediment supply on the burial and preservation of organic carbon in marine shales. Geochim. Cosmochim. Acta 60, 1577-1593.

Calvert, S.E., Pederson, T.F., Naidu, P.D., and Von Stackelberg, U., 1995. On the organic carbon maximum on the continental slope of the eastern Arabian Sea. J. of Mar. Res. 53, 269-296.

Canfield, D.E. and Raiswell, R., 1991. Carbonate precipitation and dissolution. In: P.A. Allison and D.E.G. Briggs, (Eds.), Taphonomy; releasing the data locked in the fossil record. Plenum Press, New York, pp. 411-453.

Caralp, M.H., 1984. Impact de la matière organique dans des zones de forte productivité sur certains foraminifères bentiques. Oceanol. Acta 7, 509-515.

Caralp, M.H., 1989. Abundance of *Bulimina exilis* and *Melonis barleeanum*: Relationship to the quality of marine organic matter. Geo-Marine Letters 9, 37-43.

Clemens, S., Prell, W., Murray, D., Shimmield, G. and Weedon, G., 1991. Forcing mechanisms of the Indian Ocean monsoon. Nature 353, 720-725.

Codispoti, L.A., 1991, Primary productivity and carbon and nitrogen cycling in the Arabian Sea. In: S.L. Smith, K. Banse, J.K. Cochran, L.A. Codispoti, H.W. Ducklow, M.E. Luther, D.B. Olson, W.T. Peterson, W.L. Prell, N. Surgi, J.C. Swallow, and K. Wishner, (Eds.), U.S. JGOFS: Arabian Sea Process Study. U.S. JGOFS Planning Report 13, 75-85.

Corliss, B.H. and Chen, C., 1988. Morphotype patterns of Norwegian Sea deep-sea benthic foraminifera and ecological implications. Geology 16, 716-719.

Corliss, B.H., 1985. Microhabitats of benthic foraminifera within deep-sea sediments. Nature 314, 435-438.

Corliss, B.H., 1991. Morphology and microhabitat preferences of benthic foraminifera from the northwest Atlantic Ocean. Mar. Micropaleontol. 17, 195-236.

Corliss, B.H., and Emerson, S., 1990. Distribution of Rose Bengal stained deep-sea benthic foraminifera from the Nova scotian continental margin and Gulf of Maine. Deep-Sea Res. 37, 381-400.

Cullen, J.L. and Prell, W.L., 1984. Planktonic foraminifera of the northern Indian Ocean: distribution and preservation in surface sediments. Mar. Micropaleontol. 9, 1-52.

Dansgaard, W., Johnsen, S.J., Clausen, H.B., Dahl-Jensen, D., Gundestrup, N.S., Hammer, C.U., Hvidberg, C.S., Steffensen, J.P., Sveinbjörnsdottir, A.E., Jouzel, J., and Bond, G., 1993. Evidence for general instability of past climate from a 250-kyr ice-core record. Nature 374, 218-220.

De Stigter H.C., Jorissen F.J., and Van der Zwaan, G.J., 1996. Evidence for the control of organic flux on the bathymetric zonation of benthic foraminifera. In: Recent and fossil benthic foraminifera in the Adriatic Sea: distribution patterns in relation to organic carbon flux and oxygen concentration at the seabed (thesis). Geologica Ultraiectina 144, 121-142.

De Stigter, H.C., Jorissen, F.J., and Van der Zwaan, G.J., 1998. Bathymetric distribution and microhabitat partitioning of live (Rose bengal stained) benthic foraminifera along a shelf to bathyal transect in the southern Adriatic Sea. J. Foram. Res. 28, 40-65.

Dean, W.E., Gardner, J.V., and Andersen, R.Y., 1994. Geochemical evidence for enhanced preservation of organic matter in the oxygen minimum zone of the continental margin of northern California during the late Pleistocene. Paleoceanography 9, 47-61.

Den Dulk, M., Reichart, G.J., Memon, G.M., Roelofs, E.M.P., Zachariasse, W.J., and Van der Zwaan, G.J., 1998. Benthic foraminiferal response to variations in surface water productivity and oxygenation in the northern Arabian Sea. Mar. Micropaleontol. 35, 43-66 (Chapter 1, this thesis).

Den Dulk, M., Reichart, G.J., Van Heijst, S., Zachariasse, W.J, Van der Zwaan, G.J., 1999. Benthic foraminifera as proxies of organic matter flux and bottom water oxygenation ?: *A case history from the northern Arabian Sea* (Palaeogeog., palaeoclimatol., Palaeoecol., in press, Chapter 3, this thesis).

Denne, R.A., and Sen Gupta, B.K., 1991. Association of bathyal foraminifera with water masses in the northwestern Gulf of Mexico. Mar. Micropaleontol. 17, 173-193.

Des Combes, H.J., Caulet, J.P., Tribovillard, N.P., 1999. Pelagic productivity changes in the equatorial area of the northwest Indian Ocean during the last 400,000 years. Mar. Geol. 159, 27-55.

Deuser, W.G., Ross, E.H., and Mlodzinska, Z.J., 1978. Evidence for rate of denitrification in the Arabian Sea. Deep-Sea Res. 25, 431-445.

Dietrich, P., and Marchig, V., 1996. Sedimentation und Frühdiagenese im Bereich der Sauerstoff-Minimum-Zone vor der Indus-Münndung (Pakistan, Arabisches Meer). Zbl. Geol. Paläontol. 1995 (I), 45-61.

Douglas, R.G., and Woodruff, F., 1981. Deep sea benthic foraminifera. In: C.

Emiliani, (Ed.), The Sea; Vol. 7; The oceanic lithosphere. Wiley-Interscience, New York, 1233-1327.

Douglass, F., 1996. Monsoonal Variations: Evidence from a Sediment Core from the North-eastern Arabian Sea. B.Sc. Thesis, University of British Columbia, Vancouver, 46 pp.

Duplessy, J.C., Shackleton, N.J., Fairbanks, R.G., Labeyrie, L., Oppo, D., and Kallel, N., 1988. Deepwater source variations during the last climatic cycle and their impact on the global deepwater circulation. Paleoceanography 3, 343-360.

Dymond, J., Suess, E., Lyle, M., 1992. Barium in deep-sea sediment: a geochemical proxy for palaeoproductivity. Paleoceanography 7 (2), 163-181.

Emeis, K.C., Anderson, D.M., Doose, H., Kroon, D., and Schulz-Bull, D., 1995. Sea-surface temperatures and the history of monsoon upwelling in the northwestern Arabian Sea during the last 500,000 years. Quat. Res. 43, 355-361.

Fariduddin, F., and Loubere, P., 1997. The surface ocean productivity response of deeper water benthic foraminifera in the Atlantic Ocean. Mar. Micropaleontol. 32, 289-310.

Fontugne, M.R., and Duplessey, J.C., 1986. Variations of the monsoon regime during the upper Quaternary: evidence from carbon isotopic record of organic matter in north Indian ocean sediment cores. Palaeogeogr. Palaeoclimatol. Palaeoecol. 56, 69-88.

Gooday, A.J., 1986. Meiofaunal foraminiferans from the bathyal Porcupine Seabright (northeast Atlantic): size structure, standing stock, taxonomic composition, species diversity and vertical distribution in the sediment. Deep-Sea Res. 33, 1345-1373.

Gooday, A.J., 1993. Deep-sea benthic foraminiferal species which exploit phytodetritus: Characteristic features and controls on distribution. Mar. Micropaleontol. 22, 187-205.

Gooday, A.J., 1994. The Biology of Deep-Sea Foraminifera: A Review of Some Advances and their Applications in Paleoceanography. Palaios 9, 14-31.

Gooday, A.J., and Rathburn, A.E., 1999. Temporal variability in living deep-sea benthic foraminifera: a review. Earth Sci. Rev. 46, 187-212.

Grousset, F., Labeyrie, L., Sinko, J.A., Cremer, M., Bond, G., Duprat, J., Cortijo, E., and Houon, S., 1993. Patterns of ice-rafted detritus in the glacial North Atlantic. Paleoceanography 8 (2), 175-193.

Guichard, S., 1997. Evolution de l'environment dans la zone de l'upwelling mauritanien pendant les derniers 236,000 ans; le temoignage de l'ecosysteme benthique. (These) l'Universite Bordeaux I, N° d'ordre: 1799, pp 400.

Guo, Z., Liu, T., Guiot, J., Wu, N., Lü, H., Han, J., Liu, J., and Gu, Z., 1996. High-frequency pulses of East Asian monsoon climates in the last two glaciations: link with the North Atlantic. Climate Dyn. 12, 701-709.

Herguera, J.C., and Berger, W.H., 1991. Paleoproductivity from benthic foraminifera abundance: Glacial to postglacial change in the west-equatorial Pacific. Geology 19, 1173-1176.

Hermelin, J.O.R., 1991. The benthic foraminiferal faunas of sites 725, 726, and 728 (Oman Margin, northwestern Arabian Sea. Proc. Ocean Drilling Prog. Ser. 117, 55-87.

Hermelin, J.O.R., and Shimmield, G.B., 1990. The Importance of the Oxygen Minimum Zone and Sediment Geochemistry in the Distribution of Recent Benthic Foraminifera in the Northwest Indian Ocean. Mar. Geol. 91, 1-29.

Hermelin, J.O.R., and Shimmield, G.B., 1995. Impact of productivity events on the benthic foraminiferal fauna in the Arabian Sea over the last 150,000 years. Paleoceanography 10, 85-116.

Hughen, K.A., Overpeck, J.R., Peterson, L.C., and Trumbore, S., 1996. Rapid climate changes in the tropical Atlantic region during the last deglaciation. Nature 380, 51-54.

Imbrie, J., Hays, J.D., Martinson, D.G., Mcintyre, A., Mix, A.C., Mortley, J.J., Pisias, N.G., Prell, W.L. and Shackleton, N.J., 1984. The orbital theory of Pleistocene climate: Support from a revised chronlogy of the marine $\delta^{18}O$ record. In: A.L. Berger, J. Imbrie, J. Hays, G. Kukla, B. Saltzman, (Eds.),: Milankovitch and Climate, Part I, Reidel Dordrecht, pp. 269-305.

Jannink, N.T., Van der Zwaan, G.J., and Zachariasse, W.J., 1998. Living (Rose Bengal stained) foraminifera from an upwelling environment: the continental margin south of Karachi, Arabian Sea. Deep-Sea Res. I 45, 1483-1513.

Jasper, J.P., and Gagosian, R.B., 1990. The sources and deposition of organic matter in the Late Quaternary Pigmy Basin, Gulf of Mexico. Geochim. Cosmochim. Acta 54, 1117-1132.

Johnsen, S.J., Clausen, H.B., Dansgaard, W., Fuhrer, K., Gunde-strup, N., Hammer, C.U., Iversen, P., Jouzel, J., Stauffer, B., and Steffensen, J.P., 1992. Irregular glacial interstadials recorded in a new Greenland ice core. Nature 359, 311-313.

Jones, R.W., 1994. The challenger foraminifera. Oxford University Press, Oxford, 149 pp.

Jongman, R.H.G., Ter Braak, C.J.F, and Van Tongeren, O.F.R., 1995 Data analysis in community and landscape ecology, Cambridge University Press, pp 299,

Jonkers, H.A., 1984. Pliocene benthonic foraminifera from homogeneous and laminated marls on Crete. Utrecht Micropaleontol. Bull. 31, 179 pp.

Jorissen, F.J., 1999. Benthic foraminiferal successions across Late Quaternary Mediteranean sapropels. Mar. Geol. 153, 91-101.

Jorissen, F.J., and Wittling, I., 1999. Ecological evidence from live-dead comparison of benthic foraminiferal faunas off Cape Blanc (Northwest Africa). Palaeogeogr. Palaeoclimatol. Palaeoecol. 149, 151-170.

Jorissen, F.J., Barmawidjaja, D.M., Puskaric, S., and Van der Zwaan, G.J., 1992. Vertical distribution of benthic foraminifera in the northern Adriatic Sea: The relation with the organic flux. Mar. Micropaleontol. 19, 131-146.

Jorissen, F.J., De Stigter, H.C., and Widmark, J.G.V., 1995. A conceptual model explaining benthic foraminiferal microhabitats. Mar. Micropaleontol. 26, 3-15.

Jorissen, F.J., Wittling, I., Peypouquet, J.P., Rabouille, C., and Relexans, J.C.,1998. Live benthic foraminiferal faunas off Cape Blanc, NW-Africa: Community structure and microhabitats. Deep-Sea Res. I 45, 2157-2188.

Josefson, A.B., and Widbom, B., 1988. Differential response of benthic macrofauna and meiofauna to hypoxia in the Gullmar Fjord basin. Mar. Biol. 100, 31-40.

Kabanova, Y.G., 1968. Primary production of the northern part of the Indian Ocean. In: Oceanology, of the academy of sciences of the USSR (English translation). Vol. 19, 214-225.

Kaiho, K., 1994. Benthic foraminiferal dissolved-oxygen index and dissolved-oxygen levels in the modern ocean. Geology 22, 719-722.

Kaiho, K., 1999. Effect of organic flux and dissolved oxygen on the benthic foraminiferal oxygen index (BFOI). Mar. Micropaleontol. 37, 67-76.

Kitazato, H., 1994. Foraminiferal microhabitats in four marine environments around Japan. Mar. Micropaleontol. 24, 29-41.

Kuhnt, W., Hess, s., and Jian, Z., 1999. Quantitative composition of benthic foraminiferal assemblages as a proxy indicator for organic carbon flux rates in the South China sea. Mar. Geol. 156, 123-157.

Laanbroek, H.J., 1990. Bacterial cycling of minerals that affect plant growth in waterlogged soils: a review. Aquatic botany 38, 109-125.

Loeblich, A.R., and Tappan, H., 1988. Foraminiferal genera and their classification. Van Nostrand Reinhold, New York, 970 pp.

Loubere, P., 1996. The surface ocean productivity and bottom water oxygen signals in deep-water benthic foraminiferal assemblages. Mar. Micropaleontol. 28, 247-261.

Lückge, A., Boussafir, M., Lallier-Verge`s, E., and Littke, R., 1996. Comparative study of organic matter preservation in immature sediments along the continental margins of Peru and Oman, Part I. Results of petrographical and bulk geochemical data. Org. Geochem. 24 (4), 437-451.

Lutze, G.F., and Coulbourn, W.T., 1984. Recent benthic foraminifera from the continental margin of northwest Africa: community structure and distribution. Mar. Micropaleontol. 8, 361-401.

Mackensen, A., Sejrup, H.P., and Jansen, E., 1985. The distribution of living benthic foraminifera on the continental slope and rise off southwest Norway. Mar. Micropaleontol. 9, 275-306.

Madhupratap, M., Kumar, S.P., Bhattathiri, P.M.A., Kumar, M.D., Raghukumar, S., Nair, K.K.C., and Ramaiah, N., 1996. Mechanism of the biological response to winter cooling in the northeastern Arabian Sea. Nature 384, 549-552.

Madhupratap, M., Kumar, S.P., Bhattathiri, P.M.A., Kumar, M.D., Raghukumar, S., Nair, K.K.C., and Ramaiah, N., 1996. Mechanisms of the biological response to winter cooling in the north-eastern Arabian Sea. Nature 384, 549-552.

Martinson, D.G., Pisias, N.G., Hays, J.D., Imbrie, J., Moore Jr, T.C., and Shackleton, N.J., 1987. Age dating and the orbital theory of the ice ages: development of a high-resolution 0-300,000 year chronostratigraphy. Quat. Res.

27, 1-29.
McCorkle, D.C., Corliss, B.H., and Farnham, C.A., 1997. Vertical distribution and stable isotopic compositions of live (stained) benthic foraminifera from the North Carolina and California continental margins. Deep-Sea Res. I 44, 983-1024.
Melkert, M., Ganssen, G., Helder, W., and Troelstra, S.R., 1992. Episodic preservation of pteropod oozes in the deep northeast Atlantic Ocean; climate change and hydrothermal activity. Mar. Geol. 103, 407-422.
Meyer, I., and Klosa, D., 1997. Mineralbestimmungen in Sediment-gesteinen mit dem Computerprogramm TRIO C . Z. Angew. Geol. 43, 118-123.
Miao, Q., and Thunell, R.C., 1993. Recent deep-sea benthic foraminiferal distributions in the South China and Sulu Sea. Mar. Micropaleontol. 22, 1-32.
Miller, K.G., and Lohmann, G.P., 1982. Environmental distribution of recent benthic foraminifera on the northeast United States continental slope. Geol. Soc. of Am. Bull. 93, 200-206.
Moodley, L., and Hess, C., 1992. Tolerance of infaunal bentic foraminifera for low and high oxygen concentrations. Biol. Bull. 183, 94-98.
Moodley, L., Schaub, B.E.M., Van der Zwaan, G.J., and Herman, P.M.J., 1998b. Resistance of benthic foraminifera (Protista: Sarcodina) to hydrogen sulphide. Mar. Ecol. Prog. Ser. 169, 77-86.
Moodley, L., Van der Zwaan, G.J., Herman, P.M.J., Kempers, L., and Van Breugel, P., 1997. Differential response of benthic meiofauna to anoxia with special reference to foraminifera (Protista: Sarcodina). Mar. Ecol. Prog. Ser. 158, 151-163.
Moodley, L., Van der Zwaan, G.J., Rutten, G.M.W., Boom, R.C.E., and Kempers, A.J., 1998a. Subsurface activity of benthic foraminifera in relation to porewater oxygen content: laboratory experiments. Mar. Micropaleontol. 34, 91-106.
Morse, J.W., and Mackenzie, F.T., 1990. Geochemistry of sedimentary carbonates. Developments in Sedimentology, 48. Elsevier, New York, pp. 707.
Müller, P.J., and Suess, E., 1979. Productivity, sedimentation rate and sedimentary organic matter in the oceans-I. Organic carbon preservation. Deep-Sea Res. 26A, 1347-1362.
Müller, P.J., Schneider, R., and Ruhland, G., 1994. Late Quaternary pCO_2 variations in the Angola current: Evidence from organic carbon $\delta^{13}C$ and alkenone temperatures. In: R. Zahn et.al., (Eds.), Carbon Cycling in the Glacial Ocean: Constraints on the Ocean's Role in Global Change. NATO ASI Ser. 117, 673-685.
Mullineaux, L.S., and Lohmann, G.P., 1981. Late quaternary stagnations and recirculation of the eastern Mediterranean: Changes in the deep water recorded by fossil benthic foraminifera. J. Foraminiferal Res. 11, 20-39.
Murray, D.W. and Prell, W.L., 1992. Late Pleistocene climatic oscillations and monsoon upwelling recorded in sediments from the Owen Ridge, northwestern Arabian Sea. In: C.P. Summerhayes, W.L. Prell and K.C. Emeis, (Eds.),

Upwelling systems: Evolution since the Early Miocene. Geol. Soc. Spec. Publ. 64, 197-213.

Murray, J.W., 1991. Ecology and Palaeoecology of Benthic Foraminifera. Longman, New York, 397 pp., ISBN 0-582-05122-3.

Naidu, P.D., and Malmgren, B.A., 1995. Do benthic foraminifer records represent a productivity index in oxygen minimum zone areas? An evaluation from the Oman Margin, Arabian Sea. Mar. Micropaleontol. 26, 49-55.

Nolet, G.J., and Corliss, B.H., 1990. Benthic foraminiferal evidence for reduced deep-water circulation during sapropel deposition in the eastern Mediterranean. Mar. Geol. 94, 109-130.

Olson, D.B., Hitchcock, G.L., Fine, R.A., and Warren, B.A., 1993. Maintenance of the low-oxygen layer in the central Arabian Sea. Deep-Sea Res. 40, 673-685.

Olson, D.B., Hitchcock, G.L., Fine, R.A., and Warren, B.A., 1993. Maintenance of the low-oxygen layer in the central Arabian Sea. Deep-Sea Res. 40, 673-685.

Oppo, D.W., and Lehman, S.J., 1993. Mid-depth circulation of the sub-polar north Atlantic during the last glacial maximum. Science 259, 1148-1152.

Oppo, D.W., Raymo, M.E., lohman, G.P., Mix., a.C., Wright, J.D., Prell, W.L., 1995. A $\delta^{18}O$ record of the Upper north Atlantic deep water during the past 2.6 million years: Paleoceanography 10, 373-94.

Pedersen, T.F., Shimmield, G.B., and Price, N.B., 1992. Lack of enhanced preservation of organic matter in sediments under the oxygen minimum zone of the Oman Margin. Geochim. Cosmochim. Acta. 56, 545-551.

Perez-Cruz, L.L., and Machain-Castillo, M.L., 1990. Benthic foraminifera of the oxygen minimum zone, continental shelf of the Gulf of Tehuantepec, Mexico. J. Foram. Res. 20, 312-325.

Peterson, L.C., Overpeck, J.T., Kipp, N.G., and Imbrie, J., 1991. A high-resolution late Quaternary upwelling record from the anoxic Cariaco Basin, Venezuela. Paleoceanography 6, 99-119.

Phleger, F.B., and Soutar, A., 1973. Production of benthic foraminifera in three east Pacific oxygen minima. Micropaleontology 19, 110-115.

Popp, B.N., Takigiku, R., Hayes, J.M., Louda, J.W., and Baker, E.W., 1989. The post-Palaeozoic chronology and mechanism of 13 C depletion in primary marine organic matter. Am. J. Sci. 289 (4), 436-454.

Porter, S., and Zhisheng, A., 1995. Correlation between climate events in the North Atlantic and China during the last glaciation. Nature 375, 305-308.

Prell, W.L., 1984. Monsoonal climate of the Arabian Sea during the late Quaternary: a response to changing solar radiation. In: A.L. Berger, J. Imbrie, J. Hays, G. Kukla and B. Saltzman, (Eds.), Milankovitch and Climate, Part I, Reidel Dordrecht, pp. 349-366.

Prell, W.L., 1993. Variation of monsoonal upwelling: A response to changing solar radiation. In: J.E. Hansen and T. Takahasi, (Eds.), Climatic processes and climate sensitivity, Vol. 29, Geophysical Union Geophys. Monogr. Ser., Washington D.C., pp. 48-57.

Prell, W.L., Hutson, W.H., Williams, D.F., Be, A.W.H., Geitzenauer, K., and Molfino, B., 1980. Surface circulation of the Indian ocean during the Last Glacial Maximum, approximately 18,000 yr B.P.. Quat. res. 14, 309-336.

Prell, W.L., Niitsuma, N., Emeis, K.C. et al., 1990. Oman Margin/Neogene Package. Proc. ODP, Sci. Results, 117, 638 pp.

Prins, M. A. and Weltje, G. J., 1999. End-member modeling of siliciclastic grain-size distributions: The late Quaternary record of eolian and fluvial sediment supply to the Arabian Sea and its paleoclimatic significance. In: J. Harbaugh, L. Watney, G. Rankey, R. Slingerland, R., Goldstein, and E. Franseen (Eds.), Numerical experiments in stratigraphy: Recent advances in stratigraphic and sedimentologic computer simulations. SEPM, (Society for Sedimentary Geology) Special Publication 62, 91-111.

Qasim, S.Z., 1982. Oceanography of the northern Arabian Sea. Deep Sea Res. 29, 1041-1068.

Rathburn, A.E., and Corliss, B.H., 1994. The ecology of deep-sea benthic foraminifera from the Sulu Sea. Paleoceanography 9, 87-150.

Rathburn, A.E., and Corliss, B.H., 1994. The ecology of living (stained) deep-sea benthic foraminifera from the Sulu Sea. Paleoceanography 9, 87-150.

Rau, G.H., Takahashi, T., and Des Marais, D.J., 1989. Latitudinal variations in plankton $\delta^{13}C$: implications for CO_2 and productivity in the past oceans. Nature 341 (10), 516-518.

Reichart, G.J., 1997. Organic carbon preservation and oxygen minimum zone (OMZ) variability in the northern Arabian Sea. In: Late Quaternary variability of the Arabian Sea monsoon and oxygen minimum zone, (thesis). Geologica Ultraiectina 154, 121-152.

Reichart, G.J., Den Dulk, M., Visser, H.J., Van der Weijden, C.H., and Zachariasse, W.J., 1997. A 225 kyr record of dust supply, paleoproductivity and the oxygen minimum zone from the Murray Ridge (northern Arabian Sea). Palaeogeogr. Palaeoclimatol. Palaeoecol. 134, 149-169.

Reichart., G.J., Lourens, L.J., and Zachariasse, W.J., 1998. Temporal variability in the northern Arabian Sea Oxygen Minimum Zone (OMZ) during the last 225,000 years. Paleoceanography, 13, 607-621.

Ripley, E.M., Shaffer, N.R., and Gilstrap, M.S., 1990. Distribution and geochemical characteristics of metal enrichment in the New Albany Shale (Devonian-Mississipian), Indiana. Econ. Geol. 85, 1790-1807.

Rohling, E.J., and Zachariasse, W.J., 1996. Red sea outflow during the last glacial maximum. Quaternary Int. 31, 77-83.

Sarnthein, M., Winn, K., Duplessy, J.C., and Fontugne, M.R.,1988. Global variations of surface ocean productivity in low and mid-latitudes: influence on CO_2 reservoirs of the deep ocean. Paleoceanography 3, 361-399.

Satyanarayana, Y., and Ramana, V., 1994. Distribution of minor elements in the shelf and deep sea sediments of the northern Arabian Sea. Mar. Chem. 47, 215-226.

Savrda, C.E., Bottjer, D.J., and Gorsline, D.S., 1984. Development of a comprehensive oxygen-deficient marine biofacies model: evidence from Santa Monica, San Pedro, and Santa Barabara Basins, California Continental Borderland. Bull. Am. Assoc. Pet. Geol. 89, 1179-1192.

Schenau, S.J., Reichart, G.J., De Lange, G.J.,. 1999. Oxygen Minimum Zone controlled Mn redistribution in the Arabian Sea sediments during the Late Quaternary. In: , (thesis). Geologica Ultraiectina 154, pp 184.

Schmiedl, G., Mackensen, A., and Müller, P.J., 1997. Recent benthic foraminifera from the eastern South Atlantic ocean: Dependence on food supply and water masses. Mar. Micropaleontol. 32, 249-287.

Schoell, M., 1984, Wasserstoff- und Kohlenstoffisotope in organischen Substanzen. Erdoel, Erdgas Geol. Jahrb. D, 67.

Schubert, C.J., Villanueva, J., Calvert, S.E., Cowie, G.L., von Rad, U., Schulz, H., Berner, U., and Erlenkeuser, H., 1998. Stable phytoplankton community structure in the Arabian Sea over the past 2000,000 years. Nature 394, 563-566.

Schulte, S., 1997. Erhaltung und frühe Diagenese von organischem Material in Sedimenten vom pakistanischen Kontinentalrand. Ph.D. Thesis, University of Oldenburg, 175 pp.

Schulz, H., Von Rad, U., and Erlenkeuser, H., 1998. Correlation between Arabian Sea and Greenland climate oscillations of the past 110,000 years. Nature 393, 54-57.

Schulz, H., Von Rad, U., Von Stackelberg, U., 1996. Laminated sediments from the Oxygen-Minimum Zone of the Northeastern Arabian Sea.-In: A.E.S. Kemp (Ed.), Paleoclimatology and Paleoceanography from Laminated sediments, Geol Soc (London) Spec. Publ. 116, 185-207.

Sen Gupta, B.K., and Machain-Castillo, M.L., 1993. Benthic foraminifera in oxygen-poor habitats. Mar. Micropaleontol. 20, 183-201.

Shaw, T.J., Gieskes, J.M., and Jahnke, R.A., 1990. Early diagenesis in differing depositional environments: The response of transition metals in pore water. Geochem. Cosmochim. Acta 54, 1233-1246.

Shimmield, G.B., 1992. Can sediment geochemistry record changes in coastal upwelling paleoproductivity? Evidence from northwest Africa and the Arabian Sea. In: C.P. Summerhayes, W.L. Prell and K.C. Emeis, (Eds.), Upwelling systems: Evolution since the Early Miocene. Geol. Soc. Spec. Publ. 64, 29-46.

Shimmield, G.B., and Mowbray, R.S., 1991. The inorganic geochemical record of the northwest Arabian Sea: a history of productivity variation over the last 400 k.y. from Sites 722 and 724. Proc. ODP, Sci. Results 117, 409-429.

Shimmield, G.B., Price, N.B., and Pederson, T.F., 1990. The influence of hydrography, bathymetry and productivity on sediment type and composition of the Oman Margin and in the North-west Arabian Sea. In: Robertson, A.H.F. et al. (Eds.), The Geology and Tectonics of the Oman Region. Special Publication, Geological Society, London, pp. 759-769.

Sirocko, F., 1996. The evolution of the monsoon climate during the last 24,000

years. Palaeoecol. Afr. 24, 53-84.
Sirocko, F., Garbe-Schönberg, D., McIntyre, A., and Molfino, B., 1996. Teleconnections between the subtropical monsoons and high-latitude climates during the last deglaciation. Science 272, 526-529.
Sirocko, F., Sarnthein, M., Erlenkeuser, H., Lange, H., Arnold, M., and Duplessy, J.C., 1993. Century-scale events in monsoonal climate over the past 24,000 years. Nature 364, 322-324.
Smith, R.L., and Bottero, J.S., 1977. On upwelling in the Arabian sea. In: M. Angel, (Ed.), A voyage of discovery, George Deacon 70th anniversary. Pergamon Press, 291-304.
Stuiver, M., and Braziunas, T.F., 1993. Modelling atmospheric ^{14}C ages of marine samples to 10,000 BC. Radiocarbon 35 (1), 137-189.
Swallow, J.C., 1984. Some aspects of the physical oceanography of the Indian Ocean. Deep-Sea Res. 31, 639-650.
Ten Kate, W.G.H.Z., Sprenger, A., Steens, T.N.F., and Beets, C.J., 1994. Late Quaternary monsoonal variations in the western Arabian Sea based on cross spectral analyses of geochemical and micropaleontological data (ODP Leg 117, core 728A). Spec. Publs Int. Ass. Sediment 19, 127-143.
Thiede, J., Suess, E., and Müller, P.J., 1982. Late Quaternary fluxes of major sediment components to the sea floor at the North-west African continental margin. In: von Rad, U., Hinz, K., Sarntheim, M., Seibold, E. (Eds.), Geology of the Northwest African Continental Margin. Springer, Berlin, pp. 605-631.
Tyson, R.V., 1995. Sedimentary organic matter: Organic facies and palynofacies. Chapmann & Hall, London, 615 pp.
Tyson, R.V., and Pearson, T.H., 1991. Modern and ancient shelf anoxia: an overvieuw. In: R.V. Tyson and T.H. Pearson, (Eds.), Modern and Ancient Shelf Anoxia. Geol. Soc. Spec. Publ. 58, 1-24.
Van Bennekom, A.J., and Hiehle, M.A., 1994. CTD operations and calibrations during legs D1, D2 and D3 of the Netherlands Indian Ocean Programme. In: W.J.M. van der Linden and C.H. van der Weijden, (Eds.), Geological study of the Arabian Sea. Netherlands Geosciences Foundation, The Hague, pp. 37-66.
Van Bennekom, J., Hiehle, M., Van Ooyen, J., Van Weerlee, E., and Van Koutrik, M., 1995. CTD and hydrography. In: Van Hinte, J.E., Van Weering, T.C.E., and Troelstra, S.R., (Eds.). Tracing a seasonal upwelling. Netherlands Geosciences Foundation, The Hague, pp. 41-62.
Van der Weijden, C.H., Reichart, G.J., and Visser, H.J., 1999. Enhanced preservation of organic matter in sediments deposited within the oxygen minimum zone in the northeastern Arabian Sea. Deep-Sea Res. 46, 807-830.
Van der Zwaan, G.J., Almogi-Labin, Duijnstee, I.A.P., Jannink, N.T., Jorissen, F.J. Apparent oxyphilic benthic foraminifera a proxy for quantitative reconstruction of oxygen contents in paleoceanography, submitted.
Van der Zwaan, G.J., and Jorissen, F.J., 1991. Biofacial patterns in river-induced shelf anoxia. In: R.V. Tyson and T.H. Pearson, (Eds.), Modern and Ancient

Continental Shelf Anoxia. Geol. Soc. Spec. Publ. 58, 65-82.

Van der Zwaan, G.J., Jorissen, F.J., and De Stigter, H.C., 1990. The depth dependency of planktonic foraminiferal ratios: Constraints and applications. Mar. Geol. 95, 1-16.

Van Leeuwen, R.J.W., 1989. Sea-floor distribution and Late Quaternary faunal patterns of planktonic and benthic foraminifers in the Angola basin. Utrecht Micropaleontol. Bull. 38, 1-287.

Van Marle, L.J., 1991. Eastern Indonesian, Late Cenozoic smaller benthic foraminifera. Verhandelingen der Konninklijke Academie van Wetenschappen, Afd. Natuurkunde, Eerste Reeks, deel 34, Amsterdam, 328 pp.

Verhallen, P.J.J.M., 1991. Late Pleistocene to early Pleistocene Mediterranean mud-dwelling foraminifera; influence of a changing environment on community structure and evolution. Utrecht Micropaleontol. Bull. 40, 219 pp.

Von Breymann, M.T., Emeis, K.-C., and Suess, E., 1992. Water depth and diagenetic constraints on the use of barium as a palaeoproductivity indicator. In: Summerhayes, C.P., Prell, W.L., and Emeis, K.C. (Eds.), Upwelling Systems: Evolution since the Early Miocene. Geol. Soc. London Spec. Publ. 64, 273- 284.

Von Rad, U., Schaaf, M., Michels, K.H., Schulz, H., and Sirocko, F., 1999. A 5,000-year record of climate change in varved sediments from the Oxygen Minimum Zone off Pakistan (north-eastern Arabian Sea). Quat. Res. 51, 39-53.

Von Rad, U., Schulz, H., Riech, V., Den Dulk, M., Berner, U., and Sirocko, F., 1999. Repeated monsoon controlled brakdown of oxygen minimum conditions during the past 30,000 years documented in laminated sediments off Pakistan. Palaeogeogr. palaeoclimatol. Palaeoecol., 152, 129-161 (Chapter 2, this thesis).

Von Rad, U., and Schulz, H., SONNE 90 Scientific Party, 1995. Sampling the Oxygen Minimum Zone off Pakistan: glacial/interglacial variations of anoxia and productivity. Mar. Geol. 125, 7-19.

Von Rad, U., and Tahir, M., 1997. Late Quaternary sedimentation on the outer Indus shelf and slope (Pakistan): evidence from high-resolution seismic data and coring. Mar. Geol. 138, 193- 236.

Von Stackelberg, U., 1972. Faziesverteilung in Sedimenten des indisch.-pakistanischen Kontinentalrandes (Arabisches Meer). 'Meteor'-Forsch.-Ergeb. C9, 1-73.

Wang, L., Sarnthein, M., Erlenkeuser, H., Grimalt, J., Grootes, P., Heilig, S., Ivanova, E., Kienast, M., Pelejero, C., and Pflaumann, U., 1999. East Asian monsoon climate during the Late Pleistocene: high-resolution sediment records from the South China Sea. Mar. Geol. 156, 245-284.

Weber, M., Wiedicke, M.H., Kudrass, H.R., Hübscher, C., and Erlenkeuser, H., 1997. Active growth of the Bengal Fan during sea-level rise and highstand. Geology 25 (4), 315-318.

Wells, P., Wells, G., Cali, J., and Chivas, A., 1994. Response of deep-sea benthic foraminifera to Late Quaternary climate changes, southeast Indian Ocean, offshore Western Australia. Mar. Micropaleontol. 23, 185-229.

Wells, P., Wells, G., Cali, J., and Chivas, A., 1994. Response of deep-sea benthic foraminifera to Late Quaternary climate changes, southeast Indian Ocean, offshore Western Australia. Mar. Micropalaeontol. 23, 185-229.

Wetzel, A., 1991. Ecologic interpretation of deep-sea trace fossil communities. Palaeogeogr., Palaeoclimatol., Palaeoecol. 85, 47-69.

Wishner, K.F., Gowing, M.M., and Gelfman, C., 1998. Mesozooplankton biomass in the upper 100 m in the Arabian Sea: overall seasonal and geographic patterns, a relationship to oxygen gradients. Deep-Sea Res. 45, 2405-2432.

Wyrtki, K., 1971. Oceanographic atlas of the international Indian Ocean expedition. Amerind Publishing Co. Pvt. Ltd., New Delhi, 531 pp.

Wyrtki, K., 1973. Physical Oceanography of the Indian Ocean. In: B. Zeitschel, (Ed.) The biology of the Indian Ocean. Springer-Verlag, New York, Heidelberg, Berlin, pp.18-36.

You, Y., and Tomczak, M., 1993. Thermocline circulation and ventilation in the Indian Ocean derived from water mass analyses. Deep-Sea Res. 40, 13-56.

Zahn, R., and Pedersen, T.F., 1991. Late Pleistocene evolution of surface and mid-depth hydrography at the Oman margin: planktonic and benthic isotope records at site 724. In: W. Prell, and N. Niitsuma, (Eds.), Proc. O.D.P., Sci. Results 117, 291-308.

Zobel, B., 1973. Biostratigraphische Untersuchungen an Sedimenten des Indisch-Pakistanischen Kontinentalrandes (Arabisches Meer). "Meteor" Forsch.-Ergebnisse C(12), 9-73.

Taxonomic notes

Below follows the faunal reference list of most (common) taxa identified in the Late Quaternary Arabian Sea benthic foraminiferal record, and taxa and/or genera constituting the groupings made for faunal analysis.

Astrononion spp. includes

Astrononion novozealandicum (Cushman and Edwards) = *Astrononion novozealandicum* Cushman and Edwards, 1937, p. 35 OD; Loeblich and Tappan, 1988, p. 620, pl. 694, figs. 11-15; this thesis, pl. 3, fig. 2a,b.

Astrononion stelligerum (d'Orbigny) = *Nonionina stelligera* d'Orbigny, 1839, p. 128, pl. 3, figs. 1, 2; *Astrononion stelligerum* (d'Orbigny), Cushman and Edwards, 1937, p. 31, pl. 3, fig. 7; Barker, 1960, p. 224, pl. 109, figs. 3, 4; this thesis, pl. 3, fig. 1a,b.

Bolivina alata (Sequenza) = *Vulvulina alata* Sequenza, 1862, p. 115, pl. 2, fig. 5; *Bolivina alata* (Seguenza), Cushman, 1937b, p. 106, pl. 13, figs. 3-11; this thesis, pl. 1, fig. 1.

Bolivina cf. *B. dilatata* Reuss = *Bolivina dilatata* Reuss, 1850, p. 381, pl. 48, figs. 15a, b, c; Macfadyen, 1930, p. 57, pl. 2, fig.1; Cushman, 1937b, p. 78, pl. 9, fig. 17-20; *Bolivina robusta* Brady, 1881, in Jones, 1994, pl. 53, fig. 7; this thesis, pl. 1, fig. 2, 3.

Bolivina pygmaea Brady = *Bolivina pygmaea* Brady, 1881, p. 57 (nomen nudum), Brady, p.421, pl. 53, fig. 5-6; *Brizalina pygmaea* (Brady), Van Marle, 1991, p. 305, pl. 17, figs. 17, 18; this thesis, pl. 1, fig. 5.

Bolivina cf. *B. seminuda* Cushman = *Bolivina seminuda* Cushman, 1911; in Barmawidjaja et al., 1992, pl. 2, fig 1-4; this thesis, pl. 1, fig. 4.

Bolivinita quadrilatera (Schwager) = *Textilaria quadrilatera* Schwager, 1866, p. 253, pl. 7, fig. 103; *Bolivinita quadrilatera* (Schwager), Van Marle, 1991, pl. 6, figs. 4-6.

Bulimina marginata d'Orbigny =*Bulimina marginata* d'Orbigny 1826, p. 269, pl. 12, figs. 10-12; Murray, 1971, p. 119, pl. 49; this thesis, pl. 2, fig. 1.

Bulimina aculeata (*aculeata* type) = *Bulimina aculeata* d'Orbigny, 1826, p. 269, mod. 7; Brady, 1884, p. 406, pl. 51, fig. 7-9; Fornasini, 1902, p. 153, fig. 4; Jones, 1994, pl. 51, figs. 7, 8, 9; this thesis, pl. 2, fig. 3.

Bulimina aculeata (*marginata* type) = *Bulimina aculeata* d'Orbigny, 1826, partim; included are morphotypes with a distinctive undercut as in *Bulimina marginata* but with spines distributed as in *B. aculeata*-type; this thesis, pl. 2, fig. 2.

Bulimina alazanensis Cushman = *Bulimina alazanenesis* Cushman, 1927, p. 161, pl. 25, fig. 4; Phleger, Parker and Peirson, 1953, p. 32, pl. 6, fig. 23; this thesis, pl. 2, fig. 5.

Bulimina exilis Brady = *Bulimina elegans* d'Orbigny var. *exilis* Brady, 1884, p. 339, pl. 50, figs. 5, 6; *Bulimina exilis* Brady, Cushman and Parker, 1947, p. 124, pl. 28, fig. 29; this thesis, pl. 1, fig. 14.

Bulimina sp.1; this thesis, pl. 1, figs. 12,13.

Bulimina striata d'Orbigny = *Bulimina striata* d'Orbigny, 1826, p. 269; fig. in Fornasini, 1902, p. 372, pl. 1; this thesis, pl. 2, fig. 4.

Cancris spp. includes

Cancris auricula (Fichtel and Moll) = *Nautilus auricula* Fichtel and Moll, 1798, p. 108, 110, pl. 20, figs. a-c (var. a), figs. d-f (var. b); *Cancris auricula* (Fichtel and Moll), Murray, 1971, p. 136, 137, pl. 57, figs. 1-7.

Cancris oblongus (d'Orbigny) = *Valvulina oblonga* d'Orbigny 1839c , p. 136, pl.1, figs. 40-42; *Rotalina oblonga* Williamson, 1858, p. 51, pl 4, figs. 98-100.

Cassidulina laevigata d'Orbigny = *Cassidulina laevigata* d'Orbigny, 1826, p.282, pl. 15, figs 4, 5; Cushman, 1922a, p. 122, pl. 24, fig. 4; Dieci, 1959, p. 84, pl. 7, fig.7; this thesis pl. 3, fig.7a,b.

Cassidulinoides bradyi (Norman) = *Cassidulina bradyi* Norman, 1881; in Brady, 1884, p431, pl.54, fig.6-9; Jones, 1994, pl. 54, figs. 6-9; this thesis, pl. 4, fig. 1.

Cassidulina carinata Silvestri = *Cassidulina laevigata* d'Orbigny var. *carinata* Silvestri, 1896; p. 104, pl. 2, fig. 10; Barker, 1960, p. 110, pl. 54, figs. 2, 3; this thesis, pl. 3, figs. 6a,b.

Cassidulina crassa d'Orbigny = *Cassidulina crassa* d'Orbigny, 1839b, p56, pl. 7, figs. 18-20; Barker, 1960, p. 112, pl. 54, figs. 4, 5; this thesis, pl. 3, figs. 4a,b.

Cassidulina cf. *C. inflata* Leroy = *Cassidulina inflata*, Leroy 1944, Loeblich and Tappan, 1994, p. 116, pl. 226, fig. 1-12; this thesis, pl. 3, fig. 5a,b.

Cassidulina sp.1; this thesis pl. 3, fig. 3ab

Cassidulina subglobosa Brady = *Cassidulina globosa* Hantken, 1876 = *Cassidulina subglobosa* Brady, 1881; p. 60, fig. in Brady, 1884, p. 430, pl. 54, fig. 17; Barker, 1960, p. 112, pl. 54, fig. 17; this thesis, pl. 3, fig. 8,9.

Ceratobulimina pacifica (Cushman and Harris) = *Bulimina contraria* Brady (not Reuss), 1884, p. 409, pl. 54, figs. 18a,b; *Ceratobulimina pacifica* Cushman and Harris, 1927, p. 176, pl. 29, figs. 9a-c; this thesis, pl. 9, fig. 5a,b.

Chilostomella oolina Schwager = *Chilostomella oolina* Schwager, 1878, p.527, pl. 1, fig. 16; Barker, 1960, p. 114, pl. 55, figs. 12-14, 17, 18; this thesis, pl. 2, fig. 16.

Cibicides ungerianus (d'Orbigny) = *Rotalina ungeriana* d'Orbigny, 1846, p. 157, pl. 8, figs. 16-18; *Cibicides ungerianus* (d'Orbigny), Marks, 1951, p. 73, pl. 8, figs. 2a, b; this thesis, pl. 6, figs. 1a,b,c.

Cibicides pseudoungerianus (Cushman) = *Truncatulina pseudoungeriana* Cushman, 1922a, p. 97, pl. 20, fig. 9; *Cibicides pseudoungeriana* Cushman, 1931, p. 123, pl. 22, fig. 3-7; *Cibicides pseudoungerianus* Cushman, Longinelli, 1956, p. 183, pl. 6, figs. 9a,b; this thesis, pl. 6, figs. 3a,b,c,.

Cibicides bradyi (Trauth) = *Truncatulina bradyi* Trauth, 1981, p. 235; *Cibicides bradyi* (Thrauth), Barker, 1960, pl. 95, fig.5; Pflum and Frerichs, 1976, pl. 3, figs 6, 7; this thesis, pl. 6, figs. 2a,b.

Cibicides kullenbergi (Parker) = *Cibicidoides kullenbergi* Parker, 1958, p. 49, pl. 11, figs. 7, 8; Wright, 1978, p. 713, pl. 4, figs. 5-7; this thesis, pl. 6, figs. 5a,b,c.

Cibicides cf. *C. dutemplei* (d'Orbigny) = *Rotalina dutemplei* d'Orbigny, 1846; *Cibicides dutemplei* (d'Orbigny), Batjes, 1958, p. 157, pl. 8, fig. 9; *Heterolepa dutemplei*, Loeblich and Tappan, 1964, p. C759, pl. 623, figs. 3a-c; Verhoeve, 1971, p. 108, pl. 5, figs. 18a-c); this thesis, pl. 7, figs. 2a,b.

Cibicides wuellerstorfi (Schwager) = *Anomalina wuellerstorfi* Schwager, 1866; *Planulina wuellerstorfi* (Schwager) Phleger, Parker and Peirson, 1953; this thesis, pl. 6, figs. 6a,b,c.

Cibicides sp.1; this thesis, pl. 7, figs. 1a,b,c.

Lenticulina spp. includes

Lenticulina peregrina (Schwager) = *Cristellaria peregrina* Schwager, 1866, p. 245, pl. 7, fig. 89; *Lenticulina peregrina* (Schwager), Barker, 1960, p. 144, pl. 68, figs. 11-16; this thesis, pl. 9, fig. 2.

Lenticulina sp.1; this thesis, pl. 9 fig.3

Saracenaria sp.1; this thesis, pl. 9, fig. 4

Epistominella exigua Brady = *Epistominella exigua* (Brady), Phleger, Parker and Peirson, 1953, p. 43, pl. 9, figs. 35, 36; Todd, 1965, p. 30, pl. 10, fig. 1; this thesis, pl. 7, figs. 4a, b.

Ehrenbergina pacifica Cushman = *Ehrenbergina pacifica* Cushman, 1927b, p. 5, pl. 2, fig. 2; Jones, 1994, pl. 55, figs. 4, 6, 7; this thesis, pl. 2, figs. 8.

Fursenkoina bradyi (Cushman) = *Virgulina bradyi* Cushman, 1922, p. 115, pl. 24, fig. 1; Phleger, Parker and Peirson, 1953, p. 34, pl. 7, figs. 4, 5; this thesis, pl. 1, figs. 7a,b.

Fursenkoina sp.1= this species looks similar to *Cassidulinoides tenuis* Phleger and Parker, 1951; Jones,1994, pl. 52, figs. 7, 8; this thesis, pl. 1, figs. 6.

Gavelinopsis lobatulus (Parr) = *Discorbis lobatulus* Parr, 1950, p. 354, pl. 13, figs. 23-25; *Gavelinopsis lobatulus* (Parr), Barker, 1960, p. 182, pl. 88, fig. 1; this thesis, pl. 4, figs. 6a, b, c.

Globobulimina affinis (d'Orbigny) = *Bulimina pupoides* d'Orbigny, 1846, p.125, pl.11, figs. 11-12; *Praeglobobobulimina pupoides* (d'Orbigny), Loeblich and Tappan, 1946, C561, pl. 442, figs. 14, 15; Van Marle, 1991, pl.5, figs. 13, 14; this thesis, pl. 1, fig. 11. Included are morphotypes similar to *Bulimina elegans* d'Orbigny.

Globobulimina spp. = we lumped all globobuliminids, excl. *Globobulimina affinis*, because intraspecific variation in this genus can cover a wide range (see also van der Zwaan, 1982); this thesis, pl. 1, figs. 9, 10, 11a,b.

Globobulimina sp.1 = this species is rather similar to *Globulimina pacifica* Cushman, 1927a, p.67, pl. 14, figs. 12a,b; Van Marle, 1991, p. 90, pl. 5, figs. 11, 12; included are slender, fragile morphotypes with the final chamber almost completely covering the test. We later lumped these under *Globulimina* spp.

Gyroidina spp. includes:

Gyroidina polia (Phleger and Parker) = *Eponides polius* Phleger and Parker, 1951, p. 21, pl. 11, figs. 1, 2; Phleger, Parker and Peirson, 1953, p. 41 pl 9, figs. 3, 4; Van Leeuwen, 1989, pl. 12, figs. 4-6; this thesis, pl. 8, figs. 3a, b, c.

Gyroidina orbicularis d'Orbigny = *Gyroidina orbicularis* d'Orbigny, 1826, p. 278, mod. 13; Parker, Jones and Brady, 1865, pl. 3, fig. 85; Loeblich and Tappan, 1964, p.C750, pl. 614, figs. 5, 6; Van Marle, 1991, p. 293, pl. 11, figs. 8, 9, 10; this thesis pl. 8, figs. 1a,b,c,.

Gyroidina sp.1 = this species is similar to *Gyroidina* sp.1; Van Leeuwen, 1989, pl. 12, figs. 7-9; this thesis, pl. 8, figs. 4a,b,c.

Gyroidina altiformis R.E. and K.C. Stewart = *Gyroidina soldanii* d'Orbigny var. *altiformis* R.E. and K.C. Stewart, 1930, p. 67, pl. 9, fig. 2; *Gyroidinoides soldanii* (d'Orbigny, 1826), Jones; 1994, p. 106, pl. 107, fig. 6a,b,c.

Gyroidina soldanii (d'Orbigny) = *Rotalina soldanii* d'Orbigny, 1846, p. 155, pl. 8, figs. 10-12; *Gyroidina soldanii* (d'Orbigny), Cushman, 1929a, p. 38, pl. 8, figs. 3-8; Longinelli, 1956, pl. 14, figs. 16a, b; this thesis, pl. 8, figs. 2a,b,c..

Hanzawaia boueana (d'Orbigny) = *Truncatulina boueana* d'Orbigny, 1846, p. 169, pl. 9, figs. 24-26; Cibicides boueanus (d'Orbigny), Marks, 1951, p. 72, pl. 8, fig. 9; *Hanzawaia boueana* (d'Orbigny), Batjes, 1958, p. 154, pl. 8, fig. 5; this thesis, pl. 4, figs. 8a,b,c.

Hoeglundina elegans (d'Orbigny) =*Rotalia* (*Turbuline*) *elegans* d'Orbigny, 1826, p. 276, no. 54; *Hoeglundina elegans* (d'Orbigny), Cushman, 1915, p. 63, pl. 26, figgs. 3a-c; Loeblich and Tappan, 1964, C775, figs. 636, 3-5; this thesis, pl. 9, figs. 6a,b.

Hyalinea balthica (Schroeter) = *Nautilus balthicus* Schroeter, 1783, p. 20, pl. 1, fig. 2; *Hyalinea balthica* (Schroeter), Barker, 1960, p. 230, pl. 112, figs. 1, 2; this thesis, pl. 4, figs. 9a,b.

Karreriella bradyi (Cushman) = *Gaudryina pupoides* (not d'Orbigny, 1840), Brady, 1884, p. 378, pl. 46, figs. 1-4; *Gaudryina bradyi*, Cushman, 1911, p. 67, pl. 2, figs. 107a-c; *Karreriella bradyi* (Cusman), Dieci, 1959, p. 21, pl. 1, fig. 15; this thesis, pl. 10, figs. 4,5.

Lagenids s.l. includes many forms:

Amphycorina hirsuta (d'Orbigny) = *Amphycorina hirsuta* (d'Orbigny, 1826), Jones, 1994, p. 75, pl. 63, figs. 12-15; this thesis, pl. 5, figs. 15.

Amphycorina scalaris (Batsch) = *Nodosaria scalaris* (Battsch), Brady, 1884, p 510, pl. 63, figs. 28-31; *Amphycorina scalaris* (Batsch), Barker 1960, p. 134, pl. 63, figs. 28-31, p. 136, pl. 65, figs. 7-9; Van Marle, 1991, Loeblich and Tappan, 1994, p. 71, pl. 127, figs. 1-18; pl. 2, figs. 3, 4; this thesis, pl. 5, figs. 12, 13.

Dentalina advena (Cushman) = *Dentalina advena* (Cushman), Barker, 1960, p. 132, pl. 63, fig. 1; Van Marle, 1991, pl. 1, figs. 13; this thesis, pl. 5, figs. 17.

Dentalina subsoluta (Cushman) = *Nodosaria soluta* Brady (not Reuss), p. 503, pl. 62, figs. 13-16; *Dentalina subsoluta* (Cushman), Barker, 1960, p. 130, pl. 62, figs. 13-16; this thesis, pl. 5, figs. 16.

Glandulina laevigata (d'Orbigny) = *Nodosaria* (*Glandulina*) *laevigata* d'Orbigny, 1826, p. 252, pl. 10, figs. 1-3; Brady, 1884, p. 490, pl. 61, figs. 20-22; *Glandulina laevigata* (d'Orbigny), Loeblich and Tappan, C537, pl. 421, figs. 1,2.

Lagena sp. 1; this thesis, pl. 5, figs. 11

Nodosaria sp.1; this thesis, pl. 5, figs. 14.

Oolina cf. *O. apiopleura* (Loeblich and Tappan) = *Oolina apiopleura* (Loeblich and Tappan, 1953), Jones, 1994, p. 66, pl 58, fig. 21; this thesis, pl. 5, figs. 10.

Melonis barleeanum (Williamson) = *Nonionina barleeana* Williamson, 1858, p. 32, pl. 3, figs, 68, 69; *Melonis barleeanum* (Williamson), Corliss, 1979, p. 10, pl. 5, figs 7, 8; this thesis, pl. 4, figs. 7a,b.

Miliolids includes:

Nummuloculina sp.1; this thesis, pl. 5, figs. 7.

Nummuloculina irregularis (d'Orbigny) = *Biloculina irregularis* d'Orbigny, 1839a, p. 67, pl. 8, figs. 20-31; *Nummuloculina irregularis* (d'Orbigny), Barker, 1960, p. 2, pl. 1, figs. 17-18; Van Marle, 1991, pl. 4, fig. 3. this thesis, pl. 5, fig. 8.

Pyrgo murrhina (Schwager) = *Biloculina murrhina* Schwager, 1866, p. 203, pl , figs. 15a-c; Van Marle, 1991, p. 274, pl. 3, fig. 3; this thesis, pl. 5, fig. 4.

Pyrgo subsphaerica (d'Orbigny) = *Biloculina subsphaerica* d'Orbigny, 1839a, p. 162, pl. 8, figs. 25-27; Van Marle, 1991, p. 274, pl. 3, fig. 4, 5.

Pyrgo williamsoni (Sylvestri) = *Biloculina williamsoni* Silvestri, 1923, figured by Williamson, 1858, pl. 6, figs. 169-170, pl. 7, fig. 171; Murray, 1971, p. 70, pl. 27, figs. 5-7; this thesis, pl. 5, fig. 6.

Pyrgo sp.1; this thesis, pl. 5, fig. 5.

Quinqueloculina seminulum.(Linnaeus) = *Quinqueloculina seminulum* (Linnaeus), Brady, 1884, p. 157, pl. 5, figs. 6a-c; Barker, 1960, p. 10, pl 5, figs. 6a-c; this thesis, pl. 5, figs. 2, 3.

Sigmoilopsis schlumbergeri (Silvestri): *Sigmoilina schlumbergeri* Silvestri, 1904, p. 267; Loeblich and Tappan, 1964, p. C466, pl. 353, figs. 2a-c; this thesis, pl. 5, figs. 9.

Triloculina cf *T. tricarinata* d'Orbigny = *Triloculina tricarinata* d'Orbigny, 1826, p.299, mod. No. 94, *Miliolina tricarinata* (d'Orbigny), Brady, 1884, p. 165, pl. 3, figs. 171a,b; *Triloculina tricarinata* (d'Orbigny), Cushman, 1929, p.56, pl. 13, fig. 3; this thesis, pl. 5, figs. 1.

Oridorsalis umbonatus (Reuss) = *Rotalina umbonata* Reuss, 1851, p 75, pl. 5, fig. 35; and *Oridorsalis umbonatus* (Reuss), Lohmann, 1978, p. 26 pl. 4, figs. 1-3 (non Reuss, 1851), *Oridorsalis umbonata* (Reuss), Jones, 1994, pl. 95, fig. 11; *Oridorsalis umbonatus* var 1&2, Van Leeuwen, pl. 17, figs. 1-3, 7-13; this thesis, pl. 7, figs. 3a,b,c.

Osangularia spp includes

Osangularia sp.1 = this species looks similar to *Osangularia bengalensis* (Schwager) = *Anomalina bengalensis* Schwager, 1866, p. 259, pl. 7, fig. 111; *Osangularia bengalensis* (Schwager), Loeblich and Tappan, 1964, C752, pl.615, figs. 3, 4; Van Marle, 1991, pl. 11, fig. 16, pl. 12, fig. 1; this thesis, pl. 4, figs. 5a,b.

Osangularia culter (Parker and Jones) = *Planorbulina culter* Parker and Jones, 1865, p. 421, pl. 19, fig. 1, *Osangularia cultur* (Parker and Jones), Todd, 1965, p. 25, pl. 15, fig. 1; this thesis, pl. 4, figs. 4a,b.

Pullenia bulloides (d'Orbigny) = *Nonionina bulloides* d'Orbigny ,1846, p. 107, pl. 5, figs. 9, 10; *Pullenia bulloides* (d'Orbigny), Dieci, 1959, p. 87, pl. 7, fig. 16; Christodolou, 1960, p. 56, pl. 2, figs, 11, 12.; Loeblich and Tappan, 1988, pl. 696 fig. 3-4; this thesis, pl. 4, figs. 2.

Pullenia quinqueloba (Reuss): *Nonionina quinqueloba* Reuss, 1851, p. 71, pl. 5, fig. 31; *Pullenia quinqueloba* (Reuss), Brady, 1884, p. 617, pl. 84, figs. 14, 15; Marks, 1951, p. 69, pl. 7, fig. 19; this thesis, pl. 4, figs. 3a,b.

Rotaliatinopsis semiinvoluta (Germeraad) = *Pulleniatina semiinvoluta* (Germeraad, 1946), Loeblich and Tappan, 1988, p. 184, pl. 714, figs. 7-11; this thesis, pl. 2, figs. 6, 7.

Robertinoides includes:

Robertina subcylindrica (Brady) = *Robertina subcylindrica* Brady, 1881, figured in Jones, 1994, p. 55, pl. 50, fig. 16a,b.

Robertinoides wiesneri Parr = *Robertinoides wiesneri* Parr, 1950, p. 369, pl. 15, fig. 9, Loeblich and Tappan, 1994, p. 99, pl. 178, figs. 10-14.

Shallow water taxa: includes

Ammonia beccarii (Linnaeus) = *Nautilus beccarii* Linnaeus, 1758, p. 710, pl. 1, figs. 1a-c; *Rotalia beccarii* (Linnaeus), Cushman, 1931, p. 58, pl. 12, figs. 1-7; *Ammonia beccarii* (Linnaeus), Loeblich and Tappan, 1964, p. C607, pl. 479, figs. 2, 3; this thesis, pl. 10, fig. 1a,b.

Cibicides lobatulus (Walker and Jacob) = *Nautilus lobatulus* Walker and Jacob, 1798, in Kanmacher, p. 642, pl. 14, fig. 36; *Cibicides lobatulus* (Walker and Jacob), Longinelli, 1956, p. 182, pl. 6, fig. 12; Hageman, 1979, p. 91, pl. 3, figs. 6a,b, pl. 4, figs. 1a,b; this thesis, pl. 6, figs. 4a,b.

Rosalina vilardeboana d'Orbigny = *Rosalina vilardeboana* d'Orbigny, 1839a, p.44, pl. 6, figs. 13-15; Barker, 1960, p. 178, pl. 86, fig. 9; Van Marle, 1991, p. 156, pl. 14, figs. 13, 14; this thesis, pl. 9, figs. 10a,b,c.

Rosalina sp.1; this thesis, pl. 9, figs. 8a,b,c.

Discorbidae sp.2; this thesis, pl. 10, figs. 2a,b.

Discorbidae sp.3; this thesis, pl. 10, figs. 3a,b.

Sphaeroidina bulloides d'Orbigny = *Sphaeroidina bulloides* d'Orbigny 1826, p. 267, mod. 65; d'Orbigny, 1846, p. 284, pl. 20, figs. 19, 20; Longinelli, 1956, p. 77, pl. 10, fig. 1; this thesis, pl. 9, fig. 1.

Spiroloculina spp. includes:

Spiroloculina rotunda d'Orbigny = *Spiroloculina rotunda* d'Orbigny, 1826, p.299 (nomen nomen), Barker, 1960, p. 18, pl. 9, figs 15, 16.

Spiroloculina communis (Cushman and Todd) = *Spiroloculina excavata* Brady (not d'Orbigny), 1884, p. 151, pl. 9, figs 5, 6; *Spiroloculina communis*, Cushman and Todd, 1944, p.63, pl. 9, figs. 4, 5, 7, 8; this thesis, pl. 5, fig. 18.

Spiroplectammina var, includes:

Spiroplectammina sp.1; this thesis, pl. 10, figs. 7.

Spiroplectammina sp.2; this thesis, pl. 10, figs. 8.

Spiroplectammina sp.3; this thesis, pl. 10, figs. 9.

Textularia var, includes:

Textularia cf. *T. saggitula* Defrance = *Textularia saggitula* (Defrance, 1824), Murray, 1971, p. 30, pl. 8, figs. 1-9); this thesis, pl. 10, fig. 10.

Siphotextularia sp.1; this thesis, pl. 10, figs. 11.

Tritaxia tricarinata Brady = *Tritaxia tricarinata* Brady (not Reuss), 1884, p. 389, pl. 49, figs. 8,9; this thesis, pl. 10, fig. 6.

Trifarina angulosa (Williamson) = *Uvigerina angulosa* Williamson, 1858, p. 67, pl. 5, fig. 140; *Angulogerina angulosa* (Williamson), Barker, 1960, p. 154, pl. 74, figs. 15, 16; this thesis, pl. 2, figs. 15.

Uvigerina spp. included are:

Uvigerina peregrina Cushman = *Uvigerina peregrina* Cushman, 1923, p. 166, pl. 42, fig. 7-10; Van Marle, 1991, pl. 7, figs. 14-15; (partim included are *Uvigerina peregrina* Cushman var. *dirupta* Todd, 1948, p. 267, pl. 43, fig. 3; Van Marle, 1991, p. 104, pl. 7, figs. 16-17, and *Uvigerina peregrina* var. *hollecki*, Thalman, 1950, Figured in Van der Zwaan et al, 1986, p. 222, pl. 13, figs. 1-7, pl. 14, figs. 1-4; this thesis pl. 2, figs. 10, 11.

Uvigerina hispida Schwager = *Uvigerina hispida* Schwager, 1866, p.249, fig. 95; Van der Zwaan et al, 1986, p. 216, pl. 11, figs. 1-4; this thesis pl. 2, figs. 12.

Uvigerina porrecta Brady = *Uvigerina porrecta* Brady 1879, p. 274, pl. 8, figs. 15, 16; Van Marle, 1991, pl. 8, figs. 7-8; this thesis, pl. 2, figs. 14.

Uvigerina proboscidea Schwager = *Uvigerina proboscidea* Schwager 1866, p. 250, pl. 7, fig. 96;Van marle, 1991, pl. 8, figs. 12-14; this thesis, pl. 2, figs. 9.

Uvigerina semiornata d'Orbigny = *Uvigerina semiornata* d'Orbigny, 1846 = *Uvigerina crassicostata* Schwager, 1866, p. 248, pl. 7, fig. 94; Van Marle, 1991, pl. 7, figs. 12-13; this thesis, pl. 2, figs. 13.

Valvulineria spp. includes:

Valvulinaria cf. *V. laevigata* Phleger and Parker = *Valvulinaria laevigata* Phleger and Parker, 1951, p. 25, pl. 13, figs. 11,12; Boltovskoy, p. 173, pl. 8, figs. 42,43;) this thesis, pl. 9, figs. 7a,b.

Valvulineria minuta (Schubert) = *Valvulineria minuta* (Schubert), Parker, 1954, p.527, pl.9, figs. 4-6; Loeblich and Tappan, 1994, p. 505, pl. 268, figs, 4-9; this thesis, pl. 9, figs. 9a,b.

Taxonomic references

Barker, R.W., 1960, Taxonomic notes on the species figured by H.B. Brady in his Report on the Foraminifera dredged by the H.M.S. Challenger during the years 1873 - 1876. Soc. Econ. Pal. And Mineral., Spec. Publ., 9, Tulsa, Oklahoma.

Batjes, D.A.J., 1958, Foraminifera of the Oligocene of Belgium, Mém. Inst. Roy. Sci. Belg., Vol. 143, 188 pp., Brussels.

Brady, H.B., 1881, Notes on some of the reticularian Rhizopoda of the Challenger Expedition, Pt. 3, Quart. J. Micr. Sci., vol. 21, London.

Brady, H.B., 1884, Report on the Foraminifera dredged by H.M.S. Challenger, during the years 1873-1876, In: Report on the Scientific Results of the Voyage of H.M.S. Challenger during the years 1873-1876. Zoölogy, Vol. 9, 814 pp., London.

Christodolou, G., 1960, Geologische und mikropaläontologische Untersuchungen auf der Insel Karpathos (Dodekanesos), Paläontographica, Abt. A, Bd. 115 , 143 pp., 16 Tafeln, 23 Abb., Stuttgart.

Corliss, B.H., 1979. Taxonomy on recent deep-sea benthonic foraminifera from the southeast Indian Ocean. Micropaleontol. 25/1, 1-19.

Cushman, J.A., 1911, A monograph of the Foraminifera of the North Pacific Ocean, Pt. 2: Textulariidae, U.S. Nat. Mus. Bull., Vol. 71, 108 pp., Washington D.C.

Cushman, J.A., 1922a, The Foraminifera of the Atlantic Ocean, Pt. 3: Textulariidae, U.S. Nat. Hist. Mus. Bull., 104, 143 pp., Washington D.C.

Cushman, J.A., 1922b, Shallow-water Foraminifera of the Tortugas region, Carnegie Inst. Washington, Publ. No. 311 (Dept. Mar. Biol. Pap., Vol. 17), p. 1-85.

Cushman, J.A., 1927a, Proc. U.S. Nat.Mus., Vol. 72, No. 2716, art. 20 Sret n.i. L&T, kan qua telling

Cushman, J.A., 1923. The foraminifera in the Atlantic Ocean partIV: Lagenidae. U.S. Nat. Mus. Bull. 104, 228 p.

Cushman, J.A.,1927b, Recent foraminifera of the genus Siphonina and related genera. U.S. Nat Mus. Proc.72/2716, 1-15.

Cushman, J.A., 1929a, The Foraminifera of the Atlantic Ocean, Pt. 6: Miliolidae, Ophtalmidiidae and Fisherinidae, U.S. Nat. Mus. Bull., 104., Washington D.C.

Cushman, J.A., 1929b, U.S. Geol. Surv. Prof. Paper, 191

Cushman, J.A., 1931, The Foraminifera of the Atlantic Ocean, Pt. 8: Rotaliidae, Amphisteginidae, Calcarinidae, Cymbaloporettidae, Globorotaliidae, Anomalinidae, Planorbulinidae, Rupertiidae, and Homotremidae, U.S. Nat. Mus. Bull., Vol. 104, Washington D.C.

Cushman, J.A., 1937b, A monograph of the Foraminiferal family Virgulininae of the foraminiferal family Buliminidae, Cushman Lab. Foram. Res., Spec. Publ., 9, 228 pp.

Cushman, J.A., and Harris, R.W., 1927. Some notes on the genus Ceratobulimina. Cushman lab. Foram. Res., Contr. 3/4; 171-179.

Cushman, J.A. and Edwards, P.G., 1937, Astrononion, a new genus of the Foraminifera, and its species, Contr. Cushman Lab. Foram. Res., Vol. 13, pt. 1, p. 29-36.

Cushman, J.A. and Parker, F.L., 1937b, Notes on some European Eocene species of Bulimina and Buliminella, Contr. Cushman Lab. Foram. Res., Vol. 13, Pt. 2, p. 46-54.

Czjzek, J., 1848, Beitrag zur Kenntniss der fossilen Foraminiferen des Wiener Beckens, Haidinger's Naturwiss. Abh., Vol. 2, Pt. 1, p. 137-150.

Dieci, G, 1959, I foraminiferi Tortoniani di Montegibbio e Castelvetro, Paleont. Ital., Vol. 54, 113 pp.

d'Orbigny, A.D., 1826, Tableau méthodique de la classe des Céphalopodes, Ann. Sci. Nat. Paris, série 1, Vol. 7, p. 245-315 (fide Loeblich and Tappan, 1964).

d'Orbigny, A.D., 1839A, Voyage dans l'Amérique méridionale - Foraminifères, Vol. 5, Pt. 5, 86 pp., 9 Pl., Pitois-Levrault et Ce (Paris), V. Levrault (Strasbourg).

d'Orbigny, A.D., 1839B, Foraminifères, in: R. de la Sagra, Histoire physique, politique et naturelle de l'île de Cuba, atlas, 12 pl.

d'Orbigny, A.D., 1839C, Foraminifères des Iles Canaries. In Barker-Webb and Berthelot, Histoire naturelle des Iles canaries, Vol. 2/2; 119-146.

d'Orbigny, A.D., 1846, Foraminifères fossiles du Bassin Tertiaire de Vienne (Autriche), 312 pp., 21 Pl., Gide et Compe , Paris.

Fichtel, L. von and Moll, J.P.C. von, 1798, Testacea Microscopica alia que minuta ex generibus Argonauta et Nautilus, ad natura pictura et descripta (Mikroskopsche und andere kleine Schaltiere aus den geschlechtern Argonaute und Schiffer), Camesina, Wien.

Fornasini, C., 1902, Contributo alla conoscenza de le Bulimine Adriatiche, Mem. R. Accad. Sci. Ist., Bologna, ser. 5, Vol. 9.

Hageman, J., 1979, Benthic foraminiferal associations from Plio-Pleistocene open bay to lagoonal sediments of the western Peloponnesus (Greece), UMB 20, 171 pp.

Hantken, M. von, 1875, Die Fauna der Clavulina Szabói Schichten, Teil 1, Foraniniferen, Magy. Kir. Földt int. évkönyve, (Mitt. Jahrb. K. Ung. Geol. Anst.) Vol. 4.

Heron-Allen, E. and Earland, A., 1930, The foraminifera of the Plymouth district, Pt. 1, J. Roy. Micr. Soc., London. (B plic ps-pl).

Jones, R.W., 1994. The challenger foraminifera. Oxford University Press, Oxford, 149 pp.

Kanmacher, F., 1798. G. Adams essays on the miroscope containing a practical description of the most improved microscopes: a general history of insects, their transformations, peculiar habits, and economy. Second Ed., Dillon and keating London, p724.

Loeblich, A.R. and Tappan, H., 1964, Sarcodina, chiefly "Thecamoebians" and

Foraminifera, Vol. 1, 2, In: R.C. Moore, Ed., Treatise on invertebrate paleontology, pt. C, Protista 2, The Geol. Soc. of Am. and the Univ. of Kansas Press.
Loeblich, A.R. and Tappan, H., 1988, Foraminiferal genera and their classification, Van Nostrand Reinhold, New York.
Loeblich, A.R. and Tappan, H., 1994, Foraminifera of the Sahul shelf and Timor Sea, In: S.J. Culver, Ed., Cushman Foundation for Foraminiferal Research Special Publication no. 31.
Longinelli, A., 1956, Foraminifera del Calabriano e Piacenziano di Rosignano marittimo e della Val di Cecina, Paleontogr. Ital., nov. ser., Vol. 19, 116 pp.
Macfadyen, W.A., 1930, Miocene Foraminifera from the clysmic area of Egypt and Sinaï Egypt, Geol. Surv., Cairo.
Marks, P., 1951, A revision of the smaller Foraminifera from the Vienna Basin, Contr. Cushman Found. Foram. Res., Vol. 2, Pt. 2.
Murray, J.W., 1971, An atlas of British Recent Foraminiferids, Heinemann Educ. Books Ltd., London.
Norman, A.M., 1881, A list of the post-Tertiary foraminifera of the North-east of Ireland, Quart. J. Micr. Soc., London, new ser., Vol. 21.
Parker, F.L., 1958, Swedish Deep Sea Exped., vol. 7
Parker, W.K., andJones, T.R., 1865, On some foraminifera from the North Atlantic Arctic Oceans, including Davis Straits and Baffin's bay. Roy. Soc. London Phil. Trans. 155, 325-441.
Parker, W.K., Jones, T.R. and Brady, H.B., 1871. On the nomenclature of the Foraminifera. Pt. 12: The species enumerated by d'Orbigny in the "Annales des Sciences Naturelles", Vol. 7, 1826, Ann. & Mag. Nat. Hist., ser. 3, Vol. 16, p. 15-41.
Parr, W.J.,1950, Foraminifera. B.A.N.Z. Res. Exped. 1929-1931 Rep., Ser. B (Zool. Bot.), 5/6, 116-218.
Perconig, E., 1955, Boll. Ital. Serv. Geol., Vol. 77.
Pflum, C.E. and Frerichs, W.E., 1976. Gulf of Mexico deep water foraminifers. Cushman Found. Foram. Res., Spec. Publ., 14.
Phleger, F.P., and Parker, F.L, 1951. Ecology of foraminifera, northwest Gulf of Mexico. Part 2: Foraminifer species. Geol. Soc. Am. Mem. 46, 1-64.
Phleger, F.P., Parker, F.L. and Peirson, J.F., 1953, North Atlantic Foraminifera, Rep. Swedish Deep Sea Exped., Vol. VII, Sediment cores from the North Atlantic Ocean, Mar. For. Lab., Scripps Inst. Ocean., California.
Reuss, A.E., 1850, Neue Foraminiferen aus den Schichten des österreichischen Tertiärbeckens, Denkschr. K. Akad. Wiss. Wien, Math.-Nat. Cl., Vol. 1, p. 365-390.
Reuss, A.E., 1851, Über die fossilen Foraminiferen und Entomostraceen des Septarientonen der Umgegend von Berlin, Deutsch. Geol. Gesellsch. Zeitschr., Vol. 3, p. 49-91.
Schroeter, J.S., 1783. Einleitung in die Conchylienkenntnis nach Linne. Band I.J.J.

Gebauer, Halle, pp. 860.
Schwager, C., 1866, Fossile Foraminiferen von Kar-Nicobar, Novara Exp., 1857-1859, Geol. Theil, Vol. 2, p. 187-268.
Schwager, C., 1878, Nota su alcuni foraminiferi nuovi del tuffo di Stretto preso Girgenti, Boll. Uff. Geol. (R. Com. Geol. Ital.), Vol. 9, Roma.
Seguenza, G., 1862, Prime recerche intorno ai Rizopodi fossili delle argile Pleistoceniche dei dintorni di Catania, Accad.Gioenia Sci. Nat. Catania, ser. 2, vol. 18, Atti, Catania.
Silvestri, A., 1896, Foraminiferi Pliocenici della Provincia di Siena, Pt. 1, Mem. Accad. Pont. Nuovi Lincei, Vol. 12.
Silvestri, A., 1904, Ricerche strutturali su alcune forme dei trubi di Bonfornello (Palermo), Mem. Accad. Pont. Rom. Nuovi Lincei, Vol. 22, Rome.
Stewart, R.E. and Stewart, K.C., 1930, Post-Miocene foraminifera from the Ventura Quadrangle, Ventura County, California, J. Paleont., Vol. 4, no. 1.
Todd, R.,1965, The foraminifera of the tropical collections of the 'Albatross', 1899-1900. Part 4: Rotaliform Families and Planktonic Families. Smitsonian Inst., U.S. Nat. Mus., Bull. 161, 1-139.
Trauth, F., 1918, Das Eozänvorkommen bei Radstadt im Pongau und seine Beziehungen zu den gleichalterigen Ablagerungen beu Kirchberg am Wechsel und Wimpassing am Leithagebirge, Denkschr. K. Akad. Wissensch. Wien, Math. -Nat. Cl., Vol. 95, p. 171-278.
Van Leeuwen, R.J.W., 1989. Sea-floor distribution and Late Quaternary faunal patterns of planktonic and benthic foraminifers in the Angola basin. Utrecht Micropaleontol. Bull. 38, 1-287.
Van Marle, L.J., 1991. Eastern Indonesian, Late Cenozoic smaller benthic foraminifera, Verhandelingen der Konninklijke Academie van Wetenschappen, Afd. Natuurkunde, Eerste Reeks, deel 34, Amsterdam, 328 pp.
Van der Zwaan , G.J., Jorissen, F.J., Verhallen, P.J.J.M., and Von Daniels, C.H., 1986. Atlantic-European Oligocene to recent Uvigerina, taxonomy, paleoecology and paleobiogeography. Utr. Micropaleontol. Bull., 35, pp. 239.
Verhoeve, D., 1971, Benthonic foraminifera of the Neogene Asteri Dhramia and Francocastello Formations from western Crete (Greece), Kon. Ul. Dep. Aardwet., Leuven.
Von Daniels, 1970, Göttinger Abh. Geol. Pal., 8
Walker, G. and Jacob, E., 1798, Adams' essays on the microscope, In: F. Kanmacher, London, edition 2.
Williamson, W.C., 1848. On the british recent species of the genus *Lagena*. Ann. Mag. Nat. Hist., ser. 2, I, 1-20.
Williamson, W.C., 1858, On the Recent Foraminifera of Great Britain, Ray Soc., London.
Wright, R., 1978, Neogene benthic foraminifers from DSDP leg 42A, Mediterranean Sea. Init. Rep. DSDP, Vol. 42, pt. 1, Washington D.C.

Plate 1

Fig. 1 *Bolivina alata* (Sequenza), sample NIOP455-89

Fig. 2, 3 *Bolivina* cf. *B. dilatata* Reuss, sample NIOP455-11

Fig. 4 *Bolivina* cf. *B. seminuda* Cushman, sample NIOP455-98

Fig. 5 *Bolivina pygmaea* Brady, sample NIOP455-1

Fig. 6 *Fursenkoina* sp.1, sample NIOP55-47

Fig. 7 *Fursenkoina bradyi* (Cushman), sample NIOP455-59

Fig. 8-10 *Globobulimina* spp, sample NIOP455-62, -703, -388

Fig. 11 *Globobulimina affinis* (d'Orbigny), sample NIOP464-96

Fig. 12, 13 *Bulimina* sp.1, sample NIOP455-120, -62

Fig. 14 *Bulimina exilis* Brady, sample NIOP455-17

Scale bar = 100 μm

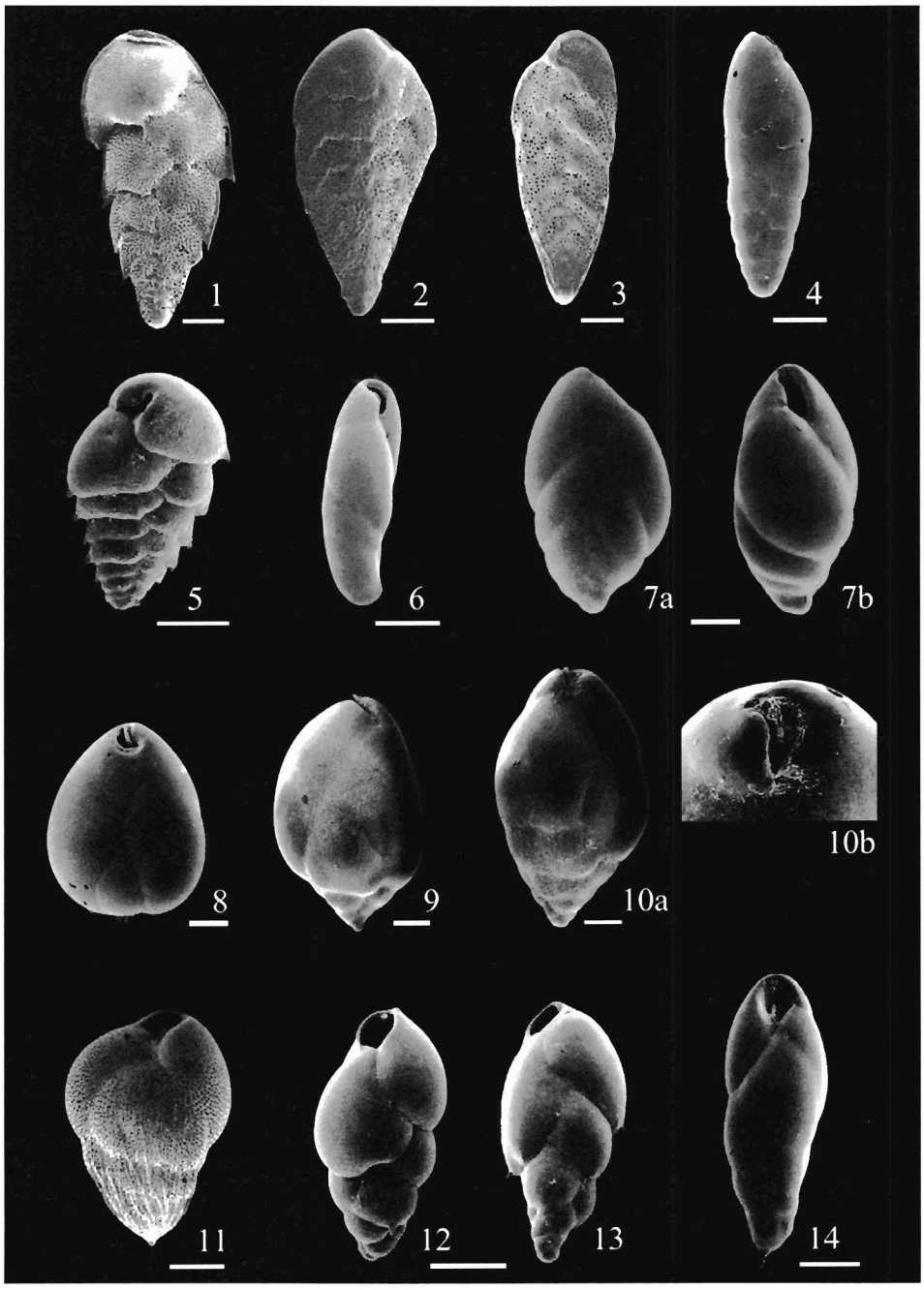
1
2
3
4
5
6
7a
7b
8
9
10a
10b
11
12
13
14

Plate 2

Fig. 1 *Bulimina marginata* d'Orbigny, sample 137KA/885cm

Fig. 2 *Bulimina aculeata* (*marginata* type), sample NIOP455-23

Fig. 3 *Bulimina aculeata* (*aculeata* type), sample NIOP455-23

Fig. 4 *Bulimina striata* d'Orbigny, sample NIOP455-47

Fig. 5 *Bulimina alazanensis* Cushman, sample NIOP455-5

Fig. 6, 7 *Rotaliatinopsis semiinvoluta* (Germeraad), sample NIOP455-104

Fig. 8 *Ehrenbergina pacifica* Cushman, sample NIOP464-12

Fig. 9 *Uvigerina proboscidea* Schwager, sample 137KA/885

Fig. 10, 11 *Uvigerina peregrina* Cushman, sample NIOP463-b5

Fig. 12 *Uvigerina hispida* Schwager, sample NIOP464-39

Fig. 13 *Uvigerina semiornata* d'Orbigny, sample NIOP463-b5

Fig. 14 *Uvigerina porrecta* Brady, sample NIOP455-56

Fig. 15 *Trifarina angulosa* (Williamson), sample NIOP464-85

Fig. 16 *Chilostomella oolina* Schwager, sample NIOP455-8

Scale bar = 100 μm

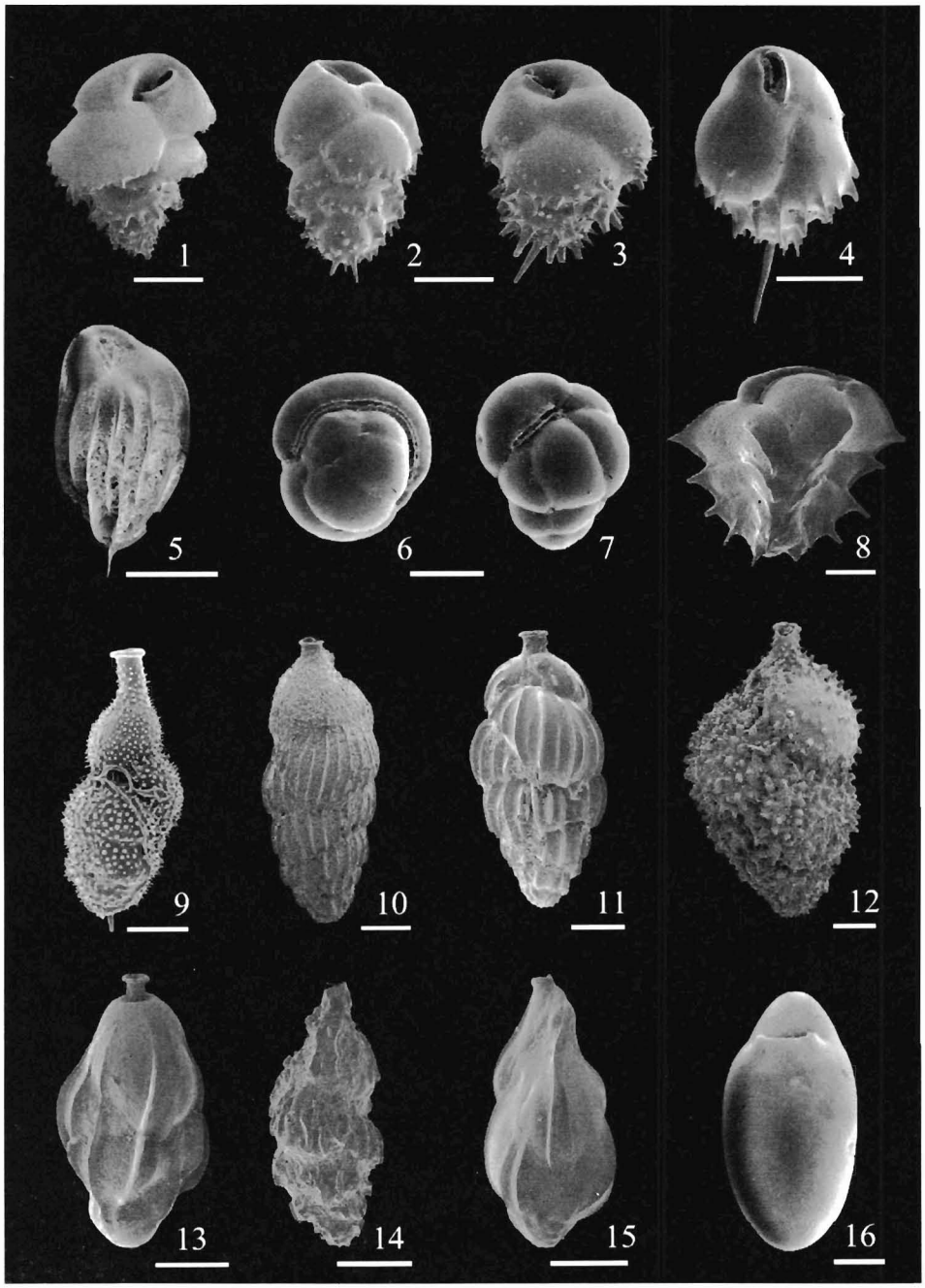
1
2
3
4
5
6
7
8
9
10
11
12
13
14
15
16

Plate 3

Fig. 1 *Astrononion stelligerum* (d'Orbigny), sample 137KA/885cm

Fig. 2 *Astrononion novozealandicum* (Cushman and Edwards), sample NIOP464-211

Fig. 3 *Cassidulina* sp. 1

Fig. 4 *Cassidulina crassa* d'Orbigny, sample 137KA/885cm

Fig. 5 *Cassidulina* cf. *C. inflata* Leroy, sample NIOP463-b5

Fig. 6 *Cassidulina carinata* Silvestri, sample NIOP455-47

Fig. 7 *Cassidulina laevigata* d'Orbigny, sample 137KA/865cm

Fig. 8 *Cassidulina subglobosa* Brady, sample NIOP455-44

Fig. 9 *Cassidulina subglobosa* Brady, sample NIOP464-138

Scale bar = 100 μm

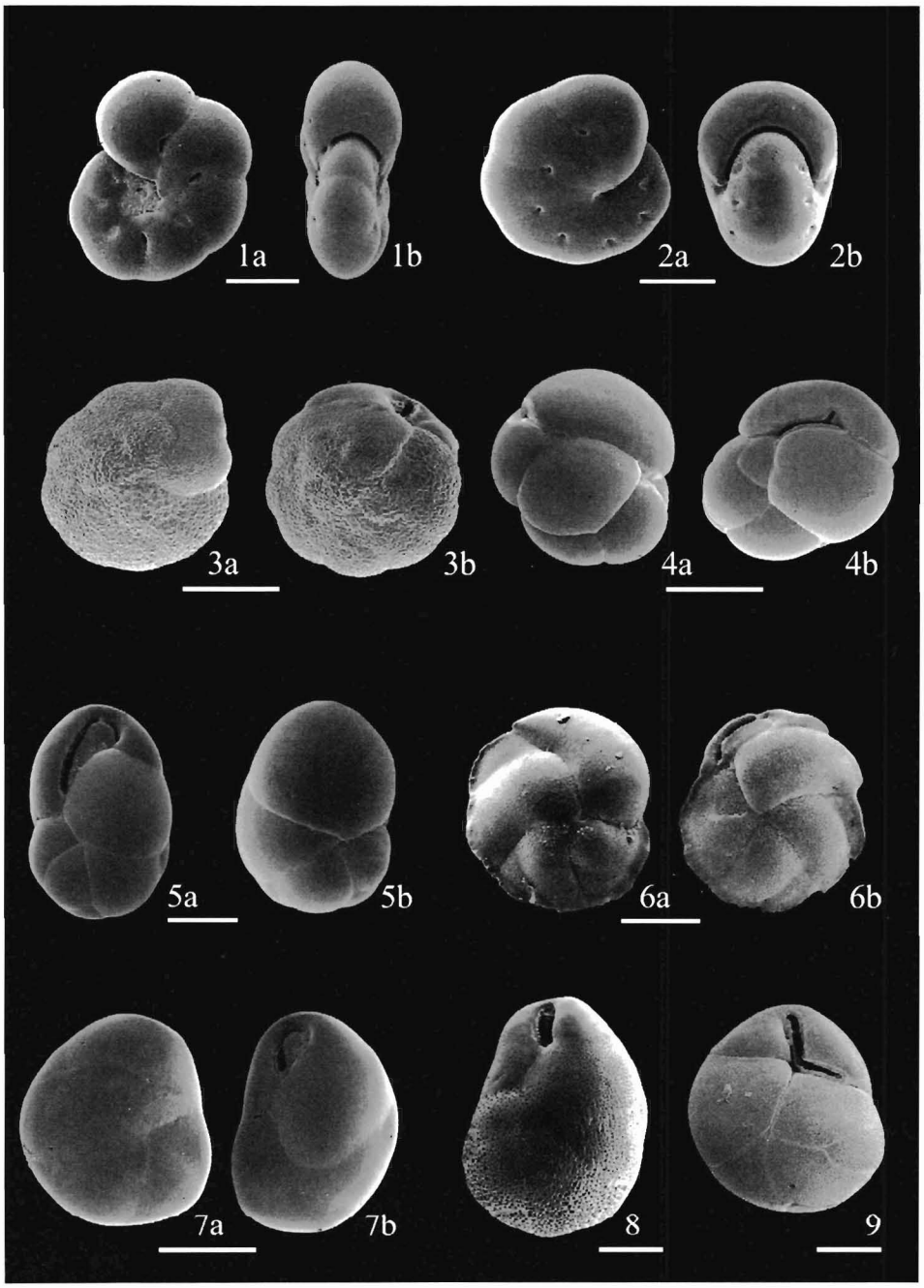
1a
1b
2a
2b
3a
3b
4a
4b
5a
5b
6a
6b
7a
7b
8
9

Plate 4

Fig. 1 *Cassidulinoides bradyi* (Norman), sample NIOP463-b5

Fig. 2 *Pullenia bulloides* (d'Orbigny) , sample NIOP455-47

Fig. 3 *Pullenia quinqueloba* (Reuss), sample NIOP463-b5

Fig. 4 *Osangularia culter* (Parker and Jones), sample NIOP464-211

Fig. 5 *Osangularia* sp.1, sample NIOP463-b5

Fig. 6 *Gavelinopsis lobatulus* (Parr), sample NIOP455-47

Fig. 7 *Melonis barleeanum* (Williamson), sample NIOP455-47

Fig. 8 *Hanzawaia boueana* (d'Orbigny), sample 137KA/885cm

Fig. 9 *Hyalinea balthica* (Schroeter), sample NIOP455-47

Scale bar = 100 μm

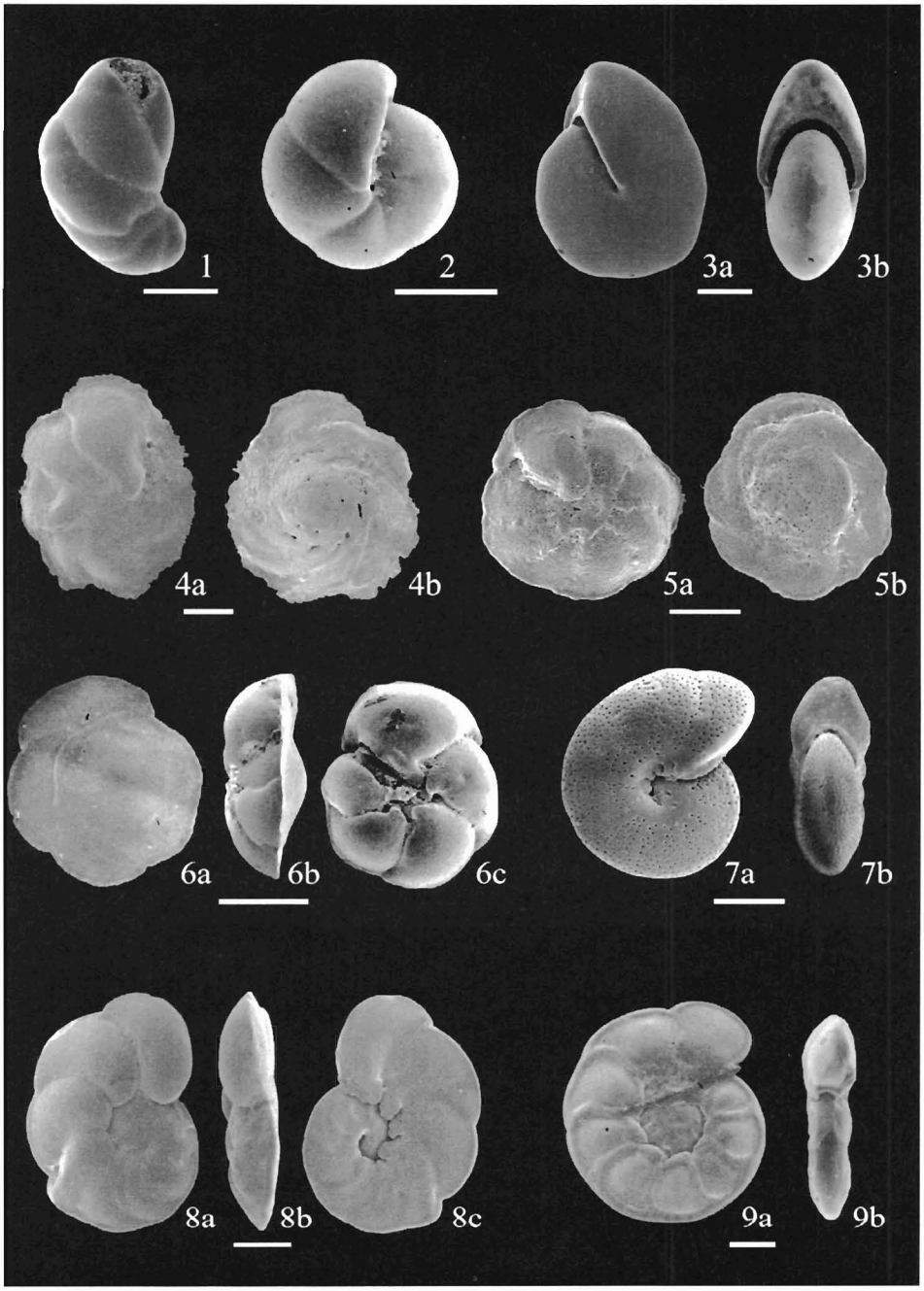
1
2
3a
3b
4a
4b
5a
5b
6a
6b
6c
7a
7b
8a
8b
8c
9a
9b

Plate 5

Fig. 1 *Triloculina* cf. *T. tricarinata* d'Orbigny, sample NIOP455-23

Fig. 2, 3 *Quinqueloculina seminulum*.(Linnaeus), sample NIOP455-47, -23

Fig. 4 *Pyrgo murrhina* (Schwager), sample NIOP455-23

Fig. 5 *Pyrgo* sp.1, sample NIOP464-96

Fig. 6 *Pyrgo williamsoni* (Sylvestri), sample 137KA/885cm

Fig. 7 *Nummuloculina* sp.1, sample NIOP464-73

Fig. 8 *Nummuloculina irregularis* (d'Orbigny), sample NIOP464-83

Fig. 9 *Sigmoilopsis schlumbergeri* (Silvestri), sample NIOP455-23

Fig. 10 *Oolina* cf. *O. apliopleura*, sample NIOP464-96-7

Fig. 11 *Lagena* sp.1, sample NIOP455-23

Fig. 12, 13 *Amphycorina scalaris* (Batsch), sample NIOP455-11, 137KA/885cm

Fig. 14 *Nodosaria* sp. 1, sample NIOP455-47

Fig. 15 *Amphycorina hirsuta* (d'Orbigny), sample NIOP455-23

Fig. 16 *Dentalina subsoluta* (Cushman), sample NIOP455-23

Fig. 17 *Dentalina adveana* (Cushman), sample NIOP464-211

Fig. 18. *Spiroloculina communis* (Cushman and Todd), sample NIOP137ka/885

Scale bar = 100 μm

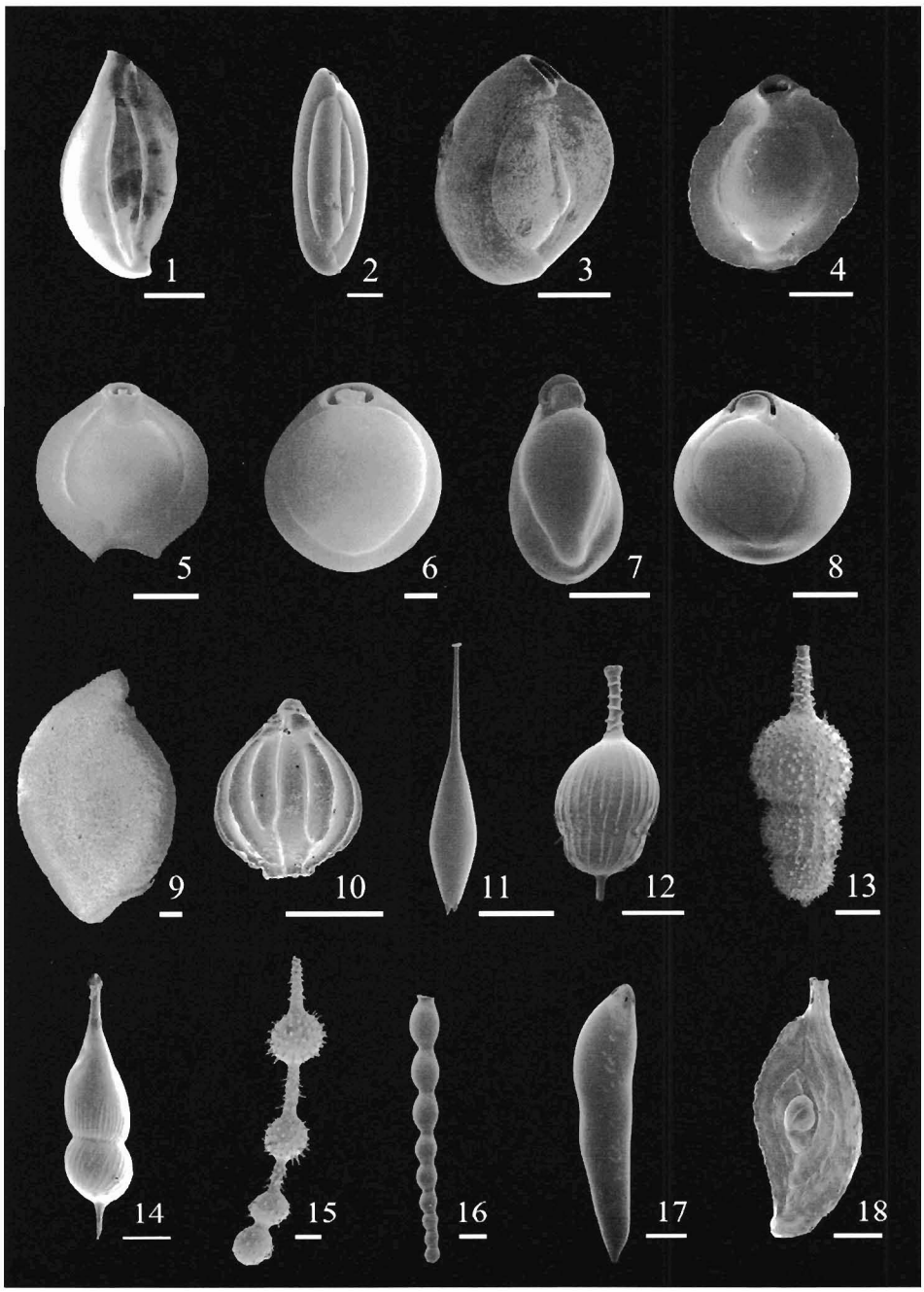
1
2
3
4
5
6
7
8
9
10
11
12
13
14
15
16
17
18

Plate 6

Fig. 1 *Cibicides ungerianus* (d'Orbigny), sample NIOP455-47

Fig. 2 *Cibicides brady* (Trauth), sample NIOP464-211

Fig. 3 *Cibicides pseudoungerianus* (Cushman), sample NIOP464-112

Fig. 4 *Cibicides lobatulus* (Walker and Jacob), sample NIOP464-96 (included in Shallow water species.)

Fig. 5 *Cibicides kullenbergi* (Parker), sample NIOP464-96

Fig. 6 *Cibicides weullerstorfi* (Schwager), sample NIOP464-39

Scale bar = 100 μm

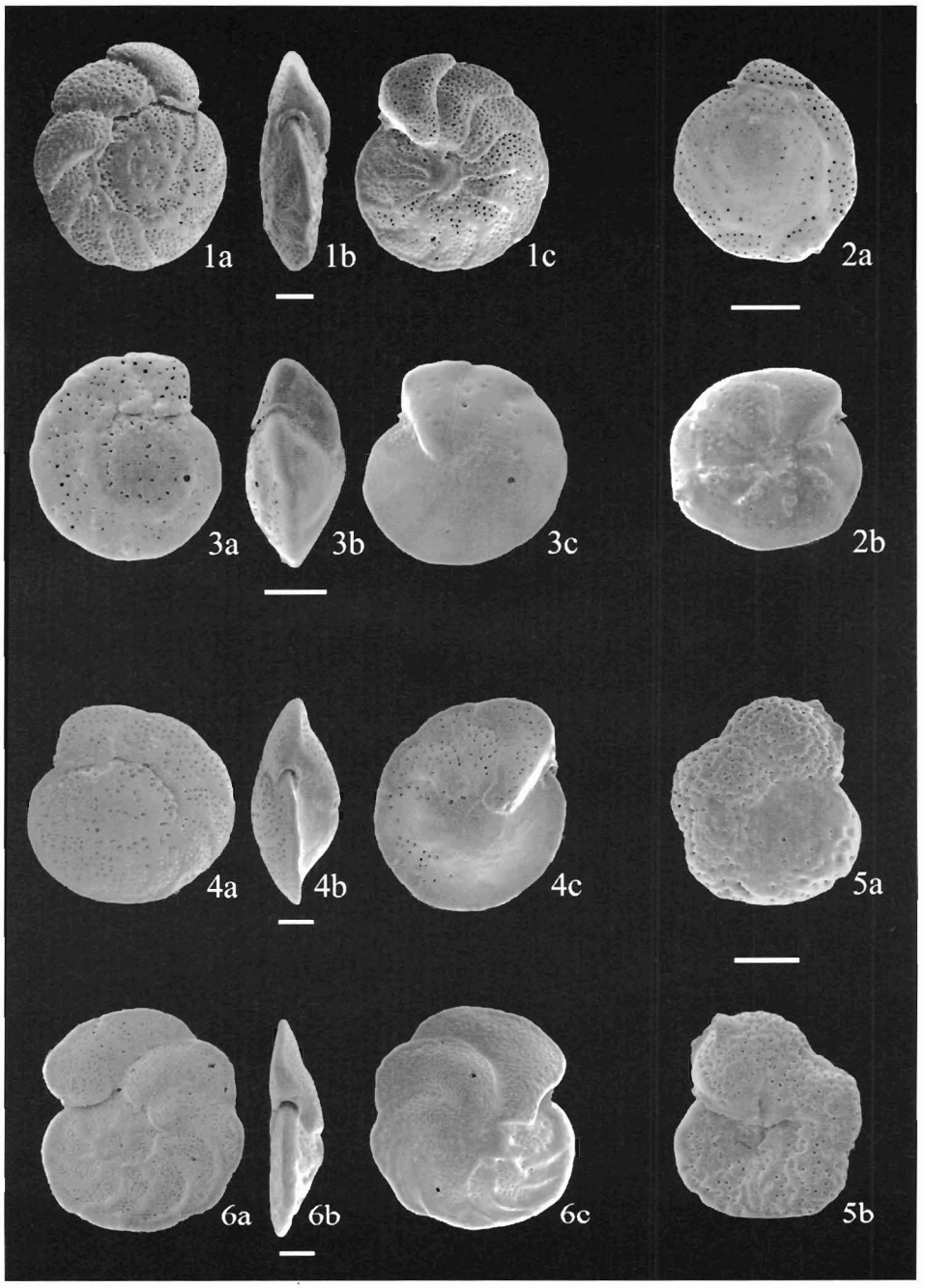
1a
1b
1c
2a
3a
3b
3c
2b
4a
4b
4c
5a
6a
6b
6c
5b

Plate 7

Fig. 1 *Cibicides* sp.1, sample NIOP464-112

Fig. 2 *Cibicides* cf. *C. dutemplei*, sample 137KA/563cm

Fig. 3 *Oridorsalis umbonatus* (Reuss), sample NIOP455-23

Fig. 4 *Epistominella exigua* Brady, sample NIOP464-25

Scale bar = 100 μm

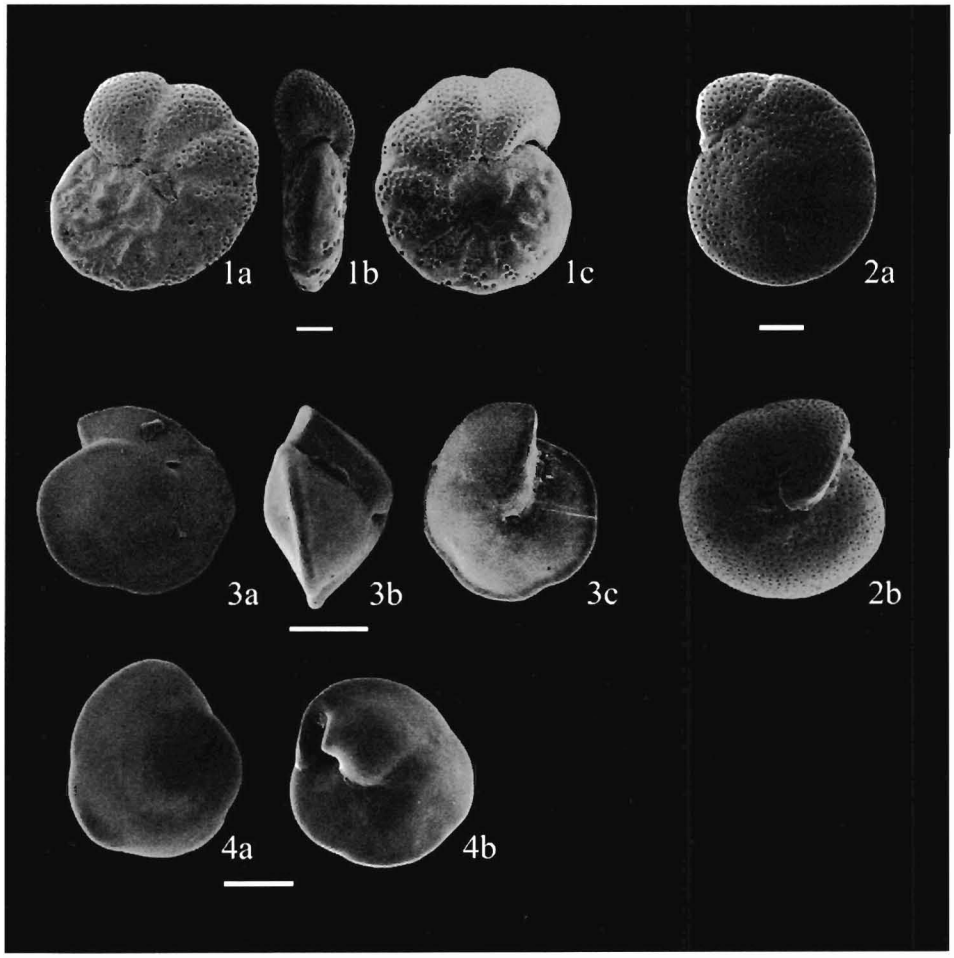
1a
1b
1c
2a
3a
3b
3c
2b
4a
4b

Plate 8

Fig. 1 *Gyroidina orbicularis* d'Orbigny, sample NIOP464-112

Fig. 2 *Gyroidina soldanii* (d'Orbigny), sample NIOP

Fig. 3 *Gyroidina polia* (Phleger and Parker), sample NIOP464-211

Fig. 4 *Gyroidina* sp.1, sample 137KA/885cm

Scale bar = 100 μm

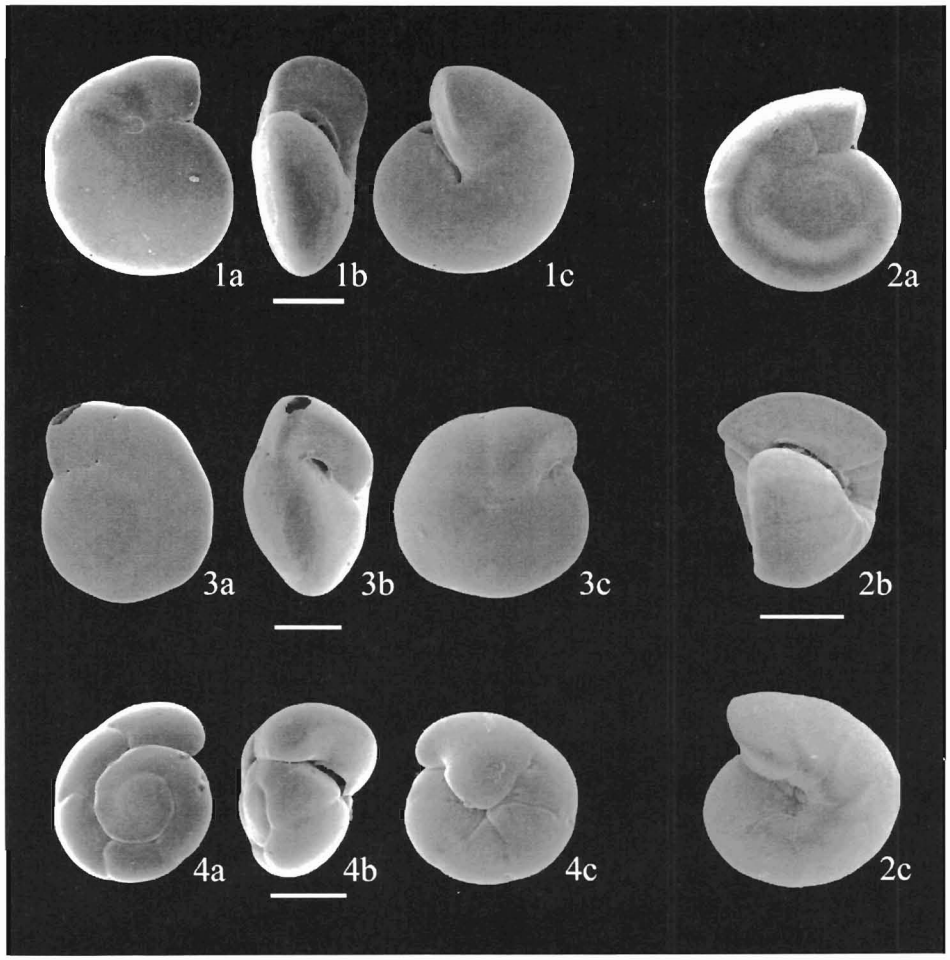
1a
1b
1c
2a
3a
3b
3c
2b
4a
4b
4c
2c

Plate 9

Fig. 1 *Sphaeroidina bulloides* d'Orbigny, sample NIOP455-47

Fig. 2 *Lenticulina peregrina* (Schwager), sample 137KA/885cm

Fig. 3 *Lenticulina* sp.1 , sample 137KA/885cm

Fig. 4 *Sarasenaria* sp.1, sample NIOP455-23 (included in *Lenticulina* spp.)

Fig. 5 *Ceratobulimina pacifica* (Cushman and Harris), sample NIOP464-112

Fig. 6 *Hoeglundina elegans* (d'Orbigny), sample NIOP455-47

Fig. 7 *Valvulinaria* cf. *V. laevigata*, NIOP464-83

Fig. 8 *Rosalina* sp.1, sample 137KA/885cm

Fig. 9 *Valvulinaria minuta* (Schubert),NIOP455-11

Fig. 10 *Rosalina vilardeboana* d'Orbigny, sample NIOP455-23

Scale bar = 100 μm

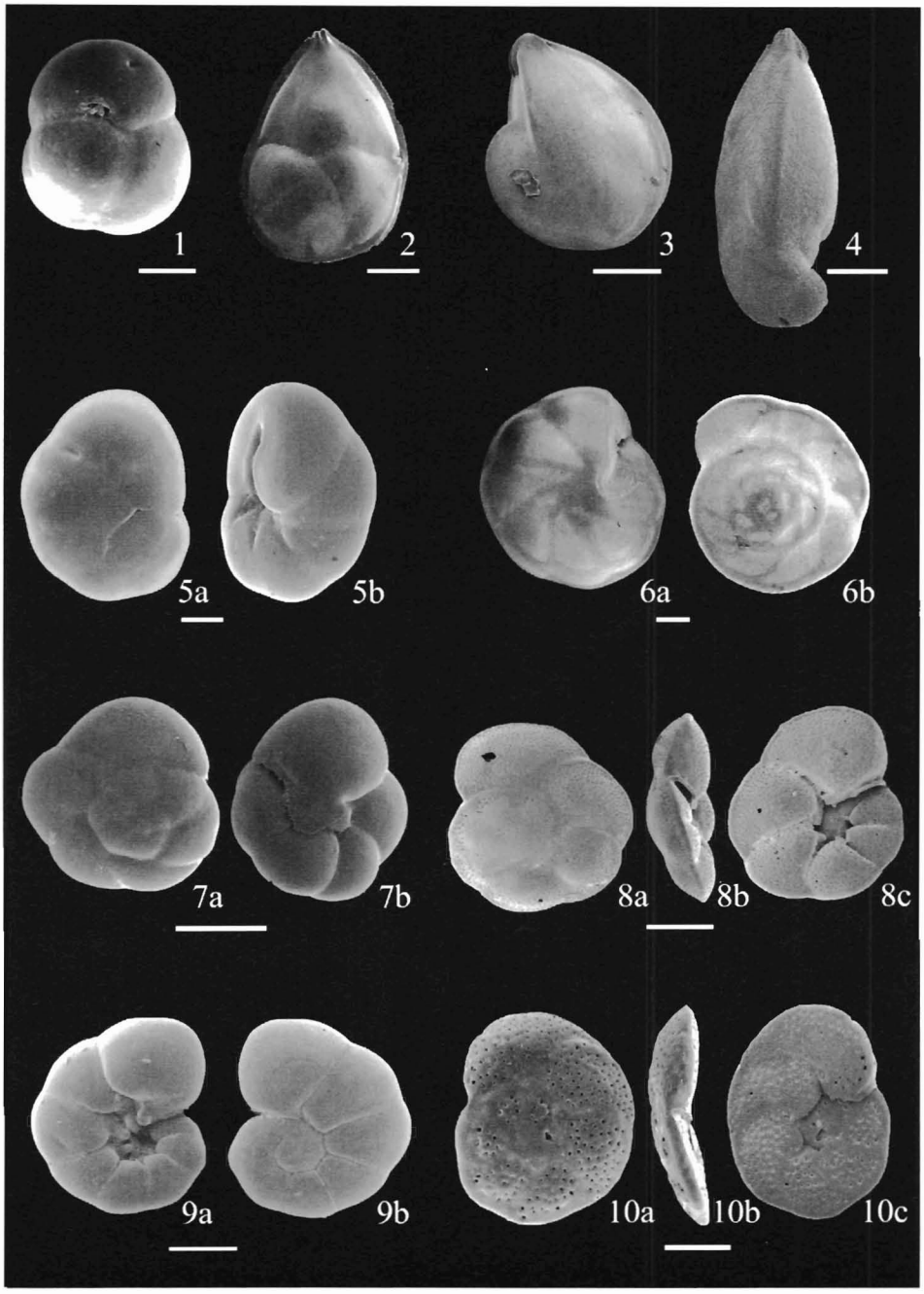
1
2
3
4
5a
5b
6a
6b
7a
7b
8a
8b
8c
9a
9b
10a
10b
10c

Plate 10

Fig. 1 *Ammonia beccarii* (Linnaeus), sample NIOP455-23

Fig. 2 *Discorbidae* sp.2, sample 137KA/865

Fig. 3 *Discorbidae* sp.3, sample 137KA/865

Fig. 4,5 *Karreriella bradyi* (Cushman) , sample NIOP464-211, -455-23

Fig. 6 *Tritaxia tricarinata* Brady, sample 137KA/865cm

Fig. 7 *Spiroplectammina* sp.1, sample NIOP464-211

Fig. 8 *Spiroplectammina* sp.2, sample NIOP463-b5

Fig. 9 *Spiroplectammina* sp.3, sample NIOP455-23

Fig. 10 *Textularia* sp.1, sample NIOP455-23

Fig. 11 *Textularia* cf. *T. saggitula*, sample NIOP137KA/885cm

Fig. 12 *Siphotextularia* sp.1, sample NIOP455-11

Scale bar = 100 µm

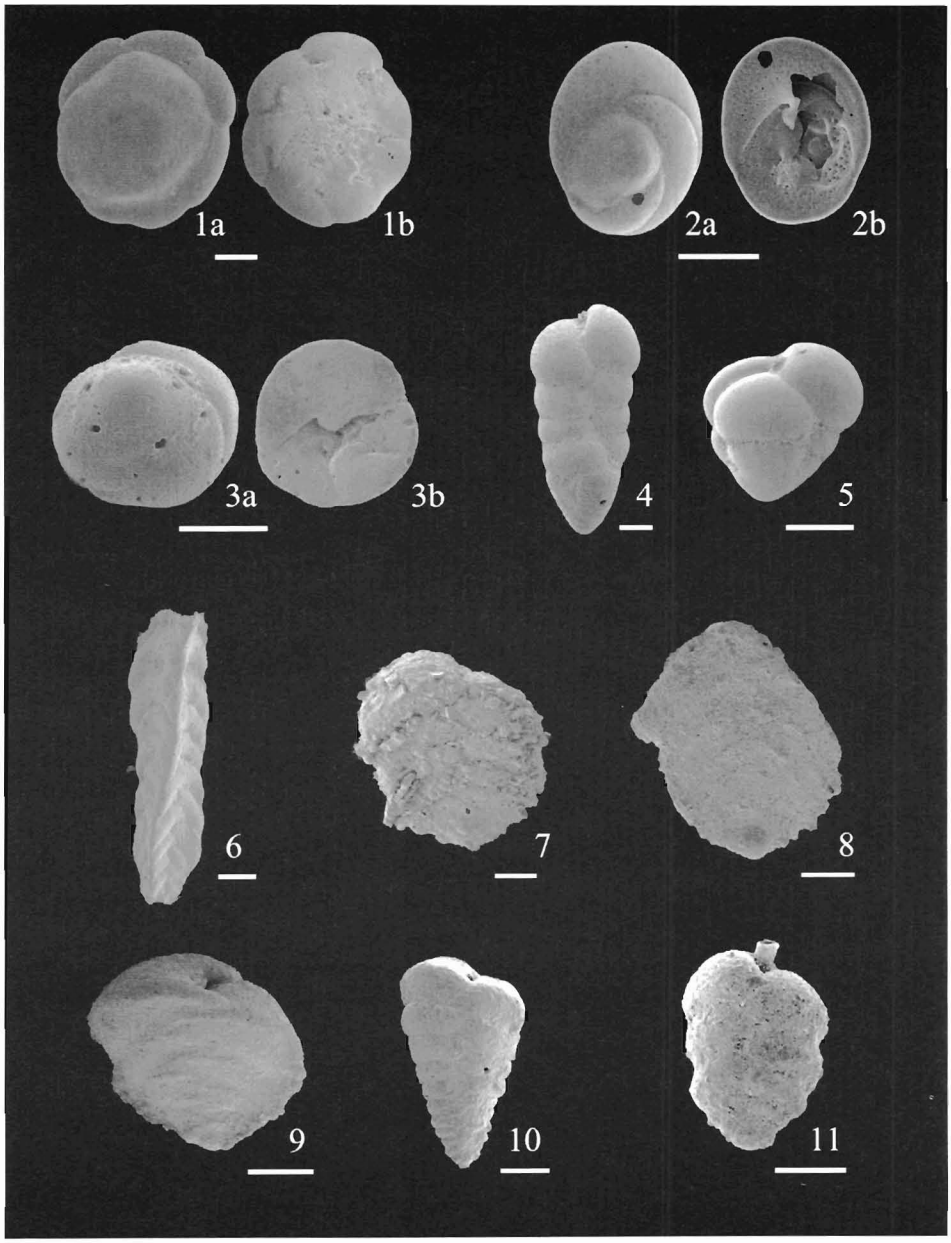
1a
1b
2a
2b
3a
3b
4
5
6
7
8
9
10
11

Introductie en samenvatting (Summary in Dutch)

Doha (Qatar), mijn woonplaats tussen 1975 en 1980:
Meer dan eens waren we genoodzaakt terug te keren naar de hoofdstad Doha. We werden verrast door plotseling opstekende zandstormen gerelateerd aan de Shamal winden, in een jaargetijde dat anders ideaal zou zijn geweest voor een uitstapje in de natuur. Hevig teleursgesteld vanwege het feit dat het kampeer weekendje naar een van Qatar's geweldige, verlaten zandstranden en ondiepe lagunes niet door kon gaan.

Later, gedurende mijn promotieonderzoek, leerde ik dat de Shamal winden op het Arabisch continent het begin inluiden van de Aziatische zomer-moesson.

Continenten in de tropen worden geregeerd door een halfjaarlijkse omkering van de windrichting, 'moesson' genaamd. Het Aziatische moesson-systeem zorgt voor seizoenale regenval in het overgrote deel van Azië en beïnvloedt zodoende de landbouw, de economie en het ecosysteem als geheel. De inwoners van het Aziatische continent zijn sterk afhankelijk van dit moesson-klimaat en zijn voorspelbaarheid. Het feit dat meer dan 60% van de wereldbevolking in deze regio leeft, illustreert het belang van dit klimaatsysteem, alsmede de hoeveelheid mensen die potentieel gebaat is bij onderzoek naar de mechanismen van dit systeem.

De richting en kracht van de Aziatische moessonwinden worden bepaald door de luchtdrukgradient, opgebouwd tussen het Aziatisch continent en de subtropische Indische Oceaan. De positie van de Inter Tropische Convergentie Zone in dit gebied, en de daaraan gerelateerde tropische depressie, schommelt jaarlijks ongeveer tussen de Kreeftskeerkring en 10° zuiderbreedte als gevolg van de cyclus van maximale instraling van de zon. De Arabische Zee, gelegen in het noordwestelijke deel van de Indische Oceaan, wordt ingesloten door noordoost Afrika, het Arabisch schiereiland en India. In de zomer zorgt de opwarming van het Tibetaanse Plateau ten noorden van India voor een versterking van de luchtdrukgradient, en daarmee voor de ontwikkeling van een krachtige zomer-moesson. Vochtige lucht afkomstig van de Indische Oceaan verplaatst zich naar het noorden over de Arabische Zee via sterke zuidwesten winden en wordt dan geforceerd op te stijgen aan de voet van het Himalayagebergte. Dit resulteert in hevige regenval in het noorden van India. In de winter is de luchtdrukgradient omgekeerd. De lage instraling van de zon en toegenomen reflectie als gevolg van de sneeuwlaag op de Himalaya zorgen voor hoge drukgebieden boven Centraal Azië. De

resulterende koude noordoosten winden gaan gepaard met een droog seizoen in India.

Dankzij de moesson is de Arabische Zee een van 's werelds biologisch meest 'productieve' watermassa's. Aanhoudende zuidwesten winden gedurende de zomer-moesson resulteren in het opwellen van het diepere, voedselrijke water. Deze situatie leidt tot een grootschalige, snelle groei van mariene algen en een daaruit voortvloeiende aanwas van de mariene fauna. De export van organisch materiaal naar dieper water en de zeebodem is navenant hoog. De afbraak van dit geëxporteerde organisch materiaal veroorzaakt op zijn beurt een verhoogde zuurstofconsumptie in de waterkolom. In combinatie met een matige ventilatieratio resulteert dit in een intense 'Zuurstof Minimum Zone' (OMZ: Oxygen Minimum Zone) op waterdieptes tussen 150 en 1200 meter. Op plaatsen waar deze OMZ de zeebodem raakt, heeft dit verregaande consequenties voor biologische en chemische processen ter plaatse.

Doordat de omstandigheden extreem zijn, vooral wat betreft productiviteit en zuurstofconcentratie, heerst in de Arabische Zee een unieke situatie voor het bestuderen van de snelheid waarmee het organisch materiaal wordt afgevoerd uit de 'epipelagische' voedselketen naar het diepere bodemleven. De extreme 'OMZ'- condities stellen ons in staat duidelijke uitspraken te doen over de rol van zuurstof in dit benthonisch-biologische systeem, alsmede over de diagenetische processen die van invloed zijn op de opslag van organisch- en ander fossiel materiaal. De hieruit verkregen kennis kan op zijn beurt weer gebruikt worden voor reconstructie-studies van het paleomilieu. Veel van dit soort onderwerpen, inclusief paleomilieu-reconstructies en klimatologische variaties, worden momenteel bestudeerd door tal van wetenschappelijk onderzoekers in diverse internationale onderzoeksprojecten.

Paleomilieu-reconstructies en benthonische foraminiferen

Biologische, chemische en sedimentologische parameters, representatief voor veranderingen in het milieu, hebben hun nut bewezen bij het ontrafelen van de condities in fossiele situaties. Belangrijke biologische hulpmiddelen daarbij zijn onder andere benthonische foraminiferen: eencellige organismen waarvan een groot aantal soorten een uitwendig kalkskelet bouwt. Hun wijdverbreide voorkomen in grote aantallen en hun hoge kans op fossilisatie maken, dat zij tot de meest bruikbare faunistische elementen behoren in

paleomilieu-reconstructies.

Momenteel worden benthonische foraminiferen vooral als nuttig beschouwd bij de reconstructie van fluctuaties in biologische productie en de zuurstof concentratie van bodemwater. Studies naar dode en levende benthonische foraminiferen, alsmede laboratoriumstudies, hebben tot het inzicht geleid dat zuurstof en organische flux bepalend zijn in de structurering van associaties van benthonische foraminiferen. Tegelijkertijd is van diverse taxa bekend, dat zij zuurstof-arme of zelfs zuurstofloze (anoxische) omstandigheden voor lange tijd kunnen doorstaan, terwijl de meeste meiofauna- en macrofaunagroepen niet meer opgewassen zijn tegen de sterk verslechterde omstandigheden. Dit maakt dat benthonische foraminiferen optimaal bruikbaar zijn bij reconstructies van extreme milieus, zoals in de Arabische Zee.

Dit proefschrift bediscussieert benthonische foraminiferen uit monsters van Laat-Kwartaire ouderdom. Aangezien, volgens de huidige opvatting, multiproxy studies een brede basis geven voor paleo-reconstructies, is bij dit onderzoek gekozen voor een multidisciplinaire opzet. Vooral diverse chemische 'tracers' zijn ingezet (hoofdstukken 2-4, 6), maar ook is er een vergelijk gemaakt met enkele lithologische proxies (hoofdstuk 3). In grote lijnen getuigen de proxies van grote fluctuaties van de OMZ gedurende de laatste 25.000 jaar en tonen aan dat de basis van de OMZ soms aanmerkelijk dieper lag dan de huidige positie (~1200 m). Variaties in de intensiteit van de OMZ verlopen synchroon met variaties in astronomische cycliciteit, maar treden daarnaast op met hogere frequenties. Ze worden verklaard door: 1) variaties in de windkracht gedurende de zomer-moesson, die op zijn beurt de hoogte van de biologische productie bepaalt via kustnabije en open oceanische opwelling van water, en daarmee tevens de mate van zuurstofconsumptie in de waterkolom, en 2) diepe mixing door convectie gedurende versterkte, koude winter-moessons. De sterke correlatie tussen 'sub-astronomische' moesson-gedreven OMZ-variaties in de Arabische Zee en snelle klimatologische veranderingen, zoals geregistreerd in sedimenten van hogere breedtegraden, suggereert dat er een sterke koppeling bestaat tussen het klimaat op hogere en lagere breedtegraden (hoofdstuk 3).

De ontwikkeling van omgevingsproxies en de continue evaluatie van hun nauwkeurigheid en betrouwbaarheid spelen een belangrijke rol in de reconstructie van paleomilieus. Dit is onmiskenbaar gerelateerd aan de complexiteit van milieu processen, maar eveneens aan de ontwikkeling en toepassing van nieuwe analytische methoden, die leiden tot gedetailleerdere gegevens, wat weer nieuwe vragen doet rijzen. Bijvoorbeeld, bij het bestuderen

van levende benthonische foraminiferen verschaft micro-electrode-technologie een meer gedetailleerde analyse van 'microhabitats' (distributie van soorten in de sedimentkolom) in relatie tot de zuurstofgradient in het poriewater. Dit roept nieuwe vragen op, bijvoorbeeld het verband met achterliggende ecologische principes van microhabitat-distributies. Het gros van de toegepaste proxies heeft in enig opzicht nadelen, voornamelijk als gevolg van verminderde betrouwbaarheid door degradatie en/of diagenetische processen. Benthonische foraminiferen vormen hierop geen uitzondering. Met de huidige kennis van de ecologie van benthonische foraminiferen, en rekening houdend met mogelijke valkuilen, wordt in hoofdstuk 4 ingegaan op de vraag hoe maatgevend benthonische foraminiferen kunnen zijn met betrekking tot de zuurstofconcentratie in het bodemwater en biologische productie in paleomilieustudies.

Daar de meeste proxies niet zijn gekalibreerd, verstrekken zij hun informatie over de vroegere milieucondities in relatieve zin. Echter, de behoefte aan steeds nauwkeuriger reconstructies lijkt groter dan ooit, vooral met het oog op de mogelijke consequenties van een sterk toenemende menselijke invloed op het milieu. Als gevolg hiervan wordt in toenemende mate gepoogd de geobserveerde, empirische relaties tussen proxies en milieu-parameters te kwantificeren door middel van zogenoemde 'transferfuncties'. Hoofdstuk 6 verkent de mogelijkheden van een op benthonische foraminiferen gebaseerde transferfunctie voor zuurstofconcentraties bij het reconstrueren van de beluchtingsgeschiedenis van de OMZ in de Arabische Zee. Hieruit blijkt dat deze transferfunctie hoogst waarschijnlijk betrouwbare kwantitatieve reconstructies van zuurstofconcentraties in het bodemwater oplevert.

Dankwoord

Ik wil graag iedereen bedanken die heeft bijgedragen tot de realisatie van dit proefschift. Om te beginnen mijn promotoren en co-promotoren Johan Meulenkamp, Bert van der Zwaan, Jan Willem Zachariasse en Gert-Jan Reichart. Bert van der Zwaan en Jan Willem Zachariasse wil ik speciaal bedanken voor hun enthausiasme en deskundige begeleiding ieder op hun eigen vakgebied. Gert-Jan Reichart ben ik veel dank verschuldigd voor de vele uren monsteren als voorbereiding op mijn verdere analyses, zijn deskundige input op het gebied van de geochemie, en niet in de laatste plaats voor zijn bereidheid iedere keer weer te helpen met allerhande vragen en analytische problemen.

Natasja Jannink en Tanja Kouwenhoven, waarmee ik voor het grootste deel van mijn promotie een kamer deelde en die tevens mijn paranimfen zijn, hebben veel bijgedragen in de vorm van morele steun en uitgebreide discussies m.b.t de ecologie van benthonische foraminiferen. Ook Ivo Duijnstee en Sander Ernst hebben enthausiast bijgedragen aan deze wetenschappelijke discussies. Natasja Jannink heeft verder een belangrijke basis gelegd voor de interpretatie van mijn resultaten, door de 'levende' benthonische foraminiferen in box-cores van de Arabische Zee te analyseren. Een stimulerende bron, tevens resulterend in een bredere kennis van paleo-klimatologische c.q. oceanografische ontwikkelingen in de Arabische Zee, is de uitwisseling van kennis met de utrechtse en amsterdamse (NIOP) collega's Sjoerd Schenau, Maarten Prins, Karin Zonneveld, Katja Ivanova, Frank Peeters en Sandrine Conan, geweest.

Ook andere collega's (en ex-collega's) wil ik bedanken voor hun bijdrage; dit was veelal door hun interesse te tonen, bemoedigende woorden te uiten, praktische hulp en/of tips te geven, of door simpelweg tijd te maken om een gezellig gesprek te voeren: Hayfaa Abdul Azis, Paul Anten, Poppe de Boer, Hans de Bruin, Jelmer Cleveringa, Jan van Dam, René Fraaye, Max van Heijst, Frits Hilgen, Tom van Hinte, Marloes van Hoeve, Lucas Lourens, Albert van der Meulen, Michiel van der Meulen, Albert Oost, Hilde Passier, George Postma, Joris Steenbrink, Henko de Stigter, Jan-Berend Stuut, Johan ten Veen. Hendrik Jan Visser wil ik speciaal bedanken omdat hij samen met Gert-Jan de monsters voor mijn analyses heeft genomen, Marlies Roelofs en Sander van Heijst voor de bijdrage die ze hebben geleverd middels hun afstudeer onderzoek aan benthonische foraminiferen van de Arabische Zee.

Ook aan andere, niet Nederlandse collega's heb ik veel te danken. I want to thank Ulrich von Rad, Hartmut Schulz, Ulrich Berner, Volkher Riech and

Frank Sirocko for their fruitful cooperation leading to a joint publication, which is also one of the chapters in this thesis. I especially want to thank Ulrich von Rad for all the effort he put into retrieving and converting the files of the figures for this chapter. Many thanks are also due to Andrea Thies and Prof. Dr. W. Kuhnt for exchanging supportive ideas. Many thanks also to Elena Turco and Kati Baldi for the nice talks concerning a wide variety of topics.

Gerrit van 't Veld en Geert Ittman wil ik speciaal bedanken voor het wassen van de monsters, Gijs Nobbe, Arnold van Dijk en Helen de Waard voor de chemische analyses. Wil den Hartog heeft de foto's gemaakt en ontwikkeld, en Paul van Oudenallen wil ik bedanken voor het maken van de omslag van mijn proefschrift. Ank Pauw en Marnella van der Tol zijn altijd bereid geweest om te helpen bij allerhande administratieve zaken.

Aan Eelco Rohling heb ik mijn introductie in de micropaleontologie en de aanzet naar het doen van dit onderzoek te danken. Rob Speijer gaf mij een door ervaring geleerd goed advies mee; 'helaas, toch blijkt veel werk weer op de laatste maanden aan te komen, ook de platen!'.

Mijn familie en vrienden wil ik bedanken voor hun belangstelling, steun en de noodzakelijke afleiding. Gerton Kalberg wil ik in het bijzonder bedanken voor zijn eindeloze begrip en onuitputtelijke stroom relativerende en bemoedigende woorden.

I would like to thank the members of the dissertation committee: Prof. Dr. P. van Cappellen, Dr. A.J. Gooday, Prof. Dr. J.W. de Leeuw, Dr. A. Mackensen, Prof. Dr. H. Visscher, for thorough reading of the manuscript and for valuable suggestions.

Curriculum Vitae

Maryke den Dulk werd geboren op 11 December, 1967 te Cardón (Venezuela). In 1980 begon zij haar middelbare school opleiding aan het Christelijk Lyceum Dr. W.A. Visser 't Hooft te Leiden. Na het behalen van het VWO diploma in 1987, begon zij in datzelfde jaar met de studie geologie aan de Universiteit Utrecht. Deze studie werd in 1993 afgesloten met het doctoraal examen Exogene Geologie. In de eerste helft van 1994 heeft zij een aanstelling als toegevoegd onderzoeker gehad bij de Faculteit Aardwetenschappen van de Universiteit Utrecht. Aansluitend werd zij van juli 1994 tot juli 1998 door de Nederlandse Organisatie voor Wetenschappelijk Onderzoek bij dezelfde faculteit aangesteld als Onderzoeker in Opleiding. In deze functie verrichtte zij onderzoek, waarvan de resultaten in dit proefschrift zijn beschreven.

Erratum

When this thesis went into print a preliminary version of the plate captions and taxonomic notes was added to the plates by mistake. Corrections to the captions are given below. Taxonomic notes should be corrected correspondingly.

Plate 3:

Fig. 8,9 *Cassidulina subglobosa* group, sample NIOP455-44, NIOP464-138

Plate 4:

Fig. 2 *Pullenia quinqueloba* (Reuss), sample NIOP455-47

Fig. 3 *Pullenia* cf. *P. quinqueloba* (Reuss), sample NIOP463-b5

Plate 5:

Fig. 2,3 *Quinqueloculina seminulum* group, sample NIOP455-47, -23

Fig. 4 *Pyrgo* cf. *P. murrhina* (Schwager), sample NIOP455-23

Fig. 8 *Nummuloculina* cf. *N. irregularis* (d'Orbigny), sample NIOP464-83

Plate 6:

Fig. 4 *Cibicides kullenbergi* (Parker), sample NIOP464-96

Fig. 5 *Cibicides lobatulus* (Walker and Jacob), sample NIOP464-96 (included under shallow water taxa in taxonomic notes)

Fig. 6 *Cibicides wuellerstorfi* (Schwager), sample NIOP464-39

Plate 10:

Fig. 1 *Ammonia beccarii* (Linnaeus), sample NIOP455-23

Fig. 2 *Discorbis* sp.1, sample 137KA/865

Fig. 3 *Discorbis* sp.2, sample 137KA/865

Fig. 4,5 *Karreriella bradyi* (Cushman), sample NIOP464-211, -455-23

Fig. 6 *Tritaxia tricarinata* Brady, sample 137KA/865cm

Fig. 7 *Spiroplectammina* sp.1, sample NIOP464-211

Fig. 8 *Spiroplectammina* sp.2, sample NIOP463-b5

Fig. 9 *Textularia* sp.1, sample NIOP455-23

Fig. 10 *Textularia* cf. *T. saggitula* Defrance, sample NIOP137/885cm

Fig. 11 *Siphotextularia* sp.1, sample NIOP455-11